Aus der Universitätsklinik für Anästhesiologie und operative Intensivmedizin
an der Martin-Luther-Universität Halle-Wittenberg,
(Direktor: Prof. Dr. med. J. Radke)
dem Institut für Pathophysiologie des Bereiches Medizin
an der Friedrich-Schiller-Universität Jena
(komm. Direktor: PD Dr. med. R. Bauer)
und der Klinik für Anästhesiologie und Intensivmedizin
am Krankenhaus Martha-Maria Halle-Dölau gGmbH,
Akademisches Lehrkrankenhaus der Martin-Luther-Universität Halle-Wittenberg
(Chefarzt: Dr. med. Harald Fritz)

elektronisches dokument
ULB Sachsen-Anhalt

Effekte der milden Hypothermie auf das traumatisierte Gehirn und extrazerebrale Organe des juvenilen Schweines

H A B I L I T A T I O N

zur Erlangung des akademischen Grades

Dr. med. habil

vorgelegt der Medizinischen Fakultät
der Martin-Luther-Universität Halle-Wittenberg

von Dr. med. Harald Georg Fritz
geboren am 09. September 1958 in Erfurt

Gutachter:

1. Univ.-Prof. Dr. med. Jürgen Piek, Rostock
2. Univ.-Prof. Dr. med. Christian Werner, Mainz
3. Univ.-Prof. Dr. med. Eberhard Kochs, München

urn:nbn:de:gbv:3-000013881
[http://nbn-resolving.de/urn/resolver.pl?urn=nbn%3Ade%3Agbv%3A3-000013881]

Referat

Nach ischämischer und traumatischer Hirnschädigung wird die Hypothermie als therapeutische Option diskutiert. Während sie für die globale ischämische Schädigung bereits in therapeutischen Konzepten etabliert ist, wird der Nutzen der Hypothermie für die traumatische Hirnschädigung derzeit kontrovers diskutiert. Spezifische Indikationen, z.B. das kindliche SHT, befinden sich derzeit in klinischer Prüfung. Experimentell ist die therapeutische Anwendung der Hypothermie beim kindlichen Schädel-Hirn-Trauma bis heute vergleichsweise wenig untersucht, obwohl das Schädel-Hirn-Trauma eine der Hauptaufnahmediagnosen auf pädiatrischen Intensivstationen und häufig mit schweren Komplikationen oder Tod assoziiert ist. Obwohl das Schädel-Hirn-Trauma für das Erwachsenenalter experimentell gut untersucht ist, gibt es bis heute nur wenige Daten für das Neugeborenen- und Kleinkindalter.

Ziel der eigenen Untersuchungen war es, an geeigneten experimentellen Modellen kliniknahe die Frühphase eines kindlichen Schädel-Hirn-Traumas nachzuvollziehen und die Beeinträchtigung der zerebralen Hämodynamik und des zerebralen Metabolismus zu quantifizieren. Nachfolgend sollten die Effekte der Hypothermie auf Hämodynamik und Metabolismus des Gehirns sowie den histopathologischen Schaden untersucht werden. Damit im Zusammenhang stehend wurde der Einfluss der Hypothermie auf die Pharmakokinetik von Fentanyl analysiert.

Mit den gewählten experimentellen Modellen waren zerebrale hämodynamische und metabolische Frühveränderungen reproduzierbar zu quantifizieren. Die Anwendung der milden Hypothermie verminderte den histopathologischen Schaden und verbesserte die metabolische und funktionelle Toleranz gegenüber einer akuten intrakraniellen Drucksteigerung. Die Hypothermie beeinträchtigt die Pharmakokinetik von Fentanyl nachhaltig.

Die Ergebnisse der vorliegenden Untersuchungen belegen neuroprotektive Effekte der Hypothermie auch für das traumatisch geschädigte juvenile Gehirn. Insbesondere scheint die Hypothermie zu einer Reduktion der intrakraniellen Drucksteigerung und somit zu einer verbesserten zerebralen Compliance zu führen.

Fritz, Harald: Effekte der milden Hypothermie auf das traumatisierte Gehirn und extrazerebrale Organe des juvenilen Schweines. Halle, Univ., Med. Fak. Diss., 148 Seiten, 2007

Inhaltsverzeichnis

Abkürzungsverzeichnis I
1. Einleitung 1
1.1. Epidemiologie und Pathophysiologie des kindlichen Schädel-Hirn-Traumas 1
1.1.1. Epidemiologische Aspekte des kindlichen SHT 1
1.1.2. Pathophysiologische Aspekte des kindlichen SHT 1
1.1.3. Altersabhängige Aspekte neurochemischer Dysfunktion des kindlichen SHT 3
1.2. Experimentelle Modellierung der traumatischen Hirnschädigung des nicht ausgereiften Gehirns 4
1.3. Therapeutische Anwendung der Hypothermie 5
2. Zielstellung der Arbeit 8
3. Material und Methoden 10
3.1. Experiment 1 – schrittweise CPP-Reduktion 10
3.1.1. Anästhesie und chirurgische Präparation zur Messung hämodynamischer Parameter 10
3.1.2. Chirurgische Präparation und Instrumentierung für Neuromonitoring und kontrollierte ICP-Steigerung 11
3.1.3. Graduelle CPP-Reduktion unter externer ABP- Kontrolle 11
3.1.4. Messung physiologischer Parameter 12
3.1.4.1. Messung von HZV und Hirndurchblutung mittels CMS 12
3.1.4.2. Durchführung der Durchblutungsmessungen mittels CMS 13
3.1.4.3. Analyseprozeduren und Bestimmung funktioneller Parameter 14
3.1.4.4. Monitoring der kortikalen Funktion mittels ECoG 16
3.1.5. Experimentelle Protokolle – Experiment 1 16
3.1.5.1. Evaluation der zerebralen Durchblutung und des oxydativen Hirnmetabolismus während schrittweiser CPP-Reduktion 16
3.1.5.2. Einfluss der milden Hypothermie auf den zerebralen Metabolismus und die elektrokortikale Funktion während schrittweiser CPP-Reduktion 17
3.2. Experiment 2 – Flüssigkeitsvermitteltes Perkussionstrauma 17
3.2.1. Anästhesie und chirurgische Präparation zur Messung hämodynamischer Parameter 17

3.2.2. Instrumentierung für Neuromonitoring und Applikation des Hirntraumas 18
3.2.3. Das flüssigkeitsvermittelte Perkussionstrauma 19
3.2.4. Messung von physiologischen Parametern 20
3.2.5. Gewebefixation, histologische und immunhistochemische Aufarbeitung 21
3.2.5.1. Immunhistochemie 21
3.2.5.1.1. ßAPP und MAP2 21
3.2.5.1.2. TUNEL-Reaktion 23
3.2.5.1.3. Auswertekriterien 24
3.2.5.1.3.1. Quantifizierung der MAP2-Immunhistochemie 24
3.2.5.1.3.2. Quantifizierung der ßAPP-Markierung 24
3.2.5.1.3.3. Quantifizierung der TUNEL-Markierung 25
3.2.6. Experimentelle Protokolle – Experiment 2 26
3.2.6.1. Auswirkungen der Hypothermie auf das Ausmaß der Hirnschädigung 26
3.2.6.2. Evaluation der Traumaschwere 27
3.2.6.3. Auswirkungen der Hypothermie auf Plasmaspiegel und Biotransformation von Fentanyl sowie die intestinale Durchblutung 28
3.2.6.3.1. In vivo Experiment (intestinale Durchblutung und Fentanyl-Plasmaspiegel) 28
3.2.6.3.2. In vitro Experiment (Temperaturabhängigkeit der CYP3A4-Aktivität) 29
3.3. Statistische Auswertung 29
4. Ergebnisse 31
4.1. Schrittweise CPP-Reduktion und der Einfluss der Hypothermie auf den zerebralen Sauerstoffmetabolismus und die elektrokortikale Funktion 31
4.2. FP-Trauma und Auswirkungen der milden Hypothermie auf das Ausmaß der histologischen Hirnschädigung 36
4.3. Flüssigkeitsvermitteltes Perkussionstrauma mit unterschiedlicher Traumaschwere 42
4.4. Auswirkungen der Hypothermie auf Plasmaspiegel und Biotransformation von Fentanyl und die intestinale Durchblutung 46
5. Diskussion 50

5.1. Effekte der Hypothermie auf das traumatisierte nicht ausgereifte Gehirn 49
5.2. Effekte der Hypothermie auf die intestinale Durchblutung und die CYP3A4-Aktivität 54
5.3. Therapeutisches Fenster für die Anwendung der Hypothermie 57
5.4. Die Wahl der experimentellen Modelle 59
6. Schlussfolgerungen 62
7. Zusammenfassung 63
8. Literaturverzeichnis 65
9. Anlagen 82
10. Weitere, im Zusammenhang mit der Thematik stehende Publikationen 141
11. Thesen zur Habilitationsschrift 142
12. Lebenslauf 146
13. Danksagung 148

Abkürzungsverzeichnis

A.	Arteria
Ae.	Arteriae
ABF	Absoluter Blutfluss
ABP	arterieller Blutdruck
AE	Absorptionseinheit
ANOVA	Analysis of Variance (Varianzanalyse)
AP	Alkalische Phosphatase
AK	Antikörper
ßAPP	ß-Amyloid-Präkursor-Protein
BV	Blutvolumen
$C_{(a-hv)}O_2$	arterio-hirnvenöse Sauerstoffgehaltsdifferenz
CBF	zerebraler Blutfluss
CBV	zerebrales Blutvolumen
CCI	Controlled-Cortical-Impact
Ch	Charrier
CMS	farbmarkierte Mikrosphären (colored microspheres)
$CMRO_2$	zerebrale Sauerstoffumsatzrate
CMRglu	zerebrale Glukoseumsatzrate
CPP	zerebraler Perfusionsdruck
DA	Dopamin
DAB	3,3-Diamino-Benzidin-Tetrahydrochlorid
DAI	Diffuse axonale Schädigung ("diffuse axonal injury“)
DMFA	Dimethylformamid
DNA	Desoxyribonukleinsäure
D_cO_2	zerebrales Sauerstoffangebot
dUTP	Desoxyuridin Triphosphatase
ECoG	Elektrokortikogramm
FiO_2	inspiratorische Sauerstoff-Fraktion
FFT	Fast Fourier Transformation
FP	Fluid-Percussion (Flüssigkeitsvermittelte Percussion)
ICP	intrakranieller Druck

I.D.	Innendurchmesser
g	Gramm
Hb	Hämoglobin
HE	Hämatoxylin und Eosin
HI	Herzindex
H_2O	Wasser
H_2O_2	Wasserstoffperoxid
Hz	Hertz
HZV	Herzzeitvolumen
iv	intravenös
KCl	Kaliumchlorid
kD	Kilodalton
KG	Körpergewicht
K-HT	Kontrollgruppe Hypothermie
K-NT	Kontrollgruppe Normothermie
KOH	Kaliumhydroxid
LDF	Laser-Doppler-Flow
M	molar
MAP	mittlerer arterieller Blutdruck
MAP2	Mikrotubuli assoziiertes Protein 2
mAb	monoklonaler Antikörper
mbar	Millibar
min	Minute
ml	Milliliter
MP	Messpunkt
ms	Millisekunde
MW	Mittelwert
NaCl	Natriumchlorid
N_2O	Stickoxydul (Lachgas)
n.s.	nicht signifikant
O_2	Sauerstoff
OH	hydroxyl
RIA	Radioimmunoassay
P_aCO_2	arterieller Kohlendioxidpartialdruck

P_aO_2	arterieller Sauerstoffpartialdruck
PBS	Phosphat gepufferte NaCl-Lösung
PID	Proprotional-Intergral-Differential
PIP	inspiratorischer Spitzendruck
PEEP	positiver endexspiratorischer Druck
pH	potentia Hydrogenii
$P_{hv}O_2$	hirnvenöser Sauerstoffpartialdruck
PU	Polyurethan
rCBF	regionaler zerebraler Blutfluss
s	Sekunde
SAB	Subarachnoidalblutung
S_aO_2	arterielle Sauerstoffsättigung
SD	Standardabweichung
SHT	Schädel-Hirn-Trauma
$S_{hv}O_2$	hirnvenöse Sauerstoffsättigung
TdT	Terminale-Desoxinukleotidyl-Transferase
$t_{Hirn}pO_2$	Hirngewebs-Sauerstoffpartialdruck
T-HT	Traumagruppe Hypothermie
TierSchG	Tierschutzgesetz
T-NT	Traumagruppe Normothermie
$T\text{-}NT_N$	Traumagruppe Normothermie (kein ICP-Anstieg)
$T\text{-}NT_{ICP}$	Traumagruppe Normothermie (sekundärer ICP-Anstieg)
TUNEL	terminal-desoxyuridine-transferase mediated biotinylated desoxyuridine-triphosphate nick end labeling
u.a.	unter anderem
V.	Vena
Vgl.	Vergleich
Vol%	Volumenprozent

1. Einleitung

1.1. Epidemiologie und Pathophysiologie des kindlichen Schädel-Hirn-Traumas

1.1.1. Epidemiologische Aspekte des kindlichen SHT

Obwohl tödliche Verletzungen im Kindesalter zu etwa einem Drittel durch Schädel-Hirn-Verletzungen verursacht werden und das SHT damit die häufigste Todesursache im Alter unter 15 Jahren darstellt (27), finden sich in der Literatur nur relativ wenige Untersuchungen zu den Pathomechanismen des kindlichen SHT (65). Dies ist umso erstaunlicher, da trotz besserer Überlebensraten die resultierenden Langzeitschäden schwerwiegende soziale und ökonomische Konsequenzen nicht nur für die Betroffenen selbst, sondern auch für ihre Angehörigen mit sich bringen (64, 158). So wurden 1996 in Deutschland ca. 83400 Kinder unter 15 Jahren nach Schädelverletzungen im Krankenhaus behandelt. Dabei handelte es sich überwiegend um intrakranielle Verletzungen, die in 80% als leichtes SHT imponierten, aber in 20% als schwere intrakranielle Verletzungen (27). Durch die wenigen vorliegenden epidemiologischen Untersuchungen ist bekannt, dass besonders häufig Kinder im Vorschulalter ein SHT erleiden und Kinder unter 4 Jahren die schlechteste Überlebensrate besitzen (112). Dabei sind Kinder unter einem Jahr am schwersten betroffen, sie weisen eine 2-3mal so hohe Mortalität auf wie Kinder über einem Jahr (204). Dagegen haben Schulkinder im Vergleich zu Erwachsenen eine doppelt so hohe Überlebensrate (114, 120).

1.1.2. Pathophysiologische Aspekte des kindlichen SHT

Ursachen sind altersspezifische Unterschiede bezüglich der Schädigungsmechanismen sowie der strukturellen und funktionellen Reife des Nervensystems (3, 153). So sind die Fähigkeiten des nicht ausgereiften kindlichen Gehirns nach einer Hirntraumatisierung, funktionell zu regenerieren, wesentlich vom Myelinisierungsgrad (51), dem Grad der dendritischen Verzweigungen, dem Beginn der Synaptogenese und der gliären Proliferationsfähigkeit abhängig (82), die im Kleinkindalter noch nicht abgeschlossen sind (202). Experimentell scheint das Ausmaß einer histopathologischen Schädigung nach diffusem Hirntrauma beim

juvenilen Gehirn geringer auszufallen als beim ausgereiften (7, 85, 154, 167). Ähnliche Befunde wurden nach experimenteller fokaler Hirnschädigung beschrieben (56).

Strukturelle Unterschiede zum reifen Gehirn bestehen im höheren Wassergehalt des kindlichen Hirngewebes, einer größeren Kapillardichte (63) und einem größeren zerebralen Blutvolumen (15).

Neben dem ungünstigen Verhältnis von Kopfgewicht zu Nackenmuskulatur ist der Schutz des Gehirns durch umgebende Strukturen, wie Schädelknochen und Hirnhäute, nicht ausgereift. Untersuchungen der eigenen Arbeitsgruppe haben gezeigt, dass der dünnere Schädelknochen und die unvollständige Kalzifizierung eine höhere Elastizität der Kalotte bedingen. Hierdurch werden mechanische Kräfte weniger stark absorbiert, so dass der Energietransfer auf das Hirngewebe wesentlich intensiver vonstatten geht (209). Daraus ergeben sich im Vergleich zum Erwachsenen großflächigere Schädelverformungen und kinetische Belastungen des Hirngewebes, die eher zu diffusen Hirnschädigungen führen (130). Die diffuse Hirnschwellung erhöht bei Kindern mit traumatischer Hirnschädigung das Mortalitätsrisiko um das 3-Fache (10).

Die Mechanismen, welche für diese diffuse Hirnschwellung verantwortlich gemacht werden, scheinen beim unreifen Gehirn andere zu sein als beim ausgereiften Gehirn. So wurde sehr häufig eine posttraumatische Hypoperfusion in den ersten 24 Stunden nach SHT bei Kindern beobachtet, die bei Unterschreiten der Ischämieschwelle für das schlechte Outcome verantwortlich war (6). Experimentell wurde eine deutliche Altersabhängigkeit dieser zerebrovaskulären Reaktion nachgewiesen. So wurde beim neugeborenen Ferkel eine ausgeprägte und länger anhaltende Vasokonstriktion der Pia-Arterien aufgrund einer entwicklungsbedingt noch verminderten NMDA-Rezeptor vermittelten Vasodilatation mit Senkung der zerebralen Perfusion gezeigt (13, 12).

Die ausgeprägten posttraumatischen Flüssigkeitsverschiebungen im immaturen Gehirn werden mit reifungsspezifischen Besonderheiten erklärt, wenngleich bislang eine kausale Detailaufklärung nur unzureichend vorliegt. Offensichtlich ist die Reifung spezifischer zerebraler Wasserkanäle (Aquaporin 4-Kanäle, AQP4), die besonders im Hirn exprimiert werden, für die zerebrale Gewebswasser-Homöostase besonders relevant (11). So werden diese APQ4-Kanäle im Gehirn der adulten Ratte nach fokalem SHT hochreguliert, wodurch die Wasserresorption beeinflusst wird (197).

Neugeborene Ratten besitzen dagegen nur 2% dieser glialen AQP4-Kanäle im Vergleich zum adulten Gehirn (212). Die Ausreifung erfolgt über mehrere Wochen, so dass im unreifen Gehirn eine deutlich eingeschränkte Kapazität zur adäquaten Kompensation nach Störung der zerebralen Gewebswasser-Homöostase vermutet werden kann (16).

Es gibt aber auch Untersuchungen, die auf Ähnlichkeiten zum adulten Gehirn hinweisen, wie etwa die vasogene und zytotoxische Komponente des posttraumatischen Hirnödems (107). Jedoch ist die Blut-Hirn-Schranke unabhängig von den mechanischen Alterationen durch den oxidativen Stress infolge der regional verminderten antioxidativen Kapazität gefährdet. Für die zytotoxische Komponente werden mindestens zwei unterschiedliche Mechanismen verantwortlich gemacht – zum einen eine anhaltende posttraumatische zerebrale Hypoperfusion (6), zum anderen eine vermehrte Glutamatrezeptor-Expression (169), die für den verstärkten Natriumeinstrom verantwortlich ist und letztendlich den intrazellulären Wassergehalt erhöht.

1.1.3. Altersabhängige Aspekte neurochemischer Dysfunktion des kindlichen SHT

Die posttraumatische Freisetzung exzitatorischer Neurotransmitter wie Glutamat führt im Hirngewebe über die Aktivierung von NMDA und metabotropen Glutamat-Rezeptoren zu einer dramatischen intrazellulären Kalziumüberladung, mit nachfolgendem Zusammenbruch der zellulären Ionen- und Wasserhomöostase (zytotoxisches Hirnödem). Die Sensitivität der NMDA-Rezeptoren auf die Freisetzung exzitatorischer Aminosäuren differiert altersabhängig, denn eine Aktivierung von NMDA-Rezeptoren führt im immaturen Gehirn zu einem stärkeren Kalziumeinstrom als im adulten Gehirn (32).

Es wird angenommen, dass unter den akuten traumatischen Bedingungen neurotoxische Effekte des Dopamins die Sensitivität der Neuronen auf exzitatorische Transmitter erhöhen (80) sowie die Produktion freier Radikale verstärken können. In diesem Zusammenhang wurde ein verminderter antioxidativer Schutz für das kindliche SHT beschrieben (20). Offensichtlich ist das unreife Gehirn selektiv empfindlich für oxidativen Stress nach traumatischer Hirnschädigung.

Ungeachtet der Hinweise, dass Veränderungen der dopaminergen Aktivität die Ausprägung von Langzeitschäden nach SHT nachhaltig beeinflussen, gibt es bisher

nur wenige Untersuchungen zur Rolle des DA-Systems in der akuten Pathogenese des SHT. So konnte gezeigt werden, dass während der Rehabilitation nach SHT eine medikamentös bedingte Dopaminanreicherung im synaptischen Spalt zur verbesserten räumlichen Wahrnehmung und Beschleunigung der kognitiven Verarbeitung führte (213), wobei die Verlangsamung der Informationsverarbeitung ein generelles Problem des kindlichen SHT darstellt (110). Experimentelle Untersuchungen der eigenen Arbeitsgruppe konnten in der Frühphase nach SHT eine Aktivierung im mesotelenzephalischen dopaminergen System für neugeborene, jedoch nicht für jugendliche Schweine belegen (210).

1.2. Experimentelle Modellierung der traumatischen Hirnschädigung des nicht ausgereiften Gehirns

Ungeachtet der Erkenntnis, dass die komplexe Dynamik der Pathogenese des kindlichen SHT eine Reihe von Aspekten aufweist, die grundsätzlich vom SHT des Erwachsenen differiert, existiert bis heute nur eine begrenzte Anzahl von experimentellen Untersuchungen.

Adäquate experimentelle Tiermodelle sind erforderlich, um die spezifischen Aspekte des SHT im Kindesalter zu untersuchen (4). Jedoch ist es unmöglich, die ganze Komplexität der traumatischen Hirnschädigung in einem Modell darzustellen (167). So werden je nach Zielstellung verschiedene Hirntraumamodelle verwendet. Die umfangreichsten Untersuchungen zur physiologischen Antwort nach einer diffusen traumatischen Hirnschädigung am unreifen Gehirn wurde mit dem Fluid Percussion - Modell durchgeführt (167). Charakterisiert ist dieses Modell durch die rasche Ausbreitung einer Flüssigkeit in den Epiduralraum, wobei alle Schweregrade des Hirntraumas induziert werden können. Mit dem schweren FP-Trauma lassen sich neben fokalen kortikalen Kontusionen und histopathologischen Schädigungen der subkortikalen Strukturen und des Hippocampus (88, 187) auch Gehirnerschütterung (Konkussion), SAB, Hirnkontusionen und DAI generieren (49, 163).

Obwohl andere experimentelle Modelle, wie das Weight-Drop-Modell (62, 68, 133) oder das Controlled-Cortical-Impact-Modell (122), die Mechanismen des primären Schadens besser abbilden, sind die nach lateralem FP-Trauma auftretenden pathophysiologischen Folgen und funktionellen Defizite dem SHT des Menschen näher (203).

Die überwiegende Zahl tierexperimenteller Untersuchungen zum Hirntrauma des nicht ausgereiften Gehirns ist an Ratten durchgeführt worden, die ein lisenzephales Gehirn aufweisen (9, 25, 55, 67, 78, 83, 96, 97, 169, 168). Das lisenzephale Gehirn erlaubt jedoch keine ausreichende Darstellung der vielschichtigen Veränderungen der Gyri und Sulci nach traumatischer Hirnschädigung. Des Weiteren unterscheidet sich die systemische physiologische Antwort der Ratte von der des Menschen beträchtlich. Hinsichtlich Gyrierung und Reifung sowie systemischer physiologischer Antwort des Gehirns stellt u.a. das Schwein eine dem Menschen ähnlichere Tierspezies dar (164), die sich insbesondere für Modelle der Hirnschädigung des nicht ausgereiften Gehirns eignet (56).

1.3. Therapeutische Anwendung der Hypothermie

Die Anwendung der Hypothermie als therapeutisches Verfahren reicht weit zurück in die Geschichte bis hin zu den Ägyptern, Griechen und Römern. Bereits Hippokrates beschrieb die topische Anwendung der Hypothermie mittels Eis und Schnee zum Zwecke der Analgesie und zur Reduktion des Blutverlustes (90). In ähnlicher Weise wurde die Hypothermie als therapeutische Strategie auch von Celsius und Galaenus beschrieben (36, 75). Auf Napoleons Leibarzt Dominique Jean Larrey geht die Beobachtung zurück, dass verletzte, nahe am Lagerfeuer abgelegte Soldaten eher ihren Verwundungen erlegen sind, als solche, die weiter entfernt von der Wärme des Feuers abgelegt wurden. Eispackungen und Schnee dienten des Weiteren zur Schmerzlinderung nach Gliedmaßen-Amputationen (118)

Die ersten wissenschaftlichen Publikationen auf dem Gebiet der Hypothermie gehen auf den Amerikaner Temple Fay zurück, der in den 40er Jahren des vergangenen Jahrhunderts über die systemische Anwendung der Hypothermie bei Hirntraumatisierten und Tumorpatienten berichtete (61). Anfang der 50er Jahre verhalf die präoperative Induktion einer systemischen Hypothermie der Kardiochirurgie zum Durchbruch, da nun Operationen am kardiopulmonalen Bypass ohne neurologische Schädigungen möglich wurden (22, 173). In den folgenden Jahren wurde eine Vielzahl von Indikationen für die systemische Hypothermie insbesondere in der Neurochirurgie untersucht, jedoch verhinderten deletäre Nebenwirkungen, wie die Zunahme der Blutviskosität, schwere

Herzrhythmusstörungen und Blutungskomplikationen während der Wiedererwärmung, ihre klinische Etablierung (53).

Seit Ende der 80er Jahre belebte sich das wissenschaftliche und klinische Interesse an der Hypothermie zur Hirnprotektion neu, nachdem eine Reihe pharmakologischer Ansätze zur Neuroprotektion nur partiell effektiv war (147). In experimentellen Studien konnte eindrucksvoll belegt werden, dass zum Erzielen einer signifikanten Neuroprotektion (Reduktion der histopathologischen Schädigung und neuropathologischer Verhaltensmuster) die Hirntemperatur nicht unter 30°C abgesenkt werden muss (35, 47, 50, 109, 155). Mit dieser milden bis moderaten Hypothermie (31-35°C) (161) ließen sich schwerwiegende Nebenwirkungen erheblich reduzieren.

Auch klinische Studien konnten diese positiven Effekte bestätigen. So sei auf zwei Studien aus dem Jahr 2002 verwiesen, welche bei Anwendung der Hypothermie nach Reanimation eine Verbesserung des neurologischen Outcomes nach 6 Monaten um 60% belegen konnten (21, 201). Ähnlich ermutigend sind die Ergebnisse bei ischämischer Hirnschädigung in der Perinatalperiode (81, 84, 182).

Dagegen gibt es bis heute widersprüchliche Ergebnisse klinischer Studien zum SHT. Während kleinere monozentrische Studien klinisch relevante Verbesserungen des neurologischen Outcomes belegen konnten (39, 131, 142, 184), zeigte die Hypothermie in einer großen multizentrischen Studie keine Vorteile gegenüber der Normothermie (41). Es gibt jedoch Hinweise, dass bei bestimmten Patientengruppen das Outcome nach SHT durch Hypothermie positiv beeinflusst werden kann (72). Die Analyse von Subpopulationen dieser multizentrischen Studie von Clifton et al.(40) ergab, dass jüngere Patienten mit einem Alter unter 45 Jahren und einer Körpertemperatur von <35°C bei Krankenhausaufnahme ein deutlich besseres Outcome (keine oder leichte funktionelle Einschränkungen) aufwiesen als eine Vergleichsgruppe, die nach Aufnahme im Krankenhaus wieder erwärmt wurde (Hypothermie beibehalten: 48%; Normothermie angestrebt: 24%, p=0.03). Ein vergleichbares neurologisches Outcome (gutes neurologisches Outcome nach 6 Monaten) wurde bei Patienten zwischen 18 und 45 Jahren nach SHT erzielt, wenn die Hypothermie für eine längere Dauer (5 Tagen) aufrechterhalten wurde. Diese langdauernde Hypothermie verhinderte den oft nach kürzerer Kühldauer beschriebenen Effekt des ICP-Rebounds (100). Auch für das kindliche SHT wurde

erst kürzlich in einer Phase-II-Studie die günstige Beeinflussung des ICP mit daraus resultierender Optimierung des CPP durch die Hypothermie belegt (8).

Dennoch besteht eine unübersehbare Diskrepanz zwischen den Ergebnissen experimenteller Untersuchungen und klinischen Daten zur Anwendung der Hypothermie nach SHT (71). Dies ist einer Vielzahl von Faktoren geschuldet, welche die Translation von Ergebnissen experimenteller Untersuchungen in die Klinik beeinflussen (52, 191). Die Wahl des Analgosedierungs-Regimes hat dabei bisher nur wenig Beachtung gefunden. Während in experimentellen Untersuchungen (28, 50, 129, 155, 216, 219) überwiegend volatile Anästhetika verwendet wurden, kommen in klinischen Studien ausschließlich intravenöse Anästhetika und Analgetika zur Anwendung. So wurde mit einer Untersuchung an Ratten gezeigt, dass z.B. Fentanyl das Outcome nach Hypothermiebehandlung sogar negativ beeinflusst (190). Das Kontusionsvolumen war nach fokaler Hirnschädigung (CCI) in der Hypothermiegruppe (32°C) größer im Vergleich zur Normothermiegruppe. Des Weiteren waren die Plasmaspiegel von Dopamin und Noradrenalin in der Hypothermiegruppe im Vergleich zur Normothermie signifikant erhöht, was auf eine erhöhte Stressantwort hinweist. Aus verschiedenen Untersuchungen ist wiederum bekannt, dass hohe Dosierungen von Fentanyl die neuronale Exzitabilität erhöhen (104, 200). Die Hypothermie allein vermag mit der Analgesie durch Fentanyl die gesteigerte exzitatorische Antwort nicht ausreichend zu unterdrücken (190). Des Weiteren alteriert die Hypothermie selbst die Pharmakokinetik von Anästhetika und Analgetika (111, 119, 175, 190).

2. Zielstellung der Arbeit

Die Besonderheiten des kindlichen SHT finden in den therapeutischen Strategien oft nur unzureichend Beachtung (16), obwohl im Jahr 2003 von der amerikanischen Brain Trauma Foundation erstmals Leitlinien zur Akutbehandlung des schweren SHT bei Kindern publiziert worden sind. Diesen Leitlinien liegen oft jedoch nur wenige Studien oder vom SHT des Erwachsenen abgeleitete Ergebnisse zugrunde (5, 54).

Ziel der eigenen Arbeit war es, an verschiedenen Modellen und Altersgruppen zur zerebralen Schädigung am gyrierten nicht ausgereiften Gehirn des Schweines die pathophysiologischen Veränderungen in der Akutphase nach einer Hirnschädigung nachzuvollziehen und die milde Hypothermie als therapeutische Intervention hinsichtlich der Beeinflussung der zerebralen Schädigung auf hämodynamischer, metabolischer, funktioneller und histopathologischer Ebene zu evaluieren.

So sollte erstens ein experimentelles Modell zur Untersuchung der Auswirkungen einer intrakraniellen Drucksteigerung auf das noch nicht ausgereifte Gehirn entwickelt werden, um eine Reduktion des CPP zu simulieren (19). Hierbei wurde die schrittweise CPP-Reduktion mittels epiduraler Volumenexpansion durch einen Ballonkatheter erzielt. Da jedoch die Zunahme des ICP frühzeitig systemische hämodynamische Alterationen (31, 180) verursacht, wodurch die Reproduzierbarkeit von Messungen der zerebralen Hämodynamik während der CPP-Reduktion beinahe unmöglich wird, wurde zur Konstanz des arteriellen Blutdruckes während der jeweiligen Messphase ein externer ABP-Kontroller installiert (93). Die externe ABP-Kontrollschleife ermöglichte auf dem jeweiligen Niveau der ICP-Steigerung, den ABP in engen Grenzen konstant zu halten.

Mit diesem Modell sollte zunächst das Ausmaß der Beeinträchtigung des rCBF und der $CMRO_2$ unter gradueller CPP-Reduktion untersucht werden. In einem zweiten Schritt wurde der Einfluss einer milden Hypothermie (32°C) auf diese ICP induzierten Störungen der zerebralen Perfusion, des Metabolismus und der kortikalen Funktion untersucht.

In einem zweiten experimentellen Ansatz wurden die Auswirkungen des schweren SHT auf das nicht ausgereifte Gehirn untersucht. Hierzu entwickelten wir ein kliniknahes Hirntraumamodell, das auf der Modifikation des 1976 von Sullivan publizierten flüssigkeitsvermittelten Perkussionstrauma-Modells beruht (196) (Abb. 3). Zunächst wurde das Modell von Sullivan auf das juvenile Schwein adaptiert und

als kliniknaher Aspekt unmittelbar nach dem Trauma ein 30%iger Blutverlust induziert, der eine sekundäre Schädigung durch kurzzeitige arterielle Hypotension simulieren sollte (74). Es ist für das adulte Gehirn der Ratte hinlänglich bekannt, dass eine sekundäre Schädigungsnoxe, wie z.B. eine zusätzliche Hypoxie, das Ausmaß der histologischen Schädigung (38, 98), des Energiestoffwechsels (185) und des zytotoxischen Hirnödems (99) zusätzlich verstärkt. Untersuchungen dieser Art sind bisher für das nicht ausgereifte Gehirn nur sporadisch beschrieben, so dass es unser Ziel war, eine traumatische Hirnschädigung mit sekundärer Schädigungsnoxe (Blutvolumenentzug) am nicht ausgereiften gyrierten Gehirn zu modellieren.

Des Weiteren sind protektive Effekte der Hypothermie (Verminderung des Defizites in Motorik und räumlicher Wahrnehmung) in experimentellen Untersuchungen nach traumatischer Hirnschädigung sowohl beim CCI-Modell (50) als auch FP-Modell (28) beschrieben, doch fehlte diesen Untersuchungen die Komplexität der sekundären Schädigungsnoxe. Die Effektivität der Hypothermie nach SHT mit sekundärer Schädigung wird bisher kontrovers diskutiert (172), insbesondere vor dem Hintergrund der bisher durch klinische Studien nicht eindeutig belegten Vorzüge der Hypothermie.

So war es unser Ziel, den therapeutischen Effekt einer milden Hypothermie nach traumatischer Hirnschädigung mit nachfolgendem Blutvolumenentzug am Ausmaß des histopathologischen Schadens zu quantifizieren (30).

Parallel hierzu wurden die Auswirkungen einer 6-stündigen milden/moderaten Hypothermie während einer 24-stündigen Monitoringphase auf die systemische Hämodynamik und die metabolische Aktivität untersucht (73). Da in klinischen Studien bisher die Langzeitanwendung von volatilen Anästhetika nicht ausreichend untersucht ist, hatten wir für unser Modell die Verwendung eines für die klinische Routine üblichen Analgosedierungs-Regimes mit Midazolam und Fentanyl gewählt. Wir untersuchten die Effekte der Hypothermie auf die Pharmakokinetik des Analgosedierungs-Regimes vor dem Hintergrund, dass die Anästhesie das Ausmaß der Schädigung in beträchtlichem Umfang beeinflussen kann (190).

3. Material und Methoden

Alle chirurgischen Verfahren und experimentellen Protokolle wurden nach §8 Abs.1 TierSchG durchgeführt und von der Tierschutzkommission des Landes Thüringen genehmigt.

3.1. Experiment 1 – schrittweise CPP-Reduktion

3.1.1. Anästhesie und chirurgische Präparation zur Messung hämodynamischer Parameter

37 weibliche Ferkel (Alter: 14 Tage, Körpergewicht: 4400±530g) wurden initial mit Ketaminhydrochlorid (50 mg/kg KG) intramuskulär anästhesiert. Die Narkoseaufrechterhaltung erfolgte nach Tracheotomie über einen Endotrachealtubus (5,5 Ch) und künstlicher Beatmung (Servo Ventilator 900C, Siemens-Elema, Schweden) mit 0,8 Vol% Isofluran in einem N_2O/O_2 von 70/30 % und intravenöser Muskelrelaxierung mit Pancuroniumbromid (0,2 mg/kg/h). Zur Volumensubstitution (Ringerlactat: 5ml/kg/h) wurde ein zentralvenöser Katheter in der V. jugularis externa sinistra platziert. Die Einhaltung der Normoventilation wurde durch kontinuierliches CO_2-Monitoring und regelmäßige arterielle Blutgasanalysen realisiert.
Zur Messung des arteriellen Blutdruckes und Gewinnung von Referenzblut für die CBF-Messung mittels farbmarkierter Mikrosphären wurde ein arterieller Katheter über die A. femoralis in die Aorta abdominalis eingebracht. Die Mikrosphären-Applikation erfolgte über einen weiteren, von der A. carotis communis dextra in den linken Ventrikel des Herzens vorgeschobenen Katheter. Für die Gewinnung von hirnvenösen Blutproben wurde zusätzlich ein Katheter über den Sinus sagittalis superior im Confluens sinuum platziert.
Zur kontinuierlichen arteriellen, linksventrikulären und zentralvenösen Druckmessung wurden Flüssigkeitsdrucktransducer (P23Db, Statham Instruments, Hato Rey, Puerto Rico) verwendet. Das EKG wurde mit den Standard-Extremitätenableitungen über Nadelelektroden registriert. Alle physiologischen Parameter wurden auf einem Multikanal-Polygraphen (MT95K2®, Astro-Med, USA) aufgezeichnet.
Die Rektaltemperatur wurde während des gesamten Experimentes bei 38°C mit einer thermostatkontrollierten Wassermatte und einer feedbackkontrollierten Wärmelampe konstant gehalten.

3.1.2. Chirurgische Präparation und Instrumentierung für Neuromonitoring und kontrollierte ICP-Steigerung

Über Bohrlochtrepanationen wurden links frontal eine fiberoptische ICP-Messsonde in die subkortikale weiße Substanz (Camino Laboratories, San Diego, U.S.A.) und eine Hirngewebs-pO_2-Elektrode (Clark-Typ) gemeinsam mit einer Temperatursonde (LICOX pO_2 Monitor, GMSmbH, Kiel-Mielkendorf, Germany) 3 bis 5 mm tief in den parietalen Kortex eingebracht. Ein Latexkatheter (8,5 Ch) mit einem epiduralen Ballon wurde rechts parietal über ein ovales Bohrloch (10x3 mm) bei intakter Dura mater parallel zum Sinus sagittalis so eingeführt, dass er über dem rechten frontoparietalen Kortex zu liegen kam. Die Bohrlöcher wurden mit Knochenwachs verschlossen und die Sonden sowie der epidurale Ballonkatheter zur Vermeidung von Dislokationen mit Dental-Acrylat fixiert (Abb.1).

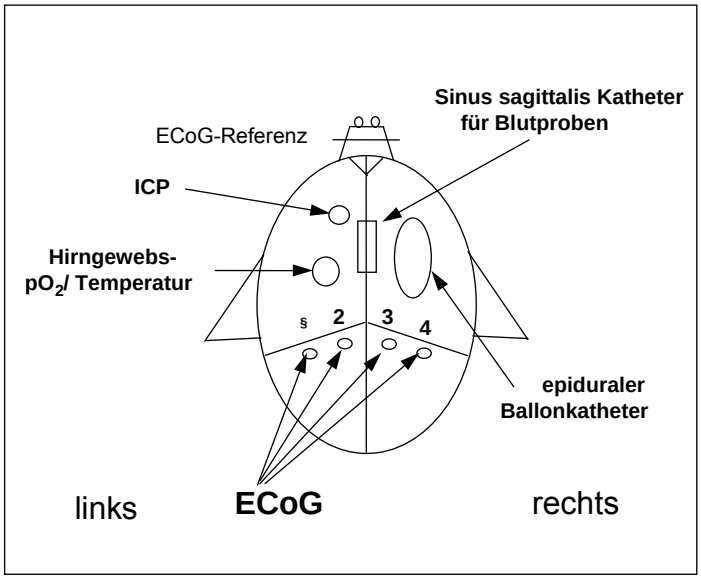

Abbildung 1 Präparation des Kopfes – Trepanationen für den epiduralen Ballonkatheter, die ICP und Gewebs-pO_2/Temperatur-Messung sowie die Lokalisation der ECoG-Ableitungen, modif. nach (70).

3.1.3. Graduelle CPP-Reduktion unter externer ABP- Kontrolle

Während der schrittweisen CPP-Reduktion wurde der MAP in engen Grenzen (85 mmHg) konstant gehalten. Die Verwendung eines speziellen externen Blutdruck-Regelkreises gestattete es, den CPP als Differenz von MAP und ICP präzise stabil zu halten und den Einfluss reaktiver MAP-Änderungen infolge der schrittweisen ICP-Erhöhung zu reduzieren.

Dabei wird die Änderung des Blutvolumens genutzt, um mittels einer durch einen externen Regelkreis per PC gesteuerten Infusions/Absaug-Pumpe (Syringe Pump SP210iw, World Precision Instruments Inc., Sarasota, USA) den Blutdruck auf einem

vorgegebenen Blutdruckniveau konstant zu halten. Da das Zusammenspiel zwischen physiologischem Blutdruckregelkreis und dem mathematisch-technischen Regler Proportional-Integral-Differential (PID) Eigenschaften mit deutlicher Nichtlinearität aufwies, war zuvor durch experimentelle Untersuchungen eine Anpassung des Reglers erforderlich (93). Die dabei ermittelte Integrationszeit-Konstante von K_1 = 6,94 mmHg/min wurde für ausreichend angesehen. Die zuverlässige Einstellung von steady-state-Zuständen ist auch bei deutlichen Abweichungen vom physiologischen Optimum in methodischen Studien belegt worden (18).

3.1.4. Messung physiologischer Parameter

3.1.4.1. Messung von HZV und Hirndurchblutung mittels CMS

Die Bestimmung des Herzzeitvolumens und der regionalen Hirndurchblutung erfolgte mittels farbmarkierter Mikrosphären (113, 208). Eine definierte Menge (~1 x 10^6 je Injektion) farbmarkierter Polystyrene-Mikrosphären (rot, weiß, gelb, blau, violett) wurde zu fünf Zeitpunkten in den linken Ventrikel des Herzens appliziert und mit dem Blutstrom zu den Organen transportiert.

Der Transport der Partikel aus dem linken Ventrikel entspricht einer Dilutionskurve, wobei der weitaus größte Teil der Mikrosphären innerhalb von 30 s im Gefäßsystem verteilt wird. Nach ca. 90 s ist die Auswaschung der CMS nahezu vollständig erfolgt.

Zur Bestimmung der nutritiven Durchblutung wurden Mikrosphären mit einem Durchmesser von 15,5±0,33 µm (Dye-Trak®, Triton Technology, San Diego, CA, U.S.A.) gewählt. Durch die Größe und die im Vergleich zu Erythrozyten fehlende Verformbarkeit werden die CMS im präkapillären Stromgebiet irreversibel fixiert und repräsentieren damit die aktuelle Durchblutung im jeweiligen Organ oder Gewebe. Zur Quantifizierung des Blutflusses wurde eine Referenzblutprobe als artifizielles Organ entnommen.

Da nach dem Lambert-Beerschen Gesetz eine lineare Beziehung zwischen Konzentration und Absorption besteht, kann die Konzentration der CMS über die Bestimmung der Absorption des durch Lösungsmittel von den Mikrosphären gelösten Farbstoffes ermittelt werden.

Das Absorptionsspektrum wurde mit einem Spektrophotometer (Beckmann DU 7500) registriert. Dabei handelt es sich um ein Summationsspektrum, das sich aus den

spezifischen Absorptionsspektren der einzelnen Farben zusammensetzt. Da das spezifische Absorptionsmaximum einer jeden Farbe in der entsprechenden Referenzblutprobe bestimmt wurde, ließ sich der Anteil der verschiedenen Farben am Summationsspektrum berechnen. Die Auflösung in die Einzelspektren erfolgte durch die inverse Matrixtechnik (179).

Die simultane Bestimmung der Farbstoffkonzentrationen in der jeweiligen Organ- bzw. Gewebeprobe und der Referenzblutprobe ermöglichte die Bestimmung des absoluten Blutflusses zu den fünf Messzeitpunkten. Die Bestimmung der Mikrosphärenzahl erfolgte durch Verwendung der spezifischen Absorption der einzelnen Farben nach Herstellerangaben als Proportionalitätsfaktor.

Der absolute Blutfluss in der jeweiligen Gewebeprobe wurde nach folgender Formel berechnet:

$$ABF_{Gewebe} = CMS\text{-}Zahl_{Gewebe} \cdot (ABF_{Referenz} / CMS\text{-}Anzahl_{Referenz})$$

Dabei entsprach $ABF_{Referenz}$ der Rate der Entnahmepumpe für die Referenzblutprobe aus der Aorta abdominalis. Der Blutfluss wird in Milliliter pro Minute pro 100g Gewebe angegeben.

Der zerebrovaskuläre Widerstand (CVR = MABP / globaler CBF) und die zerebrale Sauerstoffumsatzrate [$CMRO_2$ = Großhirnblutfluss x (arterieller - hirnvenöser O_2-Gehalt)] wurden zu jedem Messzeitpunkt bei jedem Tier bestimmt.

Des Weiteren konnte durch die exakte Gewichtsbestimmung der gemessenen Gewebeproben und des Gesamtorgans der rCBF zum Zeitpunkt der Mikrosphäreninjektion errechnet werden, indem der absolute Blutfluss bezüglich des betreffenden Probengewichtes normiert wurde.

3.1.4.2. Durchführung der Durchblutungsmessungen mittels CMS

Vor der Applikation wurden die Farbmikrosphären im Wasserbad auf 38°C vorgewärmt und im Ultraschallbad (Transonic 460/H, Singen, Germany) aufgeschüttelt, um eine optimale Suspension zu erreichen. Zu den Messzeitpunkten wurden jeweils $7{,}5 \times 10^6$ bis 9×10^6 Mikrosphären innerhalb von 20 s über den linksventrikulären Katheter in den Ventrikel injiziert. Nach der Injektion wurden die Spritze und der arterielle Katheter mit 1 ml physiologischer Kochsalzlösung gespült. Die Referenzblutprobe wurde über den A. femoralis-Katheter aus der Aorta abdominalis entnommen. Die Probenentnahme erfolgte kontinuierlich, beginnend 15 s vor Injektion der CMS über einen Zeitraum von 2 min mit einer Geschwindigkeit von

1.5 ml/min (Syringe Pump SP210iw, World Precision Instruments, Inc., Sarasota, USA).

Nach Versuchsende und Tötung der Tiere mittels intrakardialer Injektion einer 30%igen KCl-Lösung wurden die Gehirne entnommen und zur Bestimmung des rCBF in einzelne Hirnregionen geteilt, so dass die Regionen Hirnstamm (bestehend aus Medulla oblongata, Pons und Mesenzephalon), Zerebellum, Hippocampus, Großhirn, Nucleus caudatus, Thalamus, weiße Substanz (Corpus callosum, periventrikulär) und kortikale graue Substanz (gepoolt aus frontalem, parietalem, temporalem und occipitalem Kortex) erhalten wurden.

Nach Partitionierung des Hirngewebes wurden die 0,15-2,5 g großen Proben und die Referenzblutproben zur Rückgewinnung der Mikrosphären mit 3 ml/g Verdauungslösung (4N KOH mit 4% Tween 80 in deionisiertem H_2O) versetzt und für mindestens 4 h in einem 60°C warmen Wasserbad verflüssigt. Zur Rückgewinnung der CMS wurden die Proben dann über eine Polyestermembran mit einer Porengröße von 8 µm (Fa. Costar, Bodenheim) unter Laminar-Flow-Bedingungen filtriert. Im Anschluss wurden die Filtermembranen zunächst mit deionisiertem Wasser und 2 % Tween 80 und danach mit 70% Äthanol gespült.

Nach einer Trocknungszeit von 4 h wurden die CMS zusammen mit den Filtermembranen in Zentrifugengläschen gefüllt und anschließend nach Zusatz von 150 µl DMFA zur Ablösung des Farbstoffes zentrifugiert. Nach Entfernung der Membranen wurde erneut zentrifugiert und die Überstände zur Farbstoffkonzentrationsmessung abpipettiert. Die Absorptionsspektren der Farbgemische wurden mit einem Diodenarray-Spektrophotometer (Modell 7500, Beckman Instruments, Fullerton, USA; Wellenlänge von 300-800nm, optische Bandbreite 2 nm) gemessen. Bei einer Absorption >1,3 AE (1AE = -lg [10% Lichttransmission/100%]) wurde die betreffende Probe verdünnt und wiederholt gemessen, um die Linearität zwischen Absorption und Farbkonzentration zu gewährleisten. Zur Auswertung wurde eine kommerzielle Software (MISS®, Triton Technology, San Diego, U.S.A.) verwendet.

3.1.4.3. Analyseprozeduren und Bestimmung funktioneller Parameter

Hämoglobinwert, Sauerstoffsättigung und Blutgaswerte wurden unmittelbar nach Entnahme der Blutproben mit Standardlaborgeräten (Hämoxymeter OSM2®, ABL 50® Blood-Gas-Analyzer, Radiometer Kopenhagen, Dänemark) bestimmt. Alle

Messungen erfolgten temperaturkorrigiert. Die Bestimmung der Blutplasmakonzentrationen von Glukose und Laktat erfolgte mit dem Metabolit-Elektrolyt-Analyzer EML 105 (Radiometer Kopenhagen, Dänemark). Alle entnommenen Blutvolumina wurden direkt nach Entnahme durch Ersatzblut ausgeglichen.

Unter der Annahme, dass die Sauerstoffkapazität des Blutes beim Schwein 1,39 ml O_2/g Hb beträgt (34), wurde die arterio-hirnvenöse Sauerstoffgehaltsdifferenz unter Berücksichtigung des gebundenen und gelösten Sauerstoffanteils nach folgender Formel kalkuliert:

$$C_{(a\text{-}hv)}O_2 = 1.39 \bullet Hb \bullet (S_aO_2 - S_{hv}O_2) + 0.0031 \bullet (P_aO_2 - P_{hv}O_2)$$

Die zerebrale Sauerstoffumsatzrate wurde berechnet als:

$$CMRO_2 = CBF \bullet C_{(a\text{-}hv)}O_2$$

Die Blutproben aus dem Confluens sinuum repräsentieren den gemischtvenösen Sauerstoffgehalt von supratentoriell gelegenen Hirnregionen (34). Aus diesem Grund wurden zur Berechnung der $CMRO_2$ die regionalen Durchblutungen jener Hirnregionen gemittelt, deren venöses Blut vorwiegend in den Confluens sinuum drainiert (frontaler, basaler, parietaler, medianer, temporaler und occipitaler Kortex, sowie Hippocampus, Nucleus caudatus, Striatum, Thalamus und weiße Substanz des Großhirns). Für die Betrachtung des Zusammenhanges von CBF, $CMRO_2$ und mittlerer Hirntemperatur wurde als CBF der mittlere Blutfluss all jener Hirnregionen definiert, der für die Berechnung der $CMRO_2$ verwendet wurde.

Der zerebrale Gefäßwiderstand berechnet sich nach:

$$CVR = \frac{MAP}{CBF}$$

Das regionale zerebrale O_2-Angebot wurde als Produkt von arteriellem O_2-Gehalt und rCBF berechnet.

Die zerebrale Glukoseumsatzrate berechnete sich analog zur $CMRO_2$ aus dem Produkt von CBF und der zerebralen arteriovenösen Glukosedifferenz.

Das totale Blutvolumen der Tiere wurde mit 12% des Körpergewichtes kalkuliert (166).

3.1.4.4. Monitoring der kortikalen Funktion mittels ECoG

Vier als Schrauben ausgeführte Elektroden wurden zur unipolaren Ableitung des ECoG in der Schädelkalotte über dem somatosensorischen Kortex (Referenzelektrode über dem Nasion) unmittelbar kaudal der Koronarnaht und 5 bzw. 10 mm lateral der Sagittalnaht platziert (Abb. 1). Die ECoG-Signale wurden verstärkt, gefiltert und unter Verwendung eines Analog/Digital-Wandlers (DT2821F, Data Translation, Marlboro, USA) auf einen PC übertragen. Zur Offline-Auswertung wurden die Daten auf einer Festplatte gespeichert (Abtastrate 512 Hz). Das ECoG wurde während jedes Messzeitpunktes für jeweils 3 min registriert und mittels Spektralanalyse quantifiziert. Hierzu wurden die spektrale Bandleistung (Gesamtband: 1–30 Hz, δ-Band: 1–4 Hz; τ- Band: 5–8 Hz; α-Band: 9–12 Hz; β-Band: 13–30 Hz) und die δ-Ratio ([α-Band+ β-Band]/[δ-Band]) ausgewertet.

3.1.5. Experimentelle Protokolle – Experiment 1

3.1.5.1. Evaluation der zerebralen Durchblutung und des oxydativen Hirnmetabolismus während schrittweiser CPP-Reduktion

Nach Beendigung der chirurgischen Präparation wurde für alle Tiere eine Stabilisierungsphase von 60 min eingehalten. Nach Registrierung der Ausgangswerte der physiologischen Parameter (baseline) wurde der externe ABP-Kontroller zur Blutdruckregulation installiert und nach 30 min eine zweite Kontrollmessung durchgeführt (control 2).

Danach begann die schrittweise Erhöhung des ICP auf 15, 25, 35 und 45 mmHg für jeweils 30 min mittels entsprechender Inflation des epiduralen Ballons (Abb. 2). Während dieser schrittweisen ICP-Erhöhung wurde der Blutdruck bei ca. 85 mmHg konstant gehalten. Aus diesem Vorgehen resultierte bei einem ICP von 25 mmHg eine CPP-Reduktion auf etwa 70% des Ausgangswertes (Messpunkt 3), bei ICP = 35 mmHg auf 50% (Messpunkt 4) und bei ICP = 45 mmHg auf etwa 30% des Ausgangswertes (Messpunkt 5).

Mit der Aufzeichnung sämtlicher oben aufgeführter Messparameter wurde jeweils zur 25. Minute begonnen. Bei ICP=15 mmHg wurde keine CMS-Messung durchgeführt. Am Ende des Experimentes wurden die Tiere durch intrakardiale KCl-Injektion zur Entnahme und Aufarbeitung der Gehirne getötet.

3.1.5.2. Einfluss der milden Hypothermie auf den zerebralen Metabolismus und die elektrokortikale Funktion während schrittweiser CPP-Reduktion

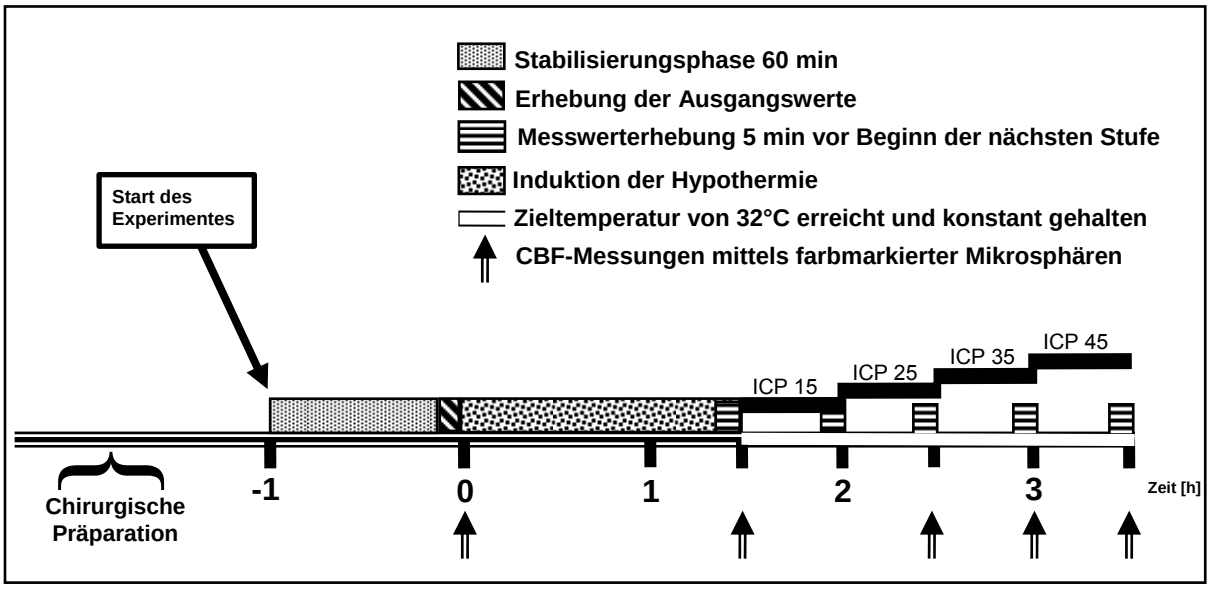

Abbildung 2 Zeitlicher Ablauf der Experimente zur Hypothermie bei schrittweiser CPP-Reduktion durch kontrollierte ICP-Erhöhung

Nach chirurgischer Präparation und Stabilisierungsphase sowie Erhebung der Kontrollwerte wurden die Tiere randomisiert entweder auf 32°C Körperkerntemperatur mittels Oberflächenkühlung gekühlt oder normotherm bei 38°C während der gesamten Versuchsdauer gehalten (Abb. 2). Nach Erreichen der Zieltemperatur erfolgte die schrittweise ICP-Erhöhung auf 25, 35 und 45 mmHg. Bei den normothermen Tieren wurde Messpunkt 3 (ICP25mmHg) nach einem Zeitintervall, welches der Kühlphase der Hypothermie-Tiere entsprach, erhoben.
Die Hypothermie wurde durch zerkleinerte Eiswürfel und eine gekühlte Wassermatte induziert und für das gesamte Experiment konstant bei 32°C Rektaltemperatur gehalten.

3.2. Experiment 2 – Flüssigkeitsvermitteltes Perkussionstrauma

3.2.1. Anästhesie und chirurgische Präparation zur Messung hämodynamischer Parameter

Alle 35 weiblichen Schweine im Alter von 6 Wochen (Deutsches Hausschwein) wurden zunächst mit Ketaminhydrochlorid (20 kg/kg KG) und Midazolam (1mg/kg) sediert. Sie atmeten über einen Nasentrichter Isofluran (2 Vol-%) in einem N_2O:O_2 -

Gemisch von 70:30 %. Die Tiere wurden dann tracheotomiert (Tracheoflex-Kanüle: Größe: 5,5 mm ID; Fa. Rüsch, Kernen, Deutschland) und ein zentralvenöser Katheter über die V. jugularis externa dextra zur Medikamenten- und Flüssigkeitsadministration (Ringerlactat: 4 ml/kg/h) mittels Venae sectio wurde platziert. Die Anästhesie wurde nun durch kontinuierliche Infusion von Fentanyl (15 µg/kg/h) und Midazolam (1 mg/kg/h) sowie Pancuroniumbromid (0,4 mg/kg/h) zur Muskelrelaxierung aufrechterhalten. Die Tiere wurden mit einem O_2/Luft-Gemisch (FiO_2 = 0,35) druckkontrolliert beatmet (PIP: 15–20 mbar, PEEP: 2–4 mbar; Servo Ventilator 900C, Siemens-Elema, Schweden). Die Normoventilation (P_aCO_2 35–40mmHg) wurde mittels kontinuierlichem CO_2-Monitoring und stündlichen arteriellen Blutgasanalysen überwacht.

Zum kontinuierlichen Blutdruckmonitoring wurde ein Katheter in der A. brachialis sinistra platziert. Ein weiterer Katheter wurde von der A. femoralis sinistra in die Aorta abdominalis zur Referenzblutaspiration während der CMS-Applikation vorgeschoben. Des Weiteren wurde ein Thermodilutionskatheter zur Messung des HI über die A. saphena sinistra in der Aorta abdominalis platziert. Weitere Katheter wurden nach linksseitiger Thorakotomie in den linken Herzvorhof für die CMS-Injektionen und in eine Pulmonalarterie des linken Lungen-Unterlappens zur Gewinnung von gemischt-venösen Blutproben eingeführt.

Die EKG-Ableitungen und die Registrierung der hämodynamischen Parameter sowie die Temperaturkontrolle erfolgten wie unter Experiment 1 beschrieben.

3.2.2. Instrumentierung für Neuromonitoring und Applikation des Hirntraumas

Nach Umlagerung wurde zunächst über eine links frontale Bohrlochtrepanation eine ICP-Messsonde (Camino Laboratories, San Diego, USA) in der subkortikalen weißen Substanz platziert. Über eine weitere links parietale Trepanation kranial und medial der Traumaapplikationsstelle erfolgte die Implantation einer Hirngewebs-pO_2-Elektrode vom Clark-Typ, einer Temperatursonde (LICOX pO_2 Monitor, GMS mbH, Kiel-Mielkendorf, Germany) und einer LDF-Sonde (Laser Blood Flow Monitor MBF 3D, Moore Instruments, Axminster, England) über eine Drei-Wege-Schraube 3-5 mm in den darunterliegenden Kortex. Eine weitere Trepanation erfolgte in der Mittellinie 20 mm rostral des Bregma zur Platzierung eines Katheters für Blutentnahmen aus

dem Confluens sinuum, der über den Sinus sagittalis superior vorgeschoben wurde (Abb. 3).
Die Katheter und Sonden wurden mit Dental-Acrylat fixiert und die Trepanationsstellen mittels Knochenwachs verschlossen.
Zur Ankopplung der Tiere an die Schlagvorrichtung wurde ein zylindrischer FP-Adapter an der Kalotte über dem linken parietalen Kortex zwischen Lambdanaht und Bregma nach Bohrlochtrepanation mittels Schräubchen und Dental-Acrylat fixiert. Während dieser Manipulationen wurde streng auf die Unversehrtheit der Dura mater geachtet.
Anschließend wurden wie in Experiment 1 die Elektroden zur Ableitung des ECoG in der Kalotte über dem somatosensorischen Kortex platziert.

3.2.3. Das flüssigkeitsvermittelte Perkussionstrauma

Das Hirntrauma wurde mittels einer modifizierten Schlagvorrichtung nach Sullivan appliziert (196). Der FP-Adapter wurde hierzu an ein zylindrisches Gehäuse konnektiert, in welches ein Drucktransducer (Typ 5011, Fa. Kistler, Ostfilden, Deutschland) eingeschraubt war. Dieses Gehäuse war mit der eigentlichen FP-Schlagvorrichtung verbunden. Die Vorrichtung besteht aus einem mit physiologischer Kochsalzlösung gefüllten 25 cm langen zylindrischen Plexiglas-Reservoir und einem abgedichteten beweglichen Metallkolben, der in dem Plexiglasrohr entlanggleitet. Der Metallkolben ist am freien Ende mit einer Gummiabdeckung versehen, auf das ein 6.2 kg schweres Pendel aufschlägt (Abb. 3).
Die Schwere des Traumas ist dabei von der Fallhöhe des Pendels und der damit pro Zeiteinheit in den Epiduralraum eindringenden Flüssigkeit abhängig. Die rasche Injektion der Flüssigkeitssäule in den Epiduralraum generiert eine diffuse Hirnbewegung mit typischen Verletzungsmustern eines schweren SHT, wie Subarachnoidalblutungen, Hirnkontusionen sowie diffusen axonalen Schäden (49, 163). Der resultierende Druckpuls diente zur Quantifizierung der Traumaschwere und wurde über den Drucktransducer registriert und auf einem Oszilloskop gespeichert (54600B Oszilloskop, Hewlett Packard, Colorado Springs, USA).
Unmittelbar nach der Trauma-Applikation wurde ein am Plexiglas-Reservoir befestigter Dreiwegehahn zur Druckentlastung geöffnet.

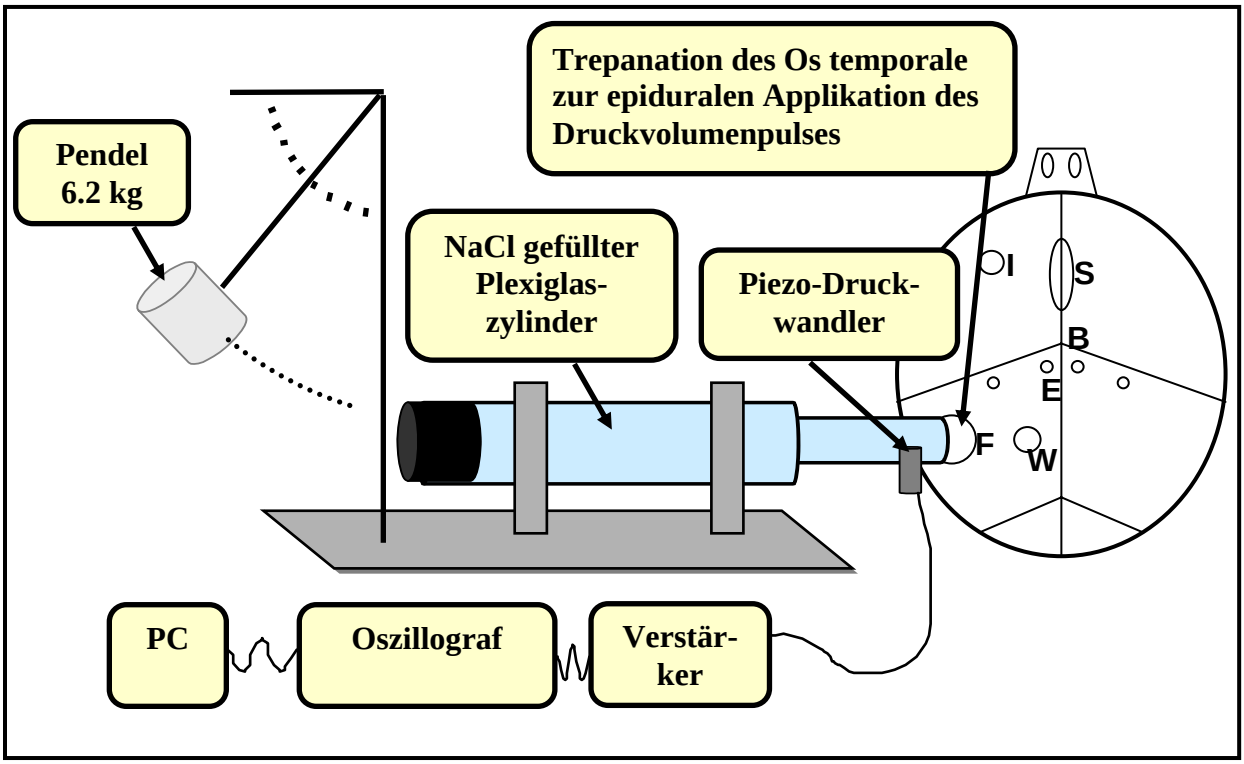

Abbildung 3 Versuchsanordnung zur Applikation des FP-Traumas; mod. nach Sullivan (196). Rechts im Bild die schematische Darstellung der instrumentierten Kalotte des Schweines (I= ICP-Sonde; S= Sinus sagittalis-Katheter, W = 3-Wege-Schraube mit $t_{Hirn}pO_2$-, Temperatur- und LDF-Sonde; F= FP-Adapter für Traumaapplikation, E = ECoG-Elektroden, B = Bregma)

3.2.4. Messung von physiologischen Parametern

Die kardiovaskulären Parameter, die Parameter des zerebralen Metabolismus und der Hirndurchblutung wurden, wie in Experiment1 beschrieben, gemessen.

CMS-Messungen wurden als Ausgangswert, am Ende des Blutentzuges, nach Volumensubstitution sowie nach 8 h (entspricht dem Ende der Hypothermiephase) und 24 h zum Ende des Experimentes durchgeführt.

Die Bestimmung des HI erfolgte mittels Thermodilutionstechnik bei Mittelung aus mindestens drei Einzelmessungen pro Messzeitpunkt.

Die Messung von Blutgasen, Elektrolyten, Glukose und Laktat im Serum erfolgte in stündlichen Abständen sowie am Ende des Blutentzuges und unmittelbar nach Substitution des Blutvolumens in der unter Experiment 1 beschriebenen Weise. Ebenso erfolgte die Aufzeichnung des ECoG in Analogie zu Experiment 1. Die auszuwertenden Analysezyklen betrugen jeweils 5 min während der Messung der metabolischen und kardiovaskulären Parameter.

3.2.5. Gewebefixation, histologische und immunhistochemische Aufarbeitung

Zur intravitalen Hirnperfusion wurde eine weitlumige Kanüle in der A. ascendens platziert und die Aorta angeschlungen. Die Aorta descendens, beide Ae. subclaviae und die V. cava inferior wurden abgeklemmt und das rechte Herzohr eröffnet. 500ml heparinisierte körperwarme physiologische NaCl-Lösung wurden nun über die Perfusionskanüle druckinfundiert, bis die aus dem rechten Herzohr zurücklaufende Lösung klar war. Nun erfolgte eine Druckinfusion von 1500 ml einer gepufferten 4%-igen Formaldehyd-Lösung zur intravitalen Hirnfixation. Nach Dekapitierung und Fixierung für 48 h in einer 4%igen Formaldehyd-Lösung bei 4°C wurden die Gehirne entnommen und zur weiteren makro- und mikropathologischen Auswertung aufgearbeitet. Hierzu wurden die Gehirne zunächst fotografiert, anschließend mit Hilfe einer Schneidevorrichtung in drei 7 mm dicke koronar verlaufende Scheiben geschnitten (Frontalhirn, temporoparietales Hirn – einschließlich Diencephalon und Hippocampus, Hirnstamm auf dem Niveau von Pons und Medulla oblongata), in Paraffin eingebettet und 7µm dicke Hirnschnitte hergestellt (Abb. 4). Sie wurden mit HE für die Routinemorphologie gefärbt bzw. für die Immunhistochemie weiter aufbereitet.

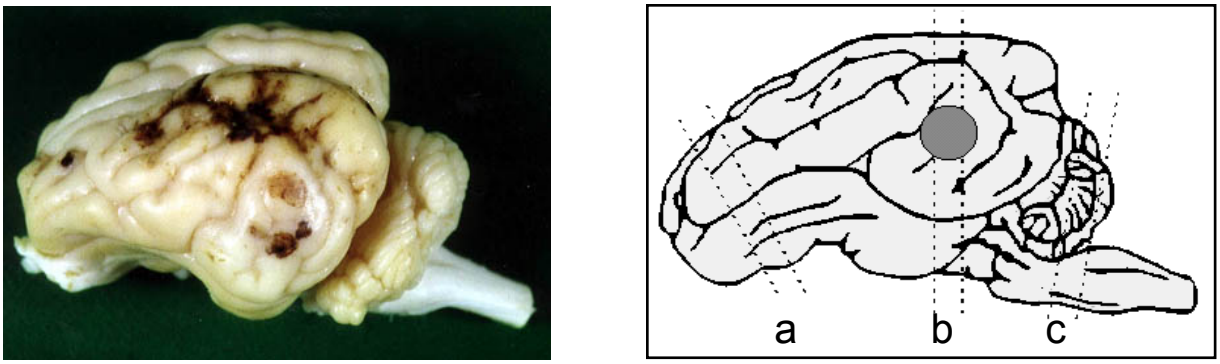

Abbildung 4 links: FP-traumatisiertes Gehirn nach Formaldehydfixierung; rechts: Schnittebenen der histologischen Aufarbeitung a)frontal, b) temporoparietal, c) Hirnstamm; der graue Kreis markiert die Lokalisation des FP-Traumas, modif. nach (30).

3.2.5.1. Immunhistochemie

3.2.5.1.1. ßAPP und MAP2

ßAPP sind Glykoproteine, die ubiquitär im ZNS, vor allem im Bereich der Synapsen, vorkommen. Lichtmikroskopisch sind sie wegen sehr geringer Konzentrationen nicht

nachweisbar (183). Im Rahmen einer Akuten-Phase-Antwort kommt es zu einer vermehrten Expression von ßAPP (171). Da ßAPP dem schnellen anterograden axoplasmatischen Transport unterliegt (135, 140), kann man bei Störungen oder Unterbrechungen der axonalen Transportfunktion intraaxonale ßAPP-Ablagerungen früher als andere axonale Proteine (z.B. Neurofilamente, Ubiquitin) nachweisen (152). Die ßAPP-Immunhistochemie hat darüber hinaus den Vorteil, dass sie im Gegensatz zu anderen axonalen Markern (Versilberungstechniken, Neurofilamente, Ubiquitin) nur geschädigte Axone markiert (1, 121).

MAP2 ist das im Gehirn quantitativ am meisten vorkommende Mikrotubuli-assoziierte Protein. Es ist vor allem in den Perikaryen und Dendriten ungeschädigter Nervenzellen anzutreffen, jedoch nicht in den Axonen. MAP2 ist ein hochmolekulares (280 kD), hitzestabiles zytoskelettales Protein, das während der normalen Hirnentwicklung Veränderungen unterliegt und bei einer Reihe neurodegenerativer Erkrankungen (Morbus Alzheimer, Morbus Pick) alteriert ist. Weiterhin gibt es Hinweise darauf, dass MAP2 eine wichtige Rolle bei Lern- und Gedächtnisprozessen spielt (214). Es liegen einige Studien über den MAP2-Verlust bei Ischämie vor (46, 106). Nach experimentellem Hirntrauma der Ratte wurde eine Abnahme der MAP2-Immunreaktivität im ipsilateralen Kortex und Hippocampus beschrieben (89).

Die ßAPP- und MAP2 - Immunhistochemie erfolgte mittels Avidin-Biotin-Peroxidase-Komplex-Methode (89). Bei den entparaffinierten Gewebeschnitten wurde zunächst die endogene Peroxidase mit 0,3% H_2O_2 in PBS-Puffer geblockt (30 Minuten bei Raumtemperatur). Nach Inhibierung unspezifischer Aldehydgruppen mit 50mg Natrium-Borhydrit auf 100 ml Aqua dest. und Blockierung unspezifischer Antigene mit Normalserum wurden die Gewebsschnitte über Nacht bei 4°C mit den primären AK inkubiert. Zur Darstellung von ßAPP-Ablagerungen (mAb Maus 22c11; Boehringer Mannheim, Indianapolis, USA) wurden ßAPP-AK und für die Markierung der MAP2-Proteine (mAb, Amersham International, Little Chalfont, GB) MAP2-AK verwendet. Nach Spülung mit Arbeitspuffer wurden die Schnitte am Folgetag mit dem sekundären biotinylierten AK (Pferd-anti-Maus IgG) über 24 h bei 4°C inkubiert. Nach erneuter Spülung wurde der ABC-Komplex als tertiärer AK mit einer Einwirkzeit von 30 min bei Raumtemperatur auf die Schnitte (Vectastain Elite Kit, Vector Laborities, Burlingham, USA) aufgetragen. Anschließend wurden die Schnitte nach erneuter mehrmaliger Spülung PBS und Aqua dest. mit dem Peroxidase-Substrat (DAB) inkubiert. Die Reaktion wurde nach 8 min mit Aqua dest. unterbrochen, anschließend

wurde mit Hämatoxylin gegengefärbt (Einwirkzeit: 15 min). Nach Dehydrierung in aufsteigender Alkoholreihe wurden die Gewebeschnitte mit DPX-Deckmedium eingedeckt.
Zur Negativkontrolle dienten mit Pferdeserum inkubierte Gewebeschnitte ohne primären AK, die keinerlei Markierungen zeigten. Als Positivkontrollen für die MAP2-Immunhistochemie wurden Gewebeschnitte vom Rattenhirn, für die ßAPP-Immunhistochemie ßAPP-positive Hirnschnitte von Alzheimerpatienten genutzt.

3.2.5.1.2. TUNEL-Reaktion

Mit der TUNEL-Methode sind die für die Apoptose charakteristischen DNA-Fragmentationen nachweisbar. Neben dem nekrotischen Nervenzelluntergang lassen sich auch Häufigkeit und Lokalisation apoptotischer Hirnzellen analysieren.
Die genomische DNA kann während des Apoptoseprozesses sowohl in niedermolekulare DNS-Doppelstrangfragmente als auch in Einzelstränge („nicks“) höheren Molekulargewichts zerbrechen. Solche DNA-Strangbrüche können in einer enzymatischen Reaktion durch die Markierung freier 3´-OH-Enden mittels modifizierter Nukleotide identifiziert werden. Bei dem verwendeten Kit („in situ cell death detection kit“, AP, Boehringer Mannheim, Indianapolis, USA) wurde das Enzym TdT, welches die Polymerisation von Nukleotiden an freien 3´-OH-DNA-Enden katalysiert, genutzt, um DNA-Strangbrüche nachzuweisen.
Während der TUNEL-Reaktion wurde mit Hilfe der TdT Fluorescein-konjugierte dUTP-Nukleotide als Antigen an die fragmentierte DNA angelagert. Für die Passage der AK in den Zellkern war jedoch eine Vorbehandlung mit proteolytischen Enzymen, wie Proteinase K, notwendig. Dieser Vorgang wurde nach 20 min Inkubation im Brutschrank bei 37°C durch dreimaliges Spülen mit PBS beendet. Für die TUNEL-Reaktion wurde in Abhängigkeit von der Größe der Gewebeproben bis zu 100ml Fluorescein-konjugierte dUTP und die TdT aufgetragen und für 1h bei 37°C inkubiert. Zur Negativkontrolle wurde nur die reine Verdünnungslösung (Fluorescein-konjugierte dUTP ohne Enzym) aufgetragen. Die TUNEL-Reaktion wurde durch dreimalige Spülung mit PBS beendet. Die Verwendung von Fluorescein-konjugierter dUTP möglichte es, die DNA-Fragmentation direkt nach der Inkubation des primären AK unter dem Fluoreszenzmikroskop zu untersuchen. Für die lichtmikroskopische Darstellung reagierte in einem zweiten Schritt der primäre AK mit einem Anti-Fluorescein-Sekundär-AK, der mit AP konjugiert war. Da es sich bei der AP um ein

ubiquitär vorkommendes Enzym handelt, wurde die endogene AP zuvor mit Magermilchpulver bzw. Kaninchenserum für 60 min inhibiert. Nach Zusatz eines Substrates für die AP wurde anschließend die Converter-AP aufgetragen und bei 37°C für 30 min inkubiert. Der Entwicklungsprozess wurde mit Blockierungslösung (NBT/BCIP, Boehringer Mannheim, Indianapolis, USA) beendet. Nach Gegenfärbung mit Kernechtrot und Eindeckung der Schnitte mit Glyceringelatine konnten die markierten Zellen lichtmikroskopisch analysiert werden. Als Positivkontrolle dienten humane Lymphomschnitte.

3.2.5.1.3. Auswertekriterien

Die Gewebeschnitte wurden ohne Kenntnis der Zugehörigkeit zur jeweiligen Versuchsgruppe ausgewertet. Die Auswertung von MAP2-Immunhistochemie und TUNEL-Reaktion erfolgte an zwei konsekutiven Schnitten, die der ßAPP-Immunhistochemie nach Prüfung der Reproduzierbarkeit an einem Schnitt. Für die histologische Auswertung und die genaue anatomische Zuordnung der untersuchten Hirnareale dienten anatomische Atlanten vom Schweinegehirn (66).

3.2.5.1.3.1. Quantifizierung der MAP2-Immunhistochemie

Die Quantifizierung der MAP2-Immunhistochemie erfolgte an Gewebeschnitten des Neokortex und Hippocampus beider Hemisphären nach Einscannen in einen PC mittels Bildbearbeitungssoftware (IMAGE, Version 1.42, NIH Public Domain, USA).
Die Bilder der Koronarschnitte wurden digitalisiert und die MAP2-Reaktivität mit einer Dichteskala (Grauwerte) zwischen 0 (weiß) und 255 (schwarz) bestimmt. Der nicht markierten subkortikalen weißen Substanz wurde dabei als Hintergrundmarkierung immer der Grauwert 0 (weiß) zugeordnet („Weißabgleich“).

3.2.5.1.3.2. Quantifizierung der ßAPP Markierung

Folgende Hirnareale wurden auf eine ßAPP-Markierung hin untersucht:

a) linke und rechte Hemisphäre auf dem Niveau des Traumas, temporoparietales Hirn mit Radiatio optica, Fasciculus subcallosus, Corpus callosum, Splenium, Commissura fornicis und Hippocampus,

b) linkes und rechtes Dienzephalon mit Fasciculus tegmenti und Thalamus;

c) Frontallappen, subkortikale weiße Substanz auf Höhe der Fissura rhinalis anterior, des rostralen Anteils des Nucleus caudatus;

d) Hirnstamm mit Commissura colliculi inferioris, Pedunculi cerebellares superiores, Lemniscus lateralis, Fasciculus tegmenti, Fasciculus longitudinalis medialis und Lemniscus medialis.

Alle ßAPP-positiven Areale wurden in die Auswertung einbezogen. Die Gewebsschnitte wurden unter 200x Vergrößerung betrachtet und auf Markierung von Axonen, deren Form und das Ausmaß der Markierung untersucht. Die Anzahl der markierten Axone sowie der zwiebelförmigen Axonauftreibungen („axonal bulbs“) wurde in einem Bereich von 0,5mm^2 ermittelt und auf die gesamte Fläche, in der positive Markierungen auftraten, extrapoliert. Zur semiquantitativen Auswertung der ßAPP-Markierung wurde folgende Graduierung genutzt (140):

Grad 0: keine Markierung von Axonen oder Nervenzellen

Grad 1: schwache und nur vereinzelte Axon- und Nervenzell-Markierungen

Grad 2: kräftige, aber nur fleckförmige Ansammlung von Axon- und Nervenzellmarkierungen

Grad 3: kräftige und weiträumige Markierungen von Axonen und Nervenzellen.

Das Vorhandensein von ‘axonal bulbs‘(zwiebelförmige Axonauftreibungen) erfolgte in separater Bewertung.

3.2.5.1.3.3. Quantifizierung der TUNEL-Markierung

Auf dem Niveau des Traumas wurden Kortex, weiße Substanz, Hippocampus und Dienzephalon (Abb. 4) auf Anwesenheit, Anzahl und Verteilung TUNEL-positiver Zellen untersucht. Die Gewebsschnitte wurden unter 200x Vergrößerung in mindestens fünf Gesichtsfeldern betrachtet (Fläche 1,5mm^2 pro Gesichtsfeld) und nach folgendem semiquantitativen Score eingeteilt:

0 = keine TUNEL-positiven Zellen

1 = bis zu 10 TUNEL-positive Zellen pro Gesichtsfeld

2 = 11 - 20 TUNEL-positive Zellen pro Gesichtsfeld

3 = mehr als 20 TUNEL-positive Zellen pro Gesichtsfeld

Die räumliche Verteilung innerhalb eines Hirnareals wurde mit einem zweiten Score analysiert:

0 = keine TUNEL-positiven Zellen

1 = Ansammlung TUNEL-positiver Hirnzellen an einem Punkt des Hirnareals

2 = Ansammlung TUNEL-positiver Hirnzellen an mehreren Punkten des Hirnareals
3 = ubiquitäres Auftreten TUNEL-positiver Hirnzellen des Hirnareals.
Die Ergebnisse dieser zwei Untersuchungen wurden zu einem Wert addiert. Somit ergab sich ein Maximalwert von sechs für jedes ausgewertete Hirnareal.
Eine genaue morphologische Beschreibung der TUNEL-positiven Zellen war erforderlich, da DNA-Schäden sowohl apoptotisch als auch nekrotisch bedingt sein können (149). Die Differenzierung TUNEL-positiver Zellen erfolgte in Typ-I- (nekrotische Zellen) und Typ-II-Zellen (apoptotische Zellen) (170). Geschwollene Zellen mit diffuser homogener TUNEL-Markierung wurden den Typ-I–Zellen zugeordnet. TUNEL-positive Zellen mit dem morphologischen Bild von Kernschrumpfung, Chromatinmargination und der Ausbildung von „apoptotic bodies“ wurden den Typ-II-Zellen zugeordnet. Ermittelt wurde sowohl die Gesamtzahl TUNEL-positiver Zellen, als auch der prozentuale Anteil von Typ-II/Typ-I-Zellen.

3.2.6. Experimentelle Protokolle – Experiment 2

3.2.6.1. Auswirkungen der Hypothermie auf das Ausmaß der Hirnschädigung

Nach Beendigung der chirurgischen Präparation und einer Stabilisierungsphase von 60 min wurden die Ausgangswerte erhoben. Danach erfolgte die Randomisierung der Tiere durch eine unabhängige Person (I.W.) und die Zuordnung zu den Kontrollgruppen [K-NT: Kontrolle-Normothermie (n=6) oder K-HT: Kontrolle-Hypothermie (n=6)] oder den Traumagruppen [T-NT: Hirntrauma-Normothermie (n=13) oder T-HT: Hirntrauma-Hypothermie (n=10)]. Das Hirntrauma wurde mit einem Auslenkwinkel des Pendels der FP-Schlagvorrichtung von 22 bis 26°, was im Mittel einem moderaten Trauma von 3,5±0,3 atm entsprach (errechnet aus der mittleren Amplitude des Druckpulses 2–5 ms nach Beginn des Traumas).
Drei Minuten nach dem Trauma wurde als sekundäre Schädigungsnoxe eine hypovolämische Hypotension induziert. Den Tieren wurde innerhalb von 18 min 30 % des kalkulierten Blutvolumens entzogen. Dabei wurde von einem BV, das ca. 8% des Körpergewichtes entspricht (166), ausgegangen. 35 min posttraumatisch wurde das entzogene BV mit einem gelatinebasierten kolloidalen Volumenersatz (Gelafusal, Serumwerke Bernburg, Deutschland) innerhalb von 10 min vollständig substituiert (Abb. 5). Am Ende der 24-stündigen Überwachungsperiode wurden die Tiere mit einer intrakardialen Injektion einer 30%igen KCl-Lösung getötet.

Bei den Tieren der Hypothermiegruppen (K-HT und T-HT) wurde mit der Kühlung 60 min nach Trauma-Applikation begonnen. Die Tiere wurden während des Experimentes auf einer wassergekühlten Matte (Wassertemperatur: 4°C) gelagert und zusätzlich mit einem Kaltluftgebläse gekühlt. Rektale und Hirntemperatur wurden kontinuierlich gemessen, wobei die thermoregulatorischen Maßnahmen nach der Rektaltemperatur gesteuert wurden. Die Tiere wurden so auf 32°C gekühlt und die rektale Temperatur für 6 h konstant gehalten. Anschließend wurden die Tiere mittels Erwärmung der Wassermatte und Warmluftgebläse innerhalb von 3 bis 4 Stunden wiedererwärmt und das Monitoring bis 24 Stunden posttraumatisch fortgeführt (Abb.5). Nach 24 h erfolgte die Beendigung des Experimentes nach der oben beschriebenen Prozedur.

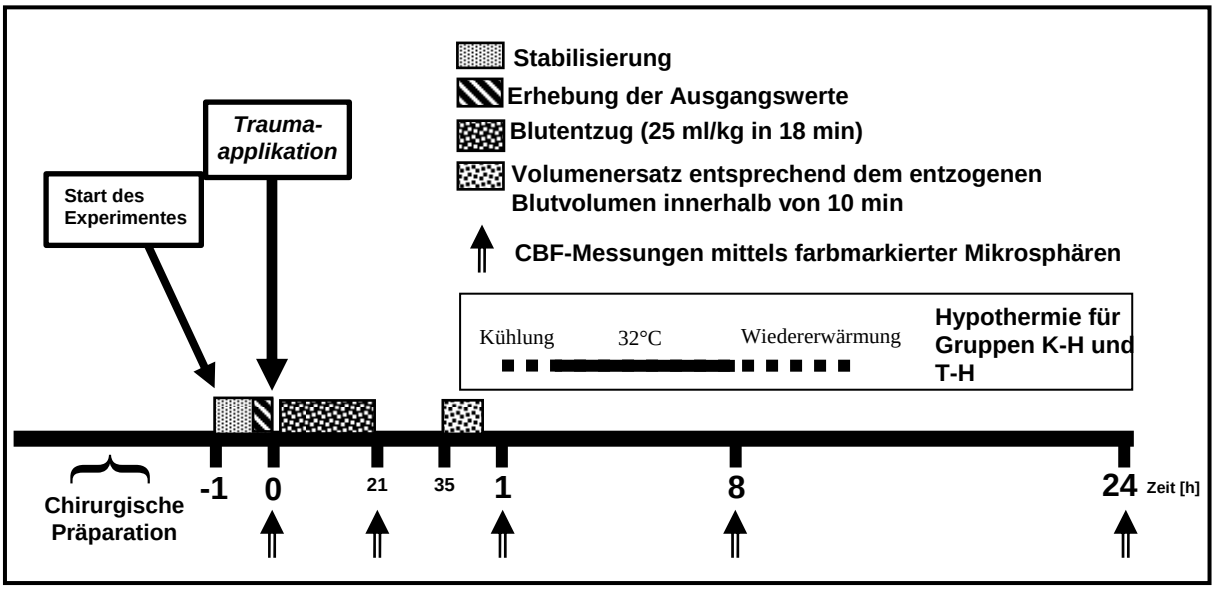

Abbildung 5 Versuchsablauf für FP-Trauma und Hypothermie

3.2.6.2. Evaluation der Traumaschwere

Die Auswertung der Traumaschwere ergab sich aus der unterschiedlichen Reaktion der Tiere hinsichtlich des Verlaufes des ICP. Ein Teil der Tiere der Gruppe T-NT entwickelte einen sekundären ICP-Anstieg (n=7), der ca. 5 h posttraumatisch begann. Die Detailanalyse ergab differierende Druckpulse, so dass alle normothermen Tiere (K-NT + T-NT; n=19) einer erneuten separaten Auswertung hinsichtlich des ICP-Verhaltens unterzogen wurden (74).

3.2.6.3. Auswirkungen der Hypothermie auf Plasmaspiegel und Biotransformation von Fentanyl sowie die intestinale Durchblutung

Die Tiere der hypothermen Kontrollgruppe (n=6) dienten in einem zusätzlichen Arm des experimentellen Settings zur Bestimmung der Fentanyl-Plasmaspiegel während milder Hypothermie (*in vivo*). In einem ergänzenden *in vitro* Experiment wurde die Temperaturabhängigkeit der CYP3A4-Aktivität mittels Monooxygenase Modell-Reaktion (Ethylmorphin N-Demethylierungsaktivität) untersucht (108).

3.2.6.3.1. In vivo Experiment (intestinale Durchblutung und Fentanyl-Plasmaspiegel)

Anästhesie und Instrumentierung sowie die Durchführung der Hypothermie erfolgten wie oben beschrieben.

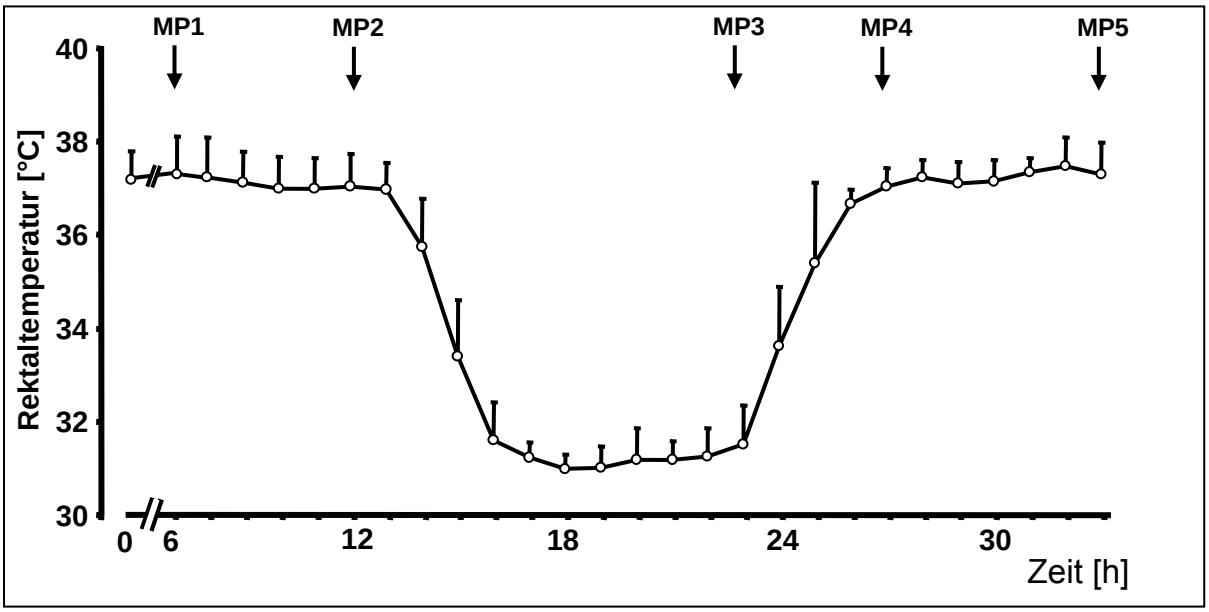

Abbildung 6 Temperaturverlauf der hypothermen Kontrolltiere (n=6) und Messpunkte (MP) für Bestimmungen der Fentanyl-Plasmaspiegel sowie CMS-Messungen für die Organdurchblutung (MW±SD), modif. nach (73)

Die Abnahme der Blutproben für die Kontrollwerte zur Bestimmung der Fentanyl-Plasmaspiegel erfolgte während der chirurgischen Präparation nach 6 und als Kontrollwert 2 während der Stabilisierungsphase 12 h nach Beginn des Experimentes. Die weiteren Blutproben wurden am Ende der Hypothermiephase, nach Wiedererwärmung und am Ende des Experimentes entnommen (Abb. 6). Gleichzeitig zu diesen Blutentnahmen erfolgte die CMS-Applikation zur Bestimmung der regionalen Durchblutung der intestinalen Organe.

Die Blutproben für die Fentanyl-Plasmaspiegel wurden nach Entnahme in kleine Glasröhrchen verbracht und bei 4°C zentrifugiert. Die Fentanyl-Plasmaspiegel wurden anschließend mittels RIA (Fa. Janssen Biotech, Olen, Belgien) gemessen (144).

Nach Tötung der Tiere am Ende des Experimentes wurden die Organe entnommen. Gewebeproben von Pankreas, Milz, Leber, Niere, Magen (Kardia, Fundus, Pylorus) und Dünndarm (Duodenum, Jejunum, Ileum) je 4 bis 6 g wurden mittels oben beschriebener CMS-Technik zur Bestimmung der regionalen Organdurchblutung aufgearbeitet.

3.2.6.3.2. In vitro Experiment (Temperaturabhängigkeit der CYP3A4-Aktivität)

Für das *in vitro* Experiment wurden die Lebern von 4 juvenilen Schweinen (Deutsches Hausschwein, Alter: 6 Wochen, KG: 12.7±1.5 kg) verwendet. Hierzu wurden die Tiere nach Narkose mittels Ketaminhydrochlorid (20 mg/kg) und Midazolam (1 mg/kg) mittels iv-Injektion von 10 ml Magnesiumchlorid getötet. Nach unmittelbarer Organentnahme wurden die Lebergewebsproben (ca. 1 g) in flüssigem Stickstoff eingefroren. Zur Präparation des 9000g Überstandes wurden die Proben in eisgekühltem 0,1 M Natriumphosphat-Puffer (pH = 7,4) homogenisiert und bei 9000g für 20 min bei 4°C zentrifugiert. Der Proteingehalt des Überstandes wurde mittels modifizierter Biuretmethode bestimmt.

Die Ethylmorphin N-Demethylierungsaktivität wurde in den 9000g-Überständen fotometrisch mit dem Reaktionsprodukt Formaldehyd gemessen (108). Für diese Reaktion wurden die Überstände 1:4 mit 0,1 M Natriumphosphat-Puffer (pH =7,4) verdünnt, mit dem Substrat Ethylmorphin versetzt und die Reaktion in einem Rüttelbad für 10 min nach einer 5 minütigen Temperatur-Äquilibrierung (26°, 32°, 38° 44°C) durchgeführt.

3.3. Statistische Auswertung

Die Daten aller Experimente sind, wenn nicht anders deklariert, als Mittelwerte ± SD dargestellt. Die Ausgangswerte wurden zwischen den Gruppen mit dem ungepaarten Student’s t-Test verglichen. Eine einfaktorielle ANOVA wurde verwendet, um die Unterschiede zwischen den Gruppen zu analysieren. Für Vergleiche innerhalb der Gruppen wurde eine einfaktorielle ANOVA für wiederholte Messungen verwendet.

Für *post hoc* Vergleiche kam der gepaarte t-Test mit Bonferroni-Holm-Korrektur für multiple Vergleiche zur Anwendung. Schließlich wurden die Daten zwischen den Gruppen mit dem ungepaarten t-Test mit Bonferroni-Holm-Korrektur für multiple Vergleiche analysiert.

Unterschiede in der Häufigkeit der mikro- und makropathologischen Merkmale wie auch die Muster des ICP-Verhaltens wurden mit dem exakten Fischer-Test analysiert. Der Vergleich der immunhistochemischen Daten erfolgte mittels Mann-Whitney U-Test. Die α-Adjustierung erfolgte nach Bonferroni und Holm.

Zur statistischen Auswertung wurde das Statistik-Programm SPSS für Windows V. 6.0 bis 10.0 (SPSS Inc. Chicago, USA) genutzt. Die Unterschiede wurden bei einem $p < 0,05$ als signifikant eingestuft.

4. Ergebnisse

Die physiologischen Parameter zu den einzelnen Experimenten sind in den im Anhang aufgeführten Originalarbeiten aufgelistet.

4.1. Schrittweise CPP-Reduktion und der Einfluss der Hypothermie auf zerebralen Sauerstoffmetabolismus und elektrokortikale Funktion

Mit dem beschriebenen experimentellen Ansatz in Experiment 1 konnte eine schrittweise CPP-Reduktion auf 69±1, 51±3 und 32±2% des Ausgangswertes (86±7 mmHg entspricht 100%) erzielt werden. Der MAP wurde während der schrittweisen ICP-Erhöhung konstant gehalten (Abb. 7) und somit eine kardiovaskuläre Beeinflussung des CPP vermieden.

Da die individuelle kardiovaskuläre Antwort auf die ICP-Erhöhung unterschiedlich ausfiel, waren diesbezüglich unterschiedlich entzogene bzw. retransfundierte Blutvolumina erforderlich (baseline: 0; control2: - 4,1±5,2; ICP25: - 8,8±8,3; ICP35: - 5,0±7,1; ICP45: 5,8±2,4 % des kalkulierten BV). Die CMS-Applikation beeinflusste die kardiovaskuläre und zerebrale Hämodynamik nicht.

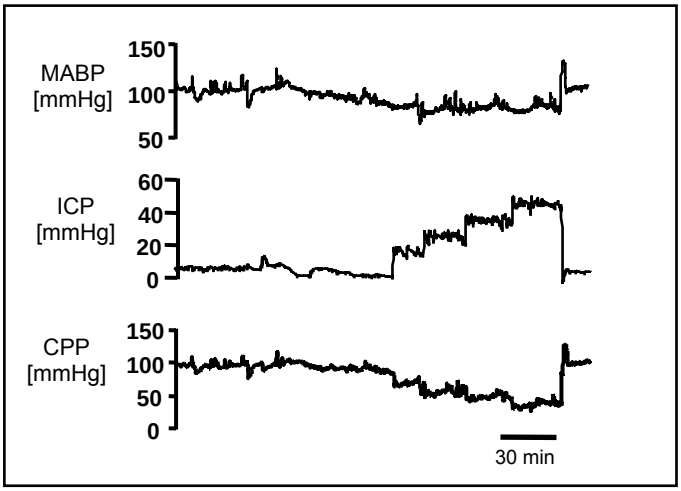

Abbildung 7 Beispiel eines typischen Verlaufes von MAP, ICP und CPP während schrittweiser CPP-Reduktion durch Inflation eines epidural platzierten Ballonkatheters bei Konstanthalten des MAP mittels ABP-Kontroller, modif. nach (19)

Bis zu einem ICP von 25±2 mmHg, der einer CPP-Reduktion auf 69±1% entsprach, blieben das zerebrale Sauerstoffangebot und die Sauerstoffumsatzrate auf dem Niveau der Ausgangswerte. Dies ging allerdings mit einer leichten Erhöhung des globalen CBF um 16% einher. Der globale CBF, das zerebrale Sauerstoffangebot und die $CMRO_2$ wiesen bei weiterer ICP-Steigerung eine CPP abhängige Reduktion auf. Bei stärkerer CPP-Reduktion auf 30% des Ausgangsniveaus reduzierte sich der globale CBF auf 24±18%, während sowohl das zerebrale Sauerstoffangebot als auch

die $CMRO_2$ eine überproportionale Reduktion auf 15±13% bzw. 16±15% vom Ausgangsniveau aufwiesen (Tab. 1).

Tabelle 1 Globale Hirndurchblutung, zerebrales Sauerstoffangebot und Sauerstoffumsatzrate bei normalem ICP (Baseline, Control2) und schrittweiser ICP-Steigerung, modif. nach (19)

	Baseline	Control2	ICP25	ICP35	ICP45
gCBF (ml/min/100g)	58±21	54±16	60±29	34±15*	12±14*
D_cO_2 (µmol/min/100g)	397±176	365±125	372±191	201±99*	68±73*
$CMRO_2$ (µmol/min/100g)	172±67	146±26	144±58	104±34*	43±56*

* p<0,0,5 vs. control2

Die einzelnen Hirnregionen wurden während der schrittweisen ICP-Steigerung unterschiedlich in ihrer Durchblutung beeinträchtigt. So zeigten die ipsilateral zum epiduralen Ballon gelegenen Hirnregionen vergleichbare Durchblutungswerte zur kontralateralen Seite. Ähnlich war dies für die meisten kortikalen Hirnregionen nachweisbar. Jedoch bestand in Hirnregionen in unmittelbarer Nähe zum epiduralen Ballon schon bei milder ICP-Steigerung auf 25 mmHg eine reduzierte regionale Durchblutung, die auch bei weiterer Hirndrucksteigerung existent war (Abb. 8).

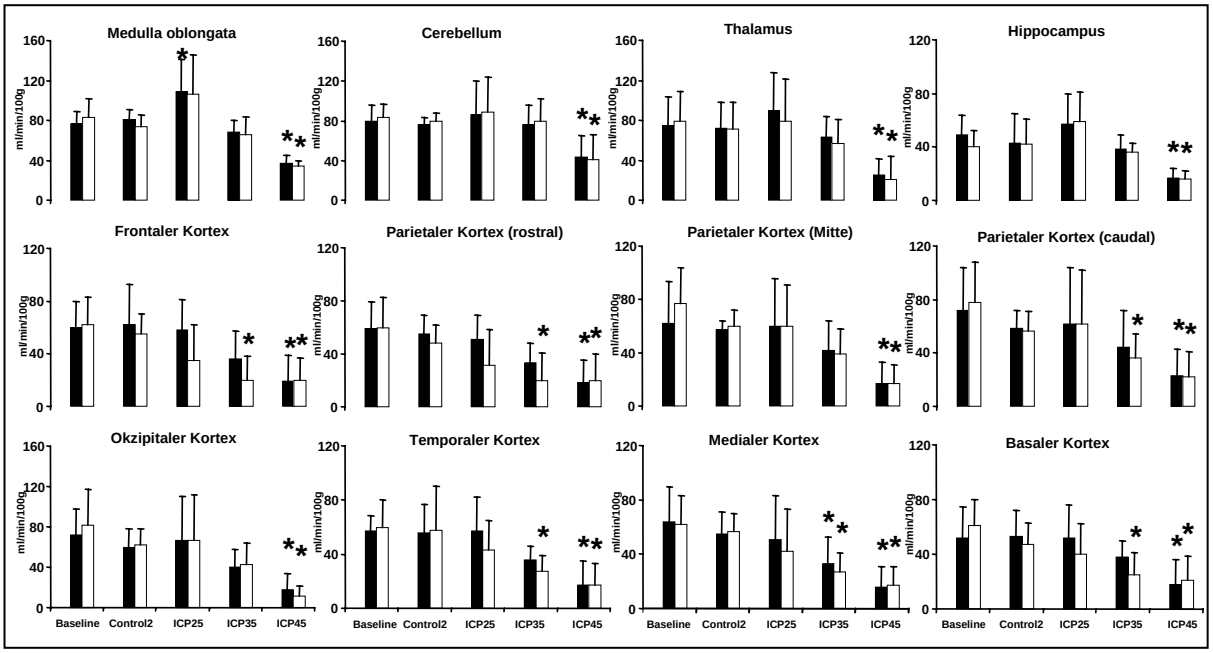

Abbildung 8 Regionale Hirndurchblutung bei schrittweiser ICP-Steigerung (MW ± SD), schwarze Balken markieren die kontralateral zum epiduralen Ballon gelegene Hemisphäre, helle Balken die ipsilateralen Hirnregionen. (*p<0,05, signifikante Unterschiede zwischen Baseline-Werten und Werten während der Stufen der schrittweisen CPP-Reduktion innerhalb der Gruppen), modif. nach (19)

Infratentorielle Hirnregionen, Thalamus und Hippocampus tendierten zwar während milder ICP-Steigerung auf 25 mmHg zu einer Durchblutungssteigerung, waren aber

zum Zeitpunkt der maximalen ICP-Steigerung auf 45 mmHg ebenso signifikant reduziert.

Bei sieben Tieren wurde unmittelbar nach Messung der Ausgangswerte (baseline) eine milde Hypothermie induziert. Die Zieltemperatur von 31,8±0,1°C wurde nach 95±24min erreicht. Unter den Ausgangsbedingungen während Normothermie und Hypothermie ohne CPP-Reduktion (Hypothermie) lag die Hirntemperatur um 0,2 bis 0,5°C ($p<0,05$) über der rektalen Temperatur. Während der Stufen der CPP-Reduktion nahm diese Temperaturdifferenz ab und invertierte während der niedrigsten CPP-Stufe (0,4–0,8°C; $p<0,05$).

Der MAP wurde in engen Grenzen konstant gehalten (MW: 81±11 mmHg), obwohl während der letzten beiden Stufen der CPP-Reduktion ein leichter aber signifikanter Abfall des MAP zu registrieren war ($p<0,05$).

Die infolge der milden Hypothermie gemessene Abnahme des CBF auf 74±20% vom Ausgangswert ging mit einer in der Relation stärker ausgeprägten Reduktion der $CMRO_2$ auf 50±15% einher ($p<0,05$; Abb. 9). Diese CBF-Veränderungen lassen sich durch höhere P_aCO_2-Werte erklären (temperaturkorrigierte Blutgasanalysen). Die regionale Hirndurchblutung war mit Ausnahme von Medulla oblongata, Thalamus und dem basalen Kortex in allen anderen Hirnregionen deutlich reduziert. Infolgedessen nahmen die $C_{(a\text{-}hv)}O_2$ um31±19% ($p<0,05$) ab und der $t_{Hirn}pO_2$ um 31±12% ($p<0,05$) zu.

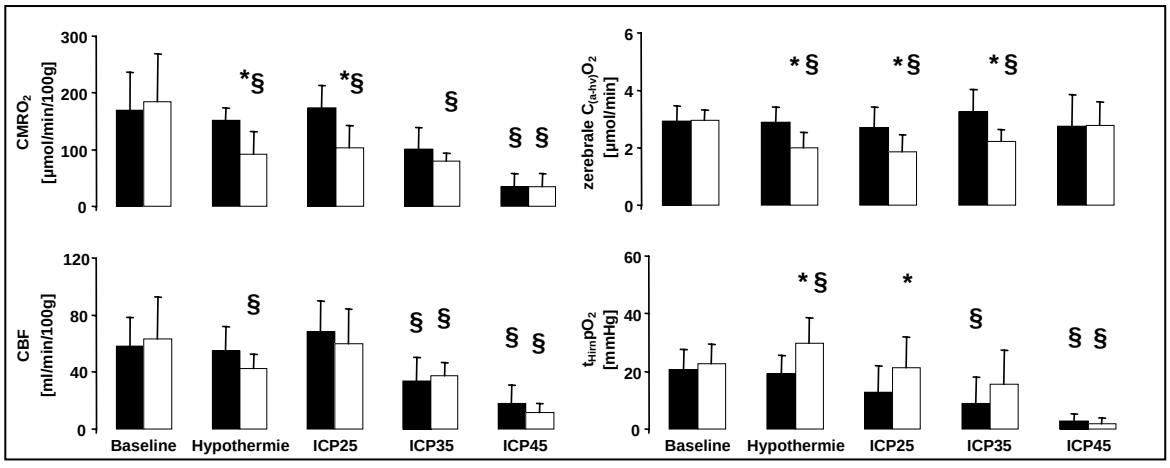

Abbildung 9 $CMRO_2$,CBF, zerebrale $C_{(a\text{-}hv)}O_2$ und $t_{Hirn}pO_2$ normothermer (■) und hypothermer (□)Tiere während schrittweiser CPP-Reduktion (MW±SD); Messpunkt „Hypothermie“ entspricht dem Messpunkt „control2“. Die nachfolgenden Stufen der CPP Reduktion wurden bei diesen Tieren unter hypothermen Bedingungen gemessen. ($p>0,05$ signifikante Unterschiede zwischen Baseline und den jeweiligen Messpunkten (§) bzw. zwischen den Gruppen (*), $p<0,05$), modif. nach (17)

Die graduelle ICP-Erhöhung mit konsekutiver CPP-Reduktion auf 70% des Ausgangswertes verursachte ungeachtet der Recovery des CBF auf das Ausgangsniveau in der HT-Gruppe zunächst keine weitere Reduktion der $CMRO_2$. Allerdings war auf dieser CPP-Stufe der für die MAP-Konstanz erforderliche Blutentzug (NT: - 9.8±6,7% BV; HT: - 4,6±6,7%BV) so groß, dass er mit einer signifikanten Abnahme des HI einherging (Baseline NT: 231±53 ml/kg/min, HT: 213±96 ml/kg/min; ICP25 NT:121±57 ml/kg/min, HT: 118±61 ml/kg/min). Des Weiteren war in der NT-Gruppe eine Umverteilung der regionalen Hirndurchblutung zu Medulla oblongata, Cerebellum, Thalamus und Hippocampus zu verzeichnen (Abb.10).

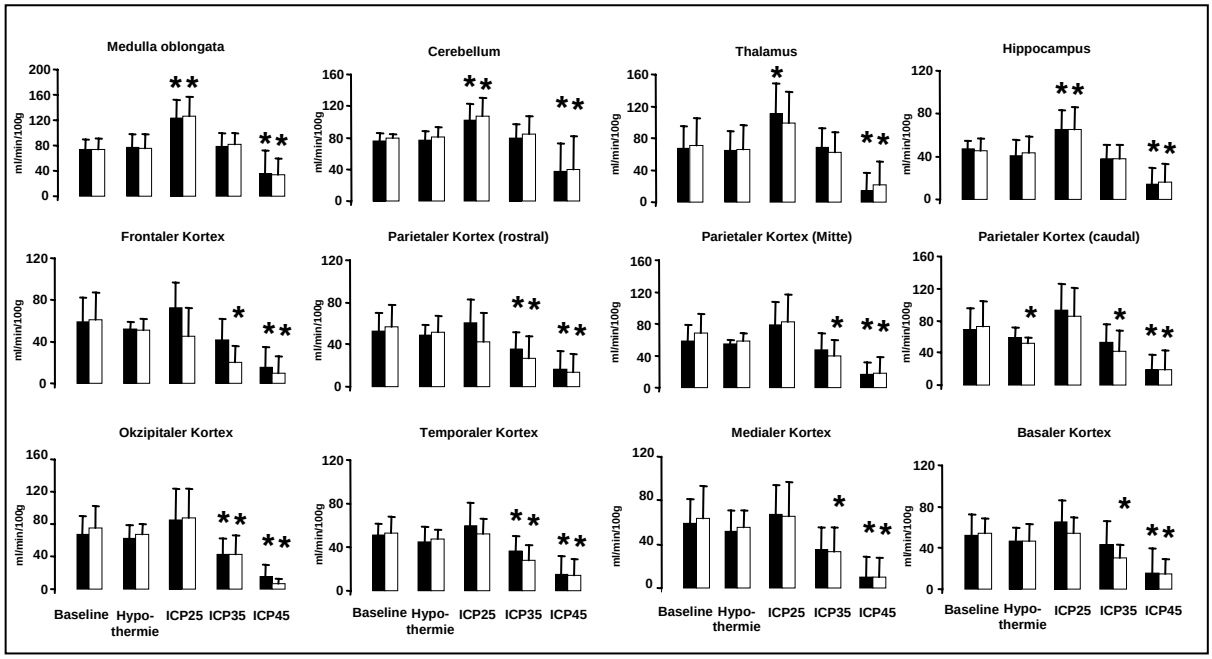

Abbildung 10 Regionale Hirndurchblutung in interessierenden Hirnregionen während schrittweiser CPP-Reduktion bei normothermen (■) und hypothermen (□)Tieren (MW ± SD), Der Messpunkt „Hypothermie“ entspricht dem Messpunkt „control2“, da in der Hypothermie-Gruppe die Zieltemperatur (31,8±0,1°C) bereits erreicht ist. Die nachfolgenden Stufen der CPP Reduktion wurden bei diesen Tieren unter hypothermen Bedingungen gemessen. (*p<0,05, signifikante Unterschiede zwischen Baseline-Werten und Werten während der Stufen der schrittweisen CPP-Reduktion innerhalb der Gruppen), modif. nach (17)

Die Inflation des epiduralen Ballons führte ipsilateral zu einer reproduzierbaren Reduktion des rCBF, die in unmittelbarer Umgebung des Ballons im frontalen Kortex mit 38% in der NT-Gruppe und 30% in der HT-Gruppe am ausgeprägtesten war. Der $t_{Hirn}pO_2$ erreichte das Ausgangsniveau, während die $C_{(a\text{-}hv)}O_2$ im Bereich der hypothermen Ausgangswerte blieb (MP: Hypothermie). Die Parameter des zerebralen Sauerstoffmetabolismus blieben in der NT-Gruppe auf der ersten Stufe der CPP-Reduktion (ICP25) unbeeinträchtigt. Die weitere CPP-Reduktion auf ca. 50% des Ausgangsniveaus verursachte eine weitere Reduktion des CBF auf

63±34% in der NT-Gruppe bzw. 66±25% in der HT-Gruppe ($p<0,05$). Diese Verminderung des CBF war im Wesentlichen durch die signifikante Reduktion des regionalen CBF in den ipsilateral zum Ballon gelegenen kortikalen Regionen, insbesondere des frontalen Kortex, verursacht.

Die weitere CPP-Reduktion auf 30% des Ausgangsniveaus führte zu einer erheblichen Verminderung des CBF in beiden Tiergruppen (NT: 35±26%; HT: 20±14%). Auch der Abfall der $CMRO_2$ (NT: 19±21%; HT: 15±15%) und $t_{Hirn}pO_2$ (NT:10±18%; HT: 9±10%) war auf dieser Stufe der CPP-Reduktion in beiden Gruppen am ausgeprägtesten. Durch die starke Inflation des epiduralen Ballons (ICP = 45mmHg) zeigte sich in allen supratentoriell gelegenen Hirnarealen eine gleichermaßen ausgeprägte Reduktion des rCBF.

Die Analyse der elektrokortikalen Funktion zeigte als Ausgangsbefund das typische delta-dominierte Frequenzmuster für Isofluran-Narkosen (siehe Anhang (70), Abb.4). Nach Erreichen der Zieltemperatur zeigte die ECoG-Gesamtaktivität eine Reduktion auf 44±117% ($p<0,05$). Innerhalb des Frequenzspektrums war eine Frequenzverschiebung zu höheren Frequenzen (θ- und α-Band) zu verzeichnen. Dementsprechend war die δ-Aktiviät reduziert (48±22% vom Ausgangswert, $p<0,05$). Diese veränderte Frequenzverteilung verdeutlichte sich auch in der Zunahme der δ-Ratio (225±25% vom Ausgangswert, $p<0,05$%). Die hypothermieinduzierten ECoG-Veränderungen gingen mit einer Reduktion des globalen CBF einher (72±13% vom Ausgangswert, $p<0,05$). Regional reagierte die Hirndurchblutung unterschiedlich auf die Temperatursenkung. Während der kortikale CBF auf 67±10% vom Ausgangswert ($p<0,05$) abfiel, nahm die regionale Durchblutung in der Medulla oblongata leicht auf 114±15% zu. Thalamus und Mesenzephalon zeigten dagegen keine Veränderungen des rCBF gegenüber den normothermen Ausgangswerten.

Die milde CPP-Reduktion auf 70% (ICP25) führte in der NT-Gruppe zur Abnahme der Gesamtaktivität (63±21% vom Ausgangswert) und einer Frequenzverlangsamung im ECoG. Die regionale Hirndurchblutung war in beiden Tiergruppen gesteigert, wobei sie in Medulla oblongata (NT: 166±24%; HT: 145±26%, $p < 0.05$) und Thalamus (NT: 151±45%; HT: 153 ± 53%, $p < 0.05$) am ausgeprägtesten war. In der NT-Gruppe konnte die Durchblutungssteigerung auch im Mesenzephalon nachgewiesen werden (158±26%, $p < 0.05$).

Die Reduktion des CPP auf 50 % (ICP35) verursachte in der NT-Gruppe einen weiteren Abfall des CBF auf 68±8% ($p<0,05$), die mit einer deutlichen Minderung der

δ-Amplitude bei gleichzeitiger Zunahme der δ-Bandaktivität auf 81±27% assoziiert war. Im Gegensatz dazu war in der HT-Gruppe bei einem reduzierten CBF auf 74 ± 5% keine Änderung des ECoG-Musters im Vergleich zum MP Hypothermie nachweisbar. Der kortikale CBF war sowohl in der NT- als auch in der HT-Gruppe signifikant vermindert (NT: 58 ± 16%; HT: 58±10%, $p < 0.05$). In der Medulla oblongata blieb der regionale CBF in beiden Gruppen erhöht, obwohl er zwischen den Gruppen signifikant (NT: 105±18%; HT: 136±14%, $p<0,05$) differierte.

Die Reduktion des CPP auf 30% vom Ausgangsniveau verursachte eine zwischen den Gruppen unterschiedliche Reduktion des globalen CBF (NT: 41±16%; HT: 28±7%, $p < 0.05$). Auch der kortikale CBF war in beiden Gruppen deutlich vermindert, wobei dies in der HT-Gruppe stärker ausgeprägt war (NT: 31±13%, HT:18±6%, $p<0,05$). Dagegen war die Durchblutung der Medulla oblongata in beiden Gruppen nur um etwa 30% reduziert.

Im ECoG der HT-Gruppe waren eine weitere Frequenzverlangsamung und eine Amplitudenreduktion zu verzeichnen. Das ECoG der NT-Gruppe war bei der Mehrzahl der Tiere vollständig supprimiert oder es traten, wie in 2 Fällen beobachtet, sporadisch Burst-Suppression-Muster auf.

4.2. FP-Trauma und Auswirkungen der milden Hypothermie auf das Ausmaß der histologischen Hirnschädigung

Die physiologischen Parameter des Experimentes sind in Tabelle 1 der Originalarbeit (30) in der Anlage aufgeführt. Der posttraumatische temporäre Blutentzug verursachte eine signifikante Reduktion des HI 44±14% ($p<0,05$), mit entsprechender Reduktion von MAP und CPP. Acht Stunden nach Applikation des Traumas stieg der ICP bei sieben normothermen traumatisierten Tieren auf 29±24 mmHg an, so dass diese Tiere im Weiteren als Subgruppe: T-NT_{ICP} bezeichnet werden. Die sechs anderen normothermen Tiere (jetzt Subgruppe: T-NT_N) und alle hypothermen Tiere (Gruppe: T-HT) wiesen keinen sekundären ICP-Anstieg auf. In der T-HT-Gruppe wurde die angestrebte Hirntemperatur von 32,2±0,5 °C innerhalb von 185±30 min mittels Oberflächenkühlung erreicht. Während der Hypothermiephase war der HI in beiden Hypothermiegruppen (K-HT, T-HT) vergleichbar reduziert (K-HT: 61±13%; T-HT: 54±7%, n.s.). Zur aktiven Wiedererwärmung wurden 259±30 min benötigt.

Makropathologisch morphologisch war das Hirntrauma im linken temporoparietalen Kortex durch Kontusionsherde, SAB, intrazerebrale Blutungen, Hirnödem und

Mittellinienverschiebung sowie sekundäre Infarzierungen gekennzeichnet. Sämtliche traumatisierten Tiere zeigten im Vergleich zu den Kontrolltieren subdural gelegene Hämatome im Bereich des Kontusionsherdes. SAB der kontralateralen Hemisphäre fanden sich in der T-NT_{ICP}-Subgruppe. Des Weiteren waren subarachnoidale Blutungen im Hirnstamm aller traumatisierten normothermen Tiere nachweisbar, jedoch nur bei 3 von 7 Tieren der T-HT-Gruppe.

Supratentorielle Parenchymblutungen fanden sich bei allen traumatisierten Tieren, überwiegend in der ipsilateralen weißen Substanz unterhalb des Kontusionsherdes. Diese Einblutungen waren regelhaft von einem perifokalen Ödem umgeben. Die Hirngewichte der normothermen Versuchstiere mit Hirndruckanstieg waren im Vergleich zu allen anderen Versuchsgruppen signifikant größer (T-NT_{ICP}: 72,6±2,2g; T-NT_N: 60,0±1,5g; T-HT: 61,8±1,8g; K-NT: 59,8±2,2g; K-HT: 66,3±2,1g; $p<0,05$). Makroskopisch zeigten drei Tiere der T-NT_{ICP}-Subgruppe schwere, vier dagegen moderate Zeichen des intrakraniellen Druckanstieges, wie Verschmälerung der Sulci, Abflachung der Gyri sowie Herniation im Bereich des Tentoriums und der Tonsillen. Bei einem dieser Tiere fand sich eine Hirnstamminfarzierung. Mikroskopisch waren Zeichen der globalen Hypoxie mit geschrumpften triangulären Nervenzellkörpern und -kernen, eosinophilem Zytoplasma und perineuronalem Ödem sowie gestaute Blutgefäße nachweisbar.

In der histologischen Untersuchung fanden sich bei allen traumatisierten Tieren kleine SAB nahe der Kraniotomie für den FP-Adapter und intraparenchymale Blutungen in der temporoparietalen subkortikalen weißen Substanz um die Kontusionen herum. Des Weiteren zeigten sich bei diesen Tieren Foci mit trianguläre hämorrhagischen Nekrosen mit nahezu komplettem Nervenzellverlust im Zentrum der Schädigung.

In den angrenzenden Arealen fanden sich geschrumpfte Neurone mit eosinophiler Homogenisation des Zytoplasmas und trianguläre dunkle Zellkerne. Daran schloss sich eine Zone mit geschrumpften Neuronen ohne Homogenisation an. Etwa 1,5 cm vom Zentrum der Schädigung entfernt fanden sich in der T-NT_N-Subgruppe morphologisch intakte Neurone, während bei den T-NT_{ICP} -Tieren geschrumpfte Neurone mit triangulären Zellkörpern und -kernen, eosinophilem Zytoplasma und perineuralem Ödem über den gesamten ipsi- und kontralateralen temporoparietalen Kortex verteilt nachweisbar waren (Abb. 11).

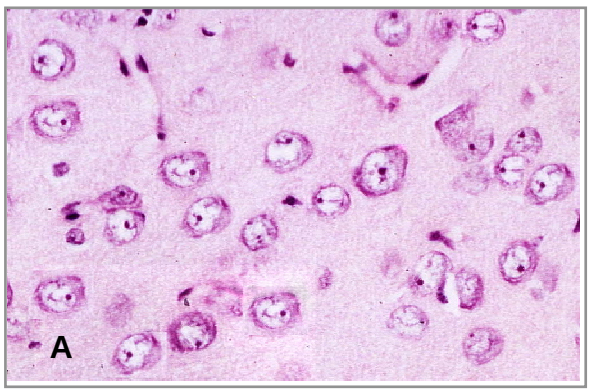

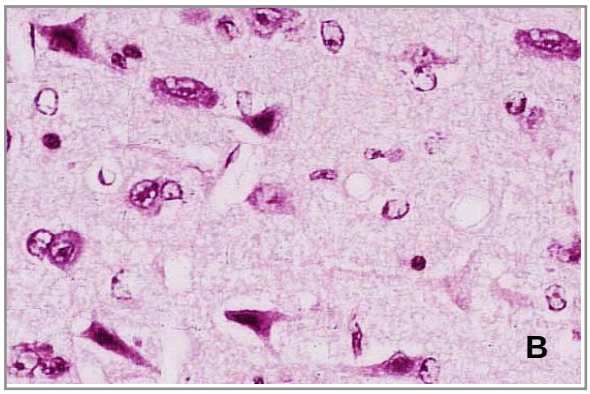

Abbildung 11 A: Runde, voluminöse Gestalt der Nervenzellkörper mit hypochromem Zellkern und deutlich erkennbarem Nucleolus der Kontrolltiere (400x-Vergrößerung; HE). B: Tiere mit Hirndruckanstieg zeigten im gesamten Kortex ein Nebeneinander von geschrumpften Nervenzellen mit eosinophilem Zytoplasma und pyknotischem Zellkern und Zellen mit "normaler" Morphologie (400x-Vergrößerung; HE).

In der T-NT_{ICP}-Subgruppe war die neuronale Schädigung in allen untersuchten Gesichtsfeldern des Hippocampus beider Hemisphären nachweisbar, während nekrotische Neurone nur bei 2 Tieren der T-NT_N-Subgruppe gefunden wurden. Diese Befunde beschränkten sich auf die CA2-Region des ipsilateralen Hippocampus. Auch bei den T-HT-Tieren fanden sich ähnliche Befunde nekrotischer Neurone nur umschrieben und im ipsilateralen Hippocampus ohne regionale Zuordnung. Neuronale Schädigungen des Hirnstamms ließen sich bei 3 Tieren der T-NT_{ICP}-Subgruppe nachweisen. In der T-NT_N-Subgruppe waren keine Hirnstammschädigungen vorhanden. Zusammenfassend ließen sich bei den T-NT_N-Tieren vor allem fokale Schäden, bei den T-NT_{ICP}-Tieren dagegen Zeichen der fokalen und diffusen Hirnschädigung nachweisen.

Die MAP2-Immunhistochemie der Kontrollgruppen (K-NT; K-HT) zeigte eine homogene Markierung in den Dendriten und Nervenzellsomata des Kortex und Hippocampus. Lange, gerade Dendriten zogen von den oberen Kortexschichten in die tieferen, während an der Mark-Rinden-Grenze stärker gefärbte Neurone mit kurzen Dendriten auffielen [siehe Originalarbeit (30), Abb. 2b, in der Anlage].

In der T-NT_N-Subgruppe und den T-HT-Tieren waren regelmäßig auf den Kontusionsherd begrenzte, nahezu vollständige MAP2-Markierungsverluste der Dendriten und der Nervenzellsomata nachweisbar. Der Kontusionsherd grenzte sich scharf von dem umgebenden, nahezu unbeeinträchtigten Gewebe ab. Im geschädigten Areal fanden sich vereinzelt fragmentierte, zum Teil geschwollene oder minder markierte Dendriten. Im Hippocampus zeigte sich eine erhaltene, aber zum Teil verwaschene Darstellung der Dendritenstruktur.

In der Subgruppe T-NT_{ICP} fand sich in drei Fällen ein nahezu kompletter Markierungsverlust auf der Traumaseite bei unauffälliger kontralateraler Hemisphäre. Die übrigen Tiere zeigten einen beidseitigen, nahezu vollständigen MAP2-Markierungsverlust in Kortex und Hippocampus. Vor allem die Neurone in den tieferen Kortexschichten zeigten eine Restmarkierung mit einer MAP2-Akkumulation in den Somata. Vereinzelt waren auch stark verkürzte Dendritenmarkierungen sowie fragmentierte oder geschwollene Dendriten nachweisbar. Histologisch zeigten die Neurone einen kondensierten Kern bei normaler Morphologie. Im Hippocampus erstreckte sich der MAP2-Verlust gleichmäßig auf alle Subregionen.

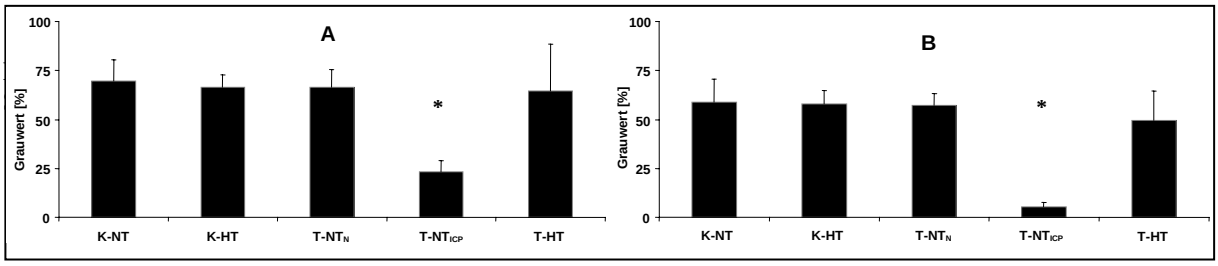

Abbildung 12 Ergebnisse der Grauwertbestimmung des Kortex (A) und Hippocampus (B) beider Hemisphären der jeweiligen Versuchsgruppen ± SD. Es ergab sich ein signifikanter Unterschied zwischen der T-NT_{ICP}-Subgruppe und den übrigen Gruppen (* $p<0,05$), modif. nach (30)

Die quantitative Auswertung mittels Grauwertbestimmung ergab signifikante Unterschiede zwischen der T-NT_{ICP}-Subgruppe und den übrigen Versuchsgruppen (Abb.12).

Die ßAPP-Markierungen waren vielgestaltig und reichten von nur gering verbreiterten Axonen, über geschwollene und torquierte Axone bis hin zu ‘axonal bulbs‘. ßAPP-Aktivität war in beiden Kontrollgruppen (K-NT, K-HT) nicht nachweisbar.

In der T-NT_N-Subgruppe war die ßAPP-Markierung eher moderat und, wenn vorhanden, in der weißen Substanz unmittelbar unter dem Kontusionsherd bei 3 von 7 Tieren (Grad 1–3) nachweisbar. Die Nervenzellen wiesen insbesondere im Traumagebiet Markierungen ihrer Somata auf. Bei vier Tieren konnten keine Axonmarkierungen (Grad 0) nachgewiesen werden. Im ipsilateralen Dienzephalon zeigten drei Tieren leichte Axonmarkierungen (Grad 1) und ein Tier kräftige und weiträumige Markierungen (Grad 3). Im rechten Dienzephalon wurden in einem Fall leichte Axonfärbungen (Grad 1) nachgewiesen. Bei zwei Tieren fand sich im Hirnstamm eine Grad 1-Markierung.

In der T-NT_{ICP}-Subgruppe zeigten sich deutliche ßAPP-markierte Axone und axonale Auftreibungen in allen untersuchten Hirnregionen (überwiegend Grad 3). Nur in den

frontalen Hirnregionen, die am weitesten vom Trauma entfernt lagen, fand sich keine ßAPP-Aktivität.

In der T-HT-Gruppe zeigten dagegen nur fünf Tiere auf der ipsilateralen Hemisphäre Axonmarkierungen (Grad 1). Kontralateral war in der SHT-HT-Gruppe keine ßAPP-Markierung nachweisbar. Im Dienzephalon ließen sich in vier von acht Fällen in der traumatisierten Hemisphäre angefärbte Axone darstellen. Dabei zeigten drei Tiere vereinzelt schwache Axon- und Nervenzellmarkierungen (Grad 1) und ein Tier vereinzelte kräftige Markierungen von Axonen und Nervenzellen (Grad 2). Im Hirnstamm wurden keine Veränderungen festgestellt (Tab.2).

Tabelle 2: Regionale Verteilung der Axonschäden (Maximum 3,0) nach FP-Trauma bei normothermen ($T\text{-}NT_N$, $T\text{-}NT_{ICP}$) und hypothermen (T-HT) Tieren, zum Vergleich sind die Kontrollgruppen K-NT und K-HT aufgeführt, modif. nach (30)

	K-NT	**K-HT**	**$T\text{-}NT_N$**	**$T\text{-}NT_{ICP}$**	**T-HT**
Frontalhirn (LH)	0	0	0	0	0
Frontalhirn (RH)	0	0	0	0	0
temporoparietales Gehirn (LH)	0	0	1,0	2,5 *	1,1
temporoparietales Gehirn (RH)	0	0	0	0,3	0
Dienzephalon (LH)	0	0	0,9	1,3	0,8
Dienzephalon (RH)	0	0	0,1	1,0	0
Hirnstamm	0	0	0,4	1,8 *	0

LH – linke Hemisphäre, RH – rechte Hemisphäre; * $p<0,05$ SHAM-NT vs. andere Gruppen

Zu den positiv markierten Arealen im Zwischenhirn gehörten bei allen Traumagruppen das Corpus geniculatum, das Pulvinar, sowie der Fasciculus tegmenti und der Lemniscus medialis. Im Hirnstamm traten die Axonmarkierungen insbesondere in beiden Pedunculi cerebelli superiores sowie im Fasciculus longitudinalis medialis auf. Die Verteilung der Axonmarkierungen ähnelte dem morphologischen Korrelat des diffusen axonalen Schadens (DAI) beim Menschen (2, 183).

In der Zusammenfassung zeigten die Tiere der $T\text{-}NT_{ICP}$-Subgruppe die qualitativ und quantitativ am stärksten ausgeprägten Axonmarkierungen. Es ergaben sich signifikante Unterschiede im Vergleich zu allen anderen Gruppen. $T\text{-}NT_N$- und T-HT-Tiere zeigten in der weißen Substanz sowie im unilateralen Zwischenhirn ähnlich geringe Werte. Unterschiede zwischen diesen beiden Gruppen fanden sich jedoch im

kontralateralen Dienzephalon und im Hirnstamm, wo bei den hypothermen Tieren keine Axonmarkierungen nachweisbar waren.

TUNEL-positive Zellen waren in Kortex, weißer Substanz, Hippocampus, Dienzephalon und Plexusgewebe nachweisbar (Tab. 3). Wir fanden nekrotische Zellen, die geschwollen erschienen und eine diffuse homogene TUNEL-Markierung besaßen (Typ-I-Zellen), und apoptotische Zellen mit Kernschrumpfungen, Chromatinmarginationen und der Ausbildung von „apoptotic bodies“ (Typ-II–Zellen). Bei den normothermen und hypothermen Kontrolltieren waren keine TUNEL-positiven Zellen nachweisbar.

Tabelle 3: Regionale Auswertung der TUNEL-Methode (Maximum 6,0) nach FP-Trauma bei normothermen (T-NT_N, T-NT_{ICP}) und hypothermen (T-HT) Tieren, zum Vergleich sind die Kontrollgruppen K-NT und K-HT aufgeführt, modif. nach (30)

	K-NT	K-HT	T-NT_N	T-NT_{ICP}	T-HT
temporoparietales Gehirn (Kortex-LH)	0	0	0	3,5	0
temporoparietales Gehirn (Kortex-RH)	0	0	0	3,0	0
temporoparietales Gehirn (weiße Substanz-LH)	0	0	1,4	5,2 *	0,7
temporoparietales Gehirn (weiße Substanz-RH)	0	0	0,3	5,2 *	0,7
Dienzephalon (LH)	0	0	0,3	4,4 *	0,7
Dienzephalon (RH)	0	0	0,3	5,3 *	0,7
Hippocampus (LH)	0	0	0,3	4,0	0,5
Hippocampus (RH)	0	0	0	4,0	0,5

LH – linke Hemisphäre, RH – rechte Hemisphäre; * $p<0,05$ SHT-NT vs. SHT-NT-ICP

Auch im Kortex der Tiere der T-NT_N-Subgruppe waren keine TUNEL-positiven Zellen nachweisbar. Jedoch fanden sich TUNEL-positive Zellen bei vier von sieben untersuchten Tieren in der weißen Substanz, hauptsächlich unterhalb des Kontusionsherdes, in einem Fall auch in der kontralateralen Hemisphäre sowie im Zwischenhirn und im Hippocampus. Insgesamt war die Anzahl der markierten Zellen gering. Der Anteil der Typ-II-Zellen an den TUNEL-positiven Zellen war mit ca. 40% jedoch recht hoch. In der Mehrzahl handelte es sich um Gliazellen.

TUNEL-positive Zellen mit variabler Morphologie wurden dagegen bei allen untersuchten Gehirnen der T-NT_{ICP}-Subgruppe gefunden. Hier war der Anteil der Typ-II-Zellen (apoptotische Zellen) mit 15% relativ gering. Die Mehrzahl TUNEL-positiver Zellen fand sich in der weißen Substanz beider Hemisphären. Die meisten TUNEL-positiven Zellen waren Gliazellen. Aufgrund der Morphologie und der GFAP-

Negativität bei Doppelfärbung (kombinierte GFAP-TUNEL-Reaktivität hier nicht dargestellt) ist anzunehmen, dass es sich vorrangig um Oligodendrozyten handelte.
Zahlreiche TUNEL-positive Zellen waren auch im Zwischenhirn und Hippocampus bei nahezu allen Tieren der T-NT_{ICP}-Subgruppe nachweisbar. Diese Zellen erschienen häufig als Typ-I-Zellen. Bemerkenswerterweise fiel im Gegensatz zu den anderen Traumagruppen eine relativ selektive Markierung kleiner Körnerzellen im Gyrus dentatus auf, während im Hippocampus meist relativ uniforme Markierungen aller Schichten und der hippocampalen Subregionen nachweisbar waren.
In der T-HT-Gruppe waren die Ergebnisse mit denen der T-NT_N-Subgruppe vergleichbar. Im Kortex ließen sich keine TUNEL-positiven Zellen nachweisen. Nur eines der zehn untersuchten Versuchstiere wies überhaupt TUNEL-positive Zellen auf (weiße Substanz, Dienzephalon, Hippocampus). Der Anteil der Typ-II-Zellen betrug ca. 20%.
Das Verhältnis von Typ-II/I-Zellen war in den Traumagruppen unterschiedlich (T-NT_N: 40%, T-NT_{ICP}: 15% und T-HT: 20%). In der T-NT_{ICP}-Subgruppe war die TUNEL-Reaktion sowohl räumlich als auch quantitativ am ausgeprägtesten. So ergaben sich signifikante Unterschiede zu den anderen Versuchsgruppen in den untersuchten Hirnarealen von weißer Substanz, Dienzephalon und Hippocampus. Demgegenüber zeigten die normothermen und hypothermen Versuchstiere ohne Hirndruckanstieg (T-NT_N, T-HT) einen geringen Anteil TUNEL-positiver Zellen. Hauptschädigungsorte waren auch in diesen Gruppen weiße Substanz und Dienzephalon.

4.3. Flüssigkeitsvermitteltes Perkussionstrauma mit unterschiedlicher Traumaschwere

Die physiologischen Daten sind im Anhang in der Originalarbeit in Tabelle 1 aufgeführt (74) (Erläuterung der Tiergruppenbezeichnung für Tab.1 der Originalarbeit: Sham = K-NT; mTBI = T-NT_N; sTBI = T-NT_{ICP}). Sowohl die Ausgangswerte der systemischen und zerebralen Hämodynamik als auch die des zerebralen Sauerstoffmetabolismus waren in allen Gruppen vergleichbar. Die Daten in der Kontrollgruppe (K-NT) blieben während des gesamten Experimentes unverändert. Während sich die systemische Hämodynamik (MAP, HF, HI) zwischen den Traumagruppen nicht unterschied, führte die höhere Intensität des FP-Traumas in der T-NT_{ICP} -Subgruppe zu einem biphasischen ICP-Anstieg.

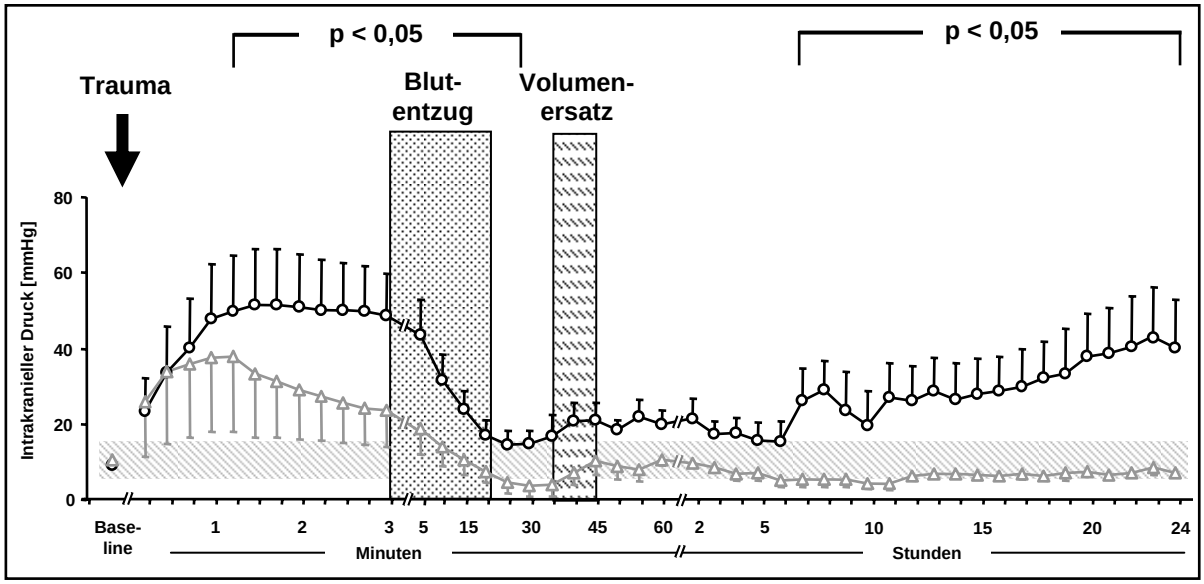

Abbildung 13 24-h-Aufzeichnung des ICP nach moderatem (Δ) und schwerem (○) FP-Trauma nachfolgendem Blutentzug und Volumenersatz innerhalb der ersten Stunde nach dem Trauma. Die Darstellung der Aufzeichnungen für die ersten 3 min alle 15 s, innerhalb der ersten Stunde alle 5 min, bis 24 Stunden stündlich. (MW ± SD). Grau unterlegt ist Bereich des ICP-Ausgangswertes ± 2 SD, modif. nach (74).

Der erste ICP-Gipfel trat nach 90 s, d.h. unmittelbar nach der Trauma-Applikation, auf und war etwa 1,5-fach höher als in der T-NTN-Subgruppe. Der ICP persistierte in dieser Gruppe und fiel erst während des Blutentzuges auf das Ausgangsniveau ab. Ein zweiter, sekundärer ICP-Anstieg entwickelte sich 5±1,5h posttraumatisch (Abb. 13).

Tabelle 4 Spezifische ICP-Muster während der 24-h-Monitoringphase in den Untersuchungsgruppen, modif. nach (74)

ICP-Muster	K-NT	$T\text{-}NT_N$	$T\text{-}NT_{ICP}$
niedriger, stabiler ICP	6/6*	$6/6^{\$}$	0/7
stabiler, erhöhter ICP	0/6	0/6	$7/7^{*\$}$
B-Wellen des ICP	0/6	0/6	$6/7^{*\$}$
Plateau-Wellen des ICP	0/6	0/6	4/7
Hohe, spitze ICP-Wellen bei akutem Blutdruckanstieg	0/6	0/6	3/7
Spitze ICP-Wellen durch Absaugmanöver	2/6	4/6	7/7*

*p<0,05 Unterschiede zwischen K-NT und $T\text{-}NT_{ICP}$, $^{\$}$p<0,05 Unterschiede zwischen $T\text{-}NT_N$ und $T\text{-}NT_{ICP}$, die Datenpaare zeigen die Zahl der Tiere mit spezifischen ICP-Mustern je experimenteller Gruppe.

Die Reduktion des CPP war in der $T\text{-}NT_{ICP}$ -Subgruppe im Vergleich zur $T\text{-}NT_N$-Subgruppe nach Trauma und Blutentzug stärker ausgeprägt ($T\text{-}NT_N$: 65±26 mmHg;

T-NT_{ICP}: 50±24 mmHg) und normalisierte sich vorübergehend nach Volumensubstitution.

Während im weiteren Verlauf des Experimentes in der T-NT_{ICP}-Subgruppe eine progressive Verschlechterung des CPP eintrat, blieb der CPP in der T-NT_N-Subgruppe auf annähernd normalem Niveau erhalten. Die Hirntemperatur fiel bei den T-NT_{ICP}-Tieren im Verlauf des Experimentes leicht ab.

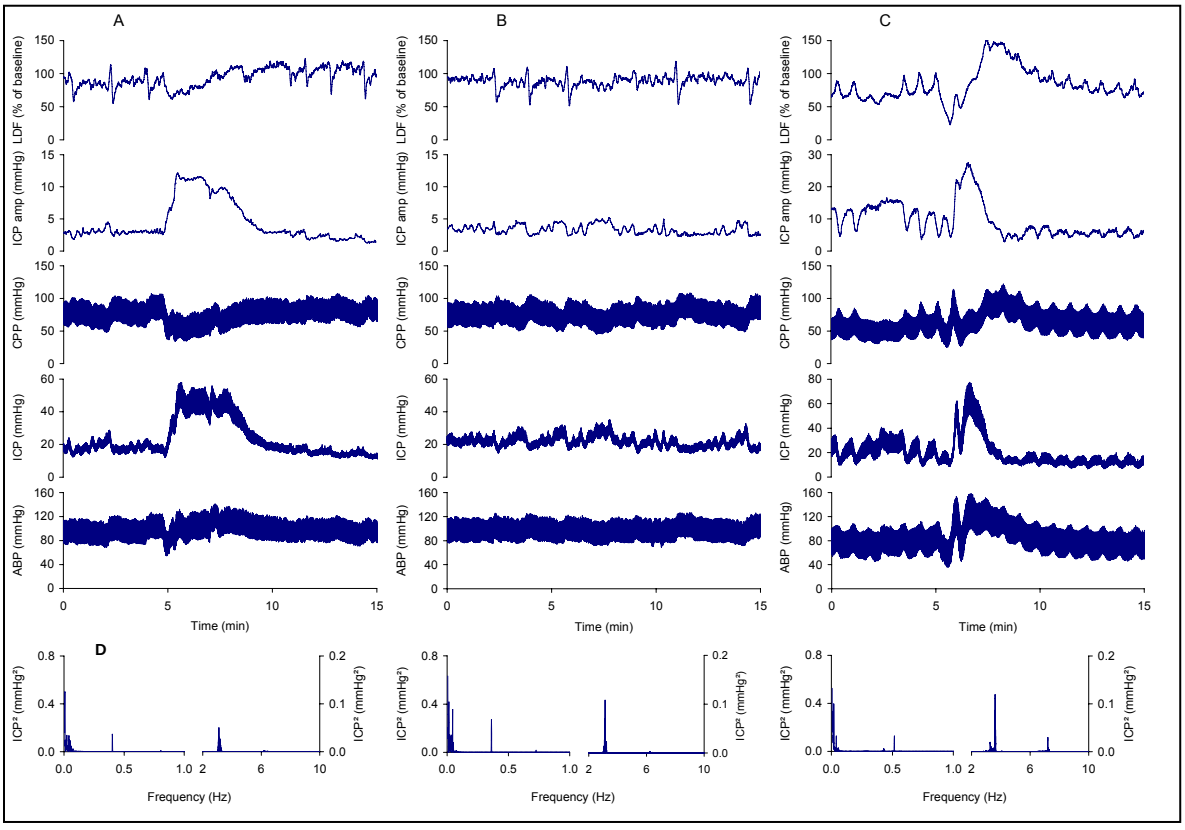

Abbildung 14 Repräsentative Aufzeichnungen von APB, ICP,CPP, ICP – Amplitude und LDF mit typischen Mustern des transienten ICP-Anstieges in der T-NT_{ICP}-Subgruppe. **(A)** ICP-Plateauwelle, die zerebrospinale kompensatorische Reserve ist niedrig. Während des ICP-Peaks sind CPP und LDF bei unbeeinträchtigtem ABP merklich reduziert. Nach der Plateauwelle fällt der ICP unter den Ausgangswert und die zerebrospinale kompensatorische Reserve scheint sich zu verbessern. **(B)** „B"-Wellen des ICP sind bei fast allen T-NT_{ICP}-Tieren nachweisbar. Sie verweisen auf eine verminderte intrakranielle Compliance und ein erhöhtes Risiko für eine intrakranielle Hypertension. **(C)** Hohe spitze ICP-Wellen, verursacht durch akuten Anstieg des ABP. Initial ist dieser Zustand mit einer erheblichen Reduktion des LDF verbunden, der eine anhaltende kortikale Hyperämie folgt, die nach ICP-Abfall und infolge eines nachfolgenden CPP-Anstieges bestehen bleibt. **(D)** Separate Darstellung der Komponenten der Frequenzanalyse der ICP-Aufzeichnungen. Hauptkomponenten der ICP-Fluktuationen, z.B. Pulswellen und Schwingungen (Frequenzbereich 2–10 Hz), atemabhängige Wellen und erste Schwingung (schmales Frequenzband von 0,4 – 0,8 Hz durch maschinelle Ventilation) und „langsame Wellen" (Frequenzbereich 0,05 – 0,0055 Hz, der 20-s bis 3-min Perioden), modif. nach (74)

Spontane ICP-Muster der beeinträchtigten intrakraniellen Compliance traten in der T-NT_{ICP}-Subgruppe häufiger auf, während kurzzeitige ICP-Anstiege durch Manipulationen, wie endotracheale Absaugung, regelmäßig auch bei den T-NT_N-

Tieren, aber auch bei den Kontrolltieren zu beobachten waren (Abb. 14, Tab. 4). Eine Steigerung des CBF war bei den Tieren der T-NT_N-Subgruppe nach Volumensubstitution zu beobachten.

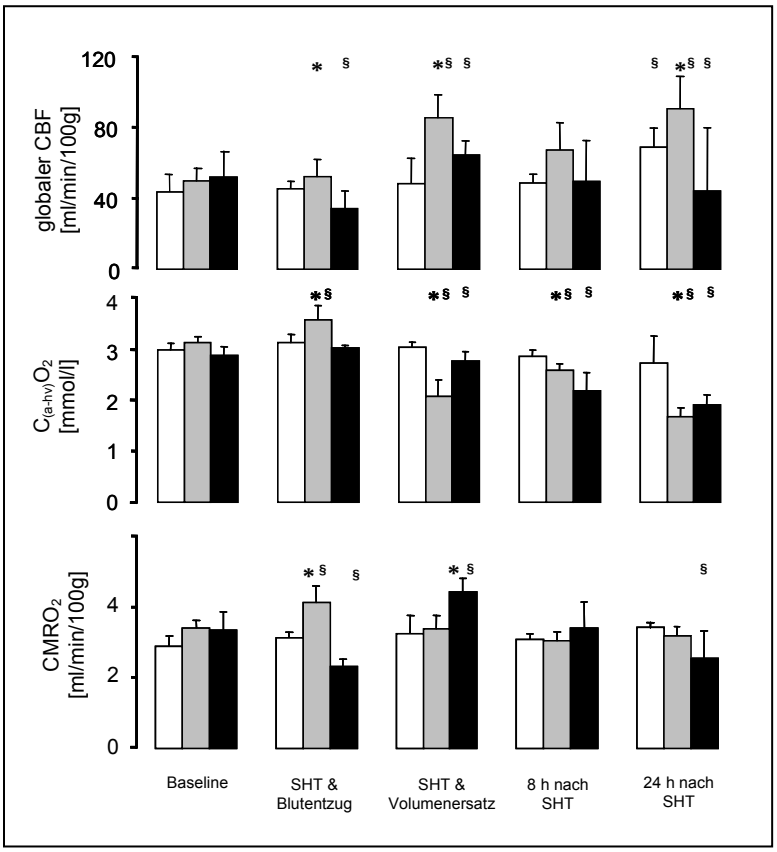

Abbildung 15 globaler CBF, zerebrale $C_{(a-hv)}O_2$ und $CMRO_2$ nach moderatem (T-NT_N,□) und schwerem (T-NT_{ICP},■) FP-Trauma, dazu im Vgl. die K-NT-Gruppe (□); (MW ± SD), §signifikanter Unterschied zu baseline innerhalb der Gruppe, ($p<0,05$); *signifikanter Unterschied zwischen T-NT_N- und T-NT_{ICP}-Tieren ($p<0,05$), modif. nach (74)

Die gesteigerte Hirndurchblutung persistierte bis zum Versuchsende. In der T-NT_{ICP}-Subgruppe dagegen fiel der CBF nach dem Blutentzug ab und erreichte während der 24-stündigen Monitoringphase das Ausgangsniveau nicht mehr. Am Ende des Experimentes betrug der CBF noch 50% im Vergleich zur T-NT_N-Subgruppe. (T-NT_N: 91±18 ml/min/100g; T-NT_{ICP}: 44±31 ml/min/100g) (Abb. 15).

Trauma-Applikation und Blutentzug induzierten in der T-NT_N-Subgruppe eine Steigerung der $CMRO_2$ auf 120±15% vom Ausgangswert. Nach Volumensubstitution fiel sie auf das Ausgangsniveau zurück und blieb für die restliche Monitoringphase weitgehend unverändert. Dagegen zeigte die $CMRO_2$ in der T-NT_{ICP}-Subgruppe zunächst eine ausgeprägte Verminderung nach Trauma-Applikation und Blutentzug auf 70±6% ($p<0,05$). Nach Volumensubstitution stieg die $CMRO_2$ überschießend auf 130±12% vom Ausgangswert an, um anschließend erneut abzufallen (24h: 75±24%, $p<0,05$).

Die posttraumatischen morphologischen Veränderungen, wie supratentorielle Parenchymblutungen bei den Tieren der T-NT_{ICP}-Subgruppe sind bereits weiter oben

beschrieben. Eine ergänzende semiquantitative Auswertung des Ausmaßes der Blutungen zeigte entsprechend höhere Scores in der T-NT_{ICP}- im Vergleich zur T-NT_N-Subgruppe (Tab. 5).

Tabelle 5 Hirn-Blutung-Oberflächen-Index (BBSI) von Tieren mit moderatem (T-NT_N) und schwerem (T-NT_{ICP}) FP-Hirntrauma, evaluiert von zwei nicht eingeweihten Untersuchern, modif. nach (74)

	K-NT (n=6)	T-NT_N (n=6)	T-NT_{ICP} (n=7)
Untersucher 1	1.4 ± 0.5	4.4 ± 1.5	6.6 ± 2.7
Untersucher 2	1.8 ± 0.6	2.8 ± 0.8	6.4 ± 2.5
Mittelwert	1.6 ± 0.6	3.6 ± 1.1$^{\$}$	6.5 ± 2.6$^{\$*}$

* $p<0,05$ T-NT_N vs. T-NT_{ICP}
$^{\$}$ $p<0,05$ Wert vs. K-NT

4.4. Auswirkungen der Hypothermie auf Plasmaspiegel und Biotransformation von Fentanyl und die intestinale Durchblutung

Die physiologischen Parameter sind in der Anlage in der Originalarbeit (73) in Tabelle 1 aufgeführt. Die Hypothermie verursachte eine Senkung des HI von 41±15% und der HF von 21±4% ($p<0,05$).

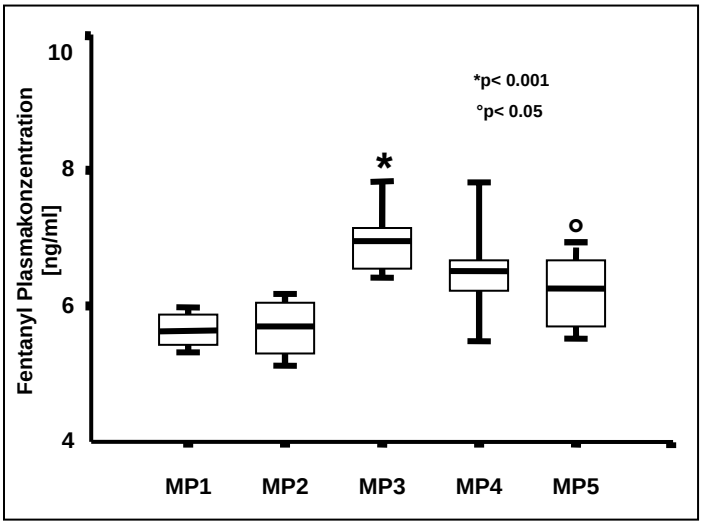

Abbildung 16 Fentanyl-Plasmakonzentrationen vor Hypothermie (MP1,MP2), am Ende der 6-stündigen Hypothermiephase (MP3), nach Wiedererwärmung (MP4) und nach 6 Stunden Normothermie (MP5). Die Boxplots sind als Median und 25% bzw. 75% interquartile Spanne angegeben. Die Fehlerbalken geben die 10. und 90. Percentile an, modif. nach (73)

Eine ähnliche Verminderung war beim systemischen Sauerstoffverbrauch (44±11% vom Ausgangswert; $p>0,05$) während der Hypothermie zu beobachten. Nach Wiedererwärmung erreichten diese Parameter wieder das Ausgangsniveau vor der Hypothermieinduktion. Dagegen wurde der Abfall des MAP (78±8%; $p<0,05$) während der Hypothermie nach Wiedererwärmung nicht kompensiert, der MAP blieb gegenüber den Ausgangswerten reduziert. Die Plasmakonzentration von Fentanyl

stieg während der Hypothermie um 25±11% (MP3; p<0,001) an. Nach Wiedererwärmung (MP4) und auch 6 Stunden nach Wiedererreichen der Normothermie blieb die Plasmakonzentration von Fentanyl noch erhöht (p<0,05) (Abb. 16).

Die arterielle Durchblutung der intestinalen Organe Niere (38±32%), Milz (45±33%), Magen (53±31%) und Darm (49±26%) war während der Hypothermie deutlich vermindert (p<0,05) und erlangte nach Wiedererwärmung das Ausgangsniveau zurück.

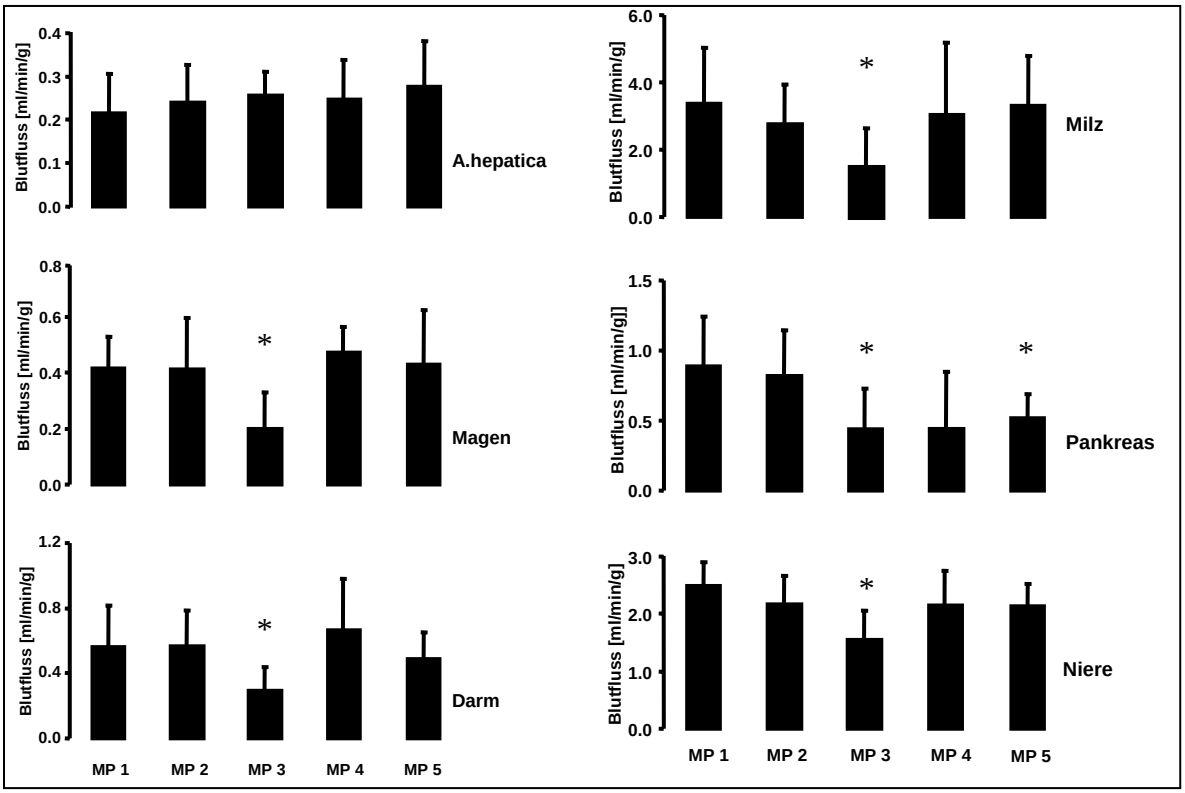

Abbildung 17 Organblutfluss vor Induktion der Hypothermie (MP1,MP2), nach 6 h Hypothermie von 31,6±0,2°C (MP3), nach Wiedererwärmung (MP4) und am Ende des Experimentes nach weiteren 6 h Normothermie (MP5) (MW ±SD; *p<0,05 MP vs. Ausgangswert MP1), modif. nach (73)

Im Pankreas war die arterielle Durchblutung während der Hypothermie ebenso reduziert (49±46%), blieb aber auch nach Wiedererwärmung vermindert (p<0,05). Dagegen blieb der hepatische arterielle Blutfluss während des gesamten Experimentes unbeeinträchtigt (Abb. 17).

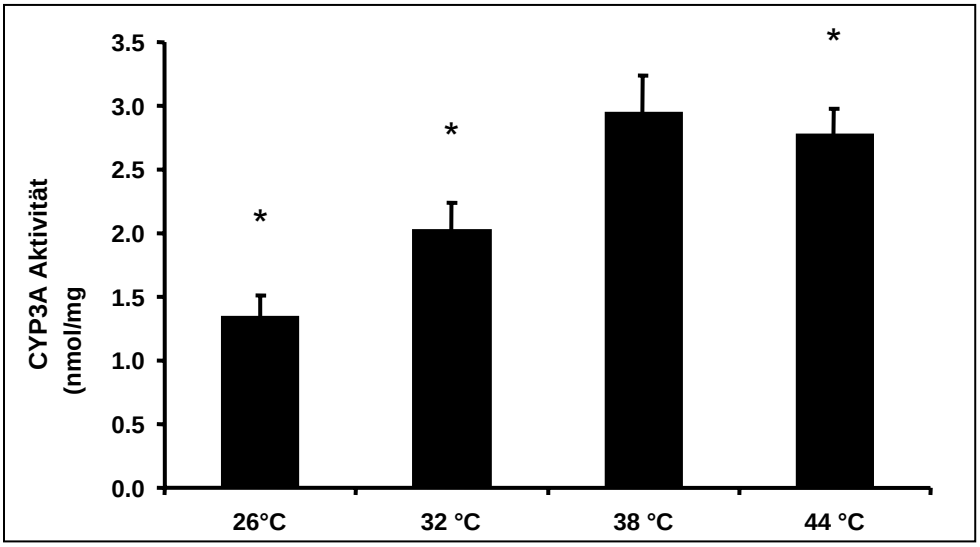

Abbildung 18 Temperaturabhängigkeit der hepatischen mikrosomalen Cytochrom P450 CYP3A4 (CYP3A)-Aktivität des Schweines. *In vitro* Bestimmung mittels Ethylmorphin-N-Demethylierung.(MW ±SD, *p<0,05 vs. 38°C), modif. nach (73)

Die hepatische CYP3A4-Aktivität zeigte eine temperaturabhängige Reduktion während der Hypothermie (bei 26°C: 48±2%, bei 32°C: 69±1% im Vgl. zu den Werten bei 38°C: 100%, p<0,001) 32°C. Aber auch der Temperaturanstieg auf 44°C verursachte eine leichte Minderung CYP3A4-Aktivität (Abb. 18).

5. Diskussion

In unterschiedlichen experimentellen Ansätzen konnte mit der vorliegenden Arbeit demonstriert werden, dass die milde Hypothermie beim nicht ausgereiften Gehirn protektive Effekte besitzt. Insbesondere bei Zuständen des kompromittierten zerebralen Metabolismus infolge akuter Hirndrucksteigerung oder komplexer traumatischer Hirnschädigung ließ sich in der Akutphase das deletäre Ausmaß der Schädigung durch die Anwendung der milden Hypothermie reduzieren.
Bis heute ist zwar eine Vielzahl von Mechanismen beschrieben, über welche die Hypothermie ihre neuroprotektiven Effekte entfaltet (124), jedoch sind hierzu spezifische Untersuchungen am nicht ausgereiften Gehirn bei komplexer Hirnschädigung nur spärlich vorhanden (8).
An einem epiduralen Ballonmodell zur intrakraniellen Drucksteigerung (19) beim 2-Wochen alten Ferkel konnten wir demonstrieren, dass die Hypothermie von 32°C die zerebrale Sauerstoffbalance durch Senkung des zerebralen Energiebedarfes verbessert (17), was in einer funktionellen Protektion (erhaltene elektrokortikale Funktion) resultiert (70). Des Weiteren zeigten wir am Modell des flüssigkeitsvermittelten Perkussionstraumas beim 6-Wochen alten Ferkel (74), dass die milde Hypothermie eine morphologische Protektion (Reduktion des histopathologischen Schadens) herbeiführt (30).
In einer ergänzenden Untersuchung wurde belegt, dass sowohl die Perfusion intestinaler Organe als auch deren metabolische Aktivität durch die milde Hypothermie beeinflusst werden. (73). Diese Effekte sind nicht nur perfusionsbedingt, sondern werden, wie am Beispiel von Fentanyl gezeigt, durch direkte Beeinflussung von Biotransformation katalysierenden hepatischen Enzymen hervorgerufen.

5.1. Effekte der Hypothermie auf das traumatisierte nicht ausgereifte Gehirn

Bei den 14-Tage alten Ferkeln resultierte die milde Hypothermie von 32°C während schrittweiser CPP-Reduktion mittels epiduralen Ballons in einer verbesserten O_2-Balance durch eine Reduktion des zerebralen O_2-Bedarfs. Die Reduktion des O_2-Bedarfes zeigte sich in einer verminderten $C_{(a\text{-}hv)}O_2$ und einem Anstieg des $t_{Hirn}pO_2$. Obwohl zum Verhalten des $t_{Hirn}pO_2$ unter Hypothermie bisher nur wenige, widersprüchliche Daten vorliegen (60), bestätigen unsere Ergebnisse Beobachtungen aus einer älteren Untersuchung an Hunden, bei der nach

Temperaturreduktion von 37°C auf 20°C eine 2- bis 4-fache Erhöhung des $t_{Hirn}pO_2$ zu verzeichnen war (211). Dagegen fand sich in einer anderen Untersuchung an Kaninchen keine Beeinflussung des $t_{Hirn}pO_2$ durch die Hypothermie (14).

Die reduzierte $C_{(a-hv)}O_2$ weist den geringeren O_2-Bedarf unter Hypothermie aus. Dies zeigt sich auch in der um ca. 50% verminderten $CMRO_2$ nach Erreichen der Hypothermie. Es ist hinreichend bekannt, dass die Hypothermie den zellulären Metabolismus durch Verlangsamung der Energieverluste reduziert (60, 124). Beim adulten gyrierten Gehirn reduziert sich die $CMRO_2$ pro 1°C um 5–7% (143). Dagegen beträgt die Reduktion der $CMRO_2$ in unserem Experiment beim juvenilen Gehirn ca. 10%/1°C und bestätigt somit ältere Untersuchungen an neugeborenen Ferkeln (33). Diese $CMRO_2$-Reduktion ist damit beinahe 50% höher als für das adulte Gehirn beschrieben (148). Im Gegensatz zu den Experimenten von Busija und Leffler (33), die ihre Untersuchungen unter leichter Hypokapnie durchführten (α-stat), war in unseren Experimenten die Verminderung des CBF geringer ausgeprägt. Wir führten unsere Untersuchungen mit einem temperaturkorrigierten Blutgasmanagement durch (ph-stat), aus der eine relative Hyperkapnie resultierte. Dieses Vorgehen wurde gewählt, da eine Reihe von Berichten über das verbesserte zerebrale Outcome bei weniger alkalisch orientiertem Blutgasmanagement (ph-stat) existiert (59, 91, 116).

Auf der höchsten Stufe der CPP-Reduktion (ICP45) zeigte sich eine generell reduzierte Sauerstoffverfügbarkeit, wodurch die Unterschiede in der $CMRO_2$ zwischen den normothermen und hypothermen Tieren nicht mehr nachweisbar waren. Jedoch war die elektrische Aktivität des Gehirnes bei den hypothermen Tieren weniger supprimiert. So haben einige Studien zeigen können, dass die Hypothermie induzierte Suppression des zerebralen Sauerstoffbedarfes, die den Einfluss auf sauerstoffverbrauchende Prozesse darstellt, von solchen Prozessen zu unterscheiden ist, welche eine barbituratinduzierte EEG-Suppression hervorrufen (143, 148, 192). Nemoto et al. (148) haben einen durch Barbiturate nicht supprimierbaren Anteil der $CMRO_2$ beschrieben, der jedoch temperatursensitiv ist. Unsere Daten belegten die Änderung eines delta-Wellen dominierten EEG (Narkose-EEG) hin zu einem delta-supprimierten EEG, mit unverändertem Anteil an höheren Frequenzen. Da höhere Frequenzmuster jedoch mit erhaltener kortikaler synaptischer Aktivität und erhaltenem Signaltransfer assoziiert sind (193), ist anzunehmen, dass ein erheblicher Teil der hypothermiebedingten $CMRO_2$-Reduktion durch die nicht EEG-assoziierte $CMRO_2$-Reduktion hervorgerufen wird. Die

Frequenzshift im ECoG ist im Allgemeinen eng an die Zunahme des CBF und des oxydativen Metabolismus gekoppelt (23). Wir fanden jedoch eine Zunahme der α-Aktivität, obwohl CBF und $CMRO_2$ während Hypothermie reduziert blieben. Die erhöhte α-Aktivität lässt sich möglicherweise mit Veränderungen der regionalen Hirndurchblutung in Zusammenhang bringen. So fanden wir unter Hypothermie eine stärker ausgeprägte Reduktion der kortikalen Durchblutung im Vergleich zum Mesenzephalon. Da die α-Aktivität nachhaltig durch die neuronale Aktivität des Mesenzephalon beeinflusst wird (101) und die Formatio reticularis des Mesenzephalon die thalamische Synchronisation und Desynchronisation moduliert (177), scheinen frequenzmodulierende Einflüsse der Formatio reticularis des Mesenzephalon somit erhalten zu bleiben. Die globale CBF-Reduktion durch Hypothermie wird also offensichtlich durch die Verminderung der kortikalen Durchblutung verursacht, die demzufolge als hauptverantwortlicher Faktor für die Reduktion der totalen Spektral-Power und der Hypovoltage zu betrachten ist.

Die moderate Verminderung des CPP (ICP35) verursachte unter Normothermie eine stärkere Beeinträchtigung der elektrokortikalen Aktivität im Vergleich zur Hypothermie. Auch auf dieser Stufe der CPP-Reduktion war eine besser erhaltene Aktivität der höheren ECoG-Frequenzen zu verzeichnen, was auf eine noch erhaltene Energieproduktion entsprechend den funktionellen Anforderungen hinweist. Das Versagen der Energieproduktion wird in Abhängigkeit vom globalen CBF beschrieben, der unterhalb der Schwelle des Versagens der neuronalen Aktivität liegt (125). So fanden sich bei den normothermen Tieren auf der höchsten Stufe der CPP-Reduktion (ICP45) ECoG-Muster (Burst-Suppression, Null-Linien), die das Unterschreiten der Schwellen für ein funktionelles und metabolisches Versagen des Gehirnes anzeigen. Im Gegensatz dazu blieb bei den hypothermen Tieren die elektrokortikale Aktivität auf niedrigem Niveau erhalten [siehe Originalarbeit Abb.4 (70), in der Anlage].

Die Neuroprotektion mittels Hypothermie nach Hirntrauma untersuchten wir mit dem zweiten experimentellen Ansatz am 6-Wochen alten Ferkel. Bei einem Teil der normothermen Tiere war mit diesem Modell ein sekundärer Hirndruckanstieg zu verzeichnen, der sich erst einige Stunden nach einem freien Intervall posttraumatisch entwickelte. Bei den Tieren, die nach Trauma-Applikation auf 32°C gekühlt wurden, war hingegen kein sekundärer ICP-Anstieg zu beobachten. Die günstige Beeinflussung des Hirndruckes durch die Hypothermie nach traumatischer

Hirnschädigung ist in klinischen Studien sowohl für Erwachsene (162) als auch für Kinder (8, 24) beschrieben worden. Als ein möglicher Mechanismus wird die temperaturabhängige Reduktion der zerebralen Stoffwechselaktivität und des Sauerstoffverbrauchs diskutiert, in deren Folge sich die Sauerstoffbilanz verbessert. Dies ist häufig mit einer Reduktion von CBF und CBV verbunden, wodurch der ICP reduziert wird (156). Diese Effekte der Hypothermie mit Senkung der $CMRO_2$ und des CBF während gradueller ICP-Erhöhung konnten wir bereits mit unserem ersten experimentellen Ansatz belegen (17).

Neben der Senkung des zerebralen Sauerstoffumsatzes (17, 143) sind die Beeinflussung der zerebrovaskulären Permeabilität und der Ödembildung (16, 37, 94), auf zellulärer Ebene die Hemmung der Freisetzung exzitatorischer Aminosäuren (35), des intrazellulären Kalzium-Einstroms (103), die Reduktion der Lipidperoxidation und die Bildung von Sauerstoffradikalen (79, 92, 102) sowie die Reduktion des histopathologischen Schadens (47, 109, 155) die wohl bedeutendsten Wirkmechanismen der Hypothermie. Die lange Monitoringphase in unserem experimentellen Ansatz erlaubte die Erfassung von histomorphologischen Veränderungen innerhalb der ersten 24 Stunden nach dem Trauma. Die sekundäre Progression der Schädigung nach einem lateralen FP-Trauma kann selektive Zelltypen schädigen (203), wie es für alle Hirnregionen, einschließlich Kortex, Hippocampus, Thalamus und Striatum beschrieben wurde (86, 176). Wir konnten neuronale Schädigungen mittels MAP2-Immunhistochemie in sehr ausgeprägter Form nur bei den Tieren mit sekundärem ICP-Anstieg nachweisen, der sowohl in tieferen Kortexschichten der traumatisierten Hemisphäre als auch im Hippocampus nachweisbar war. Diese Befunde sind mit denen aus anderen Untersuchungen an der Ratte vergleichbar, die eine Zeitabhängigkeit in der Ausprägung zeigten, welche 48 bis 72 Stunden posttraumatisch ihr Maximum erfuhr (69). Diese schweren zytoskelettalen Schäden bleiben offensichtlich lang anhaltend bestehen (89).

Die Darstellung des axonalen Schadens erfolgte in unserem Modell mittels ßAPP-Immunmarkierung. Als früher Marker des gestörten axoplasmatischen Transportes korreliert eine ßAPP-Immunpositivität sehr gut mit der Schwere des DAI (77). Die axonale Schädigung ist jedoch nicht zwingend mit dem Primärereignis des Hirntraumas verbunden. Vielmehr reflektiert auch der DAI die Progression nach einem primären traumatischen Ereignis (165). So wurde die Progression der axonalen Schädigung innerhalb von 2 Wochen nach lateralem FP-Trauma für die

Ratte beschrieben (160). Unsere Befunde der axonalen Schwellung und Auftreibungen befinden sich in Kongruenz zu den in der Literatur beschriebenen. Insbesondere bei den Tieren mit sekundärem ICP-Anstieg fanden wir 24 Stunden nach dem Trauma eine beträchtliche Zahl ßAPP-immunpositiver Axone. Die höheren ßAPP-Scores im Dienzephalon der T-NT_{ICP}-Tiere sind nicht überraschend und stehen für die sekundäre Hirnschädigung. Obwohl bisher nur wenige Untersuchungen zum Einfluss der Hypothermie auf die axonale Schädigung existieren, konnte jedoch gezeigt werden, dass die Hypothermie die Dichte geschädigter Axone zu reduzieren vermag (77, 135, 195). Dagegen fanden wir nur geringe Unterschiede in der ßAPP-Akkumulation zwischen den normothermen und hypothermen Tieren nach FP-Trauma. Jedoch fehlte die ßAPP-Immunreaktivität bei den hypothermen Tieren (T-HT) im Hirnstamm, während sie auch in dieser Region bei den normothermen Tieren ohne sekundären ICP-Anstieg (T-NT_N) nachweisbar war. In neueren experimentellen Untersuchungen scheint der Einfluss des Wiedererwärmungsregimes auf die axonale Protektion von außerordentlicher Bedeutung zu sein. So konnte gezeigt werden, dass das axonale Zytoskelett in ultrastrukturellen Untersuchungen nach langsamer Wiedererwärmung vergleichbar zu den Kontrolltieren erhalten bleibt (136).

Die TUNEL-Markierung wurde zur Bestimmung des traumatisch bedingten apoptotischen Geschehens genutzt. Hierbei ist jedoch zu beachten, dass auch nekrotische Zellen TUNEL-positiv reagieren (170), so dass wir zunächst nur den Terminus „TUNEL-positiv“ in die Auswertung einbezogen haben. Im Vergleich zu den normothermen Versuchstieren mit sekundärem Hirndruckanstieg (T-NT_{ICP}) zeigten die hypothermen Versuchstiere (T-HT) einen signifikant niedrigeren TUNEL-Index. Dies deckt sich mit der Verhinderung des Hirndruckanstieges durch die Hypothermie. Die Hypothermie reduzierte offensichtlich das Risiko für eine zerebrale Minderoxygenierung und die hieraus resultierende ischämische Schädigung. Experimentell ist belegt, dass die durch die kalziumabhängige Endonukleaseaktivität getriggerte Apoptose mittels Hypothermie reduziert werden kann (145). Für die Pathogenese der Apoptose werden derzeit zwei Wege beschrieben: ein über die Freisetzung von mitochondrialem Cytochrom C vermittelter (intrinsischer Weg) und ein rezeptorvermittelter Weg (extrinsischer Weg) (124). Es wird spekuliert, dass durch die Hypothermie beide Wege beeinflusst werden. So ist bekannt, dass sowohl die Cytochrom C-Freisetzung (217) als auch die Caspase-Aktivierung (159) durch

Hypothermie gehemmt werden. Aber auch weitere protektive Mechanismen, wie die Steigerung der endogenen Produktion des anti-apoptotischen Proteins Bcl-2 (58, 218), die Suppression des pro-apoptotischen Proteins Bax (57) und die Reduktion der DNA-Fragmentierung (151) durch Hypothermie, wurden bisher beschrieben.

Die Unterschiede in der TUNEL-Markierung zwischen den Tieren der Gruppen T-NT_N und T-HT waren nach 24 Stunden nur gering ausgeprägt. In der Hypothermie-Gruppe wurden TUNEL-positive Zellen allerdings nur bei einem der zehn untersuchten Tiere nachgewiesen, wodurch ein Trend zur verminderten TUNEL-Positivität bei den hypothermen Versuchstieren zu erkennen ist. Nach FP-Trauma der adulten Ratte waren apoptotische Zellen im ipsilateralen Kortex nach 24 Stunden nachweisbar, in der weißen Substanz bereits nach 12 Stunden. Jedoch wurde das Maximum der TUNEL-Positivität in diesen Hirnarealen erst nach einer Woche erreicht (44). Andererseits waren in einer Untersuchung mit Kryo-Schädigung des Gehirns apoptotische Zellen schon nach 12 Stunden nachweisbar (215). Das Maximum war im Kortex nach 24 h, in weißer Substanz und Hippocampus nach 48 h erreicht. Somit scheint eine Reihe von Faktoren, wie z.B. das experimentelle Setting, den zeitlichen Verlauf der posttraumatischen Apoptose zu beeinflussen. Dennoch ist es denkbar, dass der von uns gewählte Untersuchungszeitraum von 24 Sunden noch zu kurz gewählt war, um das gesamte Ausmaß signifikanter Unterschiede zwischen Normothermie und Hypothermie darzustellen.

Die direkte Beeinflussung des Ausmaßes der immunhistochemisch nachweisbaren Schädigung durch die milde Hypothermie lässt sich aus unseren Untersuchungen jedoch nicht sicher ableiten, da durch die ICP-Reduktion weitere schädigende Sekundäreffekte, wie sie z.B. durch die kompromittierte zerebrale Compliance entstehen, vermieden wurden.

5.2. Effekte der Hypothermie auf die intestinale Durchblutung und die CYP3A4-Aktivität

In einem weiteren experimentellen Ansatz untersuchten wir die Effekte einer 6-stündigen Hypothermie von 32 °C auf die intestinale Durchblutung. Wir fokussierten in diesem Ansatz auf die Bestimmung der Plasmaspiegel von Fentanyl, einem Opioid, das auch bei Patienten nach traumatischer Hirnschädigung zur Analgosedierung auf Intensivstationen eingesetzt wird. Wir konnten zeigen, dass die Hypothermie zu einer 25%igen Erhöhung der Plasmaspiegel von Fentanyl führt.

Ähnliche pharmakokinetische Effekte sind unter Hypothermie bereits für andere Medikamente mit hoher (111, 119, 137) und geringer (95) hepatischer Extraktionsrate, aber auch für Pharmaka, die durch unspezifische Esterasen (174) metabolisiert werden, nachgewiesen. Jedoch unterschieden sich diese Studien bezüglich der Applikationswege, der Untersuchungszeit und der Tiefe der Hypothermie, so dass sie nur bedingt vergleichbar sind. Fentanyl wird in der Intensivmedizin über eine lange Zeitdauer mittels kontinuierlicher Infusion verabreicht, weshalb wir einen langen Untersuchungszeitraum mit kontinuierlicher Infusion wählten. Des Weiteren führten wir unsere Untersuchungen an einem Schweinemodell durch, da Ähnlichkeiten zum Menschen bezüglich kardiovaskulärer Parameter und der regionalen Verteilung des Blutflusses bestehen (141).

Unter normalen Bedingungen erfolgt die Fentanyl-Clearance überwiegend über hepatische Biotransformation (138). Dies geschieht durch N-Dealkylierung zu Norfentanyl durch das hepatische mikrosomale Cytochrom P450 3A-Isoenzym (CYP3A4) (199). Andere Metabolisierungs- und Eliminationswege scheinen bei parentaler Fentanylgabe unwahrscheinlich (117).

Für die Erhöhung der Plasmaspiegel von Fentanyl unter Hypothermie werden verschiedene Prozesse verantwortlich gemacht. So werden durch die Hypothermie Verteilungsvolumen und totale Körper-Clearance erheblich reduziert (111). Die verminderte Körper-Clearance kann die Folge einer reduzierten hepatischen Biotransformation und/oder einer verzögerten Verteilung sein, die wiederum aus der Reduktion von Herzleistung und Organperfusion durch Hypothermie entsteht. In Simulationsuntersuchungen ist gezeigt worden, dass das von uns beschriebene Ausmaß der Perfusionsminderung tatsächlich für die erhöhten Plasmaspiegel von Fentanyl verantwortlich sein kann (26).

Hinsichtlich der hypothermiebedingten Beeinträchtigung der Fentanyl-Elimination sind verschiedene Aspekte zu beachten. Wir fanden eine stark temperaturabhängige Aktivität des CYP3A4. Bei 32°C war die Konversionsrate um ca. 1/3 reduziert. Demzufolge lässt sich ein relevanter Anteil der reduzierten Körper-Clearance auf die verminderte Biotransformation in der Leber zurückführen.

Ungeachtet des überraschenden Befundes eines unbeeinträchtigten arteriellen hepatischen Blutflusses, nehmen wir eine Verminderung des totalen hepatischen Blutflusses durch Hypothermie an. Dies lässt sich vermuten, weil der arterielle hepatische Zustrom beim juvenilen Schwein nur ein Fünftel des totalen hepatischen

Blutflusses ausmacht (206). Der überwiegende Anteil des Zustroms erfolgt über die Portalvene. Der portale Blutfluss, in unserer Untersuchung nicht direkt gemessen, muss durch die Hypothermie merklich reduziert sein, da alle Blutflussraten der Organe des Splanchnikusgebietes, die in die Portalvene drainieren, reduziert sind. Da Fentanyl eine hohe hepatische Extraktionsrate besitzt, ist die hepatische Elimination stärker von Änderungen des totalen hepatischen Blutflusses als von der enzymatischen Aktivität abhängig (178).

Die Ursache für die erhöhten prolongierten Plasmaspiegel von Fentanyl nach Temperaturnormalisierung bleibt spekulativ. Eine verlängerte Inhibition der CYP3A4 ist eher unwahrscheinlich, da sich auch nach langdauernder tiefer hypothermer Leberkonservierung die hepatische Pharmakon-Extraktion bereits 30 min nach Wiedererwärmung normalisiert hat (105). Eine vermehrte Gewebsakkumulation von Fentanyl während der Hypothermiephase und ein Rebound des Plasmaspiegels nach Wiedererwärmung infolge vermehrter Gewebeperfusion ist dagegen eher möglich. Des Weiteren ist auch die Biotransformation von Midazolam von der hepatischen CYP3A4-Aktivität abhängig, so dass in der Hypothermiephase auch Midazolam akkumulieren kann. Dies wurde von uns nicht gemessen. Sollte eine vergleichbare Reaktion wie mit Fentanyl bestehen, ist es durchaus möglich, dass eine prolongierte Akkumulation beider Medikamente zur Überschreitung der biotransformatorischen Kapazität von CYP3A4 führt. Das hat zwangsläufig eine verzögerte Normalisierung der Plasmaspiegel zur Folge. Weiterhin ist durch Midazolam eine Verstärkung der hämodynamischen Effekte der Hypothermie auf den regionalen Blutfluss und den Fentanyltransport zur Leber möglich (76).

Obwohl die Mechanismen für die persistierenden hohen Fentanyl-Plasmaspiegel spekulativ bleiben, ist die Beschreibung des Phänomens ohne Zweifel von klinischer Relevanz. So kann zum einen die Recoveryphase nach einer therapeutischen Hypothermie deutlich verlängert sein. Andererseits wird eine Fentanyl-Überdosierung während kontinuierlicher Langzeitinfusion durch die Hypothermie aggraviert, die wiederum mit nachhaltigen schwerwiegenden Nebenwirkungen behaftet ist (intestinale Motilitätsstörungen, Hypotension, akutes Fentanyl-Entzugssyndrom, verlängerte Intensivstationsverweildauer, vermehrte Kosten) (189).

Mit unseren Untersuchungen konnten wir zeigen, dass die Hypothermie sowohl indirekt über eine reduzierte Organperfusion als auch direkt durch Verminderung von Enzymaktivitäten die Pharmakokinetik von Analgetika zu beeinflussen vermag (73).

Im Gegensatz zu anderen experimentellen Untersuchungen (190) fanden wir bei Verwendung eines Analgosedierungs-Regimes mit Fentanyl dennoch nach 24 h posttraumatisch eine Reduktion des histopathologischen Schadens in der Hypothermiegruppe. Dies deutet auf die hypothermiebedingte Supprimierung von Schädigungsmechanismen hin, die unabhängig vom Analgosedierungs-Regime sind.

5.3. Therapeutisches Fenster für die Anwendung der Hypothermie

In den vorliegenden Untersuchungen haben wir eine Hypothermie assoziierte Reduktion des histopathologischen Schadens nach traumatischer Hirnschädigung für das nicht ausgereifte juvenile Gehirn des Schweines demonstrieren können. Es bleibt jedoch offen, ob durch Optimierung der Modalitäten der Hypothermie, d.h. Zeitpunkt des Beginns der Hypothermie und des Erreichens der Zieltemperatur, Hypothermiedauer und Geschwindigkeit der Wiedererwärmung, bessere Ergebnisse zu erzielen sind. Aus einer Reihe experimenteller Untersuchungen zur fokalen oder globalen zerebralen Ischämie ist bekannt, dass die intra- und frühzeitig postischämisch induzierte Hypothermie die besten Ergebnisse bezüglich der Reduktion des histopathologischen Schadens und des neurologischen Defizits aufweist (57, 58, 87, 115, 126, 198). Als einer der bedeutendsten Schädigungsmechanismen wird die neuroexzitotoxische Kaskade angesehen, die schwere Störungen der intrazellulären Ionen-Homöostase durch Akkumulation von exzitatorischen Neurotransmittern wie Glutamat hervorruft. Hierdurch wird ein langdauernder und exzessiver Kalzium-Einstrom mit zellulärer Hyperexzitabilität und Hyperaktivität verursacht, der zur Zellschwellung und Aktivierung von Proteasen führt. Dies führt dann in der Endkonsequenz zum nekrotischen Zelluntergang (207). Jedoch konnte in einem SHT-Modell der Ratte auch mit einer bis zu 60 min verzögerten Hypothermieinduktion eine signifikante Reduktion der posttraumatischen Verhaltensstörung erreicht werden (132). Eine verzögert induzierte Hypothermie wurde bisher auch in klinischen Studien mit z. T. gutem Erfolg angewendet (21, 201). In unserem Modell induzierten wir die Hypothermie 60 min posttraumatisch, was durchaus der klinischen Realität entspricht. Die Effektivität der spät einsetzenden Hypothermie zeigt, dass offensichtlich noch eine Reihe weiterer Mechanismen für die Propagation der posttraumatischen wie auch der postischämischen zerebralen Schädigung von Bedeutung ist. So können Schädigungskaskaden, die Stunden bis Tage bzw. Wochen andauern (48), wie Bildung freier Radikale,

Gerinnungsaktivierung, Blut-Hirn-Schrankenstörung, mitochondriale Schädigung, Inflammation und Apoptose, durch die Hypothermie supprimiert werden. Nach traumatischer Hirnschädigung wurde der neuroprotektive Effekt der Hypothermie auf die Apoptose bisher nur für die Ratte beschrieben (188). Unsere Untersuchungen haben belegen können, dass eine sechsstündige milde Hypothermie, die 60 min posttraumatisch induziert wird, den apoptotischen Zelluntergang auch beim gyrierten Gehirn signifikant vermindert. Nach kälteinduzierter Hirnschädigung scheint eine längere Hypothermiephase (12 h) apoptotische Prozesse jedoch noch effektiver zu supprimieren (215). Dabei reagierten die Zellen im Hippocampus deutlich sensitiver auf die Hypothermie als die Zellen der weißen Substanz oder des Kortex, was die eigenen Untersuchungen im Trend bestätigten.

Während wir in unserem Hirntraumamodell die Effektivität der Hypothermie durch Vermeidung eines sekundären ICP-Anstieges untersuchten, zielte das epidurale Ballon-Modell darauf ab, eine Neuroprotektion durch Hypothermie auch während kompromittierter zerebraler Compliance nachzuweisen. Wir konnten bei den hypothermen Tieren eine bessere funktionelle Toleranz gegenüber der reduzierten zerebralen Perfusion im Vergleich zu den normothermen Tieren belegen. Da in diesem Modell die Hypothermie jedoch bereits vor der Schädigung induziert worden ist, lassen sich die Ergebnisse nur bedingt für klinische Situationen mit beeinträchtigter zerebraler Compliance (akuter ICP-Anstieg) übertragen. Wurde vor der Schädigung nicht gekühlt, d.h., konnten die Schädigungskaskaden bis zum Zeitpunkt eines akuten ICP-Anstieges ungebremst ablaufen, so war die Effektivität der Hypothermie bezüglich einer funktionellen Protektion um so geringer, je später nach dem traumatischen Ereignis die Kühlung induziert wurde.

Aus experimentellen Untersuchungen zur globalen und fokalen zerebralen Ischämie ist bekannt, dass eine längere Hypothermiedauer auch zu einer signifikant ausgeprägteren Neuroprotektion führt. In einer Studie zur Hypothermie nach globaler Ischämie bei der Ratte korrelierte das Ausmaß der Reduktion der neuronalen Schädigung mit der Dauer der Hypothermie (42). Allerdings war die Reduktion der neuronalen Schädigung noch vergleichsweise gering, da die Hypothermie erst 2 Stunden postischämisch induziert und für eine relativ kurze Dauer erhalten wurde (30 min, 3,5 und 5 Stunden) (42). In der anderen Studie konnte nach 24-stündiger Hypothermie ein fast kompletter Erhalt der für eine Hypoxie empfindlichen CA1-Neurone (10% neuronale Schädigung vs. 85% nach 12 h

Hypothermie) nachgewiesen werden (43). Für unsere Untersuchungen wurde eine Hypothermiephase von 6 Stunden gewählt, da die Hypothermie zu einem vergleichsweise frühen Zeitpunkt induziert wurde. Nach Daten aus Studien zur globalen Ischämie ist jedoch anzunehmen, dass sich eine längere Hypothermiephase auch positiv auf die Neuroprotektion bezüglich des histopathologischen Schadens auswirkt. Das Risiko potentieller Nebenwirkungen durch zunehmende Hypothermiedauer ist dann stärker zu beachten (161).
Neben dem Zeitpunkt des Beginns und der Dauer beeinflusst vor allem die Wiedererwärmung die Effektivität der Neuroprotektion durch Hypothermie. Obwohl bisher keine spezifischen Daten über die Geschwindigkeit der Wiedererwärmung des unreifen Gehirns vorliegen, kann davon ausgegangen werden, dass sich eine zu schnelle Wiedererwärmung ebenso negativ auswirkt, wie es für das ausgereifte Gehirn beschrieben wurde. So induziert eine rasche Wiedererwärmung nach tiefer Hypothermie eine transiente Entkopplung von CBF und zerebralem Metabolismus, wohingegen die Kopplung bei langsamer Wiedererwärmung erhalten bleibt (146). Ähnliche Befunde wurden nach traumatischer Hirnschädigung mit sekundärer Hypoxie bei der Ratte beschrieben (134). Eine rasche Wiedererwärmung von 15 min korrelierte mit einer Zunahme des Kontusionsvolumens im Vergleich zur langsamen Wiedererwärmung von 120 min, was einer Wiedererwärmungsrate von 2°C/h entspricht. Dagegen war die Wiedererwärmungsrate mit ca. 1,4°C /h in unseren Experimenten um mehr als 25% geringer. Im Vergleich zu klinischen Hypothermiestudien nach globaler Hirnischämie und SHT mit Wiedererwärmungsraten deutlich < 1°C/h (21, 41, 201) erscheint unsere Wiedererwärmungsrate hoch. Obwohl sich die negative Beeinflussung unserer neuroprotektiven Ergebnisse nicht endgültig ausschließen lässt, ist dennoch anzunehmen, dass die für unsere Experimente gewählte Wiedererwärmungsrate auf Grund der vorliegenden experimentellen Daten die Kernaussagen der Untersuchungen nicht entscheidend beeinflusst hat.

5.4. Die Wahl der experimentellen Modelle

Zur Untersuchung der Auswirkungen der intrakraniellen Drucksteigerung, wie sie nach traumatischer Schädigung insbesondere beim kindlichen Gehirn beschrieben ist (8, 10, 24), wählten wir ein epidurales Ballon-Modell, mit dem graduierte und

kontrollierte Hirndrucksteigerung reproduzierbar induziert werden konnte. Die Effekte der epiduralen Volumenexpansion auf die zerebrale Hämodynamik ließen sich verlässlich messen. In der Vergangenheit wurde dieses Modell bei einer Reihe von experimentellen Untersuchungen des adulten Tieres (Kaninchen, Hund, Schwein) verwendet (123, 150, 180, 181). Im Unterschied zu anderen experimentellen Ansätzen, die dieses Modell verwendeten, konnten wir durch den Einsatz des ABP-Kontrollers Sekundäreffekte, die während der intrakraniellen Drucksteigerung durch systemische hämodynamische Reaktionen ausgelöst werden („Cushing-Reaktion“), weitgehend ausschalten. Die Menge des entzogenen Blutes differierte auf den einzelnen ICP-Druckstufen in Abhängigkeit von der erwarteten kardiovaskulären Reaktion. Auf der höchsten Druckstufe (ICP45) war dagegen die Retransfusion des entzogenen Blutes erforderlich. Die systemische hämodynamische Stabilität war mittels Blutentzug/Retransfusion während der Experimente auf jeder ICP-Druckstufe suffizient gewährleistet.

Im zweiten experimentellen Ansatz wurde das nicht ausgereifte Gehirn des Schweines einem schweren Hirntrauma mittels flüssigkeitsinduzierter Perkussion ausgesetzt. Das FP-Modell wird seit mehr als 30 Jahren für experimentelle Untersuchungen zum Hirntrauma genutzt und zeichnet sich dadurch aus, dass es sowohl fokale als auch diffuse Hirnschäden verursacht (203). Das laterale FP-Modell haben wir in modifizierter Form beim gyrierten Gehirn des juvenilen Schweines verwendet und eine zusätzliche Schädigungsnoxe, den akuten Blutverlust, ergänzend simuliert. Die lange posttraumatische Monitoringphase erlaubte im Gegensatz zu anderen Untersuchungen eine Aussage über den ICP-Verlauf innerhalb der ersten 24 Stunden (127, 128, 194). Somit konnte ein reproduzierbarer sekundärer ICP-Anstieg nach einem freien Intervall von ca. 5 Stunden beobachtet werden. Dies steht im Gegensatz zu anderen Untersuchungen mit diesem Modell, bei denen vor allem frühzeitige ICP-Anstiege unmittelbar nach dem Trauma beschrieben wurden (49, 139, 157, 205). Im Vergleich zu den genannten Untersuchungen bevorzugten wir eine lange (24 h) posttraumatische Monitoringphase (74), so dass die sekundären ICP-Veränderungen in früheren Untersuchungen möglicherweise aus diesem Grunde nicht erfasst wurden. Der sekundäre ICP-Anstieg bei den normothermen Traumatieren ($T\text{-}NT_{ICP}$) war jedoch nicht regelhaft. Zunächst blieb unklar, welche Tiere für einen sekundären ICP-Anstieg prädestiniert waren. Auch klinische Untersuchungen konnten bisher keine

sichere prädiktive Aussage zum Verhalten des ICP nach traumatischer Hirnschädigung ermöglichen (186). Eine separate Detailanalyse zum ICP-Verlauf zeigte jedoch, dass schon die geringe Modifikation des Auslenkwinkels des zur Trauma-Applikation benutzten Pendels zu einer dramatischen Verstärkung der Hirnschädigung führte. So scheint die Traumaschwere doch einer der wesentlichsten Faktoren für die Entstehung eines sekundären Hirndruckes zu sein. Mit den Untersuchungen an unserem kliniknahen SHT-Modell sind wir zwar nicht der Frage der Entstehungsmechanismen für den sekundären ICP-Anstieg nachgegangen, unser sehr aufwendiges kontinuierliches Monitoring erlaubte jedoch das Studium der funktionellen und hämodynamischen Veränderungen, aus denen sich therapeutische Konsequenzen ableiten lassen. Mit diesem experimentellen Ansatz sind definierte Interventionen, z.B. pharmakologische Hirndrucksenkung, neuroprotektive Maßnahmen wie therapeutische Hypothermie, weiter evaluierbar.

Limitiert werden unsere Ergebnisse durch die Fokussierung ausschließlich auf die Akutphase der traumatischen Hirnschädigung. Es war jedoch unser Ziel, zunächst an einem kliniknahen Modell die Akutphase des kindlichen SHT zu evaluieren. Als zusätzliche Schädigungsnoxe sollte der unmittelbar posttraumatisch induzierte Blutentzug mit konsekutiver Volumensubstitution einen Blutverlust simulieren. Die Volumensubstitution stellte den Beginn der Maßnahmen durch den Rettungsdienst dar. Im Unterschied zur klinischen Praxis erfolgte die medikamentöse Analgosedierung und Volumensubstitution aus ethischen Gründen bereits vor der Trauma-Applikation (Präparation). In der Zukunft sollten mit diesem Modell auch Langzeiteffekte therapeutischer Maßnahmen, wie z.B. der Hypothermie, untersucht werden können, da für eine abschließende Beurteilung der Qualität der Neuroprotektion nach traumatischer Hirnschädigung das neurologische Defizit nach überstandener Akutphase von herausragender Bedeutung ist. So korreliert im chronischen Experiment der Ratte, sowohl nach traumatischer (29, 28) als auch nach ischämischer (45) Hirnschädigung, die Reduktion histologischer Gewebsuntergänge durch Hypothermie mit dem Erhalt der kognitiven Funktion.

6. Schlussfolgerungen

Das FP-Trauma ermöglicht die Modellierung der zerebralen hämodynamischen Frühveränderungen einer traumatischen Hirnschädigung am gyrierten Gehirn des juvenilen Schweines. So lassen sich therapeutische Ansätze wie die Effekte der Hypothermie auf das Ausmaß der traumatischen Hirnschädigung untersuchen. Die milde Hypothermie erweist sich als hirnprotektiv hinsichtlich der Beeinflussung des Hirndruckes beim juvenilen Gehirn. Diese experimentellen Daten stimmen mit klinischen Daten aus einer Phase-II-Studie zum kindlichen SHT überein, so dass die Hypothermie als therapeutische Maßnahme beim kindlichen SHT mit ICP-Steigerung durchaus sinnvoll erscheint. Ob das neurologische Outcome beim kindlichen SHT tatsächlich positiv beeinflusst werden kann, muss allerdings in weiteren experimentellen und klinischen Untersuchungen bewiesen werden. Eine Vielzahl von Faktoren kann die Effektivität der Hypothermie beeinflussen wie z.B. die Geschwindigkeit des Erreichens der Zieltemperatur, die Dauer der Hypothermiephase und die Geschwindigkeit der Wiedererwärmung. Bisher ungeklärt bleibt, ob die Hypothermie nur bei bestimmten zerebralen Pathologien oder grundsätzlich beim SHT angewendet werden sollte, da insbesondere ältere Patienten nach den derzeit vorliegenden Studien nicht von einer Hypothermie profitieren. Des Weiteren muss das Analgosedierungs-Regime nach schwerem SHT beachtet werden, da experimentelle Daten belegen konnten, dass die Analgosedierung mit Opioiden die protektiven Effekte der Hypothermie aufzuheben vermag.

7. Zusammenfassung

An verschiedenen Modellen zur Beeinträchtigung der intrazerebralen Compliance wurde untersucht, ob die milde Hypothermie das Ausmaß einer Schädigung des juvenilen Gehirnes zu reduzieren vermag. Mit einem epiduralen Ballonmodell beim 14-Tage alten Ferkel wurden die Effekte der Hypothermie auf zerebrale Durchblutung, Metabolismus und elektrische kortikale Funktion während schrittweiser Verminderung der zerebralen Perfusion durch intrakranielle Drucksteigerung untersucht. Die Hypothermie verursacht eine signifikante Reduktion der zerebralen Durchblutung bei gleichzeitiger stärker ausgeprägter Verminderung des zerebralen Sauerstoffmetabolismus. Während schrittweiser Reduktion der zerebralen Perfusion bleibt die elektrische kortikale Funktion auf reduziertem Niveau im Vergleich zur Normothermie länger erhalten, während Unterschiede in zerebraler Durchblutung und zerebralem Metabolismus bei Reduktion des CPP auf 30% des Ausgangsniveaus nicht mehr nachweisbar sind.

Die komplexe traumatische Schädigung des kindlichen Gehirns wurde am 6-Wochen alten Ferkel mit einem flüssigkeitsinduzierten Perkussionsmodell mit sekundärer Schädigung durch temporären Blutentzug untersucht. Mit diesem Modell sind bei schwerer Schädigung nach 24 Stunden histopathologisch diffuse Hirnschäden nachweisbar. Insbesondere bei Tieren, die einen sekundären Hirndruckanstieg entwickeln, lässt sich ein beinahe kompletter Ausfall von immunhistochemischen Markern wie MAP2-Protein nachweisen. Das ßAPP ist bei diesen Tieren verstärkt bis hin zu „Retraction balls“ nachweisbar, ebenso wie ein hoher Anteil an nekrotischen Nervenzellen in der TUNEL-Färbung.

Im Gegensatz dazu ist die Hypothermie offensichtlich in der Lage, Hirndruckanstiege zu vermeiden und somit den histopathologischen Schaden nach 24 Stunden zu reduzieren. Ob die Hypothermie jedoch auch direkt den histopathologischen Schaden zu reduzieren vermag, lässt sich aus diesen Experimenten nicht ableiten.

In einem weiteren Experiment wurde der Einfluss der milden Hypothermie auf die Perfusion intestinaler Organe untersucht. So sind Niere, Pankreas, Milz und Darm während der Hypothermie geringer durchblutet, während die arterielle hepatische Durchblutung unverändert bleibt. Dennoch wird die Metabolisierung von Fentanyl erheblich verlangsamt. Es kommt während 6-stündiger Hypothermie zu einer 25%igen Erhöhung des Fentanyl-Plasmaspiegels. Auch nach Wiedererwärmung bleibt der Fentanyl-Plasmaspiegel noch mindestens 6 Stunden erhöht. Diese

verminderte Metabolisierung während Hypothermie ist assoziiert mit einer verminderten Aktivität der mikrosomalen CYP3A4-Isoform des Cytochrom P 450, was wesentlich für die Metabolisierung von Fentanyl bedeutsam ist.

8. Literaturverzeichnis

1. Abou-Hamden A, Blumbergs PC, Scott G, Manavis J, Wainwright H, Jones N, McLean J: Axonal injury in falls. J Neurotrauma 14 (1997) 699-713

2. Adams JH, Doyle D, Ford I, Gennarelli TA, Graham DI, McLellan DR: Diffuse axonal injury in head injury: definition, diagnosis and grading. Histopathology 15 (1989) 49-59

3. Adelson PD: Pediatric trauma made simple. Clin Neurosurg 47 (2000) 319-335

4. Adelson PD: Animal models of traumatic brain injury in the immature: a review. Exp Toxic Pathol 51 (1999) 130-136

5. Adelson PD, Bratton SL, Carney NA, Chesnut RM, du Coudray HE, Goldstein B, Kochanek PM et al.: Guidelines for the acute medical management of severe traumatic brain injury in infants, children, and adolescents. Chapter 1: Introduction. Pediatr Crit Care Med 4 (2003) S2-S4

6. Adelson PD, Clyde B, Kochanek PM, Wisniewski SR, Marion DW, Yonas H: Cerebrovascular response in infants and young children following severe traumatic brain injury: a preliminary report. Pediatr Neurosurg 26 (1997) 200-207

7. Adelson PD, Jenkins LW, Hamilton RL, Robichaud P, Tran MP, Kochanek PM: Histopathologic response of the immature rat to diffuse traumatic brain injury. J Neurotrauma 18 (2001) 967-976

8. Adelson PD, Ragheb J, Kanev P, Brockmeyer D, Beers SR, Brown SD, Cassidy LD et al.: Phase II clinical trial of moderate hypothermia after severe traumatic brain injury in children. Neurosurgery 56 (2005) 740-754

9. Adelson PD, Whalen MJ, Kochanek PM, Robichaud P, Carlos TM: Blood brain barrier permeability and acute inflammation in two models of traumatic brain injury in the immature rat: a preliminary report. Acta Neurochir Suppl 71 (1998) 104-106

10. Aldrich EF, Eisenberg HM, Saydjari C, Luerssen TG, Foulkes MA, Jane JA, Marshall LF et al.: Diffuse brain swelling in severely head-injured children. A report from the NIH Traumatic Coma Data Bank. J Neurosurg 76 (1992) 450-454

11. Amiry-Moghaddam M, Ottersen OP: The molecular basis of water transport in the brain. Nat Rev Neurosci 4 (2003) 991-1001

12. Armstead WM: Hypotension dilates pial arteries by KATP and kca channel activation. Brain Res 816 (1999) 158-164

13. Armstead WM, Kurth CD: Different cerebral hemodynamic responses following fluid percussion brain injury in the newborn and juvenile pig. J Neurotrauma 11 (1994) 487-497

14. Bacher A, Kwon JY, Zornow MH: Effects of temperature on cerebral tissue oxygen tension, carbon dioxide tension, and pH during transient global ischemia in rabbits. Anesthesiology 88 (1998) 403-409

15. Bauer R, Bergmann R, Walter B, Brust P, Zwiener U, Johannsen B: Regional distribution of cerebral blood volume and cerebral blood flow in newborn piglets--effect of hypoxia/hypercapnia. Brain Res Dev Brain Res 112 (1999) 89-98

16. Bauer R, Fritz H: Pathophysiology of traumatic injury in the developing brain: an introduction and short update. Exp Toxicol Pathol 56 (2004) 65-73

17. Bauer R, Fritz H, Walter B, Schlonski O, Jochum T, Hoyer D, Zwiener U et al.: Effect of mild hypothermia on cerebral oxygen uptake during gradual cerebral perfusion pressure decrease in piglets. Crit Care Med 28 (2000) 1128-1135

18. Bauer R, Hoyer D, Walter B, Gaser E, Kluge H, Zwiener U: Changed systemic and cerebral hemodynamics and Oxygen supply due to gradual hemorrhagic hypotension induced by an external PID-Controller in newborn swine. Exp Toxic Pathol 49 (1997) 469-476

19. Bauer R, Walter B, Torossian A, Fritz H, Schlonski O, Jochum T, Hoyer D et al.: A Piglet Model for Evaluation of Cerebral Blood Flow and Brain Oxidative Metabolism during Gradual Cerebral Perfusion Pressure Decrease. Pediatr Neurosurg 30 (1999) 62-69

20. Bayir H, Kochanek PM, Clark RS: Traumatic brain injury in infants and children: mechanisms of secondary damage and treatment in the intensive care unit. Crit Care Clin 19 (2003) 529-549

21. Bernard SA, Gray TW, Buist MD, Jones BM, Silvester W, Gutteridge G, Smith K: Treatment of comatose survivors of out-of-hospital cardiac arrest with induced hypothermia. N Engl J Med 346 (2002) 557-563

22. Bigelow WG, Lindsay WK, Greenwood WF: Hypothermia. its possible role in cardiac surgery: an investigation of factors govering survival of dogs at low body temperatures. Ann Surg 132 (1950)

23. Bischoff P: [Perioperative EEG monitoring: studies of the electrophysiological arousal mechanism]. Anasthesiol Intensivmed Notfallmed Schmerzther 29 (1994) 322-329

24. Biswas AK, Bruce DA, Sklar FH, Bokovoy JL, Sommerauer JF: Treatment of acute traumatic brain injury in children with moderate hypothermia improves intracranial hypertension. Crit Care Med 30 (2002) 2742-2751

25. Bittigau P, Sifringer M, Pohl D, Stadthaus D, Ishimaru M, Shimizu H, Ikeda M et al.: Apoptotic neurodegeneration following trauma is markedly enhanced in the immature brain. Ann Neurol 45 (1999) 724-735

26. Bjorkman S, Wada DR, Stanski DR: Application of physiologic models to predict the influence of changes in body composition and blood flows on the pharmacokinetics of fentanyl and alfentanil in patients. Anesthesiology 88 (1998) 657-667

27. Brambrink AM: Die Primärversorung des kindlichen Schädel-Hirn-Traumas aus der Sicht des Notarztes. Notfall & Rettungsmedizin 5 (2002) 332-335

28. Bramlett HM, Dietrich WD, Green EJ, Busto R: Chronic histopathological consequences of fluid-percussion brain injury in rats: effects of post-traumatic hypothermia. Acta Neuropathol (Berl) 93 (1997) 190-199

29. Bramlett HM, Green EJ, Dietrich WD, Busto R, Globus MY, Ginsberg MD: Posttraumatic brain hypothermia provides protection from sensorimotor and cognitive behavioral deficits. J Neurotrauma 12 (1995) 289-298

30. Brodhun M, Fritz H, Walter B, Antonow-Schlorke I, Reinhart K, Zwiener U, Bauer R et al.: Immunomorphological sequelae of severe brain injury induced by fluid- percussion in juvenile pigs--effects of mild hypothermia. Acta Neuropathol (Berl) 101 (2001) 424-434

31. Brown FK: Cardiovascular effects of acutely raised intracranial pressure. Am J Physiol 185 (1956) 510-514

32. Burnashev N, Schoepfer R, Monyer H, Ruppersberg JP, Gunther W, Seeburg PH, Sakmann B: Control by asparagine residues of calcium permeability and magnesium blockade in the NMDA receptor. Science 257 (1992) 1415-1419

33. Busija DW, Leffler CW: Hypothermia reduces cerebral metabolic rate and cerebral blood flow in newborn pigs. Am J Physiol 253 (1987) H869-H873

34. Busija DW, Leffler CW, Pourcyrous M: Hyperthermia increases cerebral metabolic rate and blood flow in neonatal pigs. Am J Physiol 255 (1988) H343-H346

35. Busto R, Dietrich WD, Globus MY, Valdes I, Scheinberg P, Ginsberg MD: Small differences in intraischemic brain temperature critically determine the extent of ischemic neuronal injury. J Cereb Blood Flow Metab 7 (1987) 729-738

36. Celcius, A. C.: De Medicina. Übersetzung: Spencer WG, Loeb Classical Library, (1Jh.n. Chr.)

37. Chi OZ, Liu X, Weiss HR: Effects of mild hypothermia on blood-brain barrier disruption during isoflurane or pentobarbital anesthesia. Anesthesiology 95 (2001) 933-938

38. Clark RS, Kochanek PM, Dixon CE, Chen M, Marion DW, Heineman S, DeKosky ST et al.: Early neuropathologic effects of mild or moderate hypoxemia after controlled cortical impact injury in rats. J Neurotrauma 14 (1997) 179-189

39. Clifton GL, Allen S, Barrodale P, Plenger P, Berry J, Koch S, Fletcher J et al.: A phase II study of moderate hypothermia in severe brain injury. J Neurotrauma 10 (1993) 263-271

40. Clifton GL, Miller ER, Choi SC, Levin HS, McCauley S, Smith KR, Jr., Muizelaar JP et al.: Hypothermia on admission in patients with severe brain injury. J Neurotrauma 19 (2002) 293-301

41. Clifton GL, Miller ER, Choi SC, Levin HS, McCauley S, Smith KR, Jr., Muizelaar JP et al.: Lack of effect of induction of hypothermia after acute brain injury. N Engl J Med 344 (2001) 556-563

42. Coimbra C, Wieloch T: Moderate hypothermia mitigates neuronal damage in the rat brain when initiated several hours following transient cerebral ischemia. Acta Neuropathol (Berl) 87 (1994) 325-331

43. Colbourne F, Corbett D: Delayed and prolonged post-ischemic hypothermia is neuroprotective in the gerbil. Brain Res 654 (1994) 265-272

44. Conti AC, Raghupathi R, Trojanowski JQ, McIntosh TK: Experimental brain injury induces regionally distinct apoptosis during the acute and delayed post-traumatic period. J Neurosci 18 (1998) 5663-5672

45. Corbett D, Hamilton M, Colbourne F: Persistent neuroprotection with prolonged postischemic hypothermia in adult rats subjected to transient middle cerebral artery occlusion. Exp Neurol 163 (2000) 200-206

46. Dawson DA, Hallenbeck JM: Acute focal ischemia-induced alterations in MAP2 immunostaining: description of temporal changes and utilization as a marker for volumetric assessment of acute brain injury. J Cereb Blood Flow Metab 16 (1996) 170-174

47. Dietrich WD, Alonso O, Busto R, Globus MY, Ginsberg MD: Post-traumatic brain hypothermia reduces histopathological damage following concussive brain injury in the rat. Acta Neuropathol Berl 87 (1994) 250-258

48. Dirnagl U, Iadecola C, Moskowitz MA: Pathobiology of ischaemic stroke: an integrated view. Trends Neurosci 22 (1999) 391-397

49. Dixon CE, Lyeth BG, Povlishock JT, Findling RL, Hamm RJ, Marmarou A, Young HF et al.: A fluid percussion model of experimental brain injury in the rat. J Neurosurg 67 (1987) 110-119

50. Dixon CE, Markgraf CG, Angileri F, Pike BR, Wolfson B, Newcomb JK, Bismar MM et al.: Protective effects of moderate hypothermia on behavioral deficits but not necrotic cavitation following cortical impact injury in the rat. J Neurotrauma 15 (1998) 95-103

51. Dobbing J: The later development of the brain and its vulnerability.In:Davis JA, Dobbing J (Eds): Scientific foundations of pediatrics Heinemann, London 1983, S.744-759

52. Doppenberg EM, Bullock R: Clinical neuro-protection trials in severe traumatic brain injury: lessons from previous studies. J Neurotrauma 14 (1997) 71-80

53. Drake CG, Barr WK, Coles JC, Gergely NF: The use of extracorporal circulation and profound hypothermia in the treatment of ruptured intracranial aneurysm. J Neurosurg 21 (1964) 575-581

54. Duhaime AC: Why are clinical trials in pediatric head injury so difficult? Pediatr Crit Care Med 8 (2007) 71

55. Duhaime AC, Margulies SS, Durham SR, O'Rourke MM, Golden JA, Marwaha S, Raghupathi R: Maturation-dependent response of the piglet brain to scaled cortical impact. J Neurosurg 93 (2000) 455-462

56. Duhaime AC, Saykin AJ, McDonald BC, Dodge CP, Eskey CJ, Darcey TM, Grate LL et al.: Functional magnetic resonance imaging of the primary somatosensory cortex in piglets. J Neurosurg 104 (2006) 259-264

57. Eberspacher E, Werner C, Engelhard K, Pape M, Gelb A, Hutzler P, Henke J et al.: The effect of hypothermia on the expression of the apoptosis-regulating protein Bax after incomplete cerebral ischemia and reperfusion in rats. J Neurosurg Anesthesiol 15 (2003) 200-208

58. Eberspacher E, Werner C, Engelhard K, Pape M, Laacke L, Winner D, Hollweck R et al.: Long-term effects of hypothermia on neuronal cell death and the concentration of apoptotic proteins after incomplete cerebral ischemia and reperfusion in rats. Acta Anaesthesiol Scand 49 (2005) 477-487

59. Erecinska M, Silver IA: Tissue oxygen tension and brain sensitivity to hypoxia. Respir Physiol 128 (2001) 263-276

60. Erecinska M, Thoresen M, Silver IA: Effects of hypothermia on energy metabolism in Mammalian central nervous system. J Cereb Blood Flow Metab 23 (2003) 513-530

61. Fay T: Observations on generalized refrigeration in cases of severe cerebral trauma. Assoc Res Nerv Men Dis Proc 24 (1945) 611-619

62. Feeney DM, Boyeson MG, Linn RT, Murray HM, Dail WG: Responses to cortical injury: I. Methodology and local effects of contusions in the rat. Brain Res 211 (1981) 67-77

63. Feher G, Schulte ML, Weigle CG, Kampine JP, Hudetz AG: Postnatal remodeling of the leptomeningeal vascular network as assessed by intravital fluorescence video-microscopy in the rat. Brain Res Dev Brain Res 91 (1996) 209-217

64. Feickert HJ, Drommer S, Heyer R: Severe head injury in children: impact of risk factors on outcome. J Trauma 47 (1999) 33-38

65. Felderhoff-Mueser U, Ikonomidou C: Mechanisms of neurodegeneration after paediatric brain injury. Curr Opin Neurol 13 (2000) 141-145

66. Felix B, Leger ME, be-Fessard D, Marcilloux JC, Rampin O, Laplace JP: Stereotaxic atlas of the pig brain. Brain Res Bull 49 (1999) 1-137

67. Fineman I, Giza CC, Nahed BV, Lee SM, Hovda DA: Inhibition of neocortical plasticity during development by a moderate concussive brain injury. J Neurotrauma 17 (2000) 739-749

68. Foda MA, Marmarou A: A new model of diffuse brain injury in rats. Part II: Morphological characterization. J Neurosurg 80 (1994) 301-313

69. Folkerts MM, Berman RF, Muizelaar JP, Rafols JA: Disruption of MAP-2 immunostaining in rat hippocampus after traumatic brain injury. J Neurotrauma 15 (1998) 349-363

70. Fritz H, Bauer R, Walter B, Schlonski O, Hoyer D, Zwiener U, Reinhart K: Hypothermia related changes in electrocortical activity at stepwise increase of intracranial pressure in piglets. Exp Toxicol Pathol 51 (1999) 163-171

71. Fritz HG, Bauer R: Secondary injuries in brain trauma: effects of hypothermia. J Neurosurg Anesthesiol 16 (2004) 43-52

72. Fritz HG, Bauer R: Traumatic injury in the developing brain--effects of hypothermia. Exp Toxicol Pathol 56 (2004) 91-102

73. Fritz HG, Holzmayr M, Walter B, Moeritz KU, Lupp A, Bauer R: The effect of mild hypothermia on plasma fentanyl concentration and biotransformation in juvenile pigs. Anesth Analg 100 (2005) 996-1002

74. Fritz HG, Walter B, Holzmayr M, Brodhun M, Patt S, Bauer R: A pig model with secondary increase of intracranial pressure after severe traumatic brain injury and temporary blood loss. J Neurotrauma 22 (2005) 807-821

75. Galaenus, C.: Opera Omnia (Medicorum Graecorum Opera). Übersetzung: Brock AJ. (129-199 n. Chr.)

76. Gelman S, Reves JG, Harris D: Circulatory responses to midazolam anesthesia: emphasis on canine splanchnic circulation. Anesth Analg 62 (1983) 135-139

77. Gentleman SM, Nash MJ, Sweeting CJ, Graham DI, Roberts GW: Beta-amyloid precursor protein (beta APP) as a marker for axonal injury after head injury. Neurosci Lett 160 (1993) 139-144

78. Giza CC, Prins ML, Hovda DA, Herschman HR, Feldman JD: Genes preferentially induced by depolarization after concussive brain injury: effects of age and injury severity. J Neurotrauma 19 (2002) 387-402

79. Globus MY, Alonso O, Dietrich WD, Busto R, Ginsberg MD: Glutamate release and free radical production following brain injury: effects of posttraumatic hypothermia. J Neurochem 65 (1995) 1704-1711

80. Globus MY, Busto R, Dietrich WD, Martinez E, Valdes I, Ginsberg MD: Effect of ischemia on the in vivo release of striatal dopamine, glutamate, and gamma-aminobutyric acid studied by intracerebral microdialysis. J Neurochem 51 (1988) 1455-1464

81. Gluckman PD, Wyatt JS, Azzopardi D, Ballard R, Edwards AD, Ferriero DM, Polin RA et al.: Selective head cooling with mild systemic hypothermia after neonatal encephalopathy: multicentre randomised trial. Lancet 365 (2005) 663-670

82. Gopinath SP, Robertson CS: Management of Severe Head Injury.In:Cotrell JE, Smith DS (Eds): Anesthesia and Neurosurgery Mosby - Year Book Inc., St.Louis 1994, S.661-684

83. Grundl PD, Biagas KV, Kochanek PM, Schiding JK, Barmada MA, Nemoto EM: Early cerebrovascular response to head injury in immature and mature rats. J Neurotrauma 11 (1994) 135-148

84. Gunn AJ, Gluckman PD, Gunn TR: Selective head cooling in newborn infants after perinatal asphyxia: a safety study. Pediatrics 102 (1998) 885-892

85. Gurkoff GG, Giza CC, Hovda DA: Lateral fluid percussion injury in the developing rat causes an acute, mild behavioral dysfunction in the absence of significant cell death. Brain Res 1077 (2006) 24-36

86. Hallam TM, Floyd CL, Folkerts MM, Lee LL, Gong QZ, Lyeth BG, Muizelaar JP et al.: Comparison of behavioral deficits and acute neuronal degeneration in rat lateral fluid percussion and weight-drop brain injury models. J Neurotrauma 21 (2004) 521-539

87. Hara A, Yoshimi N, Mori H, Iwai T, Sakai N, Yamada H, Niwa M: Hypothermic prevention of nuclear DNA fragmentation in gerbil hippocampus following transient forebrain ischemia. Neurol Res 17 (1995) 461-464

88. Hicks R, Soares H, Smith D, McIntosh T: Temporal and spatial characterization of neuronal injury following lateral fluid-percussion brain injury in the rat. Acta Neuropathol (Berl) 91 (1996) 236-246

89. Hicks RR, Smith DH, McIntosh TK: Temporal response and effects of excitatory amino acid antagonism on microtubule-associated protein 2 immunoreactivity following experimental brain injury in rats. Brain Res 678 (1995) 151-160

90. Hippokrates: De Verete Medicina. Übersetzung: Jones WHS, Withington ET, Loeb Classical Library, (460- 375 v. Chr.)

91. Hiramatsu T, Miura T, Forbess JM, Du PA, Aoki M, Nomura F, Holtzman D et al.: pH strategies and cerebral energetics before and after circulatory arrest. J Thorac Cardiovasc Surg 109 (1995) 948-957

92. Horiguchi T, Shimizu K, Ogino M, Suga S, Inamasu J, Kawase T: Postischemic hypothermia inhibits the generation of hydroxyl radical following transient forebrain ischemia in rats. J Neurotrauma 20 (2003) 511-520

93. Hoyer D, Bauer R, Walter B, Zwiener U: Adjustment of reduced arterial blood pressure--a tool for investigations into gradually reduced brain function. Biomed Tech (Berl) 42 (1997) 284-290

94. Huang ZG, Xue D, Preston E, Karbalai H, Buchan AM: Biphasic opening of the blood-brain barrier following transient focal ischemia: effects of hypothermia. Can J Neurol Sci 26 (1999) 298-304

95. Iida Y, Nishi S, Asada A: Effect of mild therapeutic hypothermia on phenytoin pharmacokinetics. Ther Drug Monit 23 (2001) 192-197

96. Ikonomidou C, Qin Y, Labruyere J, Kirby C, Olney JW: Prevention of trauma-induced neurodegeneration in infant rat brain. Pediatr Res 39 (1996) 1020-1027

97. Ip EY, Giza CC, Griesbach GS, Hovda DA: Effects of enriched environment and fluid percussion injury on dendritic arborization within the cerebral cortex of the developing rat. J Neurotrauma 19 (2002) 573-585

98. Ishige N, Pitts LH, Hashimoto T, Nishimura MC, Bartkowski HM: Effect of hypoxia on traumatic brain injury in rats: Part 1. Changes in neurological function, electroencephalograms, and histopathology. Neurosurgery 20 (1987) 848-853

99. Ito J, Marmarou A, Barzo P, Fatouros P, Corwin F: Characterization of edema by diffusion-weighted imaging in experimental traumatic brain injury. J Neurosurg 84 (1996) 97-103

100. Jiang JY, Xu W, Li WP, Gao GY, Bao YH, Liang YM, Luo QZ: Effect of long-term mild hypothermia or short-term mild hypothermia on outcome of patients with severe traumatic brain injury. J Cereb Blood Flow Metab 26 (2006) 771-776

101. Jones TA, Lawrence AF, Bickford RG: Serotonin depletion prevents electrocortical synchronization following acute midbrain deactivation. Electroencephalogr Clin Neurophysiol 55 (1983) 203-211

102. Karibe H, Chen SF, Zarow GJ, Gafni J, Graham SH, Chan PH, Weinstein PR: Mild intraischemic hypothermia suppresses consumption of endogenous antioxidants after temporary focal ischemia in rats. Brain Res 649 (1994) 12-18

103. Kataoka K, Yanase H: Mild hypothermia--a revived countermeasure against ischemic neuronal damages. Neurosci Res 32 (1998) 103-117

104. Kearse LA, Jr., Koski G, Husain MV, Philbin DM, McPeck K: Epileptiform activity during opioid anesthesia. Electroencephalogr Clin Neurophysiol 87 (1993) 374-379

105. Kelley SD, Cauldwell CB, Fisher DM, Lau M, Sharma ML, Weisiger RA: Recovery of hepatic drug extraction after hypothermic preservation. Anesthesiology 82 (1995) 251-258

106. Kitagawa K, Matsumoto M, Niinobe M, Mikoshiba K, Hata R, Ueda H, Handa N et al.: Microtubule-associated protein 2 as a sensitive marker for cerebral ischemic damage--immunohistochemical investigation of dendritic damage. Neuroscience 31 (1989) 401-411

107. Klatzko I: Neuropathological aspects of brain edema. Journal of Neuropathology and Experimental Neurology 26 (1967) 115-118

108. Klinger W, Muller D: Ethylmorphine-N-demethylation by liver homogenate of newborn and adult rats; Enzyme kinetics and age course of Vmax and Km1. Acta Biol Med Ger 36 (1977) 1149-1159

109. Koizumi H, Povlishock JT: Posttraumatic hypothermia in the treatment of axonal damage in an animal model of traumatic axonal injury. J Neurosurg 89 (1998) 303-309

110. Konrad K, Gauggel S, Manz A, Scholl M: Inhibitory control in children with traumatic brain injury (TBI) and children with attention deficit/hyperactivity disorder (ADHD). Brain Inj 14 (2000) 859-875

111. Koren G, Barker C, Goresky G, Bohn D, Kent G, Klein J, MacLeod SM et al.: The influence of hypothermia on the disposition of fentanyl--human and animal studies. Eur J Clin Pharmacol 32 (1987) 373-376

112. Koskiniemi M, Kyykka T, Nybo T, Jarho L: Long-term outcome after severe brain injury in preschoolers is worse than expected. Arch Pediatr Adolesc Med 149 (1995) 249-254

113. Kowallik P, Schulz R, Guth BD, Schade A, Paffhausen W, Gross R, Heusch G: Measurement of regional myocardial blood flow with multiple colored microspheres. Circulation 83 (1991) 974-982

114. Kraus JF, Fife D, Conroy C: Pediatric brain injuries: the nature, clinical course, and early outcomes in a defined United States' population. Pediatrics 79 (1987) 501-507

115. Kuboyama K, Safar P, Radovsky A, Tisherman SA, Stezoski SW, Alexander H: Delay in cooling negates the beneficial effect of mild resuscitative cerebral hypothermia after cardiac arrest in dogs: a prospective, randomized study. Crit Care Med 21 (1993) 1348-1358

116. Kurth CD, O'Rourke MM, O'Hara IB, Uher B: Brain cooling efficiency with pH-stat and alpha-stat cardiopulmonary bypass in newborn pigs. Circulation 96 (1997) II-63

117. Labroo RB, Paine MF, Thummel KE, Kharasch ED: Fentanyl metabolism by human hepatic and intestinal cytochrome P450 3A4: implications for interindividual variability in disposition, efficacy, and drug interactions. Drug Metab Dispos 25 (1997) 1072-1080

118. Larrey, I. J.: Memoirs of the military service and campaigns of the French armies. vol.2 Baltimore (1814)156-164

119. Leslie K, Sessler DI, Bjorksten AR, Moayeri A: Mild hypothermia alters propofol pharmacokinetics and increases the duration of action of atracurium. Anesth Analg 80 (1995) 1007-1014

120. Levin HS, Aldrich EF, Saydjari C, Eisenberg HM, Foulkes MA, Bellefleur M, Luerssen TG et al.: Severe head injury in children: experience of the Traumatic Coma Data Bank. Neurosurgery 31 (1992) 435-443

121. Lewis SB, Finnie JW, Blumbergs PC, Scott G, Manavis J, Brown C, Reilly PL et al.: A head impact model of early axonal injury in the sheep. J Neurotrauma 13 (1996) 505-514

122. Lighthall JW: Controlled cortical impact: a new experimental brain injury model. J Neurotrauma 5 (1988) 1-15

123. Linhart O, Formanek J, Nadvornik F: Experimental epidural brain compression. Acta Univ Carol [Med] (Praha) 20 (1974) 497-547

124. Liu L, Yenari MA: Therapeutic hypothermia: neuroprotective mechanisms. Front Biosci 12 (2007) 816-825

125. Lownie SP, Gelb AW: Cerebral Metabolism: Basic Considerations.In:Sebel PS, Fitch W (Eds): Monitoring the Central Nervous System Blackwell Science, Oxford 1994, S.1-25

126. Maier CM, Sun GH, Kunis D, Yenari MA, Steinberg GK: Delayed induction and long-term effects of mild hypothermia in a focal model of transient cerebral ischemia: neurological outcome and infarct size. J Neurosurg 94 (2001) 90-96

127. Malhotra AK, Schweitzer JB, Fox JL, Fabian TC, Proctor KG: Cerebral perfusion pressure directed therapy following traumatic brain injury and hypotension in swine. J Neurotrauma 20 (2003) 827-839

128. Malhotra AK, Schweitzer JB, Fox JL, Fabian TC, Proctor KG: Cerebral perfusion pressure elevation with oxygen-carrying pressor after traumatic brain injury and hypotension in Swine. J Trauma 56 (2004) 1049-1057

129. Mansfield RT, Schiding JK, Hamilton RL, Kochanek PM: Effects of hypothermia on traumatic brain injury in immature rats. J Cereb Blood Flow Metab 16 (1996) 244-252

130. Margulies SS, Thibault KL: Infant skull and suture properties: measurements and implications for mechanisms of pediatric brain injury. J Biomech Eng 122 (2000) 364-371

131. Marion DW, Penrod LE, Kelsey SF, Obrist WD, Kochanek PM, Palmer AM, Wisniewski SR et al.: Treatment of traumatic brain injury with moderate hypothermia. N Engl J Med 336 (1997) 540-546

132. Markgraf CG, Clifton GL, Moody MR: Treatment window for hypothermia in brain injury. J Neurosurg 95 (2001) 979-983

133. Marmarou A, Foda MA, van den BW, Campbell J, Kita H, Demetriadou K: A new model of diffuse brain injury in rats. Part I: Pathophysiology and biomechanics. J Neurosurg 80 (1994) 291-300

134. Matsushita Y, Bramlett HM, Alonso O, Dietrich WD: Posttraumatic hypothermia is neuroprotective in a model of traumatic brain injury complicated by a secondary hypoxic insult. Crit Care Med 29 (2001) 2060-2066

135. Maxwell WL, Donnelly S, Sun X, Fenton T, Puri N, Graham DI: Axonal cytoskeletal responses to nondisruptive axonal injury and the short-term effects of posttraumatic hypothermia. J Neurotrauma 16 (1999) 1225-1234

136. Maxwell WL, Watson A, Queen R, Conway B, Russell D, Neilson M, Graham DI: Slow, medium, or fast re-warming following post-traumatic hypothermia therapy? An ultrastructural perspective. J Neurotrauma 22 (2005) 873-884

137. McAllister RG, Jr., Tan TG: Effect of hypothermia on drug metabolism. In vitro studies with propranolol and verapamil. Pharmacology 20 (1980) 95-100

138. McClain DA, Hug CC, Jr.: Intravenous fentanyl kinetics. Clin Pharmacol Ther 28 (1980) 106-114

139. McIntosh TK, Vink R, Noble L, Yamakami I, Fernyak S, Soares H, Faden AL: Traumatic brain injury in the rat: characterization of a lateral fluid-percussion model. Neuroscience 28 (1989) 233-244

140. McKenzie KJ, McLellan DR, Gentleman SM, Maxwell WL, Gennarelli TA, Graham DI: Is beta-APP a marker of axonal damage in short-surviving head injury? Acta Neuropathol (Berl) 92 (1996) 608-613

141. McKirnan MD, White FC, Guth BD, Bloor CM: Exercise and Hemodynamic Studies in Swine.In:Stanton HC, Mersmann HJ (Eds): Swine in Cardiovascular Research CRC Press, Boca Raton 1986, S.105-120

142. Metz C, Holzschuh M, Bein T, Woertgen C, Frey A, Frey I, Taeger K et al.: Moderate hypothermia in patients with severe head injury: cerebral and extracerebral effects. J Neurosurg 85 (1996) 533-541

143. Michenfelder JD, Milde JH: The relationship among canine brain temperature, metabolism, and function during hypothermia. Anesthesiology 75 (1991) 130-136

144. Michiels M, Hendriks R, Heykants J: A sensitive radioimmunoassay for fentanyl. Plasma level in dogs and man. Eur J Clin Pharmacol 12 (1977) 153-158

145. Murakami K, Kawase M, Kondo T, Chan PH: Cellular accumulation of extravasated serum protein and DNA fragmentation following vasogenic edema. J Neurotrauma 15 (1998) 825-835

146. Nakamura T, Miyamoto O, Yamagami S, Hayashida Y, Itano T, Nagao S: Influence of rewarming conditions after hypothermia in gerbils with transient forebrain ischemia. J Neurosurg 91 (1999) 114-120

147. Narayan RK, Michel ME, Ansell B, Baethmann A, Biegon A, Bracken MB, Bullock MR et al.: Clinical trials in head injury. J Neurotrauma 19 (2002) 503-557

148. Nemoto EM, Klementavicius R, Melick JA, Yonas H: Suppression of cerebral metabolic rate for oxygen (CMRO2) by mild hypothermia compared with thiopental. J Neurosurg Anesthesiol 8 (1996) 52-59

149. Newcomb JK, Zhao X, Pike BR, Hayes RL: Temporal profile of apoptotic-like changes in neurons and astrocytes following controlled cortical impact injury in the rat. Exp Neurol 158 (1999) 76-88

150. Nilsson F, Akeson J, Messeter K, Ryding E, Rosen I, Nordstrom CH: A porcine model for evaluation of cerebral haemodynamics and metabolism during increased intracranial pressure. Acta Anaesthesiol Scand 39 (1995) 827-834

151. Niwa M, Hara A, Iwai T, Nakashima M, Yano H, Yoshimi N, Mori H et al.: Relationship between magnitude of hypothermia during ischemia and preventive effect against post-ischemic DNA fragmentation in the gerbil hippocampus. Brain Res 794 (1998) 338-342

152. Oehmichen M, Meissner C, Schmidt V, Pedal I, Konig HG, Saternus KS: Axonal injury--a diagnostic tool in forensic neuropathology? A review. Forensic Sci Int 95 (1998) 67-83

153. Ommaya AK, Goldsmith W, Thibault L: Biomechanics and neuropathology of adult and paediatric head injury. Br J Neurosurg 16 (2002) 220-242

154. Osteen CL, Moore AH, Prins ML, Hovda DA: Age-dependency of 45calcium accumulation following lateral fluid percussion: acute and delayed patterns. J Neurotrauma 18 (2001) 141-162

155. Palmer AM, Marion DW, Botscheller ML, Redd EE: Therapeutic hypothermia is cytoprotective without attenuating the traumatic brain injury-induced elevations in interstitial concentrations of aspartate and glutamate. J Neurotrauma 10 (1993) 363-372

156. Pannen BH, Loop T: [Evidence-based intensive care treatment of intracranial hypertension after traumatic brain injury]. Anaesthesist 54 (2005) 127-136

157. Pfenninger EG, Reith A, Breitig D, Grunert A, Ahnefeld FW: Early changes of intracranial pressure, perfusion pressure, and blood flow after acute head injury. Part 1: An experimental study of the underlying pathophysiology. J Neurosurg 70 (1989) 774-779

158. Pfenninger J, Santi A: Severe traumatic brain injury in children--are the results improving? Swiss Med Wkly 132 (2002) 116-120

159. Phanithi PB, Yoshida Y, Santana A, Su M, Kawamura S, Yasui N: Mild hypothermia mitigates post-ischemic neuronal death following focal cerebral ischemia in rat brain: immunohistochemical study of Fas, caspase-3 and TUNEL. Neuropathology 20 (2000) 273-282

160. Pierce JE, Trojanowski JQ, Graham DI, Smith DH, McIntosh TK: Immunohistochemical characterization of alterations in the distribution of amyloid precursor proteins and beta-amyloid peptide after experimental brain injury in the rat. J Neurosci 16 (1996) 1083-1090

161. Polderman KH: Application of therapeutic hypothermia in the intensive care unit. Opportunities and pitfalls of a promising treatment modality--Part 2: Practical aspects and side effects. Intensive Care Med 30 (2004) 757-769

162. Polderman KH, Tjong Tjin JR, Peerdeman SM, Vandertop WP, Girbes AR: Effects of therapeutic hypothermia on intracranial pressure and outcome in patients with severe head injury. Intensive Care Med 28 (2002) 1563-1573

163. Povlishock JT, Christman CW: The pathobiology of traumatically induced axonal injury in animals and humans: a review of current thoughts. J Neurotrauma 12 (1995) 555-564

164. Povlishock JT, Hayes RL, Michel ME, McIntosh TK: Workshop on animal models of traumatic brain injury. J Neurotrauma 11 (1994) 723-732

165. Povlishock JT, Jenkins LW: Are the pathobiological changes evoked by traumatic brain injury immediate and irreversible? Brain Pathol 5 (1995) 415-426

166. Pownall R, Dalton RG: Blood and plasma volumes of neonatal pigs expressed relative to bodyweight and total body water. Br Vet J 129 (1973) 583-588

167. Prins ML, Hovda DA: Developing experimental models to address traumatic brain injury in children. J Neurotrauma 20 (2003) 123-137

168. Prins ML, Hovda DA: Traumatic brain injury in the developing rat: effects of maturation on Morris water maze acquisition. J Neurotrauma 15 (1998) 799-811

169. Prins ML, Lee SM, Cheng CL, Becker DP, Hovda DA: Fluid percussion brain injury in the developing and adult rat: a comparative study of mortality, morphology, intracranial pressure and mean arterial blood pressure. Brain Res Dev Brain Res 95 (1996) 272-282

170. Rink A, Fung KM, Trojanowski JQ, Lee VM, Neugebauer E, McIntosh TK: Evidence of apoptotic cell death after experimental traumatic brain injury in the rat. Am J Pathol 147 (1995) 1575-1583

171. Roberts GW, Gentleman SM, Lynch A, Murray L, Landon M, Graham DI: Beta amyloid protein deposition in the brain after severe head injury: implications for the pathogenesis of Alzheimer's disease. J Neurol Neurosurg Psychiatry 57 (1994) 419-425

172. Robertson CL, Clark RS, Dixon CE, Alexander HL, Graham SH, Wisniewski SR, Marion DW et al.: No long-term benefit from hypothermia after severe traumatic brain injury with secondary insult in rats. Crit Care Med 28 (2000) 3218-3223

173. Rosomoff HL, Holaday DA: Cerebral blood flow and cerebral oxygen consumption during hypothermia. Am J Physiol 179 (1954) 85-88

174. Russell D, Royston D, Rees PH, Gupta SK, Kenny GN: Effect of temperature and cardiopulmonary bypass on the pharmacokinetics of remifentanil. Br J Anaesth 79 (1997) 456-459

175. Satas S, Haaland K, Thoresen M, Steen PA: MAC for halothane and isoflurane during normothermia and hypothermia in the newborn piglets. Acta Anaesthesiol Scand 40 (1995) 452-456

176. Sato M, Chang E, Igarashi T, Noble LJ: Neuronal injury and loss after traumatic brain injury: time course and regional variability. Brain Res 917 (2001) 45-54

177. Schmidt RF: Integrative Leistung des Zentralnervensystems.In:Schmidt RF, Lang, H., Thews G (Eds): Physiologie des Menschen Springer, Berlin, Heidelberg, New York 2005, S.132-175

178. Scholz J, Steinfath M, Schulz M: Clinical pharmacokinetics of alfentanil, fentanyl and sufentanil. An update. Clin Pharmacokinet 31 (1996) 275-292

179. Schosser R, Arfors KE, Messmer K: MIC-II - a program for the determination of cardiac output, arterio-venous shunt and regional blood flow using the radioactive microsphere method. Comput Programs Biomed 9 (1979) 19-38

180. Schrader H, Lofgren J, Zwetnow NN: Regional cerebral blood flow and CSF pressures during the Cushing response induced by an infratentorial expanding mass. Acta Neurol Scand 72 (1985) 273-282

181. Schrader H, Lofgren J, Zwetnow NN: Influence of blood pressure on tolerance to an intracranial expanding mass. Acta Neurol Scand 71 (1985) 114-126

182. Shankaran S, Laptook AR, Ehrenkranz RA, Tyson JE, McDonald SA, Donovan EF, Fanaroff AA et al.: Whole-body hypothermia for neonates with hypoxic-ischemic encephalopathy. N Engl J Med 353 (2005) 1574-1584

183. Sherriff FE, Bridges LR, Sivaloganathan S: Early detection of axonal injury after human head trauma using immunocytochemistry for beta-amyloid precursor protein. Acta Neuropathol (Berl) 87 (1994) 55-62

184. Shiozaki T, Sugimoto H, Taneda M, Yoshida H, Iwai A, Yoshioka T, Sugimoto T: Effect of mild hypothermia on uncontrollable intracranial hypertension after severe head injury. J Neurosurg 79 (1993) 363-368

185. Signoretti S, Marmarou A, Tavazzi B, Lazzarino G, Beaumont A, Vagnozzi R: N-Acetylaspartate reduction as a measure of injury severity and mitochondrial dysfunction following diffuse traumatic brain injury. J Neurotrauma 18 (2001) 977-991

186. Signorini DF, Andrews PJ, Jones PA, Wardlaw JM, Miller JD: Adding insult to injury: the prognostic value of early secondary insults for survival after traumatic brain injury. J Neurol Neurosurg Psychiatry 66 (1999) 26-31

187. Smith DH, Chen XH, Pierce JE, Wolf JA, Trojanowski JQ, Graham DI, McIntosh TK: Progressive atrophy and neuron death for one year following brain trauma in the rat. J Neurotrauma 14 (1997) 715-727

188. Smith SL, Hall ED: Mild pre- and posttraumatic hypothermia attenuates blood-brain barrier damage following controlled cortical impact injury in the rat. J Neurotrauma 13 (1996) 1-9

189. Soliman HM, Melot C, Vincent JL: Sedative and analgesic practice in the intensive care unit: the results of a European survey. Br J Anaesth 87 (2001) 186-192

190. Statler KD, Alexander HL, Vagni VA, Nemoto EM, Tofovic SP, Dixon CE, Jenkins LW et al.: Moderate hypothermia may be detrimental after traumatic brain injury in fentanyl-anesthetized rats. Crit Care Med 31 (2003) 1134-1139

191. Statler KD, Jenkins LW, Dixon CE, Clark RS, Marion DW, Kochanek PM: The simple model versus the super model: translating experimental traumatic brain injury research to the bedside. J Neurotrauma 18 (2001) 1195-1206

192. Steen PA, Newberg L, Milde JH, Michenfelder JD: Hypothermia and barbiturates: individual and combined effects on canine cerebral oxygen consumption. Anesthesiology 58 (1983) 527-532

193. Steriade M, Gloor P, Llinas RR, Lopes de Silva FH, Mesulam MM: Report of IFCN Committee on Basic Mechanisms. Basic mechanisms of cerebral rhythmic activities. Electroencephalogr Clin Neurophysiol 76 (1990) 481-508

194. Stern SA, Zink BJ, Mertz M, Wang X, Dronen SC: Effect of initially limited resuscitation in a combined model of fluid-percussion brain injury and severe uncontrolled hemorrhagic shock. J Neurosurg 93 (2000) 305-314

195. Suehiro E, Singleton RH, Stone JR, Povlishock JT: The immunophilin ligand FK506 attenuates the axonal damage associated with rapid rewarming following posttraumatic hypothermia. Exp Neurol 172 (2001) 199-210

196. Sullivan HG, Martinez J, Becker DP, Miller JD, Griffith R, Wist AO: Fluid-percussion model of mechanical brain injury in the cat. J Neurosurg 45 (1976) 521-534

197. Sun MC, Honey CR, Berk C, Wong NL, Tsui JK: Regulation of aquaporin-4 in a traumatic brain injury model in rats. J Neurosurg 98 (2003) 565-569

198. Takata K, Takeda Y, Sato T, Nakatsuka H, Yokoyama M, Morita K: Effects of hypothermia for a short period on histologic outcome and extracellular glutamate concentration during and after cardiac arrest in rats. Crit Care Med 33 (2005) 1340-1345

199. Tateishi T, Krivoruk Y, Ueng YF, Wood AJ, Guengerich FP, Wood M: Identification of human liver cytochrome P-450 3A4 as the enzyme responsible for fentanyl and sufentanil N-dealkylation. Anesth Analg 82 (1996) 167-172

200. Tempelhoff R, Modica PA, Bernardo KL, Edwards I: Fentanyl-induced electrocorticographic seizures in patients with complex partial epilepsy. J Neurosurg 77 (1992) 201-208

201. The Hypothermia after cardiac arrest study group (HACA): Mild therapeutic hypothermia to improve the neurologic outcome after cardiac arrest. N Engl J Med 346 (2002) 549-556

202. Thibault KL, Margulies SS: Age-dependent material properties of the porcine cerebrum: effect on pediatric inertial head injury criteria. J Biomech 31 (1998) 1119-1126

203. Thompson HJ, Lifshitz J, Marklund N, Grady MS, Graham DI, Hovda DA, McIntosh TK: Lateral fluid percussion brain injury: a 15-year review and evaluation. J Neurotrauma 22 (2005) 42-75

204. Tilford JM, Simpson PM, Yeh TS, Lensing S, Aitken ME, Green JW, Harr J et al.: Variation in therapy and outcome for pediatric head trauma patients. Crit Care Med 29 (2001) 1056-1061

205. Toulmond S, Duval D, Serrano A, Scatton B, Benavides J: Biochemical and histological alterations induced by fluid percussion brain injury in the rat. Brain Res 620 (1993) 24-31

206. Tranquilli WJ, Parks CM, Thurmon JC, Benson GJ, Koritz GD, Manohar M, Theodorakis MC: Organ blood flow and distribution of cardiac output in nonanesthetized swine. Am J Vet Res 43 (1982) 895-897

207. van Zanten AR, Polderman KH: Early induction of hypothermia: will sooner be better? Crit Care Med 33 (2005) 1449-1452

208. Walter B, Bauer R, Gaser E, Zwiener U: Validation of the multiple colored microsphere technique for regional blood flow measurements in newborn piglets. Basic Res Cardiol 92 (1997) 191-200

209. Walter B, Bauer R, Lindner S, Fritz H, Zwiener U: The developing piglet as a model of pediatric head injury. Pflugers Arch - Eur J Physiol 441 (2001) R111

210. Walter B, Brust P, Fuchtner F, Muller M, Hinz R, Kuwabara H, Fritz H et al.: Age-dependent effects of severe traumatic brain injury on cerebral dopaminergic activity in newborn and juvenile pigs. J Neurotrauma 21 (2004) 1076-1089

211. Watanabe T, Orita H, Kobayashi M, Washio M: Brain tissue pH, oxygen tension, and carbon dioxide tension in profoundly hypothermic cardiopulmonary bypass. Comparative study of circulatory arrest, nonpulsatile low-flow perfusion, and pulsatile low-flow perfusion. J Thorac Cardiovasc Surg 97 (1989) 396-401

212. Wen H, Nagelhus EA, miry-Moghaddam M, Agre P, Ottersen OP, Nielsen S: Ontogeny of water transport in rat brain: postnatal expression of the aquaporin-4 water channel. Eur J Neurosci 11 (1999) 935-945

213. Whyte J, Vaccaro M, Grieb-Neff P, Hart T: Psychostimulant use in the rehabilitation of individuals with traumatic brain injury. J Head Trauma Rehabil 17 (2002) 284-299

214. Woolf NJ: A structural basis for memory storage in mammals. Prog Neurobiol 55 (1998) 59-77

215. Xu RX, Nakamura T, Nagao S, Miyamoto O, Jin L, Toyoshima T, Itano T: Specific inhibition of apoptosis after cold-induced brain injury by moderate postinjury hypothermia. Neurosurgery 43 (1998) 107-114

216. Yamamoto M, Marmarou CR, Stiefel MF, Beaumont A, Marmarou A: Neuroprotective effect of hypothermia on neuronal injury in diffuse traumatic brain injury coupled with hypoxia and hypotension. J Neurotrauma 16 (1999) 487-500

217. Yenari MA, Iwayama S, Cheng D, Sun GH, Fujimura M, Morita-Fujimura Y, Chan PH et al.: Mild hypothermia attenuates cytochrome c release but does not alter Bcl-2 expression or caspase activation after experimental stroke. J Cereb Blood Flow Metab 22 (2002) 29-38

218. Zhang Z, Sobel RA, Cheng D, Steinberg GK, Yenari MA: Mild hypothermia increases Bcl-2 protein expression following global cerebral ischemia. Brain Res Mol Brain Res 95 (2001) 75-85

219. Zhao W, Alonso OF, Loor JY, Busto R, Ginsberg MD: Influence of early posttraumatic hypothermia therapy on local cerebral blood flow and glucose metabolism after fluid-percussion brain injury. J Neurosurg 90 (1999) 510-519

9. Anlagen - Der Habilitationsschrift zugrunde liegende Publikationen

(in Klammern: Referenz-Nummern dem Literaturverzeichnis der Arbeit entsprechend)

(70) Fritz H, Bauer R, Walter B, Schlonski O, Hoyer D, Zwiener U, Reinhart K: Hypothermia related changes in electrocortical activity at stepwise increase of intracranial pressure in piglets. Exp Toxicol Pathol 51 (1999) 163-171

(19) Bauer R, Walter B, Torossian A, Fritz H, Schlonski O, Jochum T, Hoyer D et al.: A Piglet Model for Evaluation of Cerebral Blood Flow and Brain Oxidative Metabolism during Gradual Cerebral Perfusion Pressure Decrease. Pediatr Neurosurg 30 (1999) 62-69

(17) Bauer R, Fritz H, Walter B, Schlonski O, Jochum T, Hoyer D, Zwiener U et al.: Effect of mild hypothermia on cerebral oxygen uptake during gradual cerebral perfusion pressure decrease in piglets. Crit Care Med 28 (2000) 1128-1135

(30) Brodhun M, Fritz H, Walter B, Antonow-Schlorke I, Reinhart K, Zwiener U, Bauer R et al.: Immunomorphological sequelae of severe brain injury induced by fluid- percussion in juvenile pigs--effects of mild hypothermia. Acta Neuropathol (Berl) 101 (2001) 424-434

(73) Fritz HG, Holzmayr M, Walter B, Moeritz KU, Lupp A, Bauer R: The effect of mild hypothermia on plasma fentanyl concentration and biotransformation in juvenile pigs. Anesth Analg 100 (2005) 996-1002

(74) Fritz HG, Walter B, Holzmayr M, Brodhun M, Patt S, Bauer R: A pig model with secondary increase of intracranial pressure after severe traumatic brain injury and temporary blood loss. J Neurotrauma 22 (2005) 807-821

Exp Toxic Pathol 1999; **51**: 163–171
URBAN & FISCHER

[1] Clinic for Anaesthesiology and Intensive Care,
[2] TBI and Perinatal Research Group, Institute for Pathophysiology; Friedrich Schiller University, Jena, Germany

Hypothermia related changes in electrocortical activity at stepwise increase of intracranial pressure in piglets

HARALD FRITZ[1], REINHARD BAUER[2], BERND WALTER[2], OLAF SCHLONSKI[2], DIRK HOYER[2], ULRICH ZWIENER[2], and KONRAD REINHART[1]

With 4 figures and 2 tables

Address for correspondence: HARALD FRITZ, M.D., Clinic for Anaesthesiology and Intensive Care, Dept. Neuroanaesthesia, Friedrich Schiller University, D-07740 Jena, Germany; Tel: (+49) 3641-933831; Fax: (+49) 3641-933844; e-mail: fritz@anae1.med.uni-jena.de

Key words: Hypothermia, brain oxygen metabolism; Brain oxygen metabolism, hypothermia; Electrocortical activity; Intracranial pressure; Cerebral blood flow; Electrocorticography; Intracranial pressure.

Summary

Recent experimental studies have demonstrated that mild hypothermia can be effective in the control of intracranial hypertension. However, investigations to analyze the effects of hypothermia on changes in brain oxygen metabolism and electrocortical activity caused by increased intracranial pressure (ICP) are lacking. We examined the effects of mild hypothermia on electrocorticogram (ECoG) in combination with measurement of regional cerebral blood flow (CBF) and estimation of brain oxygen metabolism during stepwise increase of ICP. For this purpose thirteen female piglets (14 days old, 4–5 kg b.w.) were anaesthetized and mechanically ventilated. An epidural balloon was gradually inflated in order to increase ICP to 25 mmHg, 35 mmHg and 45 mmHg every 30 minutes at adjusted mean arterial blood pressures (MAP). This procedure resulted in gradual cerebral perfusion pressure (CPP) reduction of about 70 %, 50 %, and 30 % of baseline [baseline CPP: normothermia (NT) 80 ± 3 mmHg; hypothermia (HT) 84 ± 3 mmHg]. Control animals were maintained in a normothermic state (38.6 ± 0.2 °C). HT animals were surface cooled and maintained at 31.9 ± 0.1 °C. ECoG, regional CBF, cerebral oxygen delivery (cDO_2) and the cerebral metabolic rate of oxygen ($CMRO_2$) were estimated during the normothermic period, after hypothermic stabilization, and after the gradual CPP reductions. The baseline ECoG showed the typical delta-dominated frequency pattern for isoflurane anaesthesia. At the hypothermic level, a frequency shift was seen from delta activity towards the higher frequencies (theta- and alpha activity) and the total spectral power was significantly reduced (56 ± 17 % from baseline, $p < 0.05$). the cortical CBF decreased markedly to 67 ± 10 % ($p < 0.05$), whereas the medulla oblongata blood flow increased slightly. During controlled increase of ICP by regional mass expansion from epidural balloon inflation, we found at mild and moderate stages of ICP increase (25 and 35 mmHg) only minimal changes in the ECoG in hypothermic animals compared to the hypothermic baseline, whereas the ECoG in normothermic animals showed a marked decrease in frequency, amplitude and total spectral power. We conclude that mild hypothermia produces an arousal-like ECoG activity with marked frequency shift to alpha activity and a change from high to low voltage activity. Furthermore, the hypothermic brain showed a preserved neuronal function at moderate stages of ICP. Obviously, hypothermia improves the functional tolerance of the brain to impaired oxygen supply.

Introduction

Traumatic head injury is the leading cause of death in children and young adults (WARD 1996). Obviously, children's brains show respond differently to injuries than adult's brains. The incidence of posttraumatic brain swelling is twice as high in the pediatric population as in the adult (ALDRICH et al. 1992), and is the common cause of an ICP. An initially increased ICP shortly after trauma is of considerable prognostic value and may correlate with adverse outcomes (BARZILAY et al. 1988; CIRICILLO et al. 1992).

Until now, the pathophysiology of brain swelling with increase of ICP following an acute space occupying lesion is not clearly understood. Factors such as duration and extent of cerebral compression accompanied with metabolic disturbance appears to be important in inducing brain swelling (MISHINA et al. 1994). Most dangerous consequence of ICP increase is the reduction of CPP as the driving force of CBF. This is accompanied by meta-

bolic disturbances, if the CPP falls below the autoregulatory threshold of CBF.

Depending on the extent of the metabolic disturbances the neuronal electrical activity becomes depressed, up to electrical silence, although the cells remain metabolically viable, at least for some period of time (NEWLON 1996). The patterns of electroencephalography (EEG) change may vary according to the type and severity of the damage, but typically, the patterns progresses from an initial loss of high-frequency activity to an increase in relatively synchronized delta-activity, and finally, a decrease in the amplitude of all activity (RAMPIL 1994).

Mild hypothermia has been reported as a therapeutic tool for protecting brain tissue to ischemic and traumatic brain injury (BUSTO et al. 1989; CLIFTON et al. 1991, POMERANZ et al. 1993). The efficiency of hypothermia lies in reducing the $CMRO_2$. The hypothermic decline in cerebral metabolism has been more closely linked to temperature effects on physicochemical processes than cerebral function, as represented by the EEG (LAFFERTY et al. 1978; NEMOTO et al. 1996). The most common findings using EEG recording is, that cooling to 33 °C may produce cerebral stimulatory effects as reflected by arousal phenomena as well as small shifts in EEG frequencies to theta- and beta-activities (BLAIR 1965, FITZGIBBON et al. 1984). However, other investigations have shown that cooling induces progressive reduction of both amplitude and frequency of EEG (MIZRAHI et al. 1989; GLARIA et al. 1990). Additionally, the combined effects of hypothermia and anesthetics have to be taken into account (KOCHS 1995).

Up to now there have not been experimental or clinical investigations of changes in electrocortical activity under conditions of hypothermia during compromized brain oxygen delivery caused by increased ICP.

Therefore, in the recent study we investigated the effects of mild hypothermia on the ECoG patterns during stepwise reduction of brain oxygen metabolism due to increased ICP. We hypothesized that in contrast to normothermic conditions, mild hypothermia may cause a distinct temporal preservation of the functional metabolism, which is indicated by special ECoG patterns during gradually decreased cerebral perfusion.

Methods

General instrumentation: All surgical and experimental procedures were approved by the ethical committee of the local authorities.

Thirteen piglets (14 days old, 4–5 kg b.w.) of female sex were anaesthetized initially with ketamine hydrochloride (50 mg/kg b.w., i.m.), and anaesthesia was maintained with isoflurane (0.8 Vol.%) in a nitrous oxide / oxygen mixture (70 % / 30 %). An endotracheal tube (5.5 Ch) was inserted through a tracheotomy. After immobilization with pancuronium bromide (0.2 mg/kg b.w./h, i.v.), the animals were artificially ventilated (Servo Ventilator 900C, Siemens-Elema, Solna, Sweden).

Local anaesthesia was infiltrated into the skin prior incision. A catheter was inserted into the left external jugular vein for injection of drugs and fluids. Another catheter was inserted via the femoral artery into the abdominal aorta for recording blood pressure and for withdrawal of reference samples for calculating CBF with colored microsphere (CMS) technique (CBF measurement see below at CMS technique). Further catheters were inserted into the left ventricle via the right common carotid artery and into the superior sagittal sinus in order to obtain brain venous blood samples.

Two burr holes were made into the left parietal skull for inserting a fiberoptic catheter into the subcortical white matter for ICP measurements (Camino Laboratories, San Diego, U.S.A.) and a Clark-type pO_2 electrode together with a thermocouple catheter (Licox pO_2 Monitor, GMS mbH, Kiel-Mielkendorf, Germany) into the parietal cortex.

An oval-shaped burr hole (10 mm to 3 mm) was gently drilled into the right parietal skull parallel to the sagittal suture. An epidural latex balloon catheter was placed in the epidural space of the right parietal region. The burr holes were sealed with bone wax and covered with dental acrylic in order to fix in place the probes and epidural balloon catheter throughout the experiment (fig.1).

Hemodynamic and blood gas monitoring: Arterial, left ventricular and central venous catheters were connected with pressure transducers (P23Db, Statham Instruments, Puerto Rico). Electrocardiogram (ECG) recordings were made from standard limb leads using stainless steel needle electrodes. Physiological parameters were recorded on a multi-channel polygraph (MT95K2, Astro-Med, USA). Body temperature was measured by a rectal thermoprobe inserted about 10 cm and was maintained throughout the general instrumentation at 38 ± 0.3 °C using a water-flow pad connected to a heating-cooling thermostat and a feedback controlled heating lamp.

Blood pH, pCO_2, and pO_2 were determined using an ABL50 blood gas analyzer (Radiometer, Copenhagen, Denmark). Blood hemoglobin and arterial oxygen saturation were measured by an OSM2 hemoxymeter (Radiometer, Copenhagen, Denmark), corrected to the body temperature at the time of sampling. The blood oxygen content was calculated as the product of blood oxygen saturation (%), oxy-

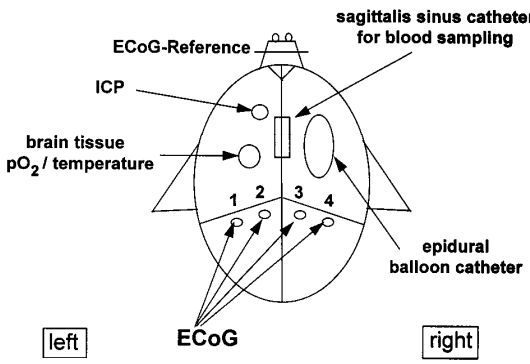

Fig. 1. Preparation of the skull – epidural balloon and monitoring device in place; ICP = intracranial pressure; ECoG = electrocorticogramm.

gen capacity of hemoglobin (1.39 mlO_2/g hemoglobin) and hemoglobin concentration (g/ml) plus dissolved O_2 and expressed in µMol/min · 100g. Cerebral O_2 delivery was calculated as the product of CBF times the arterial O_2 content. The $CMRO_2$ was calculated as arteriovenous oxygen content difference times CBF.

CPP was calculated as the difference between MAP and ICP.

CMS technique for CBF measurement: Cardiac output (CO) and regional CBF were measured by means of the reference sample color-labeled microsphere technique (KOWALLIK et al. 1991). Application and methodical considerations were presented and discussed in detail elsewhere (WALTER et al. 1997.

Briefly, in random sequence a known amount ($\approx 3 \times 10^6$ per injection) of colored polystyrene microspheres (diameter: 15.5 ± 0.33 µm) in 0.01 % Tween 80, surface coated with one of five dyes (white, yellow, red, violet, blue; Dye-Trak, Triton Technology, San Diego, U.S.A.) was thoroughly vortexed and sonicated and immediately injected in less than 20 seconds into the left ventricle. The injection line was then flushed with 2 ml saline. A blood sample was withdrawn from the descending aorta, as the reference sample beginning 15 seconds before the microsphere injection and continuing for 2 minutes with a rate of 1.5 ml/min (syringe pump SP210iw, World Precision Instruments, Sarasota, U.S.A.). The microsphere injection did not alter arterial blood pressure (ABP). After completion of the experiment the brains were removed and sectioned to determine blood flow to the following areas: brain stem (medulla oblongata, pons, midbrain), cerebellum, hippocampus, caudate nucleus, thalamus, white matter (corpus callosum and periventricular), hemispheres (gray matter pooled from frontal, parietal, temporal, and occipital lobes). Than all tissue (between 0.15 and 2.5 g) and blood samples were digested (4N KOH with 4 % Tween 80) for a minimum of four hours at 60 °C. The microspheres were retained by filtering each digested sample through an 8-µm pore PE-membrane filter (Fa. Costar, Bodenheim, Germany).

The filtration membrane was rinsed with 1 % Tween 80 and subsequently with 70 % ethanol. CMS were quantified by their dye content. The photometric absorption of each dye solution was measured by a diode-array UV/visible spectrophotometer (Model 7500, Beckman Instruments, Fullerton, U.S.A., wave length range, 300–800 nm, with a 2-nm optical bandwidth). Calculations were performed using the MISS software (Triton Technology, San Diego, U.S.A.). The number of microspheres was calculated using the specific absorbance value of the different dyes (provided by the manufacturer). Absolute flows to tissues measured by CMS were calculated by the formula: $flow_{tissue}$ = number of $microspheres_{tissue}$ · ($flow_{reference}$ / number of $microspheres_{reference}$). Flows are expressed in milliliters per minute per 100g tissue by normalizing for tissue weight.

Gradual CPP reduction controlled by an external Proportional-Integral-Differential (PID)-Controller: A detailed description of this procedure involving an external blood pressure control-loop to adjust MAP to an given set-point (like the baseline ABP value, as used in this application) has been given elsewhere (BAUER et al. 1997). Briefly, this special control-loop consists of a remote infusion/withdrawal pump, which is controlled by a PID-controller running at a PC which is serially connected. ABP is controlled by changing the blood volume by arterial blood infusion or withdrawal, respectively. The PID-controller was designed so that relevant active and passive physiological properties of the cardiovascular system are simplified and embodied in the PID-controller box. In order to get a vanishing control-error of the control-loop, an integral behavior in the controller was realized by means of the remote infusion/withdrawal pump which allowed the variation of the blood volume. Variation of volume per unit time was proportional to the difference between the measured MAP and the given set-point. The resulting effect on ABP represented an integral relation. Additionally, there was a static nonlinear transition in this technical controller calculated using Boyle's law ($p \cdot V$ = const.). A sufficient proportionality factor was found by trail and error. The use of this equipment allowed changing CPP as the difference of MAP minus ICP with good precision and stability and without any possible influences of reactive MAP changes due to stepwise ICP increase.

ECoG recording: Unipolar ECoG recordings were performed using four screw electrodes, which were drilled bilaterally into the skull above the somatosensory cortex (reference electrode on nasion). Electrode position was just posterior to the coronar suture and 5 and 10 mm lateral to the sagittal suture, respectively. ECoG signals were amplified, filtered (time constant was 0.1 second, cut off frequency was 1000 Hz), fed into a PC using a 16 channel A/D board (DT2821F, Data Translation, Marlboro, U.S.A.) and stored on the hard disk for off-line data analysis (sample rates were 512 Hz). ECoG was quantified for three minutes at each experimental period using the Fast Fourier Transformation (FFT). The spectral analysis consisted of calculating the spectral band power (total power: 1–30 Hz; delta band: 1–4 Hz; theta 5–8 Hz; alpha 9-12 Hz; beta 13–30Hz) and the delta ratio ([alpha band + beta band]/[delta band]).

Experimental protocol: After the surgical preparation had been completed, the piglets were allowed to rest for approximately 45 minutes. Then control values (control 1) recorded and randomly chosen animals, HT group (n = 7), were surface cooled by crushed ice packs and cooled water flow pads maintained a body temperature (rectal temperature) of 31.9 °C ± 0.3°C throughout the experiment. NT animals (n = 6) referred as control group to observe the effects of moderate hypothermia (control 2). At this stage the external ABP controller was established in order to adjust MAP at baseline ABP values. Then, a second series of values were obtained followed by gradual decrease of CPP by stepwise elevation of the ICP, beginning at 25 mmHg followed by 35 mmHg and 45 mmHg due to gradual epidural balloon inflation at a time of about 30 minutes each, and stabilization of the MAP by the external blood pressure control loop. Using this procedure steady state periods of reduced CPP of about 70 %, 50 %, and 30 % of baseline values were produced. Repeated measurement of all variables were recorded at the 25th minute of every steady state period. At the end of the experiments, the piglets were killed with KCl and the brains were removed for processing.

Statistical analysis: Data are reported as means ± SEM. The control variables were compared between groups with unpaired t tests. Two-way analysis of variance (ANOVA)

Table 1. Data of cerebral and systemic metabolism and hemodynamics during normothermia, hypothermia (32 °C) and stepwise increase of ICP.

		control 1	control 2	25 mmHg	35 mmHg	45 mmHg
HR [b/min]	NT	246 ± 15	244 ± 11	267 ± 14	234 ± 15	205 ± 12
	HT	233 ± 14	176 ± 6*$	176 ± 8*$	164 ± 9*$	158 ± 11*$
MAP [mmHg]	NT	85 ± 4	84 ± 2	80 ± 3	76 ± 3*	71 ± 2*
	HT	88 ± 3	82 ± 3	78 ± 3	77 ± 4*	69 ± 6*
CI [ml/min*kg]	NT	224 ± 16	225 ± 39	124 ± 22 $	184 ± 33	205 ± 24
	HT	213 ± 33	204 ± 35	125 ± 22 $	187 ± 30	181 ± 49
ICP [mmHg]	NT	7 ± 1	6 ± 1	25 ± 1*	34 ± 1*	47 ± 1*
	HT	7 ± 1	6 ± 1	25 ± 1	36 ± 1*	44 ± 1*
CPP [mmHg]	NT	80 ± 3	79 ± 3	60 ± 2*	46 ± 2*	30 ± 5*
	HT	84 ± 3	80 ± 4	59 ± 4*	44 ± 4*	27 ± 7*
$AVDO_2$ [mmol/ml]	NT	3.0 ± 0.2	2.8 ± 0.2	2.7 ± 0.3	3.2 ± 0.3	3.1 ± 0.5
	HT	3.0 ± 0.1	2.1 ± 0.2*$	2.0 ± 0.3*$	2.2 ± 0.1*$	2.8 ± 0.3
$CMRO_2$ [µmol/min*100g]	NT	179.7 ± 22.0	149.0 ± 8.4	154.9 ± 17.3	101. ± 10.6	25.1 ± 9.6*
	HT	184.3 ± 32.0	92.3 ± 16.0 *$	103.2 ± 14.6 *$	80.2 ± 5.0*	34.6 ± 9.4*
gCBF [ml/min*100g]	NT	66.8 ± 6.7	62.7 ± 4.7	73.7 ± 9.6	45.4 ± 5.6*	27.5 ± 10.9*
	HT	69.0 ± 9.7	49.7 ± 4.8*	68.3 ± 9.0	51.0 ± 3.7*	19.5 ± 4.8*
tpO_2 [mmHg]	NT	22.7 ± 3.3	20.3 ± 3.0	15.1 ± 5.0	11.5 ± 4.9*	3.3 ± 1.4*
	HT	22.7 ± 2.5	29.7 ± 3.4*$	21.2 ± 4.0 $	15.5 ± 4.4	2.3 ± 0.7*
paO_2 [mmHg]	NT	147.7 ± 8.9	150 ± 8.9	145.8 ± 9.5	149.6 ± 9.1	146.4 ± 13.2
	HT	135.5 ± 3.9	142.2 ± 8.4	128.4 ± 9.3	125.7 ± 8.7	131.4 ± 5.7
$paCO_2$ [mmHg]	NT	38.0 ± 0.4	40.2 ± 1.4	39.1 ± 0.5	38.7 ± 0.7	39.4 ± 0.8
	HT	37.3 ± 1.0	38.8 ± 1.9	39.0 ± 1.8	38.7 ± 1.3	38.2 ± 0.9
pH	NT	7.42 ± 0.01	7.40 ± 0.02	7.39 ± 0.01	7.38 ± 0.02	7.35 ± 0.03
	HT	7.44 ± 0.02	7.38 ± 0.03	7.41 ± 0.02	7.40 ± 0.02	7.39 ± 0.02
rectal temperature [°C]	NT	38.2 ± 0.3	38.2 ± 0.2	38.2 ± 0.1	38.3 ± 0.1	37.9 ± 0.3
	HT	38.0 ± 0.2	31.7 ± 0.2*$	31.8 ± 0.2 *$	31.8 ± 0.2*$	31.8 ± 0.1*$
brain temperature [°C]	NT	38.6 ± 0.2	38.3 ± 0.3	38.2 ± 0.3	38.2 ± 0.3	37.3 ± 0.3
	HT	38.4 ± 0.3	31.9 ± 0.1*$	31.7 ± 0.3*$	31.9 ± 0.1*$	31.0 ± 0.4*$

Values are mean ± SEM; NT = 6 animals; HT = 7 animals; control 1: experimental stage of normothermia in both groups; control 2: HT animals were cooled to 32 °C, this temperature was maintained throughout the experimental procedure; 25 mmHg, 35 mmHg and 45 mmHg: the ICP-levels with associated CPP reduction to about 70 %, 50 % and 30 % of baseline values (control 1).
* = significant differences to control 1 ($p < 0.05$);
$ = significant differences between NT and HT ($p < 0.05$)

with repeated measures was used to determine the effects of CPP alteration and group-CPP interaction within each variable. Subsequently, one-way ANOVA with repeated measures was performed within each group. Post hoc comparisons were made with paired t-tests using Bonferroni correction for multiple use. Between groups comparisons were made with unpaired t-tests using Bonferroni correction for multiple use. All statistical tests were done using the statistical package SPSS for Windows Release 6.0 (SPSS Inc., Chicago, U.S.A.). Differences were considered significant when $p < 0.05$.

Results

The data of cerebral and systemic hemodynamics as well as the metabolic data are shown in table 1. In the HT group after the baseline values had been recorded (control 1), the body temperature was reduced to 31.9 ± 0.3 °C by surface cooling and was maintained throughout the experiment. But, at the ICP-level of 45 mmHg the brain temperature decreased slightly more to 31.0 ± 0.4 °C.

Arterial blood gases (paO_2; $paCO_2$) and arterial pH were similar in the NT and HT group throughout the experimental procedure.

The cardiac index (CI) was unchanged during hypothermia, although the heart rate (HR) was strongly reduced by about 25 % ($p < 0.05$). During ICP increase to 25 mmHg the CI was significantly diminished to 56 ± 17 % (NT) and 58 % ± 18 % (HT) from baseline ($p < 0.05$), whereas at the higher ICP-levels (35 and 45 mmHg) the CI recovered almost completely.

MAP was virtually constant throughout the experiment (81 ± 11 mmHg), even though the MAP was reduced at the higher ICP-levels (35 and 45 mmHg, $p < 0.05$). The

Table 2. Frequency bands , total spectral power and delta ratio from ECoG - relative changes during hypothermia and stepwise increase of ICP in percent from normothermic baseline (control 1). The frequency band activity indicates percent from total spectral power at the experimental stage as 100 %.

delta band	normothermic animals (n = 6)	hypothermic animals (n = 7)
control 1	68 ± 25	69 ± 20
control 2	72 ± 25	48 ± 22*$
25 mmHg	72 ± 24	60 ± 24
35 mmHg	81 ± 27	70 ± 20
45 mmHg	85 ± 42	78 ± 48
alpha band	**normothermic animals (n = 6)**	**hypothermic animals (n = 7)**
control 1	5 ± 32	5 ± 14
control 2	5 ± 20	14 ± 21*$
25 mmHg	6 ± 35	15 ± 34*$
35 mmHg	4 ± 50	10 ± 49
45 mmHg	3 ± 39	4 ± 54
total spectral power	**normothermic animals (n = 6)**	**hypothermic animals (n = 7)**
control 1	100 ± 17	100 ± 17
control 2	98 ± 24	56 ± 17
25 mmHg	63 ± 21	55 ± 18*
35 mmHg	65 ± 23	32 ± 18*
45 mmHg	3 ± 26*	21 ± 31*$
theta band	**normothermic animals (n = 6)**	**hypothermic animals (n = 7)**
control 1	15 ± 26	17 ± 18
control 2	14 ± 22	31 ± 36*$
25 mmHg	14 ± 30	19 ± 28
35 mmHg	10 ± 38	15 ± 28
45 mmHg	9 ± 40	13 ± 49
beta band	**normothermic animals (n = 6)**	**hypothermic animals (n = 7)**
control 1	13 ± 30	9 ± 19
control 2	10 ± 30	7 ± 22
25 mmHg	8 ± 37	6 ± 14
35 mmHg	4 ± 51	5 ± 33
45 mmHg	3 ± 31$	5 ± 47
delta ratio %	**normothermic animals (n = 6)**	**hypothermic animals (n = 7)**
control 1	100 ± 55	100 ± 24
control 2	102 ± 25	225 ± 25*$
25 mmHg	62 ± 45*	105 ± 28$
35 mmHg	40 ± 69	36 ± 34*
45 mmHg	19 ± 26*	35 ± 25*$

values are mean ± SEM
* = significant differences to control 1 ($p < 0.05$);
$ = significant differences between NT and HT ($p < 0.05$)

CPP was maintained at 60, 45 and 30 mmHg using the PID-controller and showed no differences between the normothermic and hypothermic group.

The baseline ECoG exhibited the typical delta-dominated frequency pattern for isoflurane anaesthesia. At the hypothermic level (control 2), the amplitude of ECoG activity was markedly diminished, indicated by the total spectral power reduction of 44 ± 17 % ($p < 0.05$), compared with baseline (table 2). Moreover, a frequency shift was seen towards the higher frequencies (theta- and alpha-band) (fig. 2). These hypothermia induced ECoG changes were associated with a reduction of the global CBF (72 ± 13 % from the baseline, $p < 0.05$). However, the regional CBF differed considerably between the brain regions at 32 °C (control 2). the cortical CBF decreased markedly to 67 ± 10 % ($p < 0.05$), whereas the regional CBF in the medulla oblongata increased slightly (114 ± 15 % from the baseline). The regional CBF of the thalamus and of the midbrain did not changed significantly (fig. 3).

At this stage (control 2) the band power distribution of the ECoG power was markedly changed, compared with baseline values. The delta activity was reduced to 48 ± 22 % ($p < 0.05$), whereas the alpha activity increased to about three times as high and the theta activity was about twice as high as baseline (table 2, fig. 2). These changes in the band power distribution were also indicated by the increase of the delta ratio (225 ± 25 % from the baseline, $p < 0.05$).

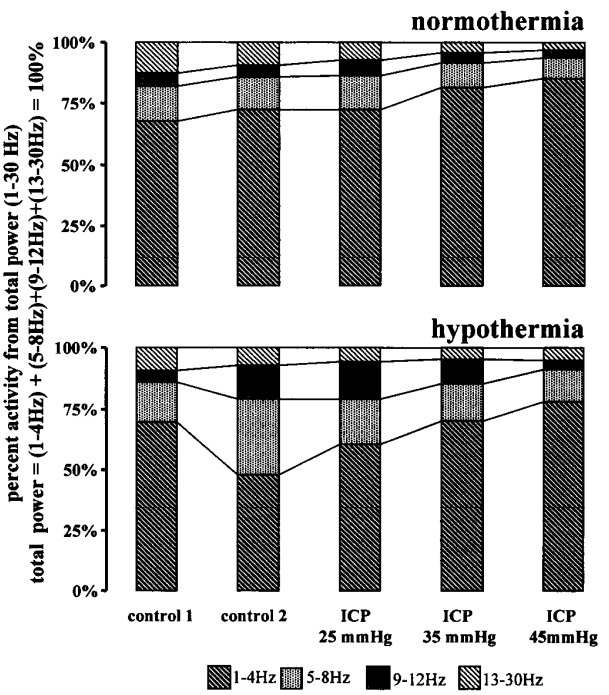

Fig. 2. Frequency distribution of neuronal electrical activity in TN and HT animals during stepwise increase of ICP.

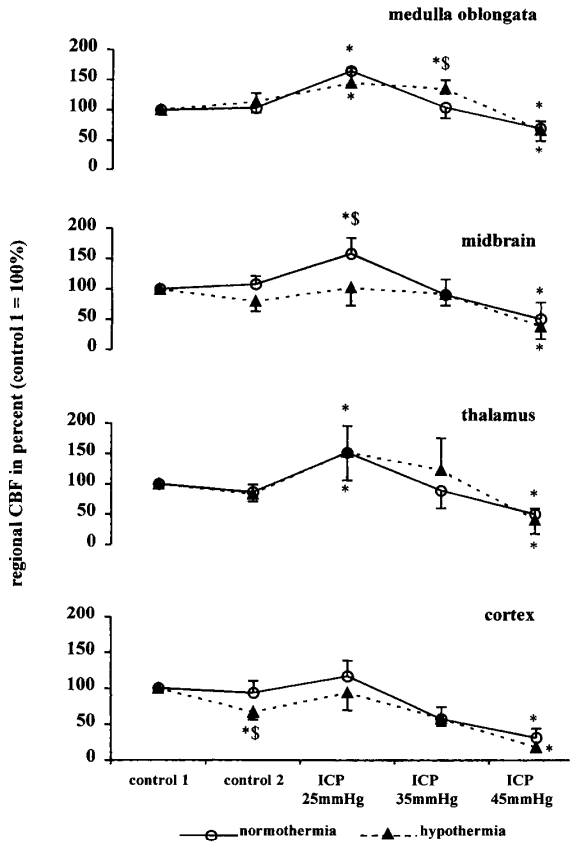

Fig. 3. Regional CBF in different brain regions during normothermia, hypothermia and stepwise increase of ICP. * = significant differences to control ($p < 0.05$); $ = significant differences between NT and HT ($p < 0.05$).

In the normothermic animals an increase of ICP to 25 mmHg with a following CPP reduction to about 70 % from baseline led to a frequency lowering of ECoG and an increase of delta activity, indicated by a reduced delta ratio (62 ± 45 %, $p < 0.05$) (table 2, fig. 2) and a slightly increased global CBF. The rise in the CBF was seen in all brain regions in both groups. The strongest increase of regional CBF was found in the medulla oblongata (NT: 166 ± 24 %; HT: 145 ± 26 %, $p < 0.05$) and in the thalamus (NT: 151 ± 45 %; HT: 153 ± 53 %, $p < 0.05$). An increase of midbrain blood flow occurred only in the NT group (158 ± 26 %, $p < 0.05$).

The ICP increase to 35 mmHg which was accompanied by a CPP reduction to about 50 % induced a marked decrease in global CBF to 68 ± 8 % in the NT and 74 ± 5 % in the HT group ($p < 0.05$), respectively. Global CBF diminishing was associated to a marked reduction of the delta amplitude in the ECoG of the NT group (fig. 4) and an increase of the delta band activity to 81 ± 27 %. In contrast, hypothermic animals exhibited ECoG patterns similar to those for control 2 stage (32 °C). Cortical CBF decreased significantly in both groups (NT: 58 ± 16 %; HT: 58 ± 10 %, $p < 0.05$). However, medulla oblongata blood flow remained elevated in both groups, nevertheless the medulla oblongata blood flow differed significantly between the normothermic (105 ± 18 %) and hypothermic (136 ± 14 %) animals ($p < 0.05$). Similar to the regional CBF in the medulla oblongata, differences occurred in the thalamus between the normothermic and the hypothermic group, still these differences were not significant.

The last stage of ICP increase (45 mmHg) caused a CCP reduction to about 30 ± 3 % from baseline. The resulting decrease of global CBF differed between the two groups (NT: 41 ± 16 %; HT: 28 ± 7 %, $p < 0.05$), but were comparable with reference to hypothermic baseline CBF (control 2) (NT: 41 ± 16 %; HT: 39 ± 10 %). Similar to the decrease of the global CBF the cortical blood flow decreased considerably in both groups, but was more pronounced in hypothermic (18 ± 6 %) than in normothermic animals (31 ± 13 %, $p < 0.05$). In contrast, medulla oblongata blood flow was only reduced by about 30 % of baseline in both groups.

In hypothermic animals a further ECoG frequency lowering, amplitude reduction (fig. 4) and maintained residual total spectral power were observed (table 2). In contrast, the ECoG activity in the normothermic group was almost completely suppressed and burst suppressions were sporadically observed in two animals (fig. 4).

Discussion

In the present study we determined the effects of hypothermia on the neuronal electrical activity in juvenile piglets during gradual increase of the ICP with consecutive CPP reduction using epidural brain compression. The major ECoG changes in the anaesthetized juvenile piglets at mild hypothermia (32 °C) were an arousal-like ECoG activity with a marked frequency shift from delta wave dominated activity to alpha wave activity and a concomitant reduction in total spectral power.

Our results are similar to those of previous studies showing that mild hypothermia levels may produce cerebral stimulatory effects as reflected by a beginning depression of amplitude, hyperresponsive reflexes and arousal phenomena in patients with depressed sensory (BLAIR 1965). These findings confirm observations by Fay (FAY 1945, 1959), who described central stimulatory effects in adult humans during cooling to 32 °C. Additionally, in humans and mammals due to mild hypothermia also unchanged or marginally altered electrocortical activity with small shifts in EEG frequencies to an increase of theta and beta activity have been described (FITZGIBBON et al. 1984; MICHENFELDER et al. 1991).

The frequency shift of the ECoG by hypothermia seems to be an electrical phenomenon, that is obviously related by the regional CBF and the oxydative metabolism. This suggestion is in agreement with findings obtained from regional CBF assessments of behavioral state

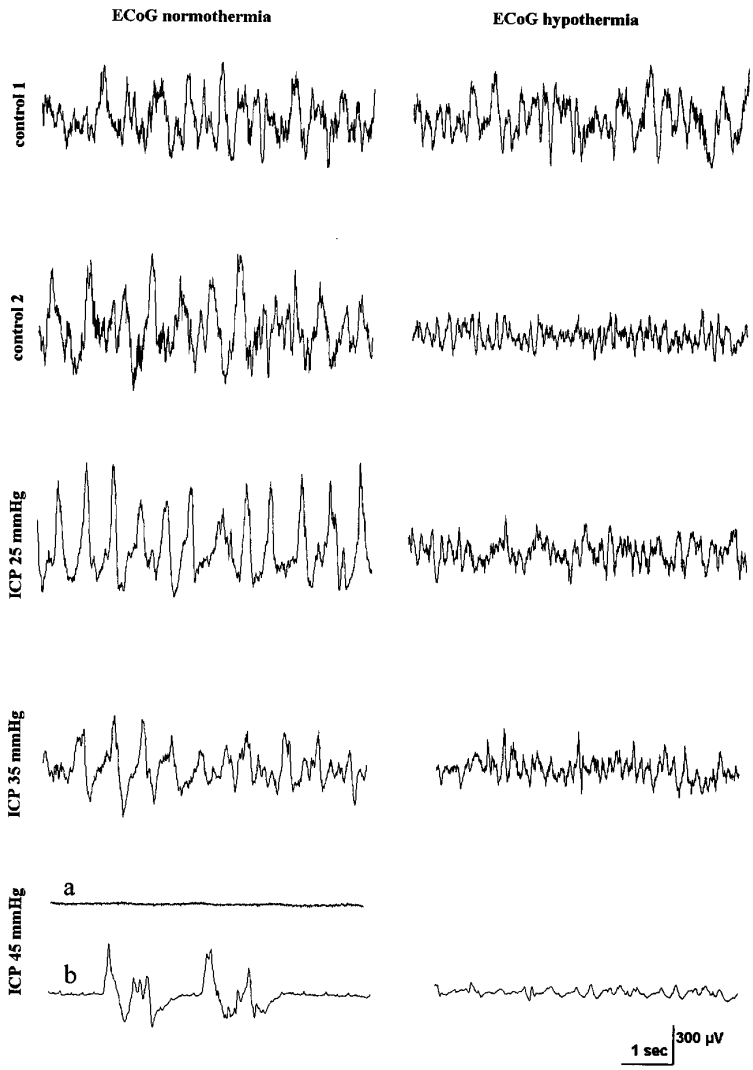

Fig. 4. Representative ECoG tracing from a normothermic and a hypothermic animal during increase of ICP.
Right side: a normothermic animal with delta wave dominated ECoG; at ICP of 45 mmHg a) electrocortical silence observed in 4 animals and b) burst suppression pattern in 2 animals.
Left side: control 2: cooling to 32 °C and maintaining this temperature throughout the experimental procedure.
Reduction of the ECoG amplitude is visible at control 2, but higher frequencies are maintained up to an ICP of 35 mmHg.

changes, where spontaneous changes from high to low voltage patterns of the ECoG were accompanied by an increase of regional CBF to areas of the brain corresponding to the arborization of the reticular formation (Jensen et al. 1986).

Commonly, an increased ECoG alpha activity is a sign for an improved cerebral activity, and is associated with an increase of CBF and cerebral oxydative metabolism (SULG et al. 1981; BISCHOFF 1994).

We found, however, at hypothermia the global CBF and CMRO2 remained suppressed, whereas the ECoG alpha activity increased. In our study we investigated the ECoG changes in relation to regional CBF measurements at hypothermia. The discovery of differences in the regional CBF, which occurred under hypothermia may help explain the increased ECoG alpha activity. At hypothermia cortical blood flow was pronouncedly reduced compared with midbrain blood flow. Normally, midbrain's reticular formation modulates the frequency of the ECoG (ZSCHOCKE 1995). It is well known that the electrocortical activity, especially the alpha activity, is remarkably influenced by the neuronal activity of the midbrain, which is able to induce and keep rhythmic activity (JONES et al. 1983). Especially, the midbrain's reticular system modulates thalamic synchronization and desynchronization (SCHMIDT 1990). The blood flow in these brain regions was not found to be influenced by hypothermia. Above all, a reduction of the global CBF by hypothermia is caused by changes of the cortical blood flow. This cortical blood flow reduction is a possible cause of the reduction of total spectral power and electrocortical high-voltage activity at mild hypothermia. Furthermore, the reticular formation has diffuse thalamocortical projections that when activated, cause desynchronization of high-voltage activity to low voltage activity (INGVAR and SÖDERBERG 1958). Presumably, the

frequency shift may be caused by the imbalance of inhibitory and stimulatory influences from the midbrain and from the thalamic frequency modulating fibres to the cortex, whose own electrical activity is suppressed by blood flow reduction at mild hypothermia. This relative stimulation evokes a partial desynchronization of the afferent reticular arousal system (BAUER et al. 1997). Another reason for these discrepancies in the results of the preserved high frequencies in the ECoG in this study and previous studies is probably due to differences in brain maturation. The other studies cited were done on adult dogs and we used juvenile piglets (STEEN et al. 1983; MICHENFELDER and MILDE 1991).

During controlled reduction of CPP by regional mass expansion due to epidural balloon inflation we found at mild and moderate stages only minimal changes in the ECoG in hypothermic animals compared to the hypothermic baseline (control 2), whereas the ECoG in normothermic animals showed a marked decrease in frequency, amplitude and total spectral power. These findings are consistent with classical pathophysiological EEG patterns observed in acute traumatic coma (IBRAHIM and ELIAN 1974; NEWLON 1996). The higher the proportion of EEG that is attributable to delta, the more likely is a poor prognosis. However, this EEG pattern in itself is not a particularly useful discriminator of outcome, because in mild and moderate traumatic head injuries the EEG pattern normalizes quickly (RUMPL 1993).

In our study, moderate brain compression (ICP 35 mmHg) caused a more pronounced affect on brain function in normothermic animals as compared with hypothermic animals. At 35 mmHg ICP differences in global CBF change between the two groups were notable. In HT animals the CBF did not change from the baseline (25 % less than normothermic baseline) with moderate ICP increase. In normothermia the CBF was reduced by about 32% from baseline with moderate ICP increase. Despite the fact that the HT animals at hypothermic baseline (control 2) and the NT animals at ICP 35 mmHg have comparable CBF and $CMRO_2$ values, there was a markedly different neuronal electrical activity. The preserved high frequency activity of HT animals is an indication of a maintenance of energy production adequate for the functional requirements of the brain. Failure of brain energy production occurs at a level of CBF somewhat lower than that causing loss of neuronal function (LOWING and GLEBE 1994). Obviously, the burst suppressions and the ECoG silence at the highest level of ICP increase to 45 mmHg, in NT animals, are caused by exceeding the threshold of neuronal and metabolic failure. In contrast, in HT animals, a residual activity of brain function is preserved.

The suppression of the cerebral metabolism at hypothermia of about 25 % in CBF and 57 % in $CMRO_2$ in our study corresponds with findings in newborn piglets and amounted to nearly fifty percent more than was reported for adult animal brains (RUPP and SEVERINGHAUS 1986; NEMOTO et al. 1996).

With the use of anaesthetics the phenomenon of the frequency shift to theta and alpha-band at hypothermia could be influenced. With the use of a minimum alveolar concentration (MAC) of 1 MAC of isoflurane there is commonly a shift to slow frequency and high amplitude ECoG (JANTZEN 1992), which we have seen at control 1. Furthermore, hypothermia normally necessitates a MAC reduction of isoflurane (SATAS et al. 1995). Accordingly, with the use of 1 MAC isoflurane, we expected a further lowering of frequency and reduction of amplitude of the ECoG with hypothermia. ECoG frequency shifts to higher frequencies with hypothermia, as seen in our study, are not explainable by influences of anaesthetics. Obviously, the influence of hypothermia on neuronal electrical activity seems to be independent from basic anaesthetics.

In summary, the present data showed in juvenile piglets with isoflurane anaesthesia during mild hypothermia an arousal-like ECoG activity with marked frequency shift to theta and alpha activity and a change from high to low-voltage activity, indicated by a reduced total spectral power in the ECoG. Furthermore, the hypothermic brain showed a preserved neuronal function at moderate stages of impaired cerebral perfusion. Obviously, hypothermia improves the functional tolerance of the brain to reduced oxygen supply. This confirms the well-known effect of mild hypothermia on a decrease of cerebral oxidative metabolism.

Acknowledgement: The authors thank Mrs. I. Witte, Mrs. U. Jäger and Mr. L. Wunder for skillful technical assistance. This study was supported by grant 01ZZ9602 from the Bundesministerium für Bildung und Forschung, Federal Republic of Germany.

References

ALDRICH EF, EISENBERG HM, SAYDJARI C, et al.: Diffuse brain swelling in severely head-injured children. A report from the NIH Traumatic Coma Data Bank. J Neurosurg 1992; **76**: 450–454.

BARZILAY Z, AUGARTEN A, SAGY M, et al.: Variables affecting outcome from severe brain injury in children. Int Care Med 1988; **14**: 417–421.

BAUER R, HOYER D, WALTER B, et al.: Changed systemic and cerebral hemodynamics and Oxygen supply due to gradual hemorrhagic hypotension induced by an external PID-Controller in newborn swine. Exp Toxic Pathol 1997; **49**: 469–476.

BAUER R, SCHWAB M, ABRAMS RM, et al.: Electrocortical and heart rate response during vibroacoustic stimulation in fetal sheep. Am J Obstet Gynecol 1997; **177**: 66–71.

BISCHOFF P: Perioperative EEG monitoring: Studies on electrophysiological arousal mechanisms. Anaesthesiol Intensivmed Notfallmed Schmerzther 1994; **29**: 322–329.

BLAIR E: A physiologic classification of clinical hypothermia. Surgery 1965; **58**: 607–618.

BUSTO R, GLOBUS MY, DIETRICH WD: Effect of mild hypothermia on ischemia-induced release of neurotrans-

mitters and free fatty acids in rat brain. Stroke 1989; **20**: 904–910.

CIRICILLO SF, ANDREWS BT, DAMRON SL, et al.: Severity and outcome of intracranial lesions in pedestrians injured by motor vehicles. J Trauma 1992; **33**: 899–903.

CLIFTON GL, JIANG JY, LYETH BG et al.: Marked protection by moderate hypothermia after experimental traumatic brain injury. J Cereb Blood Flow Metab 1991; **11**: 114–121.

FAY T: Observations on generalized refrigeration in cases of severe cerebral trauma. Assoc Res Nerv Men Dis Proc 1945; **24**: 611–619.

FAY T: Harley experiences with local and generalized refrigeration of the human brain. J Neurosurg 1959; **16**: 239–260.

FITZGIBBON T, HAYWARD JS, WALKER D: EEG and visual evoked potentials of conscious man during moderate hypothermia. Electroencephalogr Clin Neurophysiol 1984; **58**: 48–54.

GLARIA AP, MURRAY A: Monitoring brain function during cardiothoracic surgery in children and adults at two levels of hypothermia. Electroencephalogr Clin Neurophysiol 1990; **76**: 268–270.

IBRAHIM MM, ELIAN M: A reappraisal of the value of the EEG in subdural hematoma. J Neurol 1974; **207**: 117–128.

INGVAR DH, SÖDERBERG U: Cortical blood flow related to EEG patterns evoked by stimulation of the brain stem. Acta Physiol Scand 1958; **42**: 130–143.

JANTZEN JP: Zerebrale Effekte volatiler und intravenöser Anästhetika. In: RÜGHEIMER E, DINKEL M (eds.) Neuromonitoring in Anästhesie und Intensivmedizin. Berlin – Heidelberg Springer 1992: 137–155.

JENSEN A, BAMFORD OS, DAWES GS, et al.: Changes in organ blood flow between high and low voltage electrocortical activity in fetal sheep. J Dev Physiol 1986; **8**: 187–194.

JONES TA, LAWRENCE AF, BICKFORD RG: Serotonin depletion prevents electrocortical synchronization following acute midbrain deactivation. Electroencephalogr Clin Neurophysiol 1983; **55**: 203–211.

KOCHS E.: Electrophysiological monitoring and mild hypothermia. J Neurosurg Anesthesiol 1995; **7**: 222–228.

KOWALLIK P, SCHULZ R, GUTH BD, et al.: Measurement of regional myocardial blood flow with multiple colored microspheres. Circulation 1991; **83**: 974–982.

LAFFERTY JJ, KEYKHAH MM, SHAPIRO HM, et al.: Cerebral hypometabolism obtained with deep pentobarbital anesthesia and hypothermia (30 °C). Anesthesiology 1978; **49**:159–164.

LOWNIE SP, GELB AW: Cerebral metabolism: Basic considerations. In: Sebel PS, Fitch W (eds.) Monitoring the Central Nervous System. Blackwell Science, Oxford 1994: 1–25.

MICHENFELDER JD, MILDE JH: The relationship among canine brain temperature, metabolism, and function during hypothermia. Anesthesiology 1991, **75**: 130–136.

MISHINA H, YABUKI A: Relationship of cerebral blood flow, cerebral metabolism, and electroencephalography to outcome in acute experimental compression ischemia – barbiturate effects on delayed brain swelling. Neurol Med Chir Tokyo 1994; **34**: 345–352.

MIZRAHI EM, PATEL VM, CRAWFORD ES, et al.: Hypothermic-induced electrocerebral silence, prolonged circulatory arrest, and cerebral protection during cardiovascular surgery. Electroencephalogr Clin Neurophysiol 1989; **72**: 81–85.

NEMOTO EM, KLEMENTAVICIUS R, MELICK JA, et al.: Suppression of cerebral metabolic rate for oxygen ($CMRO_2$) by mild hypothermia compared with thiopental. J Neurosurg Anesthesiol 1996; **8**: 52–59.

NEWLON PG: Electrophysiological monitoring in head injury; In: NARAYAN RK, WILBERGER JE, POVLISHOCK JT (eds.): Neurotrauma. McGraw-Hill, New York 1996: 563–575.

POMERANZ S, SAFAR P, RADOVSKY A, et al.: The effect of resuscitative moderate hypothermia following epidural brain compression on cerebral damage in a canine outcome model. J Neurosurg 1993; **79**: 241–251.

RAMPIL IJ: Electroencephalography. In: SEBEL PS, FITCH W (eds.): Monitoring the Central Nervous System. Blackwell, Oxford 1994: 222-66.

RUMPL E: Craniocerebral trauma. In: NIEDERMEYER E, LOPES DA SILVA F (eds.): Electroencephalography. Williams & Wilkins, Baltimore 1993: 383–403.

RUPP SM, SEVERINGHAUS JW: Hypothermia. In: Miller RD (ed.): Anesthesia. Churchill Livingstone, New York, Edinburgh 1986: 1995–2022.

SATAS S, HAALAND K, THORESEN M, et al.: MAC for halothane and isoflurane during normothermia and hypothermia in the newborn piglets. Acta Anaesthesiol Scand 1995; **40**: 452–456.

SCHMIDT RF: Integrative Leistungen des Zentralnervensystems. In: SCHMIDT RF, THEWS G (eds.): Physiologie des Menschen. Berlin – Heidelberg, New York: Springer, 1990: 132–175.

SULG IA, SOTANIEMI KA, TOLONEN U, et al.: Dependence between cerebral metabolism and blood flow as reflected in quantitative EEG.A critical review. Advances Biol Psych 1981; **6**: 102–108.

STEEN PA, NEWBERG L, MILDE JH, et al.: Hypothermia and barbiturates: individual and combined effects on canine cerebral oxygen consumption. Anesthesiology 1983; **58**: 527–532.

WALTER B, BAUER R, GASER E, et al.: Validation of the multiple colored microsphere technique for regional blood flow measurements in newborn piglets. Basic Res Cardiol 1997; **92**: 191–200.

WARD JD: Pediatric head injury. In: NARAYAN RK, WILBERGER JE, POVLISHOCK JT (eds.): Neurotrauma. McGraw-Hill, New York 1996: 859–867.

ZSCHOCKE S:. Enstehungsmechanismen des EEG. In: ZSCHOCKE S (ed.): Klinische Elektroenzephalographie. Berlin – Heidelberg: Springer, 1995: 1–48.

Original Paper

Pediatric Neurosurgery

Pediatr Neurosurg 1999;30:62–69

Received: October 30, 1998
Accepted: December 29, 1998

A Piglet Model for Evaluation of Cerebral Blood Flow and Brain Oxidative Metabolism during Gradual Cerebral Perfusion Pressure Decrease

Reinhard Bauer[a] Bernd Walter[a] Alexander Torossian[b] Harald Fritz[b] Olaf Schlonski[a] Thomas Jochum[a] Dirk Hoyer[a] Konrad Reinhart[b] Ulrich Zwiener[a]

[a]Institute for Pathophysiology and [b]Clinic for Anesthesiology and Intensive Care, Friedrich Schiller University, Jena, Germany

Key Words

Epidural balloon inflation · Colored microspheres · Cerebral metabolic rate of oxygen · Piglets

Abstract

A piglet model was developed to study the effect of epidural volume expansion on cerebral perfusion pressure (CPP) by stepwise elevating intracranial pressure (ICP). Mean arterial blood pressure (ABP) was strictly maintained using an extracorporeal ABP controller. Two-week-old piglets (n = 10) were studied by surgically placing an epidural balloon over the right parietal region and gradually increasing the inflation to increase ICP to 25, 35 and 45 mm Hg, maintaining each pressure level for 30 min. Regional cerebral blood flow was measured using the colored microsphere technique, and cerebral oxygen delivery and cerebral metabolic rate of oxygen were calculated at baseline conditions and after reaching ICP levels of 25, 35 and 45 mm Hg. The results showed that this model of epidural volume expansion reproducibly reduces CPP to 70, 50 and 33% of baseline CPP values with elevation of ICP, and that the physiological variables remained stable throughout each increase in ICP. We conclude that the model simulates the effects of an acute intracranial focal mass expansion and is well suited for the evaluation of different therapeutical strategies for increased ICP in newborns and infants.

Introduction

Intracranial hypertension (defined as a persistent elevation of intracranial pressure, ICP, over 20 mm Hg) is a common complication following severe traumatic brain injuries in infants and young children and is closely correlated to their outcome. Recently, it was reported that approximately 60% of severely head-injured patients develop increased ICP [1], and the incidence of brain swelling following traumatic brain injuries in pediatric patients is twice that of adults [2, 3]. Moreover, a considerable number of patients suffer uncontrolled intracranial hypertension that progresses to cerebral nonperfusion and death. Much of the study to date has been in adults and older children, with little attention or investigation as to the effects of increased ICP and its cerebrovascular and brain metabolic effect in the developing brain [4]. The aim of the present study was to develop an animal model which allows sequential measures of regional cerebral blood flow (CBF) and cerebral metabolic rate of oxygen ($CMRO_2$) during the gradual reduction of cerebral perfusion pressure (CPP) by stepwise epidural balloon inflation. Through a better understanding of the physiologic changes in the brain with decreasing perfusion, strategies could be developed in the future to reduce the detrimental effects of intracranial hypertension on cerebral metabolism.

KARGER

Fax + 41 61 306 12 34
E-Mail karger@karger.ch
www.karger.com

© 1999 S. Karger AG, Basel
1016–2291/99/0302–0062$17.50/0

Accessible online at:
http://BioMedNet.com/karger

Dr. Reinhard Bauer
Institute for Pathophysiology, Friedrich Schiller University
D–07740 Jena (Germany)
Tel. +49 3641 938956, Fax +49 3641 938954
E-Mail rbau@mti-n.uni-jena.de

Material and Methods

The committee of the Thuringian State government for animal research approved this protocol. The animals were managed in accordance with the guidelines of the Americal Physiological Society.

Surgical Preparation

Ten piglets of mixed German domestic breed (14 days old, body weight 4,490 ± 611 g) were initially sedated with ketamine hydrochloride (50 mg/kg b.w.) and then anesthetized with 1.5% isoflurane in 70% nitrous oxide and 30% oxygen. A central venous catheter was introduced through the left external jugular vein and was used for administration of drugs and for volume substitution (lactated Ringer's solution: 5 ml/h). An endotracheal tube was inserted by means of a tracheotomy. After immobilization with pancuronium bromide (0.2 mg/kg b.w./h, i.v.), the animals were artificially ventilated (Servo Ventilator 900C; Siemens-Elema, Solna, Sweden). Anesthesia was maintained throughout the experiment with 0.8% isoflurane. Polyethylene catheters (inner diameter 1.5 mm) were advanced through the femoral arteries into the abdominal aorta in order to record arterial blood pressure (ABP) and withdraw reference samples for the colored microsphere technique. A further polyethylene catheter (inner diameter 0.3 mm) was inserted into the superior sagittal sinus and advanced to the confluence sinuum in order to obtain venous blood samples of the brain. The heart (left ventricle) was cannulated retrogradely via the right common carotid artery with a polyurethane catheter (inner diameter 0.5 mm). Arterial, left ventricular and central venous catheters were connected with pressure transducers (P23Db; Statham Instruments Inc., Hato Rey, Puerto Rico). Body temperature was monitored by a rectal thermoprobe and maintained throughout the experiment at 38 ± 0.3 °C using a heating-cooling thermostat and a feedback-controlled heating lamp. Physiological parameters were recorded on a multichannel polygraph (MT95K2®; Astro-Med Inc., West Warwick, R.I., USA).

After a midline skin incision and scalp retraction, a craniostomy was performed in the left frontal bone using a high-speed air drill, and an ICP monitor was implanted into the subcortical white matter for ICP measurements (Camino Laboratories, San Diego, Calif., USA). A right-sided craniostomy (10 to 3 mm) was also drilled into the frontal bone, 4 mm lateral of midline and parallel to the sagittal suture; the dura was left intact. An epidural latex balloon attached to a catheter was placed in the epidural space of the right frontoparietal region. The burr holes were sealed with bone wax and covered with dental acrylic to keep the probes and the epidural balloon catheter in place thoughout the experiment.

Experimental Protocol

After the surgical preparation had been completed, the piglets were allowed to recover for approximately 60 min. After baseline values of physiological parameters including CBF had been obtained, the external ABP controller was established to maintain the ABP at those baseline values. Following the 30-min period at controlled ABP, a second measure was performed (control 2). Then, the volume of the epidural balloon was increased so as to gradually decrease the effective CPP. This was calculated as the difference between mean ABP and ICP. A stepwise elevation of the ICP was achieved increasing the pressure to 15, 25, 35 and 45 mm Hg for 30 min at each level. The external blood pressure control loop was able to maintain a stable ABP throughout the experimental protocol. A detailed description of the procedure of mean ABP adjustment at an externally given set point (baseline ABP value, as used in this application) using an external blood pressure control loop has been given elsewhere [5]. In brief, ABP (controlled quantity) was controlled by a proportional differential integral controller running on a PC, by means of changing the blood volume by arterial blood infusion or withdrawal, respectively. An infusion/withdrawal pump was the controlling element. Since there are several nonlinear and nonstationary properties in the controlled physiological system, the parameters of the external technical controller were searched for by trial and error. Stable control of ABP was reached by means of the integrating property of the controller in particular. The integration time constant of K_I = 6.94 mm Hg·min^{-1} was found to be appropriate during all states investigated.

Physiologic Data Measurements, CBF Measures and Analysis

Blood pH, pCO_2, and pO_2 were determined with an ABL50® Blood Gas Analyzer (Radiometer, Copenhagen, Denmark). Blood hemoglobin and arterial oxygen saturation were determined using a Hemoxymeter OSM2® (Radiometer).

Regional CBF was measured by means of a reference sample obtained through color-labeled microsphere technique [6, 7]. Briefly, in random sequence, a known amount (~ 1 × 10^6 per injection) of colored polystyrene microspheres (diameter 15.5 ± 0.33 µm) in 0.01% Tween 80, surface coated with one of five dyes (white, yellow, red, violet, blue; Dye-Trak®; Triton Technology, San Diego, Calif., USA) was thoroughly vortexed and sonicated and immediately injected within 20 s into the left ventricle via the right carotid catheter and then flushed with 2 ml saline. A blood sample was withdrawn from the descending aorta as the reference sample [8], beginning 15 s before the microsphere injection and continuing for 2 min with a rate of 1.5 ml/min (syringe pump SP210iw; World Precision Instruments Inc., Sarasota, Fla., USA). The microsphere injection did not alter ABP.

At the end of the experiment, the piglet was killed with KCl, and the brain was removed for processing. The brain was sectioned to determine blood flow to the following areas: brain stem (medulla, pons, midbrain), cerebellum, hippocampus, caudate nucleus, thalamus, white matter (corpus callosum and periventricular), hemispheres (gray matter pooled from frontal, parietal, temporal and occipital lobes). After sectioning, reference blood samples and tissue samples between 0.15 and 2.5 g were covered with an appropriate volume (approximately 3 ml/g) of digestive solution (4 *N* KOH with 4% Tween 80 in deionized water). All tissue and blood samples were digested for a minimum of 4 h at 60 °C. In order to retain the microspheres, each digested sample was then filtered under vacuum suction through a PE membrane filter with 8-µm pores (Fa. Costar, Bodenheim, Germany). The filtration membrane was gently rinsed with 1% Tween 80 and subsequently with 70% ethanol. Colored microspheres were quantified by their dye content. The membranes containing the microspheres on their surface were carefully folded and put into a conically shaped glass vial. The dye was recovered from the microspheres by adding 150 µl of dimethylformamide (DMFA) and subsequent vortexing of the vial in order to moisten the membrane completely. The photometric absorption of each dye solution was measured by a diode array UV/visible spectrophotometer (Model 7500; Beckman Instruments, Fullerton, Calif., USA; wavelength range 300–800 nm, with a 2-nm optical bandwidth). Calculations were performed using the MISS® software (Triton Technology). In a manner similar to that of the overlap correction in counting radioactive microspheres, the composite spectrum of each dye solution was

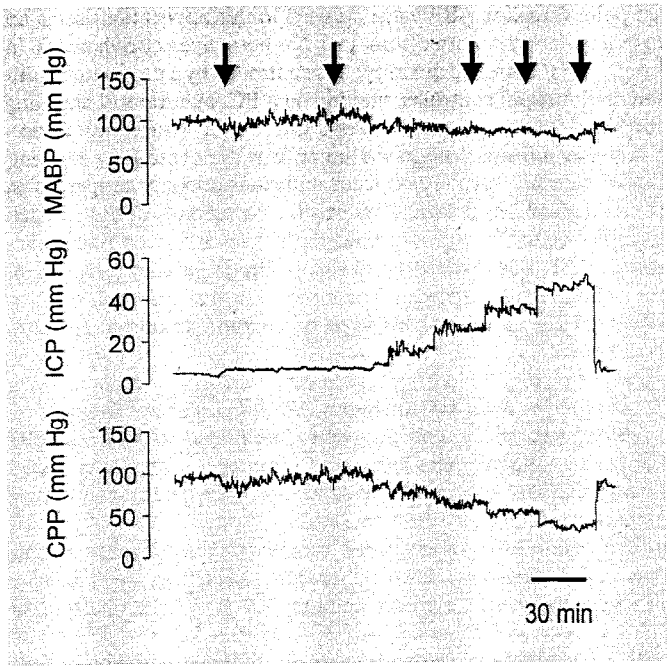

Fig. 1. Typical example of recordings of gradual CPP reduction due to a stepwise increase in ICP by epidural balloon inflation during adjusted mean ABP (MABP) in a 2-week-old piglet. Note that no Cushing response occurred even during stages of marked ICP increase. (Arrows indicate time of repeated measurements of regional CBF and related variables.)

resolved into the spectra of the individual constituents and corrected for spill over and background absorption. The amount of dye in a given sample was adjusted by appropriate dilution with DMFA to achieve absorbance values of no more than 1.3 AU (absorbance unit, 1 AU = -lg[10% light transmission/100%]) to ensure the linearity between absorbance and dye concentration according to the Lambert-Beer law. Samples with absorbances higher than 1.3 AU were further diluted with DMFA and analyzed again. The number of microspheres was calculated using the specific absorbance value of the different dyes (provided by the manufacturer). Absolute flows to tissues measured by colored microspheres were calculated by the formula: $flow_{tissue}$ = number of $microspheres_{tissue}$ × ($flow_{reference}$/number of $microspheres_{reference}$). Flows are expressed in milliliters per minute per 100 g tissue by normalizing for tissue weight.

Assuming the oxygen capacity of hemoglobin to be 1.39 ml O_2/g hemoglobin in piglets [9], blood O_2 content was calculated as equal to g hemoglobin/ml · 1.39 ml O_2/g hemoglobin · %O_2 saturation and expressed in μmol/min · 100 g. Dissolved oxygen was added by calculation, using the measured pO_2 and the temperature-corrected solubility coefficient of oxygen. Because the sagittal sinus drains the cerebral cortex, cerebral white matter and some deep gray structures (basal ganglia, hippocampus) [10], blood flow measured to the cerebrum included these structures (global CBF). $CMRO_2$ was obtained by multiplying global CBF by the difference in cerebral arteriovenous O_2 content. Cerebral O_2 delivery was calculated as the product of global CBF times the arterial O_2 content. Effective CPP was calculated as the difference between mean ABP and ICP. Total blood volume was assumed to be 12% of body weight [11].

Statistical Analysis

Data are reported as means ± SD. Data were subjected to analysis of variance for a repeated-measures design followed by the Tukey test to compare the means of parameters obtained during baseline conditions with those obtained after ABP adjustment and gradual ICP increase. Comparison of blood flow between the corresponding regions of the brain ipsi- and contralateral to the inflated epidural balloon was performed by two-way repeated-measures analysis of variance. Differences were considered significant when $p < 0.05$.

Results

Stable stages of gradually reduced CPP to 69 ± 1, 51 ± 3 and 32 ± 2% of baseline values (86 ± 7 mm Hg = 100%) could be achieved with stepwise increases in ICP to 25, 35 and 45 mm Hg, respectively (fig. 1 and table 1), by gradual epidural balloon inflation and by maintaining a constant ABP. ABP was adjusted by appropriate blood volume withdrawal/infusion (baseline: 84 ± 10 mm Hg; control 2: 87 ± 16 mm Hg; ICP 25 mm Hg: 80 ± 8 mm Hg, ICP 35 mm Hg: 76 ± 7 mm Hg; ICP 45 mm Hg: 71 ± 6 mm Hg) to ensure possible cardiovascular response effect of CPP due to the increased ICP. There was a considerable individual difference in cardiovascular ICP response as indicated by the time period and by the marked variance in the amount of changed blood volume at different experimental stages (table 1). The largest blood withdrawal was necessary at an increase in ICP to 25 mm Hg. In contrast to the earlier stages of ICP increase where blood withdrawal occurred, at the last stage of ICP increase, a complete reinfusion, partly by additional infusion of normal saline, was necessary in order to stabilize the ABP (table 1). However, at this level, a small but significant decrease in blood pressure occurred ($p < 0.05$).

Heart rate, arterial blood gases and acid-base balance, during baseline conditions and gradual ICP increase are shown in table 2. Heart rate, arterial blood gases and acid-base balance were widely unchanged throughout the earlier stages of the experimental procedure. During the last stage of CPP reduction, a small decrease in heart rate of 85 ± 15% occurred ($p < 0.05$).

Cerebral oxygen delivery and $CMRO_2$ were widely maintained up to an increase in ICP to 25 ± 2 mm Hg which corresponded to a CPP reduction of 69 ± 1% of baseline values. This was caused by a slight increase in blood flow to the cerebrum by about 16%. A further increase in ICP to 36 ± 3 mm Hg with a concomitant

Table 1. Summarized presentation of the duration of the different experimental stages, and of the behavior of ABP, ICP and CPP during the whole period of every stage and during the periods of microsphere measurement and of blood infusion/withdrawal in order to adjust ABP at baseline values using an external ABP controller

	Baseline	Control 2	ICP 25 mm Hg	ICP 35 mm Hg	ICP 45 mm Hg
Stage duration, min	29±2	62±14	30±2	29±1	30±2
ABP during whole stage, mm Hg	93±7	90±6	86±4	82±2	78±2*
ABP during microsphere measurement, mm Hg	93±8	91±7	86±7	82±2	77±3*
ICP during whole stage, mm Hg	6±2	6±3	26±3*	37±3*	47±2*
ICP during microsphere measurement, mm Hg	7±2	6±2	25±2*	36±3*	45±2*
CPP during whole stage, mm Hg	86±7	84±7	59±4*	45±3*	31±3*
CPP during microsphere measurement, mm Hg	86±7	85±8	59±4*	44±4*	28±3*
Blood infusion/withdrawal, % of the calculated blood volume	–	−4.1±5.2	−8.8±8.3	−5.0±7.1	5.8±2.4

Values are means ± SD. n = 10 animals with exception of stage ICP 45 mm Hg, because at this stage, in 2 animals an acute uncontrollable decrease in ABP occurred so that the epidural balloon had to be deflated prematurely.

* $p < 0.05$, significant differences between baseline values and values obtained at different stages of the experimental procedure.

Table 2. Physiological parameters during periods of unchanged ICP and during gradual epidural balloon inflation at adjusted ABP by extracorporeal control

	Baseline	Control 2	ICP 25 mm Hg	ICP 35 mm Hg	ICP 45 mm Hg
Heart rate, min^{-1}	240±45	243±31	259±42	226±45	200±34*
Arterial pO_2, mm Hg	154±28	154±28	151±28	154±27	152±33
Arterial pCO_2, mm Hg	38±1	40±4	39±2	39±2	39±2
Arterial pH	7.42±0.03	7.40±0.05	7.40±0.04	7.39±0.05	7.36±0.09*
Arterial O_2 content, $mmol \cdot l^{-1}$	6.6±0.8	6.7±0.8	6.2±0.7*	5.8±0.6*	5.6±0.7*
Arterial base excess, $mmol \cdot l^{-1}$	0.1±2.3	0.5±2.3	−1.1±2.6	−1.6±3.4	−1.5±3.6
Arterial glucose content, $mmol \cdot l^{-1}$	7.6±1.0	7.4±1.0	9.1±3.2	8.9±2.1	9.1±1.1*
Arterial lactate content, $mmol \cdot l^{-1}$	1.4±0.2	1.3±0.2	1.9±0.9	2.0±1.0	2.5±1.3*

Values are means ± SD. n = 10 animals with exception of stage ICP 45 mm Hg, because at this stage, in 2 animals an acute uncontrollable decrease in ABP occurred so that the epidural balloon had to be deflated prematurely.

* $p < 0.05$, significant differences between baseline values and values obtained at different stages of the experimental procedure.

CPP reduction of 51 ± 3% led to an significant reduction of global CBF (72 ± 29% of baseline value), cerebral O_2 delivery (55 ± 31% of baseline value) and $CMRO_2$ (63 ± 30% of baseline value; table 3, $p < 0.05$). The last stage of ICP increase (45 ± 2 mm Hg) resulted in a severe CBF reduction (24 ± 18% of baseline value) with a more pronounced reduction of cerebral O_2 delivery (15 ± 13% of baseline value) and $CMRO_2$ (16 ± 15% of baseline value; table 3, $p < 0.05$). Moreover, some regional CBF showed a different behavior: infratentorial brain structures, thalamus and hippocampus tended to increase CBF during mild ICP elevation (fig. 2), but CBF was significantly reduced at the highest level of ICP increase ($p < 0.05$). Furthermore, CBF to regions ipsilateral to the inflated epidural balloon was similar to that of contralateral brain regions (fig. 2). This was also true for most cortical brain regions with exception of the frontal cortex and the rostral part of the parietal cortex. Here, brain structures which were attached to the inflated epidural balloon showed a significant blood flow reduction already at mild ICP

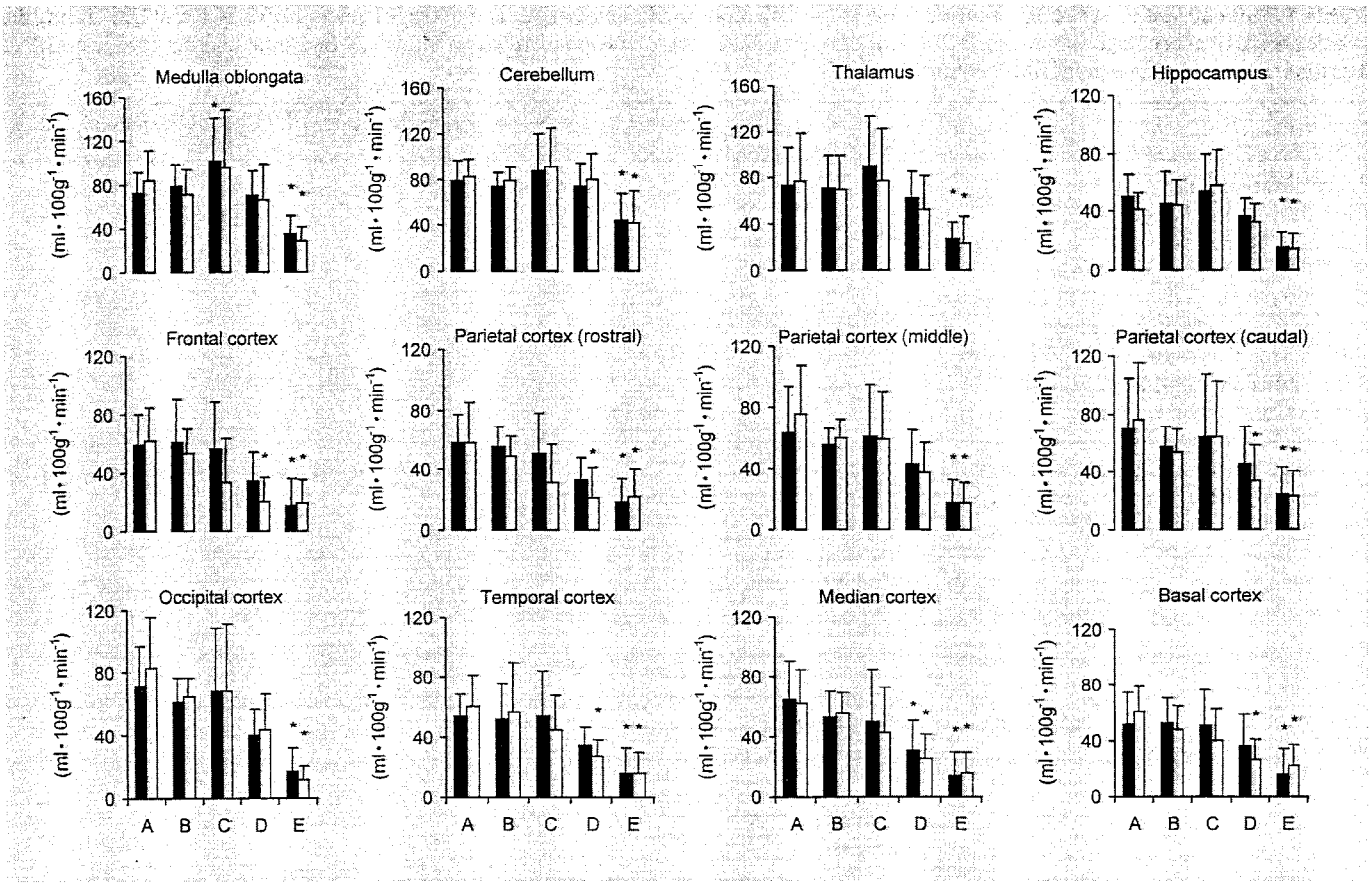

Fig. 2. Regional CBF as CPP was decreased (values are means ± SD). Black columns indicate the site contralateral and open columns the site ipsilateral to the epidural balloon. A–E indicate the different experimental stages (A = baseline, B = control 2, C = ICP 25 mm Hg, D = ICP 35 mm Hg, E = ICP 45 mm Hg). * $p < 0.05$, significant differences between baseline values and values obtained at different stages of the experimental procedure.

Table 3. Global CBF, cerebral oxygen delivery and cerebral oxygen consumption during periods of unchanged ICP and during gradual epidural balloon inflation at adjusted ABP by extracorporeal control

	Baseline	Control 2	ICP 25 mm Hg	ICP 35 mm Hg	ICP 45 mm Hg
Global CBF, ml·min^{-1}·100 g^{-1}	58±21	54±16	60±29	34±15*	12±14*
Cerebral oxygen delivery, µmol·min^{-1}·100 g^{-1}	397±176	365±125	372±191	201±99*	68±73*
Cerebral oxygen consumption, µmol·min^{-1}·100 g^{-1}	172±67	146±26	144±58	104±34*	43±56*

Values are means ± SD. n = 10 animals with exception of stage ICP 45 mm Hg, because at this stage, in 2 animals an acute uncontrollable decrease in ABP occurred so that the epidural balloon had to be deflated prematurely.

* $p < 0.05$, significant differences between baseline values and values obtained at different stages of the experimental procedure.

increase ($p < 0.05$). This side difference existed also at the next stage of ICP increase, but disappeared during the strongest ICP increase (fig. 2).

Discussion

In the present study, an experimental model was designed to create a reproducible gradual decrease in CPP to levels considered to be increasingly harmful to the immature brain. This model of an epidural balloon expansion has not been previously described in immature animals. We purposely maintained a stable period of reduced CPP in order to study the effects on regional brain hemodynamics and brain oxidative metabolism.

Methodology

The method of raising ICP by means of an inflated epidural balloon has been widely used in adult animals [12–14] but not in immature animals. Moreover, in order to use this model for studying the relationship between alterations in ICP secondary to epidural volume expansion and cerebral perfusion, one has to be aware that early alteration of systemic circulation may occur (e.g. ABP increase [15]). The experimental variability of ABP was removed by external control to guarantee that the resultant changes in CPP were the prerequisite determinant of CBF regulation. The gradual ICP increase induced by stepwise epidural balloon inflation is regularly attended by a sustained increase in the ABP, as one component of the so-called 'Cushing response' (CR) [16]. CR is defined as a triad of an elevation in ABP, bradycardia and respiratory irregularities due to brain impairment [17]. The initial response is a graded rise in ABP [16]; irregularities in breathing may not occur until the brain stem has been injured. Controversies still exist concerning the underlying mechanisms for these responses, but may include ICP [13, 15, 16, 18], reduced blood volume [19], impaired cerebral blood supply [20, 21], brain stem distortion [22, 23] or localized pressure on certain areas of the brain stem [24]. Obviously, different mechanisms mentioned may play a role at different stages of brain impairment. Gradual ICP elevation induces an ABP increase prior to alterations in CBF as a result of decreasing CPP [15], as was observed in this experimental paradigm. In order to control for the stepwise steady-state changes of CPP in piglets, an external blood pressure controller was used to adjust mean ABP to maintain it at baseline values. Moreover, in this experimental application, the amount of withdrawn/infused blood volume necessary at the different ICPs indicates the intended cardiovascular regulatory responses. Indeed, lowering of the CPP led to the need to gradually exsanguate the piglet to compensate for the ABP increase. This was true during conditions under which no relevant changes in brain oxygen metabolism occurred. Later, at the ICP of 45 mm Hg, which significantly reduced but did not eliminate brain oxygen delivery (e.g. 15 ± 13% of baseline value), maintenance of baseline ABP levels required massive reinfusion of the previously withdrawn blood volume as well as partly further volume expansion. This experimental procedure of gradual ICP increase by stepwise epidural balloon inflation and controlling for ABP also gradually reduces CPP and can be achieved with sufficient cardiovascular stability.

In order to estimate the usefulness of this experimental model in regard to the effects of ICP on forebrain oxygen metabolism, the regional deformation of the underlying cortex must be considered. Regional CBF measurements were reduced focally in the cortical regions which were in direct contact to the inflated epidural balloon (i.e. frontal lobe and the rostral part of the parietal lobe of the right hemisphere). During the initial mild balloon inflation (ICP = 25 mm Hg), a larger reduction of regional CBF was found in the ipsilateral hemisphere compared to the corresponding areas in the opposite hemisphere (fig. 2). This effect became more pronounced during moderate ICP increase, with the effect extended to other regions rostral to the tentorium. At the highest level of ICP, a homogenous decrement in CBF in both hemispheres indicates a fairly diffuse supratentorial spread of ICP and decrement in CPP. The effect of this artificial change of compartmental assignment with reference to ICP was monitored from the site opposite to the inflated balloon in order to verify effects which are representative for most parts of the brain outside the direct local effects of mass expansion.

To study a diffuse ICP increase, a comparable approach might be achieved by an intracranial fluid infusion (i.e. intraventricular or subdural infusion). Previously, this approach has induced a rapid cerebral circulatory arrest in newborn pigs [25]. Likely, it is necessary to similarly control ABP to define the effect of CPP in this model.

CBF Estimation

Regional CBF was measured using multiple colored microspheres. This technique in newborn piglets has previously been validated in our laboratory [7] for use in organ blood flow. In this study, a correlation between flow rates determined simultaneously by colored microspheres

and radioactive-labeled microsphere technique was found even for organs with low perfusion. The quality of microsphere detection is a result of the whole procedure of colored microsphere quantification. In this study, the detection error of falsely detected missing microspheres as a valid indicator of the precision of microsphere detection, found an error of approximately 1–10% [7], which was comparable with studies using radioactive-labeled microspheres [26, 27]. Another procedure to assess the quality of colored microsphere detection by spectrophotometry and matrix inversion showed a coefficient of variation between 1.28 and 3.63% [6]. The amount of falsely detected missing microspheres is of particular importance in pathophysiological conditions where regional trickle-flow or no-flow conditions can appear. Therefore, we assume that even during the low-perfusion states, a reliable estimation of regional blood flow was performed because more then 400 microspheres were found in all tissue samples which were measured. The colored microsphere method for multiple quantitative blood flow estimation was used because this method appears to be a valid alternative for regional blood flow measurement in newborn piglets, and all disadvantages (e.g. economic, legal and health considerations) arising from radioactive labeling are avoided. Regional CBF can also be measured by quantitative autoradiography using radiolabeled iodoantipyrine [28]. Despite an improved spatial resolution, this procedure appears to be inadequate in this experimental design because only one measurement per experiment can be achieved using quantitative autoradiography.

Effects on CBF and Oxidative Metabolism

Our data show that in juvenile piglets, a CPP reduction of 30% is fully compensated for by increasing CBF and stable oxidative metabolism. A further decrease in CPP up to 50% of baseline values leads to a moderate CBF reduction and a restriction in cerebral oxygen delivery and consumption. Under these conditions, oxygen metabolism of large parts of the forebrain was not disturbed. However, it has to be considered that the estimation of $CMRO_2$ was based on blood sampling from the sagittal sinus and confluence sinuum. Therefore, regional differences in oxygen consumption cannot be differentiated because of mixed venous blood obtained from the confluence sinuum from both hemispheres. Regional CBF, though, gives an estimate of regional oxygen availability. As a result, the data of regional CBF enable us to estimate the $CMRO_2$ values which likely are representative for approximately 88% of the brain, calculated as the ratio between forebrain weight and whole brain in the piglets used in this study.

Cerebral oxidative metabolism was measured under slight general anesthesia. We used a combination narcosis with a considerably low level of the narcotic component (0.8% isoflurane) which corresponds under normothermia to a MAC of about 0.34 [29]. However, the resulting effects on oxidative brain metabolism are assumed to be relevant, because earlier studies in adult dogs [30] and cats [31] have shown that an increase in isoflurane MAC from zero to 0.5 resulted in a decrease in $CMRO_2$ of about 30%. A further doubling of isoflurane MAC induced a further $CMRO_2$ reduction of 18%. Therefore, there is a nonlinear relation between isoflurane MAC increase and oxidative brain metabolism deprivation with an increased metabolic susceptibility in low MAC values. A comparable reduction in oxidative brain metabolism is likely and in line with published values of cerebral O_2 uptake in nonanesthetized piglets [32], which were about 30% higher as found in this study. Mild CPP reduction at 30% of baseline values was completely compensated for by blood flow and oxygen uptake of the cerebrum. This finding corresponds to the autoregulatory threshold in the piglets [33]. Further CPP reduction surpasses the autoregulatory threshold and hence induced a concomitant decrease in blood flow to the cerebrum combined with a similar reduction in cerebral oxygen delivery and cerebral oxygen uptake.

Outlook

This experimental model has previously been used in adult animals to study the conditions which provoke a rebound of ICP after decompression of the intracranial mass lesion [34]. It was found that this is a threshold phenomenon which depends upon the CPP during compression and the duration of the compression. Release of the compression resulted in a marked cerebral hyperperfusion which generalized to the supratentorial but not the infratentorial structures [34]. Diffuse brain swelling with fatal outcome after balloon decompression was found in a canine outcome model [35]. In this study, an increased ICP of 62 mm Hg was induced by epidural balloon inflation for 90 min, followed by intensive care for 96 h. Our study gives an experimental basis to design an outcome model in order to investigate effects of decompression after temporal epidural balloon inflation which will mimic a clinical situation of epi- or subdural hematoma evacuation which is frequent in infants and young children after nonaccidental head injury [36, 37].

In summary, the present results show that the experimental design used here provides an approach to study pathophysiological conditions comparable with situations during very severe traumatic brain lesions with excellent stability of steady-state stages in order to obtain regional brain functions.

Acknowledgment

The authors thank Mrs. U. Jäger, Mrs. I. Witte and Mr. L. Wunder for skillful technical assistance and Dr. P.D. Adelson (Pittsburgh, Pa.) for his collegial review of the manuscript. This work was supported by BMBF 01ZZ9602.

References

1 Ward JD: Pediatric head injury: A further experience. Pediatr Neurosurg 1994;20:183–185.
2 Bruce DA, Alavi A, Bilaniuk L, Dolinskas C, Obrist W, Vzzell B: Diffuse cerebral swelling following head injuries in children: The syndrom of malignant brain edema. J Neurosurg 1981;54:170–178.
3 Aldrich EF, Eisenberg HM, Saydjari C, Luerssen TG, Foulkes MA, Jane JA, Marshall LF, Marmarou A, Young HF: Diffuse brain swelling in severely head-injured children. A report from the NIH Traumatic Coma Data Bank. J Neurosurg 1992;76:450–454.
4 Shibata M, Einhaus S, Schweitzer JB, Zuckerman S, Leffler CW: Cerebral blood flow decresed by adrenergic stimulation of cerebral vessels in anesthetized newborn pigs with traumatic brain injury. J Neurosurg 1993;79:696–704.
5 Hoyer D, Bauer R, Walter B, Zwiener U: Adjustment of reduced arterial blood pressure – A tool for investigations into gradually reduced brain function. Biomed Tech 1997;42:284–290.
6 Kowallik P, Schulz R, Guth BD, Schade A, Paffhausen W, Gross R, Heusch G: Measurement of regional myocardial blood flow with multiple colored microspheres. Circulation 1991;83:974–982.
7 Walter B, Bauer R, Gaser E, Zwiener U: Validation of the multiple coloured microsphere method for measurement of regional organ blood flow in newborn piglet. Basic Res Cardiol 1997;92:191–200.
8 Makowski EL, Meschia G, Droegemueller W, Battaglia FC: Measurement of umbilical arterial blood flow to the sheep placenta and fetus in utero. Circ Res 1968;23:623–631.
9 Busija DW, Leffler CW, Pourcyrous M: Hyperthermia increases cerebral metabolic rate and blood flow in neonatal pigs. Am J Physiol 1988; 255:H343–H346.
10 Coyle MG, Oh W, Stonestreet BS: Effects of indomethacin on brain blood flow and cerebral metabolism in hypoxic newborn piglets. Am J Physiol 1993;264:H141–H149.
11 Pownall R, Dalton RG: Blood and plasma volumes of neonatal pigs expressed relative to bodyweight and total body water. Br Vet J 1973;129:583–588.
12 Linhart O, Frománek J, Nádvornik F: Experimental epidural brain compression. Acta Univ Carol [Med] (Praha) 1974;20:497–548.
13 Schrader H, Lofgren J, Zwetnow NN: Influence of blood pressure on tolerance to an intracranial expanding mass. Acta Neurol Scand 1985; 71:114–126.
14 Nilsson F, Akeson J, Messeter K, Ryding E, Rosén I, Nordström C-H: A porcine model for evaluation of cerebral hemodynamics and metabolism during increased intracranial pressure. Acta Anaesthesiol Scand 1995;39:827–834.
15 Maas AIR, Fleckenstein W, de Jong DA, Wolf M: Effect of increased ICP and decreased cerebral perfusion pressure on brain tissue and cerebrospinal fluid oxygen tension; in Avezaat CJJ, van Eijndhoven JHM, Maas AIR, Tans JTJ (eds): Intracranial Pressure VIII. Berlin, Springer, 1993, pp 233–237.
16 Cushing H: Some experimental and clinical observations concerning states of increased intracranial tension. Am J Sci 1902;124:375–400.
17 Schrader H, Zwetnow NN, Morkrid L: Regional cerebral blood flow and CSF pressures during Cushing response induced by a supratentorial expanding mass. Acta Neurol Scand 1985; 71:453–463.
18 Brown FK: Cardiovascular effects of acutely raised intracranial pressure. Am J Physiol 1956;185:510–514.
19 Downing SE, Mitchell JH, Wallace AG: Cardiovascular responses to ischemia, hypoxia and hypercapnia of the central nervous system. Am J Physiol 1963;204:881–887.
20 Guyton AC: Acute hypertension in dogs with cerebral ischemia. Am J Physiol 1948;154:45–54.
21 Dampney RAL, Kumada M, Reis DJ: Central neural mechanisms of the cerebral ischemic response. Circ Res 1979;44:48–62.
22 Thompson RK, Malina S: Dynamic axial brain stem distortion as a mechanism explaining the cardiorespiratory changes in increased intracranial pressure. J Neurosurg 1959;16:664–675.
23 Weinstein JD, Langfitt TW, Bruno L, Zaren HA, Jackson JLF: Experimental study of patterns of brain distortion and ischemia produced by an intracranial mass. J Neurosurg 1968;28:513–521.
24 Hoff JT, Reiss DJ: Localisation of regions mediating the Chushing response in CNS of cat. Arch Neurol 1970;23:228–240.
25 Leffler CW, Busija DW, Mirro R, Armstead WM, Beasley DG: Effects of ischemia on brain blood flow and oxygen consumption of newborn pigs. Am J Physiol 1989;257:H1917–H1926.
26 Buckberg GD, Luck JC, Payne DB, Hoffman JIE, Archie JP, Fixler DE: Some sources of error in measuring regional blood flow with radioactive microspheres. J Appl Physiol 1971; 31:598–664.
27 Dole WP, Jackson DL, Rosenblatt JI, Thompson WL: Relative error and variability in blood flow measurements with radiolabeled microspheres. J Am Physiol 1982;243:H371–H378.
28 Sakurada O, Kennedy C, Jehle J, Brown JD, Carbin GL, Sokoloff L: Measurement of local cerebral blood flow with iodo [14C] antipyrine. Am J Physiol 1978;234:H59–H66.
29 Sakas DE, Whitwell HL: Neurological episodes after minor head injury and trigeminovascular activation. Med Hypotheses 1997;48:431–435.
30 Stullken EH Jr, Milde JH, Michenfelder JD, Tinker JH: The nonlinear responses of cerebral metabolism to low concentrations of halothane, enflurane, isoflurane, and thiopental. Anesthesiology 1977;46:28–34.
31 Todd MM, Drummond JC: A comparison of the cerebrovascular and metabolic effects of halothane and isoflurane in the cat. Anesthesiology 1984;60:276–282.
32 Laptook AR, Hassan A, Peterson J, Corbett RJ, Nunnally RL: Effects of repeated ischemia on cerebral blood flow and brain energy metabolism. NMR Biomed 1988;1:74–79.
33 Laptook A, Stonestreet BS, Oh W: Autoregulation of brain blood flow in the newborn piglet: Regional differences in flow reduction during hypotension. Early Hum Dev 1982;6:99–107.
34 Jakobsson KE, Lofgren J, Zwetnow NN, Morkrid L: Cerebral blood flow in experimental intracranial mass lesions. II. The postdecompression phase. Neurol Res 1990;12:153–157.
35 Ebmeyer U, Safar P, Radovsky A, Obrist W, Alexander H, Pomeranz S: Moderate hypothermia for 48 h after temporary epidural brain compression injury in a canine outcome model. J Neurotrauma 1998;15:323–336.
36 Adelson PD, Kochanek PM: Head injury in children. J Child Neurol 1998;13:2–15.
37 Duhaime AC, Christian CW, Rorke LB, Zimmerman RA: Current concepts: Nonaccidental head injury in infants – The 'shaken-baby syndrome'. N Engl J Med 1998;338:1822–1829.

Effect of mild hypothermia on cerebral oxygen uptake during gradual cerebral perfusion pressure decrease in piglets

Reinhard Bauer, MD; Harald Fritz, MD; Bernd Walter, MD; Olaf Schlonski, MD; Thomas Jochum, MD; Dirk Hoyer, Dr.Ing; Ulrich Zwiener, MD, PhD; Konrad Reinhart, MD

Objective: **To study the effect of mild hypothermia on cerebral oxygen metabolism and brain function in piglets during reduced cerebral blood flow because of gradual reduction of the effective cerebral perfusion pressure (CPP).**

Design: **Comparison of two randomized treatment groups: normothermic group (NT; n = 7) and hypothermic group (HT; n = 7).**

Setting: **Work was conducted in the research laboratory of the Institute for Pathophysiology, Friedrich Schiller University, Jena, Germany.**

Subjects: **Fourteen piglets (14 days old) of mixed German domestic breed.**

Intervention: **Animals were anesthetized and mechanically ventilated. An epidural balloon was gradually inflated to increase intracranial pressure to 25 mm Hg, 35 mm Hg, and 45 mm Hg every 30 mins at adjusted mean arterial blood pressures. After determination of baseline CPP (NT, 79 ± 14 mm Hg; HT, 84 ± 9 mm Hg), CPP was reduced to ~70%, 50%, and 30% of baseline (NT, 38.1 ± 0.5°C; HT, 31.7 ± 0.5°C).**

Measurements and Main Results: **Every 25 mins after the gradual CPP reductions. Mild hypothermia induced a reduction of the cerebral metabolic rate of oxygen ($CMRO_2$) to 50% ± 15% of baseline values (baseline values, 352 ± 99 $\mu mol \cdot 100\ g^{-1} \cdot min^{-1}$) ($p < .05$). Moreover, the electrocorticogram was altered to a pattern of reduced delta activity ($p < .05$) but unchanged higher frequency activity. The cerebral oxygen balance in HT animals remained improved until CPP reduction to 50%, indicated by a reduced cerebral arteriovenous difference of oxygen but elevated brain tissue Po_2 ($p < .05$). Further CPP reduction gave rise to a strong $CMRO_2$ reduction (NT, 19 ± 21%; HT, 15 ± 15%; $p < .05$). However, the high-frequency band of electrocorticogram was less reduced in hypothermic animals ($p < .05$).**

Conclusions: **Mild whole body hypothermia improves cerebral oxygen balance by reduction of brain energy demand in juvenile piglets. The improvement of brain oxygen availability continues during a mild to moderate CPP decrease. A loss of the difference in $CMRO_2$ between the hypothermic and normothermic piglets together with the fact that brain electrical activity was less suppressed under hypothermia during severe cerebral blood flow reduction indicates that hypothermic protection may involve some other mechanisms than reduction of brain oxidative metabolism. (Crit Care Med 2000; 28:1128–1135)**

Key Words: cerebral blood flow; cerebral oxygen consumption; intracranial pressure; epidural balloon inflation; extracorporeal arterial blood pressure controller; piglets; hypothermia; colored microspheres; neurologic emergencies; brain

For infants and young children, traumatic injury is the leading cause of death and mortality is greatly increased in the presence of brain injury (1). Increased intracranial pressure (ICP) is a common complication in infants and young children suffering from severe traumatic brain injuries and is closely correlated with an adverse outcome. It was recently reported that ~60% of severe head-injury patients develop an increased ICP, mostly as a result of brain swelling (2). The incidence of brain swelling in pediatric patients was twice as high as in adults (3, 4). This concurs with recent findings in experimental studies, in which immature rats were discovered to develop cerebral edema as a main cause of brain swelling more rapidly than mature rats (5). Recently, it was shown that the cerebrovascular response to traumatic brain injury differs in immature and more mature animals. Cerebral arterioles constricted to a greater extent in newborn pigs than juvenile ones after fluid percussion induced traumatic brain injury, and the resulting decrease in cerebral blood flow (CBF) was prolonged (6). However, experimental or clinical studies on the effects of mild to moderate hypothermia on cerebral oxygen metabolism in the immature brain during compromised brain oxygen delivery because of increased ICP have not as yet been performed.

We hypothesized that mild hypothermia improves cerebral oxygen balance during stages of decreased cerebral perfusion. To test this hypothesis, we examined the effects of mild hypothermia on cerebral hemodynamics and brain oxygen metabolism in 2-wk-old piglets after a stepwise reduction in cerebral perfusion pressure, induced by gradual inflation of an epidural balloon. An experimental procedure was used that allows sequential estimation of regional CBF and cerebral metabolic rate of oxygen ($CMRO_2$). This was realized using an external closed-loop controller of arterial blood pressure (ABP) to avoid ICP-related ABP alterations.

From the Traumatic Brain Injury and Perinatal Research Group, Institute for Pathophysiology (Drs. Bauer, Walter, Hoyer, Zwiener, Mr. Schlonski, and Jochum), and the Clinic for Anesthesiology and Intensive Care (Drs. Fritz and Reinhart), Friedrich Schiller University, D-07740 Jena, Germany.

Supported, in part, by Grant 01ZZ9602 from the Bundesministerium für Bildung und Forschung, Germany.

Copyright © 2000 by Lippincott Williams & Wilkins

MATERIALS AND METHODS

This protocol was approved by the committee of the Thuringian State government for animal research. The animals were managed in accordance with the guidelines of the American Physiologic Society.

Subjects. Fourteen piglets of mixed German domestic breed (14 days old; body weight, 4517 ± 536 g) were used in the study.

Surgical Procedures. Piglets were initially sedated with ketamine hydrochloride (50 mg/kg body weight) and then anesthetized with 1.5% isoflurane in 70% nitrous oxide and 30% oxygen. A central venous catheter was introduced through the left external jugular vein and was used for the administration of drugs and for volume substitution (lactated Ringer's solution, 5 mL/kg of body weight/hr). An endotracheal tube was inserted by means of a tracheotomy. After immobilization with pancuronium bromide (0.2 mg/kg body weight/hr, iv), the animals were artificially ventilated (Servo Ventilator 900C, Siemens-Elema, Solna, Sweden). Anesthesia was maintained throughout the experiment with 0.8% isoflurane. Polyethylene catheters (inner diameter, 1.5 mm) were advanced through the femoral arteries into the abdominal aorta to record ABP and to withdraw reference samples for the colored microsphere technique. A further polyethylene catheter (inner diameter, 0.3 mm) was inserted into the superior sagittal sinus and advanced to the confluence sinuum to obtain brain venous blood samples. The left cardiac ventricle was cannulated retrogradely via the right common carotid artery with a polyurethane catheter (inner diameter, 0.5 mm). Arterial, left ventricular, and central venous catheters were connected with pressure transducers (P23Db, Statham Instruments, Hato Rey, PR). Body temperature was monitored by a rectal thermoprobe advanced for ~10 cm and was maintained throughout the general instrumentation at 38 ± 0.3°C using a water blanket connected to a heating-cooling thermostat and a feedback controlled heating lamp. Physiologic variables were recorded on a multichannel polygraph (MT95K2, Astro-Med, West-Warwick, RI).

Unipolar electrocorticogram (ECoG) recording was performed using screw electrodes. The electrode position was just posterior to the coronal suture, 10-mm lateral to the sagittal suture of the left parietal bone. The reference electrode was placed on the nasion.

Two holes were drilled into the left frontal bone, and a fiberoptic catheter was implanted into the subcortical white matter for ICP measurements (Camino Laboratories, San Diego, CA). A Clark-type Po_2 electrode (7, 8) together with a thermocouple catheter, serving as a temperature probe (LICOX Po_2 monitor, GMS mbH, Kiel-Mielkendorf, Germany), was implanted 3–5 mm into the parietal cortex. Measurements of brain tissue Po_2 were corrected to 37°C. On the right side, an oval-shaped burr hole (10–3 mm) was gently drilled into the frontal bone at a distance of 4 mm and parallel to the sagittal suture so that the dura mater was entirely intact. An epidural latex balloon attached to a catheter was placed in the epidural space of the right frontoparietal region. The burr holes were sealed with bone wax and covered with dental acrylic to fix the probes and the epidural balloon catheter in place.

Experimental Protocol. After the surgical preparation had been completed, the piglets underwent no further interventions for ~60 mins. After control values had been obtained, randomly chosen animals (n = 7) were surface cooled by crushed ice packages and cooled water through the pad to a body temperature of 31.7 ± 0.6°C. At this stage, the external ABP controller was established to adjust the ABP at baseline. A second series of values was obtained ("hypothermia"), followed by a gradual decrease of the effective cerebral perfusion pressure (CPP), which was calculated as the difference between mean ABP and ICP by stepwise elevation of the ICP in both groups, beginning at 25 mm Hg and followed by 35 mm Hg and 45 mm Hg, achieved by gradual epidural balloon inflation for ~30 mins each and stabilization of the mean ABP by the external blood pressure control loop. By using this procedure, stepwise reductions of CPP of ~70%, 50%, and 30% of baseline were produced. Considerable stability of the CPP at each stage could be reached (Table 1). Repeated measurements of all variables were recorded at the 25th min of every steady-state period.

Physiologic Measurements. Cardiac output and regional CBF were measured by means of the reference sample color-labeled microsphere technique (9). Application in piglets and methodical considerations have been presented and discussed in detail elsewhere (10). Briefly, in random sequence, a known amount (~$1.5 \cdot 10^6$/injection) of colored polystyrene microspheres (diameter, 15.5 ± 0.33 μm) in 0.01% Tween 80, surface coated with one of five dyes (white, yellow, red, violet, blue; Dye-Trak, Triton Technology, San Diego, CA) was thoroughly vortexed, sonicated, and immediately injected within 20 secs into the left ventricle. The injection line was then flushed with 2-mL of saline. A blood sample was withdrawn from the descending aorta as the reference sample (11), beginning 15 secs before the microsphere injection and continuing for 2 mins at a rate of 1.5 mL/min (syringe pump SP210iw, World Precision Instruments, Sarasota, FL). At the end of each experiment, the piglet was killed with KCl and the brain was removed for processing. The brain was sectioned into 26 tissue samples to determine blood flow to different brain regions. After sectioning, reference blood samples and tissue samples between 0.15 and 2.5 g were covered with digestive solution (4N KOH with 4% Tween 80 in deionized water). To retain the microspheres, each digested sample was then filtered under vacuum suction through an 8-μm pore polyester membrane filter. Colored microspheres were quantified by their dye

Table 1. Duration of different experimental stages and the behavior of cerebral perfusion pressure (CPP) during the whole period of every stage (normothermic baseline conditions, baseline 2/hypothermia and gradual decrease of the CPP by gradual epidural balloon inflation) and during the periods of microsphere measurement

Group	Baseline	Hypothermia	CPP-70%	CPP-50%	CPP-30%
Duration (mins)					
Normothermic	30 ± 1	89 ± 5	30 ± 2	29 ± 1	31 ± 2
Hypothermic	32 ± 3	96 ± 12	30 ± 2	30 ± 2	30 ± 1
CPP during whole stage (mm Hg)					
Normothermic	87 ± 4	84 ± 4 (96)	60 ± 3 (69)	44 ± 3 (51)	30 ± 4 (35)
Hypothermic	85 ± 5	82 ± 4 (96)	59 ± 4 (69)	44 ± 4 (51)	26 ± 5 (31)
CPP during microsphere measurement (mm Hg)					
Normothermic	87 ± 3	84 ± 3 (96)	60 ± 3 (69)	44 ± 2 (50)	27 ± 2 (32)
Hypothermic	86 ± 4	81 ± 3 (93)	59 ± 3 (69)	44 ± 3 (51)	25 ± 3 (29)

Values are mean ± SD; parentheses enclose percentage of mean CPP changes in relation to mean baseline values. n = seven animals in each group with the exception of stage CPP-30% of the normothermic group, because at this stage in one animal, an acute uncontrollable decrease of arterial blood pressure occurred so that the epidural balloon had to be deflated prematurely. "Hypothermia" indicates experimental stage of baseline 2 (normothermic group) and of that stage in which body temperature was lowered at ~32°C (hypothermic group); "CPP-70%," "CPP-50%," and "CPP-30%" indicate the lowering of CPP to ~70%, 50%, and 30% of the baseline values.

Table 2. Physiologic variables during normothermic baseline conditions, baseline 2/hypothermia, and gradual decrease of the cerebral perfusion pressure (CPP)

Group	Baseline	Hypothermia	CPP-70%	CPP-50%	CPP-30%
Heart rate (min^{-1})					
Normothermic	234 ± 45	233 ± 27	258 ± 43	221 ± 36	194 ± 17
Hypothermic	236 ± 37	176 ± 16[a,b]	176 ± 20[a,b]	164 ± 25[a,b]	158 ± 27[a,b]
Cardiac output (mL/min/kg)					
Normothermic	231 ± 53	213 ± 131	121 ± 57[b]	191 ± 91	222 ± 48
Hypothermic	213 ± 96	205 ± 102	118 ± 61[b]	182 ± 87	220 ± 125
Arterial Po_2 (mm Hg)					
Normothermic	144 ± 29	146 ± 29	140 ± 30	146 ± 30	144 ± 35
Hypothermic	133 ± 11	142 ± 22	128 ± 23	126 ± 23	131 ± 14
Arterial Pco_2 (mm Hg)					
Normothermic	38 ± 1	40 ± 5	39 ± 1	39 ± 2	39 ± 2
Hypothermic	37 ± 3	39 ± 5	39 ± 4	39 ± 3	38 ± 2
Arterial pH					
Normothermic	7.42 ± 0.04	7.40 ± 0.06	7.38 ± 0.04	7.38 ± 0.04	7.36 ± 0.08
Hypothermic	7.44 ± 0.06	7.38 ± 0.07	7.41 ± 0.06	7.40 ± 0.05	7.39 ± 0.05
Arterial oxygen content (μmol/mL)					
Normothermic	6.6 ± 0.7	6.7 ± 0.6	6.3 ± 0.6	5.9 ± 0.6	5.6 ± 0.4
Hypothermic	6.2 ± 0.7	6.5 ± 0.8	6.4 ± 0.6	6.1 ± 0.9	5.0 ± 0.6[b]
Rectal temperature (°C)					
Normothermic	38.2 ± 0.8	38.1 ± 0.6	38.2 ± 0.4	38.2 ± 0.3	37.9 ± 0.4
Hypothermic	38.0 ± 0.5	31.7 ± 0.6[a,b]	31.8 ± 0.6[a,b]	31.8 ± 0.6[a,b]	31.8 ± 0.4[a,b]

Values are mean ± SD. n = seven animals in each group with the exception of stage CPP-30% of the normothermic group, because at this stage in one animal, an acute uncontrollable decrease of arterial blood pressure occurred so that the epidural balloon had to be deflated prematurely. "Hypothermia" indicates experimental stage of baseline 2 (normothermic group) and of that stage in which body temperature was lowered at ~32°C (hypothermic group); "CPP-70%," "CPP-50%," and "CPP-30%" indicate the lowering of CPP to ~70%, 50%, and 30% of the baseline values.

[a]Significant differences between normothermic and the hypothermic animals; [b]significant differences between baseline values and values obtained at different stages of experimental procedure; $p < .05$.

content. The dye was recovered from the microspheres by adding 150 μL of dimethylformamide. The photometric absorption of each dye solution was measured by a diode-array UV/visible spectrophotometer (model 7500, Beckman Instruments, Fullerton, CA). Calculations were performed using the MISS software (Triton Technology, San Diego, CA). The number of microspheres was calculated using the specific absorbance value of the different dyes. All reference and tissue samples contained >400 microspheres.

Heart rate, ABP, ICP, cerebral perfusion pressure, arterial and brain venous pH, Pco_2, and Po_2, oxygen saturation, and hemoglobin values were measured at each study period. Blood pH, Pco_2, and Po_2 were measured with a blood gas analyzer (model ABL50, Radiometer, Copenhagen, Denmark), and blood hemoglobin and oxygen saturation were measured using a hemoximeter (model OSM2, Radiometer) and corrected to the body temperature of the animal at the time of sampling. ABP, sagittal sinus pressure, and ICP were continuously monitored.

Calculated Values and Data Analysis. Absolute flows to tissues measured by colored microspheres were calculated by the formula: $flow_{tissue}$ = number of $microspheres_{tissue}$ × ($flow_{reference}$/number of $microspheres_{reference}$). Flows are expressed in ml/min/100 g of tissue by normalizing for tissue weight.

Assuming the oxygen capacity of hemoglobin to be 1.39 mL of oxygen/g of hemoglobin in piglets (12), blood oxygen content was calculated as equal to g of hemoglobin/mL·1.39 mL oxygen/g of hemoglobin·%oxygen saturation and expressed in μmol/min·100 g. Dissolved oxygen was added by calculation, using the measured Po_2 and the temperature-corrected solubility coefficient of oxygen. Because the sagittal sinus drains the cerebral cortex, cerebral white matter, and some deep gray structures (basal ganglia, hippocampus) (13), blood flow measured to the cerebrum included these structures. $CMRO_2$ was obtained by multiplying blood flow to the cerebrum by the cerebral arteriovenous oxygen content difference ($C(a\text{-}\bar{v})o_2$). Total blood volume was assumed to be 12% of body weight (14).

ECoG signals were amplified, filtered (time constant was 0.1 secs; cut off frequency was 1000 Hz), fed into a PC using a 16-channel A/D board (DT2821F, Data Translation, Marlboro, MA), and stored on a hard disk for off-line data analysis (sample rate was 512 Hz). ECoG was quantified for 3 mins at each experimental period using Fast Fourier Transformation. Spectral band power was calculated for different frequency bands (delta band, 1.5–4 Hz; high-frequency band, 4–30 Hz) and normalized with the baseline spectral power.

A detailed description of the procedure of mean ABP adjustment at an externally given set point (baseline ABP value, as used in this application) using an external blood pressure control loop has been previously published (15, 16). In brief, ABP was controlled by a proportional-integral-differential-controller running on a personal computer, by means of changing the blood volume by arterial blood infusion or withdrawal, respectively. An infusion/withdrawal pump was the controlling element.

Statistical Analysis. If not otherwise indicated, data are reported as mean ± SD. Control variables were compared between groups with unpaired Student's *t*-tests. Two-way analysis of variance with repeated measures was used to determine the effects of CPP alteration and group CPP interaction within each variable. Subsequently, one-way analysis of variance with repeated measures was performed within each group. *Post hoc* comparisons were made with paired Student's *t*-tests using Bonferroni correction for multiple use. Comparisons between groups were made with unpaired Student's *t*-tests using Bonferroni correction for multiple use. Differences were considered significant when $p < .05$.

RESULTS

The lowering of rectal temperature to 31.8 ± 0.1°C, which was done by surface

cooling, required 95 ± 24 mins to accomplish and was maintained at this level of mild hypothermia (Table 2). The arterial blood gases and pH were similar throughout the experiment and not affected by mild hypothermia, because temperature-corrected values were used. Heart rate was strongly reduced by hypothermia by ~26% ($p < .05$). During baseline conditions and the period of hypothermia alone, brain temperature was higher than rectal temperature in normothermic as well as in hypothermic animals by 0.2–0.5°C ($p < .05$). However, in both groups during the period of decreased CPP, brain-to-body difference of temperature was first diminished, and at the lowest CPP level, the brain became cooler by 0.4–0.8°C ($p < .05$).

Gradual CPP reduction because of stepwise ICP increase (monitored contralateral to the gradually inflated epidural balloon) was determined reliably by means of epidural balloon inflation during feedback-controlled ABP stabilization (Fig. 1). ABP was maintained within small ranges throughout the experiment (81 ± 11 mm Hg), although slightly reduced ABP were found at the last two levels of reduced CPP ($p < .05$). No differences were found between normothermic and hypothermic groups in ABP, CPP, and ICP before and during mild hypothermia and during gradually reduced levels of the CPP. In contrast to the earlier stages of CPP lowering in which blood withdrawal occurred, at the last stage of CPP lowering, a complete reinfusion, partly by additional infusion of normal saline, was necessary to stabilize ABP (Table 4).

Mild hypothermia led to a significantly reduced $CMRO_2$ to 50 ± 15% of baseline values ($p < .05$; Fig. 2). This was accompanied by a smaller reduction of CBF to 74 ± 20% of baseline values. The changes in CBF are entirely attributable to higher arterial Pco_2. With the exception of the medulla oblongata, thalamus, and basal cortex, the other brain regions showed a marked blood flow reduction (Table 3). Consequently, $C(a\text{-}\bar{v})o_2$ decreased by 31 ± 19% and brain tissue Po_2 increased by 31 ± 12% ($p < .05$). Moreover, the pattern of electrocortical activity changed considerably from a delta wave-dominated pattern during normothermia to a pattern of unchanged higher frequency activity but strong reduced delta activity ($p < .05$; Fig. 3).

Gradual CPP reduction to 70% of baseline values did not change the high-

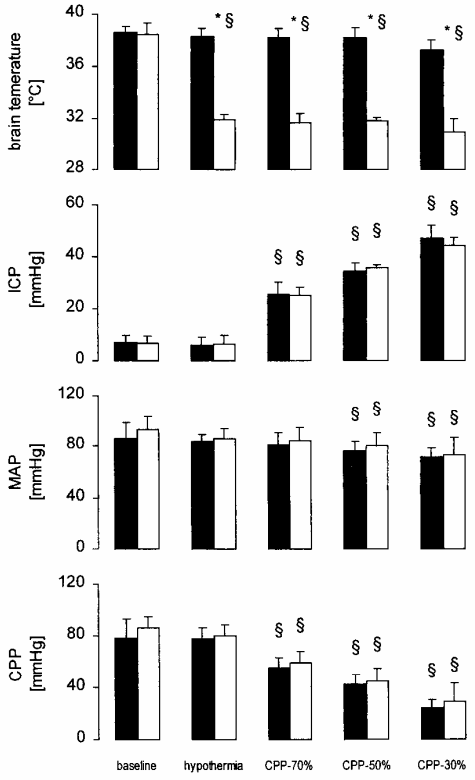

Figure 1. Brain temperature, intracranial pressure (*ICP*), mean arterial blood pressure (*MAP*), and cerebral perfusion pressure (*CPP*) in normothermic and hypothermic piglets at different stages of CPP decrease. Values are mean ± SD; n = seven animals in each group, with the exception of stage CPP-30% of the normothermic group, because at this stage in one animal an acute uncontrollable decrease of arterial blood pressure occurred so that the epidural balloon had to be deflated prematurely. *Filled columns*, normothermic group; *open columns*, hypothermic group; "hypothermia" indicates experimental stage of baseline 2 (normothermic group) and of that stage in which body temperature was lowered to ~32°C (hypothermic group). *Significant differences between the normothermic and hypothermic animals; §significant differences between baseline values and values obtained at different stages of the experimental procedure; $p < .05$.

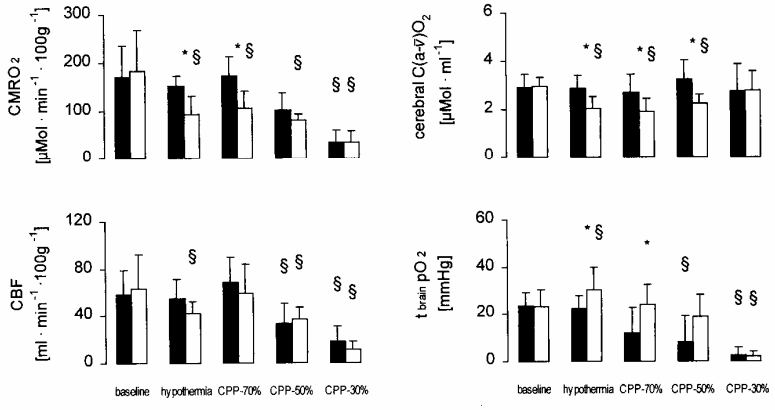

Figure 2. Cerebral metabolic rate of oxygen ($CMRO_2$) (*upper left*), cerebral blood flow (CBF) (*lower left*), cerebral arteriovenous difference of oxygen content ($C(a\text{-}\bar{v})o_2$) (*upper right*), and brain tissue Po_2 (t_{brain} Po_2) (*lower right*) in normothermic and hypothermic piglets at different stages of cerebral perfusion pressure (*CPP*) decrease. *Filled columns*, normothermic group; *open columns*, hypothermic group; "hypothermia" indicates experimental stage of baseline 2 (normothermic group) and of that stage in which body temperature was lowered to ~32°C (hypothermic group). *Significant differences between the normothermic and hypothermic animals; §significant differences between baseline values and values obtained at different stages of the experimental procedure; $p < .05$.

Table 3. Regional cerebral blood flow (ml · 100 g^{-1} · min^{-1}) for normothermic and hypothermic animals as cerebral perfusion pressure (CPP) was decreased

	Baseline	Hypothermia	CPP-70%	CPP-50%	CPP-30%
Normothermic animals					
Medulla oblongata					
CL	73 ± 16	77 ± 21	124 ± 28	79 ± 20	36 ± 26
IL	73 ± 19	75 ± 22	126 ± 31	81 ± 19	34 ± 26
Cerebellum					
CL	76 ± 10	77 ± 11	103 ± 20	79 ± 18	37 ± 36
IL	79 ± 6	81 ± 13	107 ± 24	85 ± 23	40 ± 42
Thalamus					
CL	67 ± 28	65 ± 24	111 ± 37	68 ± 25	14 ± 23
IL	71 ± 35	66 ± 30	99 ± 40	62 ± 25	22 ± 29
Hippocampus					
CL	47 ± 8	41 ± 15	65 ± 18	38 ± 13	14 ± 15
IL	45 ± 12	43 ± 16	65 ± 21	38 ± 13	16 ± 17
Occipital cortex					
CL	68 ± 22	62 ± 17	85 ± 39	43 ± 19	15 ± 15
IL	75 ± 27	67 ± 13	87 ± 37	42 ± 24	6 ± 7
Frontal cortex					
CL	59 ± 23	52 ± 7	73 ± 24	42 ± 20	15 ± 20
IL	61 ± 26	51 ± 11	45 ± 28	20 ± 16	10 ± 16
Parietal cortex (rostral)					
CL	53 ± 17	49 ± 10	60 ± 23	36 ± 16	16 ± 18
IL	57 ± 21	52 ± 15	42 ± 28	27 ± 21	13 ± 18
Parietal cortex (middle)					
CL	58 ± 21	54 ± 6	79 ± 29	47 ± 21	16 ± 16
IL	69 ± 24	58 ± 11	83 ± 34	39 ± 21	18 ± 20
Parietal cortex (caudal)					
CL	69 ± 27	59 ± 13	93 ± 33	53 ± 23	19 ± 19
IL	73 ± 32	52 ± 7	86 ± 35	41 ± 27	19 ± 24
Temporal cortex					
CL	51 ± 10	46 ± 14	60 ± 21	36 ± 14	15 ± 17
IL	53 ± 15	47 ± 9	52 ± 14	28 ± 14	14 ± 15
Median cortex					
CL	59 ± 22	52 ± 19	67 ± 27	35 ± 20	10 ± 19
IL	64 ± 29	55 ± 16	66 ± 31	33 ± 22	10 ± 18
Basal cortex					
CL	52 ± 20	47 ± 13	65 ± 21	43 ± 23	16 ± 23
IL	54 ± 15	47 ± 16	54 ± 16	30 ± 13	15 ± 14

frequency band of ECoG activity and $CMRO_2$ further in hypothermic animals, despite a recovery of CBF (Fig. 2). As shown in Table 4, during this first stage of gradual CPP lowered by stepwise ICP elevation, blood withdrawal was necessary in almost all animals to maintain ABP with the strongest compensatory blood withdrawal at stage CPP-70%. This was associated with a significant reduction of cardiac output (Table 2). Moreover, a redistribution of regional CBF was induced that significantly favored medulla oblongata, cerebellum, and the thalamus in normothermic animals (Table 3). Epidural balloon inflation led to a certain blood flow reduction ipsilateral to the inflated balloon, which was most prominent in the adjacent frontal lobe with a reduction of 38% in normothermic (NT) animals and 30% in hypothermic (HT) ones (Table 3). Brain tissue Po_2 reached baseline values, but $C(a\text{-}\bar{v})O_2$ remained at a similarly low level to before baseline in HT animals ($p < .05$; Fig. 3). Similarly mild CPP reduction because of ICP increase had no significant effects on brain oxidative variables in NT animals, but ECoG activity was significantly reduced ($p < .05$).

Further CPP reduction to an amount of ~50% of baseline values led to a CBF decrease to 64 ± 34% (NT group) and to 66 ± 25% (HT group) of baseline values ($p < .05$). This was predominantly caused by significantly reduced regional blood flows of cortical regions ipsilateral to the inflated epidural balloon, with the strongest reduction in the frontal lobe in which 48% of that flow in the contralateral frontal lobe was measured in both groups (Table 3). Moreover, the higher frequency band of ECoG was significantly reduced ($p < .05$) in HT animals, despite further unchanged $CMRO_2$.

CPP reduction to ~30% of the baseline values lead to a further considerable reduction of CBF (NT, 35 ± 26%; HT, 20 ± 14%) in both groups investigated ($p < .05$). At this stage, the reduction of $CMRO_2$ (NT, 19 ± 21%; HT, 15 ± 15%) and reduction of brain tissue Po_2 (NT, 10 ± 18%; HT, 9 ± 10%) were more pronounced in both groups. At this stage of ICP increase because of epidural balloon inflation over the right frontal lobe, a similar regional blood flow reduction occurred in all supratentorial brain regions (Table 3). Moreover, ECoG was further reduced ($p < .05$). Despite almost equalized $C(a\text{-}\bar{v})O_2$ between both groups studied, the high-frequency band of ECoG was significantly less reduced in HT animals ($p < .05$). This was confirmed with results of visual inspection of ECoG, in which an ischemic suppression of ECoG up to isoelectricity (four animals)

Table 3. Continues.

	Baseline	Hypothermia	CPP-70%	CPP-50%	CPP-30%
Hypothermic animals					
Medulla oblongata					
CL	73 ± 24	85 ± 32	108 ± 47	106 ± 30	52 ± 35
IL	74 ± 26	82 ± 31	113 ± 57	101 ± 29	51 ± 28
Cerebellum					
CL	78 ± 23	54 ± 16	66 ± 20	68 ± 22	38 ± 24
IL	75 ± 18	55 ± 17	64 ± 16	68 ± 19	36 ± 22
Thalamus					
CL	61 ± 22	52 ± 11	87 ± 50	66 ± 22	21 ± 15
IL	71 ± 32	60 ± 25	97 ± 52	64 ± 26	25 ± 16
Hippocampus					
CL	44 ± 8	30 ± 16	44 ± 19	38 ± 10	15 ± 12
IL	42 ± 8	29 ± 15	45 ± 20	37 ± 8	14 ± 11
Occipital cortex					
CL	69 ± 22	50 ± 15	76 ± 33	57 ± 18	18 ± 13
IL	65 ± 16	46 ± 12	74 ± 33	50 ± 11	15 ± 10
Frontal cortex					
CL	57 ± 11	38 ± 9	61 ± 27	39 ± 10	7 ± 6
IL	53 ± 12	39 ± 9	43 ± 21	19 ± 9	5 ± 5
Parietal cortex (rostral)					
CL	58 ± 16	44 ± 11	58 ± 25	42 ± 11	10 ± 8
IL	56 ± 12	41 ± 7	45 ± 20	21 ± 14	5 ± 5
Parietal cortex (middle)					
CL	68 ± 21	47 ± 10	72 ± 34	53 ± 10	16 ± 10
IL	60 ± 14	45 ± 13	75 ± 41	44 ± 21	14 ± 9
Parietal cortex (caudal)					
CL	68 ± 21	47 ± 13	74 ± 45	56 ± 27	19 ± 17
IL	62 ± 14	44 ± 10	79 ± 37	53 ± 17	13 ± 12
Temporal cortex					
CL	51 ± 13	48 ± 18	54 ± 22	40 ± 9	12 ± 8
IL	51 ± 15	47 ± 16	54 ± 23	32 ± 11	10 ± 7
Median cortex					
CL	59 ± 18	38 ± 11	64 ± 33	36 ± 18	9 ± 7
IL	47 ± 22	32 ± 17	52 ± 37	28 ± 18	4 ± 5
Basal cortex					
CL	49 ± 15	51 ± 22	58 ± 25	35 ± 13	9 ± 7
IL	48 ± 18	53 ± 25	55 ± 25	33 ± 14	7 ± 3

CL, contralateral; IL, ipsilateral site because of the epidural balloon.

Values are mean ± SD. n = seven animals in each group with the exception of stage CPP-30% of the normothermic group, because at this stage in one animal, an acute uncontrollable decrease of arterial blood pressure occurred so that the epidural balloon had to be deflated prematurely. "Hypothermia" indicates experimental stage of baseline 2 (normothermic group) and of that stage in which body temperature was lowered at ~32°C (hypothermic group); "CPP-70%," "CPP-50%," and "CPP-30%" indicate the lowering of CPP to ~70%, 50%, and 30% of the baseline values.

Table 4. Summarized presentation of blood infusion/withdrawal to adjust arterial blood pressure at baseline values using an external arterial blood pressure controller during normothermic baseline conditions; baseline 2/hypothermia and gradual decrease of the cerebral perfusion pressure (CPP)

Group	Baseline	Hypothermia	CPP-70%	CPP-50%	CPP-30%
Blood infusion/withdrawal (% of calculated blood volume)					
Normothermic	—	−3.6 ± 3.1	−9.8 ± 6.7	−5.9 ± 8.2	+5.0 ± 2.0
Hypothermic	—	−0.6 ± 1.4	−4.6 ± 6.7	−2.9 ± 12.9	+7.6 ± 10.5

Values are mean ± SD. n = seven animals in each group with the exception of stage CPP-30% of the normothermic group, because at this stage in one animal, an acute uncontrollable decrease of arterial blood pressure occurred so that the epidural balloon had to be deflated prematurely. "Hypothermia" indicates experimental stage of baseline 2 (normothermic group) and of that stage in which body temperature was lowered at ~32°C (hypothermic group); "CPP-70%," "CPP-50%," and "CPP-30%" indicate the lowering of CPP to ~70%, 50%, and 30% of the baseline values. –, not performed.

or burst suppression pattern (three animals) was only found in NT animals.

DISCUSSION

The data show that an improved cerebral oxygen balance by means of a marked reduction of cerebral oxygen demand results from mild hypothermia, even at stages of mild to moderate CPP restriction. The improved cerebral oxygen balance is entirely attributable to increased arterial Pco_2. The reduction in demand was shown by a reduced $C(a\text{-}\bar{v})O_2$ and an improved or maintained level of brain tissue Po_2. Preserved ECoG activity of the high-frequency band indicates an almost unchanged brain functional state. However, marked CPP reduction to ~30% of baseline with a concomitant reduced cerebral oxygen availability generally abolished these differences in $CMRO_2$ between the NT and HT groups, although brain electrical activity was less suppressed.

Mild hypothermia confers a marked protective effect on histopathologic outcome after experimental brain trauma (17), attenuating neurochemical sequels of cerebral oxygen lack and improving the behavioral outcome (18). Possible ex-

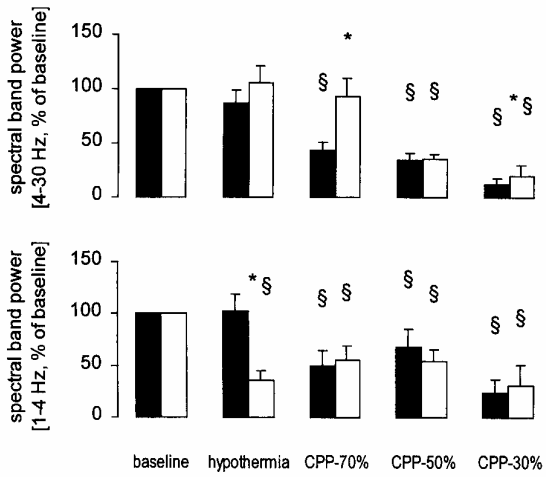

Figure 3. Spectral band power of electrocortical activity in normothermic and hypothermic piglets at different stages of cerebral perfusion pressure (*CPP*) decrease. Values are mean ± SE. *Filled columns*, normothermic group; *open columns*, hypothermic group; "hypothermia" indicates experimental stage of baseline 2 (normothermic group) and of that stage in which body temperature was lowered to ~32°C (hypothermic group). *Significant differences between the normothermic and hypothermic animals; §significant differences between baseline values and values obtained at different stages of the experimental procedure; $p < .05$.

planations for hypothermia-related improvement include the following: a) progressive reduction in cerebral metabolic rate for oxygen consumption; b) alterations in ion homeostasis (including calcium and potassium fluxes); c) increased membrane stability (including the blood-brain barrier); d) altered enzyme function (e.g., phospholipase, xanthine oxidase, nitric oxide synthase activity); e) alterations in neurotransmitter release and reuptake (e.g., glutamate); and f) changes in free radical production or scavenging (for review see References 19 and 20). Hypothermia has been evaluated as a therapeutic procedure for hastening neurologic recovery and improving the outcome in adult patients with severe traumatic brain injury (21).

The present data show a reduction in cerebral oxygen consumption caused by mild hypothermia by ~10%/°C. This corresponds with findings in newborn piglets (22) and amounted to nearly 50% more than was reported for adult brains (23, 24). However, in contrast to the results of Busija and Leffler (22) that were obtained during mild hypocapnia, obviously because of "α-stat" conditions, the corresponding blood flow reduction we observed was less pronounced.

The effect of the increased level of anesthesia because of hypothermia by the improved solubility of the anesthetics used here on $CMRO_2$ appears to be small. A reduction of brain and body temperature by 6°C at an unchanged inhalation content of 0.8% isoflurane resulted in a macroalveolar concentration increase from 0.34 to 0.45 (25).

The reason that CBF did not decrease by the same percentage as $CMRO_2$ at 32°C appears to be because of the kind of blood gas management used. We corrected blood gases and pH measurements under HT conditions to the body temperature of the animal at the time of sampling ("pH-stat"). This pH-stat management was chosen because recent reports suggest that there are mechanisms in effect during HT brain ischemia that could contribute to an improved cerebral outcome with pH-stat relative to more alkaline strategies (26–28). However, further studies are necessary to evaluate the importance of acid-base management on the relationship between cerebral oxygen delivery and demand under hypothermia and during compromised brain perfusion.

Previous studies have shown that hypothermia-induced suppression of the cerebral oxygen demand reflects influences on oxygen-consuming processes that are different from those suppressed by barbiturate-induced electroencephalogram suppression (24, 29, 30). Moreover, Nemoto and coworkers (31) also showed that the barbiturate-nonsuppressible $CMRO_2$ component of the basal $CMRO_2$ was much more temperature sensitive than the barbiturate-suppressible $CMRO_2$ component. Our study clearly showed that the ECoG pattern was changed by mild hypothermia from a delta wave-dominated ECoG to a delta wave-suppressed ECoG pattern with unchanged spectral power of the higher frequency band. Because a higher frequency pattern is associated with maintained cortical synaptic activity and signal transfer (32), we assume that at least a considerable amount of hypothermia-related $CMRO_2$ suppression was caused by the non-ECoG-associated $CMRO_2$ suppression.

The manipulation of ICP was managed by regional mass expansion because of gradual inflation of an epidural balloon. Local effects were obviously restricted to the cortical regions that were in direct contact with the inflated epidural balloon (i.e., frontal lobe and the rostral part of the parietal lobe of the right hemisphere), as was shown by respective changes in regional CBF. The effects of this artificial intracranial volume occupation with reference to ICP, brain tissue Po_2, and ECoG were monitored from sites opposite to the inflated balloon. Therefore, these effects are assumed to be representative for most parts of the brain outside the direct local effects of mass expansion.

Compared with the effects of mild hypothermia, we found that mild alterations of cerebral oxygen delivery because of gradual CPP reduction in NT animals predominantly induced a reduction of spontaneous ECoG activity, i.e., the functional $CMRO_2$ component was selectively compromised. This occurred in NT animals, even if the overall oxygen delivery and $CMRO_2$ were not reduced. The only finding that corresponded with changed ECoG activity in NT animals was an increased regional CBF to the lower brain stem and the thalamus in concordance with reduced cardiac output because of the self-controlled stabilization of ABP to prevent Cushing response-like ABP increase (33). The CBF increase to these brain regions may reflect a functional activation that could result in a desynchronization of cortical high-voltage delta activity because of diffuse thalamocortical projections of reticular formation (34, 35). However, a specific arousal-like pattern of an increased activity of high-frequency components was found only in HT animals during hypothermia and mild CPP reduction with a strong increase of alpha activity.

In summary, the present results confirm the well-known effect of mild hypo-

thermia on a decrease of cerebral oxidative metabolism. This improves the cerebral oxygen balance. However, if brain oxygen delivery was further reduced by CBF decrease induced by a gradual CPP reduction, then cerebral oxidative metabolism was obviously determined by a greater reduced oxygen delivery in brain tissue. The previously existing $CMRO_2$ differences between normothermia and hypothermia ceased, although brain electrical activity was less suppressed in HT animals.

ACKNOWLEDGMENTS

We thank U. Jäger, I. Witte, and L. Wunder for skillful technical assistance and Dr. D. Bredle (Eau Claire, WI) for collegial review of the manuscript.

REFERENCES

1. Levin HS, Aldrich EF, Saydjari C, et al: Severe head injury in children: Experience of the Traumatic Coma Data Bank. *Neurosurgery* 1992; 31:435–443
2. Ward JD: Pediatric head injury: A further experience. *Pediatr Neurosurg* 1994; 20:183–185
3. Bruce DA, Alavi A, Bilaniuk L, et al: Diffuse cerebral swelling following head injuries in children: the syndrom of malignant brain edema. *J Neurosurg* 1981; 54:170–178
4. Aldrich EF, Eisenberg HM, Saydjari C, et al: Diffuse brain swelling in severely head-injured children: A report from the NIH Traumatic Coma Data Bank. *J Neurosurg* 1992; 76:450–454
5. Grundl PD, Biagas KV, Kochanek PM, et al: Early cerebrovascular response to head injury in immature and mature rats. *J Neurotrauma* 1994; 11:135–148
6. Armstead WM, Kurth CD: Different cerebral hemodynamic responses following fluid percussion brain injury in the newborn and juvenile pig. *J Neurotrauma* 1994; 11:487–497
7. Maas AI, Fleckenstein W, de Jong DA, et al: Monitoring cerebral oxygenation: Experimental studies and preliminary clinical results of continuous monitoring of cerebrospinal fluid and brain tissue oxygen tension. *Acta Neurochir Suppl (Wien)* 1993; 59:50–57
8. Kiening KL, Unterberg AW, Bardt T, et al: Monitoring of cerebral oxygenation in severely head-injured patients: Brain tissue Po_2 vs. jugular venous oxygen saturation. *J Neurosurg* 1996; 85:751–757
9. Kowallik P, Schulz R, Guth BD, et al: Measurement of regional myocardial blood flow with multiple colored microspheres. *Circulation* 1991; 83:974–982
10. Walter B, Bauer R, Würker E, et al: Validation of the multiple coloured microsphere method for measurement of regional organ blood flow in newborn piglet. *Basic Res Cardiol* 1997; 92:191–200
11. Makowski EL, Meschia G, Droegemueller W, et al: Measurement of umbilical arterial blood flow to the sheep placenta and fetus in utero. *Circ Res* 1968; 23:623–631
12. Busija DW, Leffler CW, Pourcyrous M: Hyperthermia increases cerebral metabolic rate and blood flow in neonatal pigs. *Am J Physiol* 1988; 255: H343–H346
13. Coyle MG, Oh W, Stonestreet BS: Effects of indomethacin on brain blood flow and cerebral metabolism in hypoxic newborn piglets. *Am J Physiol* 1993; 264:H141–H149
14. Pownall R, Dalton RG: Blood and plasma volumes of neonatal pigs expressed relative to bodyweight and total body water. *Br Vet J* 1973; 129:583–588
15. Bauer R, Hoyer D, Walter B, et al: Changed systemic and cerebral hemodynamics and oxygen supply due to gradual hemorrhagic hypotension induced by an external PID-controller in newborn swine. *Exp Toxicol Pathol* 1997; 49:469–476
16. Hoyer D, Bauer R, Walter B, et al: Adjustment of reduced arterial blood pressure—A tool for investigations into gradually reduced brain function. *Biomed Technik* 1997; 42: 284–290
17. Dietrich WD, Alonso O, Busto R, et al: Posttraumatic brain hypothermia reduces histopathological damage following concussive brain injury in the rat. *Acta Neuropathol (Berl)* 1994; 87:250–258
18. Clifton GL, Jiang JY, Lyeth BG, et al: Marked protection by moderate hypothermia after experimental traumatic brain injury. *J Cereb Blood Flow Metab* 1991; 11:114–121
19. Dietrich WD: Nonpharmacological strategies—Moderate hypothermia. *In:* Neurotrauma. Narayan RK, Wilberger JE, Povlishock JT (Eds). New York, McGraw-Hill, 1996, pp 1491–1506
20. Wass CT, Lanier WL: Hypothermia-associated protection from ischemic brain injury: Implications for patient management. *Int Anesthesiol Clin* 1996; 34:95–111
21. Marion DW, Penrod LE, Kelsey SF, et al: Treatment of traumatic brain injury with moderate hypothermia. *N Engl J Med* 1997; 336:540–546
22. Busija DW, Leffler CW: Hypothermia reduces cerebral metabolic rate and cerebral blood flow in neonatal pigs. *Am J Physiol* 1987; 253:H869–H873
23. Rupp SM, Severinghaus JW: Hypothermia. *In:* Anesthesia. Miller RD (Ed). New York, Churchill Livingstone, 1986, pp 1195–2022
24. Nemoto EM, Klementavicius R, Melnick JA, et al: Suppression of cerebral metabolic rate for oxygen (CMRO2) by mild hypothermia compared with Thiopental. *J Neurosurg Anesthiol* 1996; 8:52–59
25. Satas S, Haaland K, Thoresen M, et al: MAC for halothane and isoflurane during normothermia and hypothermia in the newborn piglet. *Acta Anaesthesiol Scand* 1996; 40: 452–456
26. Jonas RA, Bellinger DC, Rappaport LA, et al: Relation of pH strategy and developmental outcome after hypothermic circulatory arrest. *J Thorac Cardiovasc Surg* 1993; 106: 362–368
27. Hiramatsu T, Miura T, Forbess JM, et al: pH strategies and cerebral energetics before and after circulatory arrest. *J Thorac Cardiovasc Surg* 1995; 109:948–957
28. Kurth CD, Orourke MM, Ohara IB, et al: Brain cooling efficiency with pH stat and alpha stat cardiopulmonary bypass in newborn pigs. *Circulation* 1997; 96(Suppl):358–363
29. Steen PA, Newberg L, Milde JH, et al: Hypothermia and barbiturates: Individual and combined effects on canine cerebral oxygen consumption. *Anesthesiology* 1983; 58: 527–532
30. Michenfelder JD, Milde JH: The relationship among canine brain temperature, metabolism, and function during hypothermia. *Anesthesiology* 1991; 75:130–136
31. Nemoto EM, Klementavicius R, Yonas H: Q10 for basal cerebral metabolic rate for oxygen (BCMRO2) in rats. *Crit Care Med* 1995; 23:A246
32. Steriade M, Gloor P, Llinas RR, et al: Report of IFCN Committee on Basic Mechanisms: Basic mechanisms of cerebral rhythmic activities. *Electroencephalogr Clin Neurophysiol* 1990; 76:481–508
33. Schrader H, Hall C, Zwetnow NN: Effects of prolonged supratentorial mass expansion on regional blood flow and cardiovascular parameters during the Cushing response. *Acta Neurol Scand* 1985; 72:283–294
34. Ingvar DH, Söderberg U: Cortical blood flow related to EEG patterns evoked by stimulation of the brain stem. *Acta Physiol Scand* 1958; 42:130–143
35. Meyer JS, Namura F, Sakamoto K, et al: Effect of stimulation of the brain stem reticular formation on cerebral blood flow and oxygen consumption. *Electroencephalogr Clin Neurophysiol* 1969; 26:125–132

Acta Neuropathol (2001) 101 : 424–434
DOI 10.1007/s004010000290

REGULAR PAPER

**Michael Brodhun · Harald Fritz · Bernd Walter
Iwa Antonow-Schlorke · Konrad Reinhart
Ulrich Zwiener · Reinhard Bauer · Stephan Patt**

Immunomorphological sequelae of severe brain injury induced by fluid-percussion in juvenile pigs – effects of mild hypothermia

Received: 6 January 2000 / Revised: 25 April 2000 / Accepted: 27 July 2000 / Published online: 16 May 2001
© Springer-Verlag 2001

Abstract Severe traumatic brain injury (TBI) often leads to a bad outcome with considerable neurological deficits. Secondary brain injuries due to a rise of intracranial pressure (ICP) and global hypoxia-ischemia are critical and may be reduced in extent by mild hypothermia. A porcine animal model was used to study the effect of severe TBI, induced by fluid percussion (FP; 3.5±0.3 atm) in combination with a secondary insult, i.e., temporary blood loss with hypovolemic hypotension. Six-week-old juvenile pigs were subjected to this kind of severe TBI; one group was then submitted to moderate hypothermia at 32°C for 6 h, starting 1 h after brain injury. Animals were killed after 24 h. TBI and hypothermia-associated alterations in the brains were investigated by immunohistochemistry with antibodies against microtubule-associated protein 2 (MAP-2) and β-amyloid precursor protein (βAPP). In addition, DNA fragmentation was investigated by the terminal deoxynucleotidyltransferase-mediated dUTP-biotin nick end labeling (TUNEL) method. Seven of the 13 normothermic TBI animals developed a secondary increase in ICP (TBI-NT-ICP) after an interval of several hours. None of the animals in the hypothermic trauma (TBI-HT) group exhibited a secondary ICP increase, indicating a protective effect of the treatment. TBI-HT animals showed significantly higher levels of MAP-2 immunoreactivity, lower levels of βAPP immunoreactivity and less DNA fragmentation than the TBI-NT-ICP animals. Differences between the TBI-HT group and normothermic animals without an ICP increase (TBI-NT) were less marked. A considerable decrease in MAP-2 outside the site of TBI-FP administration was seen only in the TBI-NT-ICP animals. MAP-2 immunohistochemistry was thus a reliable marker of diffuse brain damage. Axonal injury was present in all TBI groups, indicating its special significance in neurotrauma. Thus, severe TBI caused by FP, combined with temporary blood loss, consistently produced traumatic axonal injury and focal brain damage. Mild hypothermia was able to prevent a secondary increase in ICP and its sequelae of diffuse hypoxic-ischemic brain injury. However, hypothermia did not afford protection from traumatic axonal injury.

Keywords Trauma · Fluid percussion brain injury · Pig · Hypothermia · Immunohistochemistry

M. Brodhun · S. Patt (✉)
Institute of Pathology (Neuropathology),
Friedrich Schiller University,
Bachstrasse 18, 07740 Jena, Germany
Tel.: +49-3641-933596, Fax: +49-3641-933111

H. Fritz · K. Reinhart
Clinic of Anesthesiology and Intensive Care,
Friedrich Schiller University Jena, Jena, Germany

B. Walter · I. Antonow-Schlorke · U. Zwiener · R. Bauer
Institute of Pathophysiology, Friedrich Schiller University Jena,
Jena, Germany

Introduction

Traumatic brain injury (TBI) leads to immediate primary and delayed secondary changes [1]. Initially, there is biomechanical interaction of neurons and their processes, glial cells and blood vessels as a direct consequence of mechanical energy transfer to brain tissue. The secondary changes are much more heterogeneous and are of clinical importance due to their strong correlation to bad outcome [2]. They include biochemical and pathophysiological processes, such as decreased blood pressure, altered blood flow and brain edema, and morphological alterations, especially diffuse axonal injury (DAI).

Numerous studies have evaluated the pathomorphological and behavioral sequelae of mild to moderate TBI induced by fluid percussion (FP). For the most part, lisencephalic rats and mice have been used to study therapeutic strategies for neuroprotection after TBI [3]. Despite making valuable contributions to the understanding of the complex pathogenesis of TBI, these models have some fundamental restrictions. Studies of the biomechanical properties of the brain tissue require an animal with a large gyrencephalic brain and substantial white matter domains. Pigs fulfill these criteria [4].

Lateral FP trauma is a well-established experimental model that reproduces clinically relevant features of neurotrauma [5, 6, 7], such as alterations in intracranial pressure (ICP) [3] and cerebral blood flow [8], disruption of the blood-brain barrier [9, 10], and focal and global alterations in cerebral metabolism [11]. Importantly, the lateral FP injury device is able to produce mild, moderate or severe levels of brain damage according to the magnitude of the impact [3]. However, up to now, a procedure which is able to produce a secondary ICP increase with critically altered cerebral perfusion pressure (CPP) has not been reported.

Hypothermia has been evaluated as a therapeutic procedure to hasten neurological recovery and may have improved the outcome of patients with severe traumatic brain injury [12, 13, 14]. Hypothermia is effective in preventing secondary brain damage, especially through reducing cerebral ischemia [15]. Furthermore, it reduces the ICP, and cerebral blood flow (CBF), and reduces formation of brain edema. In addition, oxygen consumption and release of excitatory neurotransmitters is diminished [16, 17]. Although post-traumatic hypothermia has been widely studied [18, 19, 20, 21, 22, 23, 24, 25], its influence on different types of brain damage is not fully understood. To date, hypothermia-associated protection has been evaluated mostly in relation to the preservation of neurons [18, 21, 23, 24, 26], and little consideration has been given to other changes, such as secondary brain damage and axonal injury.

The purpose of the present study was to determine the extent of brain damage in severe TBI induced by FP combined with temporary blood loss in juvenile pigs with and without postinjury mild hypothermia (of 32°C). The brain damage of juvenile pigs after normo- and hypothermia was assessed with immunomorphological markers, allowing analysis of both neurons and axons. Antibodies against microtubule-associated protein 2 (MAP-2), β-amyloid precursor protein (βAPP) as a marker for axonal injury, were used. In addition the terminal deoxynucleotidyltransferase-mediated dUTP-biotin nick end labeling (TUNEL) method for DNA fragmentation was used.

Materials and methods

General instrumentation and measurement of physiological variables

Thirty-five 6-week-old pigs (mixed German breed; body weight 12.6±1.7 kg) were used. The experimental protocol was approved by the committee of animal care and use of the Thuringian State Government. Six pigs were assigned to the normothermic sham group (SHAM-NT), and 14 in the normothermic traumatic brain injury (TBI-NT) group. The hypothermic sham group (SHAM-HT) comprised 6 and the hypothermic TBI group (TBI-HT) 10 pigs. Anesthesia was induced by an intramuscular injection of ketamine hydrochloride (20 mg/kg body wt.) and midazolam (1 mg/kg body wt.) and inhalation of 70% nitrous oxide in 30% oxygen. Anesthesia was maintained throughout the experiment by a continuous infusion of fentanyl (0.015 mg/kg body wt. per h) and midazolam (1.08 mg/kg body wt. per h). Muscle relaxation was achieved with i.v. pancuronium bromide (0.4 mg/kg body wt. per h).

A polyethylene catheter (inner diameter 1.5 mm) was advanced from the femoral artery to the abdominal aorta to record arterial blood pressure and obtain samples for blood gas analysis (model ABL50, Radiometer, Copenhagen, Denmark; alpha-stat management). Body temperature was controlled by a thermoprobe advanced about 10 cm into the rectum and was maintained throughout the general instrumentation at 38±0.3°C using a water-heated pad connected to a heating-cooling thermostat and by a feedback controlled heating lamp. Physiological parameters were recorded on a multi-channel polygraph (MT95K2, Astro-Med, USA).

Two holes were drilled in the left parietal bone and a fiberoptic catheter was implanted in the subcortical white matter for ICP measurements (Camino Laboratories, San Diego, USA). A thermocouple catheter (Licox pO_2 Monitor, GMS, Kiel-Mielkendorf, Germany) was implanted in the parietal cortex. In all animals a craniotomy was made, centered between lambda and bregma over the left parietal cortex to fix a Plexiglas FP adapter with a 9-mm bore tube. The dura was kept intact. The burr holes were sealed with bone wax and covered with dental acrylic to fix the probes and FP adapter in place. CPP was calculated as the difference between mean arterial blood pressure and ICP.

Experimental protocol

Altogether, 23 randomly chosen animals were subjected to lateral FP injury (FP-TBI) using a device designed according to [27]. Briefly, the FP adapter was connected to a transducer housing, and this in turn was connected to the FP device. The device itself consisted of a cylindrical reservoir of Plexiglas 40 cm long and 5 cm in diameter. One end of the device was connected to the transducer housing, and the other had a metal piston mounted on O-rings. The exposed end of the piston was covered with a rubber pad. The entire system was filled with physiological saline solution (air bubble-free). FP-TBI was produced by allowing a 6.2-kg pendulum to strike the Plexiglas cork and generate a transient hydraulic pressure that traveled through the device and impacted upon the dura overlying the brain. The severity of the impact, determined by a transducer and recorded on a storage oscilloscope, was allowed to reach 3.5±0.3 atmospheres (mean amplitude 2–5 ms after onset of FP) and was similar in all groups investigated. This model of FP-TBI has not been fully characterized in terms of its behavioral and histopathological responses, but level of injury is considered to be a severe to high TBI in different species and ages [5, 28, 29, 30, 31, 32]. Hypovolemic hypotension was then induced by removing blood (25 ml/kg body wt., duration: 18 min) through the femoral catheter, so that blood withdrawal was completed 21 min after FP injury and then maintained for another 9 min. The same volume of plasma expander (gelatine-polysuccinate, Gelafusal, Serum-Werke Bernburg, Germany) was reinfused within 10 min. In ten animals systemic hypothermia was started 1 h after FP injury by placing the animal on a cooling blanket and by forced air cooling (TBI-HT). Sham-operated animals received the same instrumentation, and the same experimental protocol was performed except for administration of FP-TBI and temporary blood loss. Six sham-operated pigs were cooled using the same procedure (SHAM-HT). Hypothermia was guided by the temperature measured within the parietal cortex. The target brain temperature of 32°C was reached after about 3 h, and maintained for 6 h, followed by a rewarming period of about 3 h. The remaining animals were kept normothermic throughout the whole experiment. The neurometabolic and cerebrovascular findings are a subject of another manuscript (Fritz et al., in preparation).

Tissue fixation, histology, and immunohistochemistry

Animals were killed at 24 h after trauma by transcardial perfusion-fixation of the brain with a neutrally buffered solution containing 4% formalin after a short rinse with heparinized physiological saline solution. One animal of the TBI-NT-ICP group could not be adequately perfused. This brain was excluded from immunocytochemical processing, but not from TUNEL staining. Heads were

then immersion fixed for 48 h at 4°C before the brains were removed from the skulls. Three 7-mm-thick slices from the frontal lobe, temporoparietal brain, including diencephalon and hippocampus, and brain stem (ponto mid-brain site) (Fig. 1), were embedded in paraffin. They were cut into 7-μm-thick sections, which were stained with hematoxylin and eosin (H&E) for routine morphology, or prepared for immunohistochemistry. The observations were made per unit area procedure. Reactions for MAP-2 and TUNEL were performed twice on consecutive sections. βAPP immunolabeling was performed only once. The avidin-biotin-peroxidase complex (ABC) method (Vectastain Elite Kit, Vector Laboratories, Burlingame, CA), as described by Hicks et al. [33], was used for MAP-2 and βAPP immunohistochemistry. Each deparaffinized tissue section was incubated with: 10% non-immunized horse serum and 0.1% Triton X-100 for 1 h; with the primary antibody in phosphate-buffered saline (PBS) containing 5% normal horse serum at 4°C overnight; with the secondary antibody (horse anti-mouse IgG 1:200) at 4°C overnight; and with the ABC solution (1:100) for 1 h. The reaction product was visualized using 3,3-diaminobenzidine tetrahydrochloride as a chromogen. Control sections were incubated with normal horse serum in the absence of primary antibody and showed no staining. As primary antibodies we used monoclonal anti-MAP-2 mouse serum (Amersham International, Amersham, UK; 1:500), and monoclonal anti-βAPP mouse serum (mAb 22C11; Boehringer Mannheim, Indianapolis, Ind.; 1:200).

Immunostained sections were evaluated without prior knowledge of the experimental procedures performed. MAP-2 immunoreactivity in the whole neocortex and hippocampus was measured using an image analysis program (IMAGE, Version 1.42, NIH Public Domain, USA). Images of coronal sections of the brain at the level of the hippocampus were digitized onto a computer screen. The intensity of immunostaining was determined as gray scale values between 'white' (0) and 'black' (255) by outlining the brain regions of interest. Subcortical white matter of temporoparietal brain sections were used as typically non-reactive sites for MAP-2 immunostaining. These background measurements were subtracted from the values obtained from the areas of interest.

Anti-βAPP reaction was scored as ranging from accumulation of βAPP in slightly dilated axons, to accumulation of βAPP in swollen and tortuous axons (axonal swelling) or bulb formation (axonal bulbs) [34]. These features were assessed in the following brain areas: left and right hemisphere at the site of FP-TBI (i.e., radiatio optica, fasciculus subcallosus, corpus callosum, splenium, commissura fornicis), left and right diencephalons (fasciculus tegmenti, thalamus), frontal lobe (subcortical white matter at the level of fissura rhinalis anterior, rostral of caput of nucleus caudatus), and brain stem (commissura colliculi inferioris, pedunculus cerebellaris superior, lemniscus lateralis, fasciculus tegmenti, fasciculus longitudinalis medialis, lemniscus medialis) [35]. All βAPP-positive regions were taken into account. A rating score was given according to [36, 37]. If none of the features was present, a rating of 0 was given. If there was any staining of axons, however slight, a rating of 1 was made. When there were scattered areas or patches of axonal damage, a score of 2 was given. When there was extensive damage throughout large areas of white matter, the rating score was 3. In addition, numbers of axonal swelling and axonal bulbs were calculated separately (counts/0.5 mm^2, 20× objective, extrapolated for the whole βAPP-positive area) and are given as total numbers.

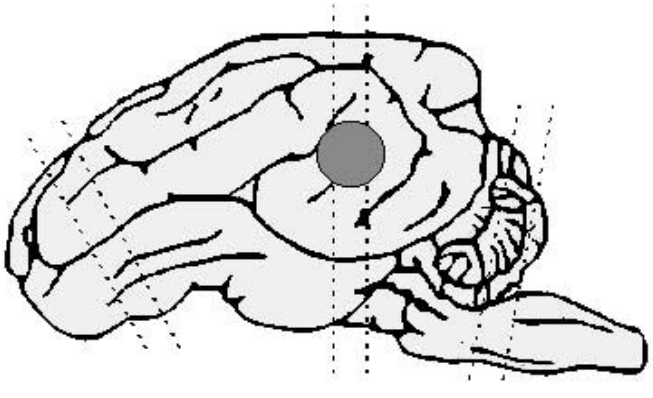

Fig. 1 Schematic drawing of placement of lateral FP-TBI in left brain hemisphere of the pig (*gray circle*) and location of the three 7-mm-thick slices taken for morphologic analysis (*disrupted lines*) (*FP* fluid percussion, *TBI* traumatic brain injury)

Fragmented DNA was detected in situ by the TUNEL method using a commercially available kit according to the manufacturer's protocol (in situ cell death detection kit "AP", Boehringer Mannheim, Germany). Sections were deparaffinized, pretreated with 20 mg/ml proteinase K, and washed in PBS prior to TUNEL staining. TUNEL staining was performed by incubation with fluorescein-conjugated digoxigenin-UTP and terminal deoxynucleotidyl transferase at 37°C for 1 h. DNA fragmentation was visualized using converter-alkaline phosphatase, NBT/BCIP and counterstaining with Kernechtrot.

Neocortical structures of parietal and temporal lobes medial and lateral to the middle suprasylvian sulcus (Fig. 1), the underlying white matter (i.e., radiatio optica, fasciculus subcallosus, corpus callosum, splenium, commissura fornicis), hippocampus, and diencephalon (corpus geniculatum laterale, corpus geniculatum mediale, pulvinar, pretectum, fasciculus tegmenti) were investigated. A semiquantitative score was used to estimate TUNEL-positive and -negative cells. When there were no positive cells in the whole section, a score of 0 was given. In cases with TUNEL positivity, positive cells were counted in 5 microscopic fields (20× objective). The scores were: 1 for up to 5 positive cells per field, 2 for 6–20 positive cells, and 3 for >20 positive cells. In addition, the distribution of TUNEL-positive cells was estimated and set as 1 for location of TUNEL-positive cells in a single dot, 2 for positive cells located in scattered areas, and 3 for ubiquitous TUNEL-positivity in the area investigated. The two scores were added together in a single value with a maximal score of 6.

Statistical analysis

Unless otherwise indicated, data are reported as means ± SD. One-way analysis of variance (ANOVA) was used to determine effects of FP-TBI and hypothermia on physiological parameters. Post hoc comparisons were made with the Student-Newman-Keuls method or with unpaired t-tests as indicated. Immunomorphological data were compared by the Mann-Whitney U-test with the alpha-adjustment procedures of Bonferroni and Holm [38,39]. The Fisher Exact Test was used to compare the distributions of treatment effects (normothermia vs hypothermia) in regard to occurrence of secondary ICP increase. Differences were considered significant when $P<0.05$.

Results

Physiological variables

Physiological parameters including intracranial pressure are shown in Table 1. These parameters remained unchanged throughout the experiment in sham-operated normothermic pigs (SHAM-NT). Temporary withdrawal of blood (25 ml/kg body wt.) immediately after FP-TBI induced a marked reduction in cardiac output of 37–49% ($P<0.05$) with a concomitant reduction in MABP and CPP (Table 1). At 8 h after TBI, ICP had increased considerably (29±24 mmHg) in seven of the normothermic animals (designated TBI-NT-ICP), whereas six normothermic animals (group TBI-NT) and all hypothermic animals

Table 1 Physiological parameters of animals. Values are means ± SD (*TBI* traumatic brain injury, *ICP* intracranial pressure, *SHAM-NT* normothermic sham-operated animals, *SHAM-HT* hypothermic sham animals, *TBI-NT* normothermic animals with fluid percussion-induced TBI, *TBI-NT-ICP* normothermic animals with TBI, which developed a secondary increase of ICP, *TBI-HT* hypothermic animals with TBI, *MABP* mean arterial blood pressure, *CPP* cerebral perfusion pressure)

		Baseline	End of blood withdrawal	8 h after TBI	24 h after TBI
ICP (mmHg)	SHAM-NT	8±2	8±2	7±3	6±2
	SHAM-HT	9±3	7±2$	5±2$	4±2$
	TBI-NT	9±3	7±3$	5±2$	5±4$
	TBI-NT-ICP	9±2	13±9	29±24*	45±27$*
	TBI-HT	6±3	6±5	6±2	6±2
MABP (mmHg)	SHAM-NT	104±13	103±10	111±13	100±25
	SHAM-HT	104±9	112±7	102±13	93±19
	TBI-NT	104±19	79±17$	82±17$*	85±16$
	TBI-NT-ICP	103±13	82±23	88±10*	71±19$
	TBI-HT	125±14*	95±22$	101±15$	82±12$
CPP (mmHg)	SHAM-NT	97±14	96±11	105±15	97±28
	SHAM-HT	96±8	105±6	97±14	89±19
	TBI-NT	95±22	73±19	77±18*	80±19
	TBI-NT-ICP	95±13	67±27$*	58±27$*	29±29$*
	TBI-HT	119±13*	88±22$	95±15$	76±12$
Cardiac output (ml/min/kg)	SHAM-NT	229±21	243±26	248±35	232±54
	SHAM-HT	205±43	202±45	128±48$*	204±33
	TBI-NT	244±18	126±19$*	257±55	302±51
	TBI-NT-ICP	240±25	128±40$*	245±46	249±80
	TBI-HT	214±26	137±37$*	109±10$*	200±42
Arterial PO_2 (mmHg)	SHAM-NT	159±15	148±22	137±34	149±15
	SHAM-HT	140±21	142±19	157±31$	133±39
	TBI-NT	139±27	139±26	139±26	133±38
	TBI-NT-ICP	144±21	141±17	157±21	149±12
	TBI-HT	146±26	155±15	180±32$	145±34
Arterial PCO_2 (mmHg)	SHAM-NT	39±4	41±1	43±3	40±6
	SHAM-HT	41±5	40±4	42±3	37±1$
	TBI-NT	43±2	42±2	41±3	41±1
	TBI-NT-ICP	40±4	40±4	37±4*	37±3
	TBI-HT	40±3	38±1	41±4	39±4
Arterial pH	SHAM-NT	7.49±0.03	7.49±0.02	7.48±0.01	7.52±0.06
	SHAM-HT	7.48±0.04	7.50±0.04	7.46±0.03	7.53±0.02$
	TBI-NT	7.45±0.01	7.44±0.04	7.46±0.05	7.51±0.04$
	TBI-NT-ICP	7.49±0.05	7.49±0.04	7.54±0.03*	7.53±0.06
	TBI-HT	7.48±0.04	7.47±0.03	7.47±0.04	7.49±0.06
Brain temperature (°C)	SHAM-NT	38.0±0.8	38.0±0.6	37.7±0.3	38.2±0.9
	SHAM-HT	38.4±0.7	38.2±0.6	32.3±0.5$*	38.8±0.5
	TBI-NT	38.8±1.0	38.6±0.9	38.9±1.0	39.1±1.0
	TBI-NT-ICP	38.5±0.7	38.3±0.6	37.5±2.2*	36.2±3.5
	TBI-HT	38.8±0.7	38.5±0.5	32.4±0.4$	38.7±0.6

*$$P<0.05; *indicates significant differences between groups compared to SHAM-NT group at the respective experimental stage; $indicates significant differences between baseline values and values obtained at different stages of the experimental procedure

did not show this secondary increase in ICP ($P<0.05$). Lowering of brain temperature to 32.2±0.5°C by surface cooling required 185±30 min, and this level of mild hypothermia was maintained for 360 min. During hypothermia cardiac output was similarly reduced in both hypothermic groups (SHAM-HT, 61±13%; TBI-HT, 54±7%; $P<0.05$). Arterial blood pressure was diminished 24 h after TBI in the TBI-NT-ICP and TBI-HT groups ($P<0.05$).

General morphological findings

In all traumatized animals, slight subarachnoidal hemorrhages were found near the craniotomy for FP-TBI administration, and small intracranial bleedings occurred in the white matter around gliding contusions. In animals from the TBI-NT-ICP group, subarachnoidal hemorrhages were also observed in the contralateral right hemisphere.

Slight subarachnoidal bleedings were present in the brain stem of all traumatized normothermic pigs, but in only three of seven animals in the TBI-HT group. At the site of trauma, circumscript triangular hemorrhagic necroses (approximately 0.8 cm^2), particularly of the gray matter, were seen. In animals from the TBI-HT group the peri-injury zones appeared macroscopically normal, but histologically showed some condensed neurons and vacuolation of tissue. There were no gross differences in the traumatic necroses between the groups. Small necrotic zones were located near the intracerebral catheters used for physiological data acquisition; they were not included in the analysis. The TBI-NT-ICP animals had increased brain weights (72.6±2.2 g; vs TBI-NT, 60.0±1.5 g; TBI-HT, 61.8±1.8 g; SHAM-NT, 59.8±2.2 g; and SHAM-HT, 66.3±2.1 g; $P<0.05$). Macroscopically, three TBI-NT-ICP animals showed severe and three animals moderate features of raised ICP, such as narrowing of sulci and flattening of gyri, reduction in size of the ventricles, tentorial and tonsillar hernia. One animal also showed brain stem infarction. Microscopically, these brains displayed microscopic signs of global neuronal hypoxia, namely shrunken and triangular cell bodies and nuclei, eosinophilic cytoplasm, and perineuronal edema. In addition, they showed blood vessel congestion. Neuronal injury in the hippocampus after secondary increase in ICP was observed in all subfields of both hemispheres, whereas in the TBI-NT group necrotic neurons were observed only in two cases and were restricted to the left hippocampus. In the TBI-HT group, the hippocampus displayed only small circumscript areas of necrotic neurons at the trauma site without predilection of hippocampal fields (like in the TBI-NT group).

MAP-2 immunostaining

Immunostaining was performed twice in each case and each region with reproducible results. In SHAM-NT (Fig. 2A, D) and SHAM-HT (not shown), immunostaining for MAP-2 gave a strong, homogeneous reaction in dendrites and somata of neurons. The dendrites appeared as fine slender structures radiating through the cerebral cortex and hippocampus. The site of FP-TBI administration in all animals was totally devoid of MAP-2 immunostaining (see arrow in Fig. 2B) or showed MAP-2-positive fragments of damaged neuronal structures. Outside the site of FP-TBI administration, the neurons of TBI-NT animals displayed nearly normal MAP-2 immunostaining (Fig. 2B, E). In TBI-NT-ICP animals, however, neurons outside the FP-TBI administration site showed markedly decreased or negative MAP-2 labeling (Fig. 2C, F). Dendrites were sometimes immunoreactive, but only in their initial portions, and appeared as short MAP-2-positive stumps.

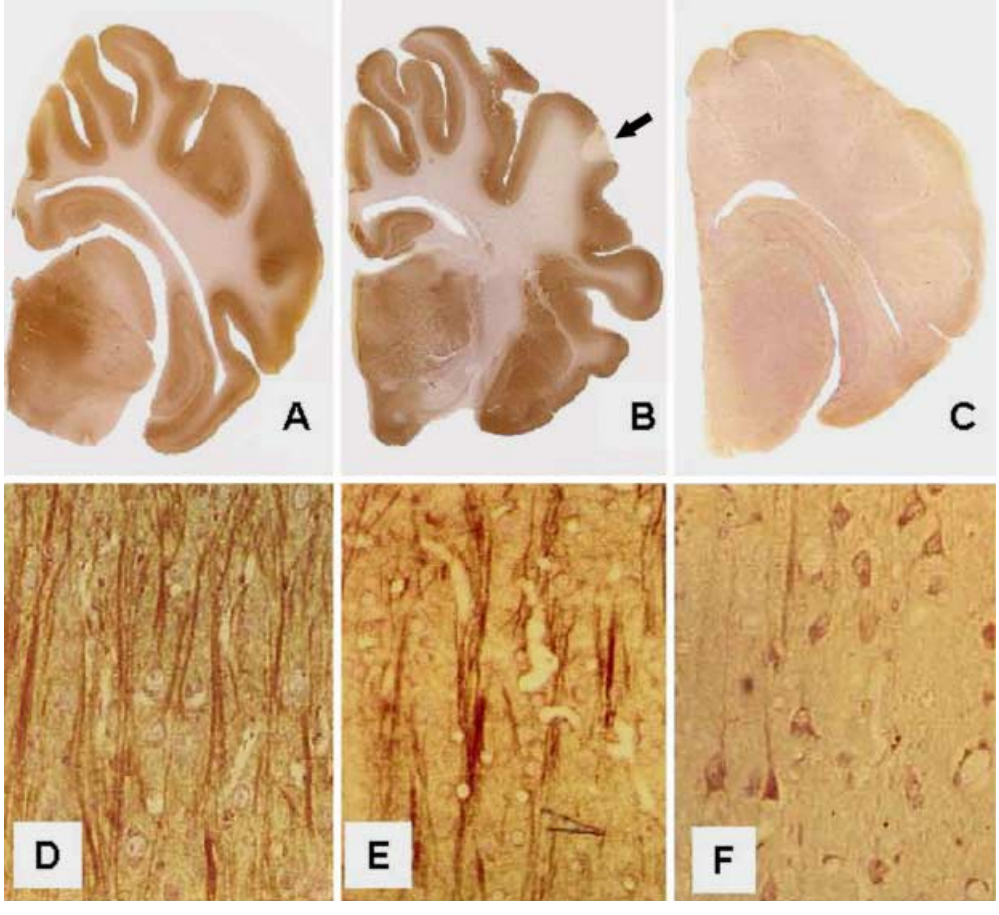

Fig. 2 MAP-2 immunostaining at low magnification in SHAM-NT (**A**), TBI-NT (**B**), and TBI-NT-ICP (**C**) groups. The site of FP-TBI administration was totally devoid of MAP-2 immunostaining (*arrow* in **B**). **D,E** MAP-2 immunoreactivity in traumatic animals outside the site of FP-TBI administration, at higher magnification. **D** Staining in dendrites and somata of neurons in SHAM-NT animals was strong and homogeneous. **E** Outside the site of FP-TBI administration, the neurons of TBI-NT animals displayed MAP-2 immunostaining comparable to that shown in **D**. **F** In TBI-NT-ICP animals, neurons outside the site of FP-TBI administration had a markedly decreased or negative MAP-2 labeling (*MAP-2* microtubule-associated protein 2, *SHAM* sham-operated, *ICP* intracranial pressure, *NT* normothermia, *NT-ICP* NT – trauma with secondary ICP increase, *HT* hypothermia). **A**–**C** ×2; **D**–**F** ×100

Three animals showed this pattern of decreased MAP-2 immunostaining in both hemispheres, three animals mostly in the left hemisphere. Histologically, these neurons had condensed nuclei but otherwise looked normal. MAP-2 immunostaining in the TBI-HT animals was similar to that in controls (TBI-NT).

Quantification of immunostaining for MAP-2 was performed separately in the two hemispheres, i.e., in left traumatized and right non-traumatized neocortex, and in left and right hippocampus (Fig. 3). There was no significant difference in MAP-2 immunoreaction between the two sides. With the exception of the FP-TBI administration site, MAP-2 values were fairly similar in the neocortex and hippocampus of sham animals and TBI-NT animals. MAP-2 values were, however, dramatically reduced in neocortex and hippocampus of TBI-NT-ICP animals (when compared to the other groups) ($P<0.05$, Fig. 3).

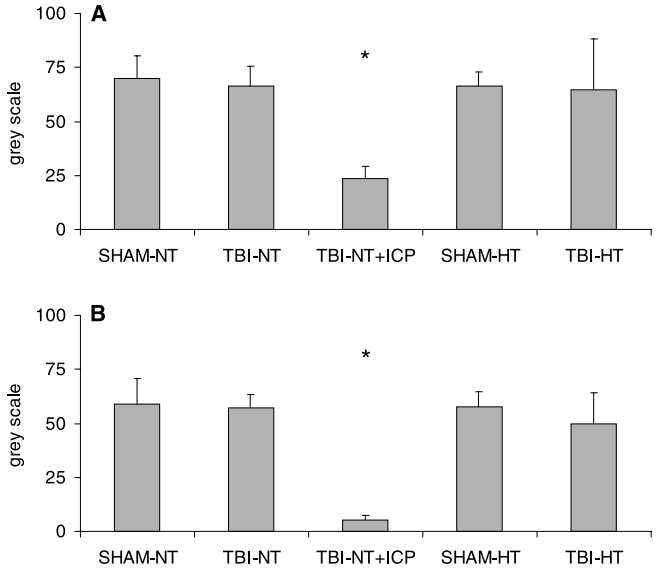

Fig. 3 Graphic presentation of the MAP-2 immunohistochemistry staining index (grey values, absolute values) in the entire neocortex (**A**) and hippocampus (**B**) of both hemispheres. Significant differences from SHAM-NT are indicated by *asterisks*

βAPP immunostaining

The following seven areas were investigated: frontal cerebral hemispheres, left and right; cerebral hemispheres at the level of FP-TBI administration, left and right; diencephalon, left and right; and brain stem. βAPP immunoreactivity was quantified using an average rating score of βAPP immunostaining (0–3) according to McKenzie et al. [36]. βAPP-immunostained axons were not observed in sham animals. Axonal swelling and axonal bulbs were found in various degrees in all traumatized animals. No immunostaining was found in the frontal lobes of either hemisphere. In the TBI-NT animals, βAPP-positivity was moderate and mainly found in the white matter underlying the traumatization (three of seven animals, score 1–3) in the diencephalon (four animals, score mainly 1) and, to a lesser extent, in the brain stem (two animals, score 1–2), but was absent in the contralateral hemisphere. In the TBI-NT-ICP pigs, many βAPP-immunoreactive axons and axonal bulbs were observed in all brains (score mostly 3) and in all areas studied except the frontal lobes, being most abundant in the traumatized hemisphere and brain stem. Hypothermic animals displayed comparable amounts of axonal swelling and axonal bulbs in the left hemisphere (five of eight animals, score mainly 1–2) and left diencephalon (four animals, score 1–2) as in the TBI-NT group, but lacked βAPP reactivity in the other areas. Dif-

Table 2 Regional βAPP immunostaining score and regional TUNEL score (*βAPP* β-amyloid precursor protein, *LH* left hemisphere, *RH* right hemisphere)

Groups	SHAM-NT	SHAM-HT	TBI-NT	TBI-NT+ICP	TBI-HT
βAPP immunostaining score (maximum 3.0)					
Frontal brain (LH)	0	0	0	0	0
Frontal brain (RH)	0	0	0	0	0
Temporoparietal brain (LH)	0	0	1.0	2.5 *	1.1
Temporoparietal brain (RH)	0	0	0	0.3	0
Diencephalon (LH)	0	0	0.9	1.3 *	0.8
Diencephalon (RH)	0	0	0.1	1.0	0
Brain stem	0	0	0.4	1.8 *	0
TUNEL score (maximum 6.0)					
Temporoparietal brain (cortex-LH)	0	0	0	3.5	0
Temporoparietal brain (cortex-RH)	0	0	0	3.0	0
Temporoparietal brain (white matter-LH)	0	0	1.4	5.2 *	0.7
Temporoparietal brain (white matter-RH)	0	0	0.3	5.2 *	0.7
Diencephalon (LH)	0	0	0.3	4.4 *	0.7
Diencephalon (RH)	0	0	0.3	5.3 *	0.7
Hippocampus (LH)	0	0	0.3	4.0	0.5
Hippocampus (RH)	0	0	0	4.0	0.5

*$P<0.05$, indicating significant differences between SHAM-NT animals and other groups

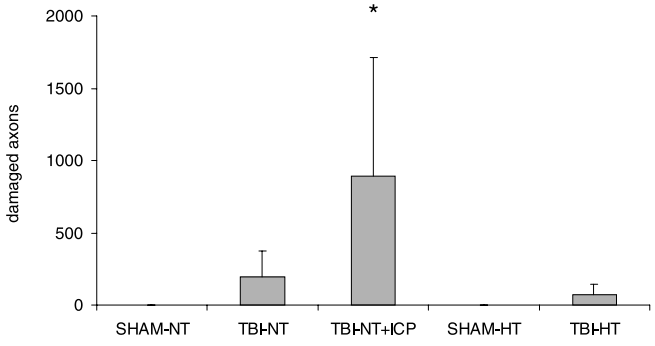

Fig. 4 Graphic presentation of βAPP-positive axons per group counted in all areas. Significant differences from SHAM-NT are indicated by an *asterisk*

ferences in βAPP immunoreactivity were statistically significant in TBI-NT-ICP pigs compared with SHAM-NT animals ($P<0.05$), but not compared with TBI-NT or TBI-HT animals (Table 2). In addition, the number of βAPP-positive damaged axons and axonal bulbs was counted in all regions (Fig. 4). The number was lower in hypothermic than in TBI-NT-ICP pigs; however, it was comparable in the TBI-NT (without secondary ICP) and TBI-HT groups.

TUNEL staining

Staining reactions were performed twice in each case and each region and yielded reproducible results. TUNEL staining was investigated in four brain areas of both hemispheres: neocortex, cerebral white matter, hippocampus, and diencephalon. TUNEL-positive cells were morphologically different. Most cells were characterized by a homogeneous dark nucleus (Fig. 5A), others showed cell shrinkage, nuclear condensation and fragmentation (apoptotic bodies) (not shown). A few cells demonstrated slight staining and without morphological changes of nuclei and cytoplasm, indicating nonspecific staining; these cells were not taken into further account. Most TUNEL-positive cells were glial cells, very few were neurons. TUNEL-positive cells were also found in the hippocampus, especially in the TBI-NT-ICP animals. Interestingly, the germinative zone of the granule cells of the dentate gyrus was selectively stained in these animals (Fig. 5B). The other animals lacked this reaction pattern (not shown).

The TUNEL reaction was semiquantified (see Materials and method) with a maximal score was 6.0. Brains of sham animals did not contain TUNEL-positive cells (score 0). TBI-NT animals displayed TUNEL-positive cells mainly in white matter areas adjacent to the FP-TBI administration site. All other areas had very low scores. TUNEL-positive cells in TBI-NT-ICP animals were abundant. The white matter of both hemispheres, the left and right hippocampus and the diencephalon were particularly involved, whereas TUNEL scores were lower in neocortex. The hippocampus, especially the germinative zone of the granular layer, showed a positive TUNEL reaction (Table 2, $P<0.05$). Hypothermic animals yielded TUNEL

Fig. 5 **A** TUNEL-positive glial cells in the white matter of a TBI-NT animal. **B** Selective TUNEL positivity in the cells of the germinative cell layer of hippocampus in a TBI-NT-ICP animal. **A** ×350; **B** ×150

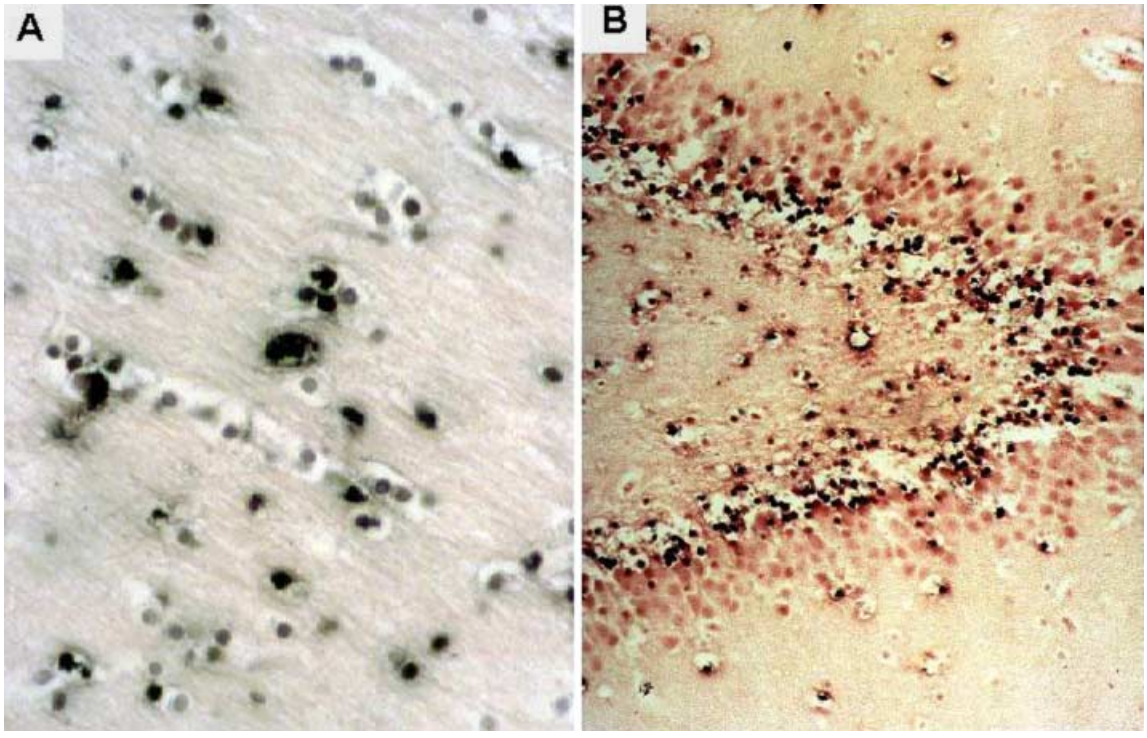

scores similar to those of TBI-NT pigs, although scores in the hemisphere of trauma were lower in TBI-HT (0.7) than in the normothermic pigs (1.4). Moreover, the TUNEL score in TBI-HT group came from only one of six animals, whereas in TBI-NT animals, TUNEL positivity was found in three of six animals (data not shown).

Discussion

Effect of lateral FP-TBI on ICP

The juvenile pigs responded differently to the modified lateral FP injury, although the severity of the trauma, verified by a transient pressure increase near the epidural application site, was similar in each experiment. A significant transfer of the fluid pulse to the brain was likely administered, since previous studies using identical experimental conditions, but with an additional transducer contralateral to the FP application site, documented that a synchronous ICP transient occurred [40]. Of the 14 normothermic traumatized animals, 7 developed a secondary ICP increase after an interval of several hours. This can not be ascribed to variation in the experimental procedure. Assignment of animals to the different experimental procedures was randomized (by means of drawing by lot). Moreover, FP-TBI administration was standardized; in particular, identical FP conditions were achieved in all TBI groups, including the kind of FP administration, the height of the falling pendulum and the hydraulic pressure transient generated. The administered FP-induced hydraulic pressure transient did not differ between TBI groups. Furthermore, we performed extensive cardiovascular, respiratory, and neurophysiological monitoring, which is summarized in Table 1 and will be presented in more detail elsewhere (Fritz et al., in preparation). We were able to show that, soon after FP-TBI, and also after temporary blood loss, no statistically significant differences occurred between TBI groups (Table 1). Thus, animal preparation, FP-TBI administration, and blood withdrawal were similarly performed in all animals with similar physiological responses. Furthermore, management of anesthesia, analgesia, fluid replacement and ventilation were similar in all experiments. Thus, the divergent response of normothermic animals with regard to ICP is not related to the care and use of the animals, and at present cannot be explained. It is, nevertheless, notable that a rise in ICP was achieved in the present experimental setting, suggesting that the model is useful for investigating secondary injuries. Although discussed in detail elsewhere (Fritz et al., in preparation), two further findings are of note; (i) animals with a secondary ICP increase could not be predicted from the physiological data, and (ii) none of the hypothermic traumatized animals had a secondary ICP increase. Our model is in this response similar to neurotrauma in man, where development of a secondary ICP increase is also hard to predict [41].

The lack of a secondary ICP increase in an animal of the hypothermic group is noteworthy. Although the numbers were rather small and a secondary ICP increase was found only in about half of normothermic pigs after TBI, hypothermia-induced neuroprotection from ICP elevation was verified significantly (P=0.018, Fisher Exact Test). This is in line with findings in clinical studies, where hypothermia is related to a lowered incidence of ICP [16].

ICP monitoring was performed using a fiberoptic system which has been shown to record pressure accurately from within the lateral ventricle, from the subdural space over the surface of the cerebral hemispheres, and from within the brain tissue itself [42, 43]. We used the intraparenchymal approach because its offered an easy and standardized placement of the fiberoptic catheter.

Altered MAP-2 immunostaining correlates with diffuse brain oxygen deprivation

Under normal conditions, the cytoskeletal protein MAP-2 is abundantly expressed in neurons, almost exclusively in dendrites and perikarya [44]. It is degraded by calcium-activated neutral proteases, such as calpain [33]. MAP-2 immunostaining can serve as a sensitive marker for neuronal impairment after brain damage of various types, including ischemia [45, 46, 47, 48, 49]. It has also been used in models of neurotrauma. The intensity and location of decreased MAP-2 immunostaining depends on the mode and severity of traumatization. For instance, rats subjected to mild lateral FP injury (1.1–1.3 atm) showed less MAP-2 loss than rats with a moderate injury (2.3–2.5 atm) [50]. Diminished or lost MAP-2 immunolabeling was found either mainly at the contusion site [51] or both at the traumatized hemisphere and outside the contused regions [52]. In a study by Folkerts et al. [52], the effect was time dependent, being observed shortly after the traumatization, with most severe loss at 48 h and a partial recovery at 72 h. Similarly, Hicks et al. [33] demonstrated decreased staining from 10 min to at least 7 days after injury (at slightly different levels). Decreased or lost MAP-2 immunostaining was correlated with signs of neuronal death in histological sections [33], but sometimes preceded morphological changes [53]. Whether MAP-2 loss implies a state of transition leading to an irreversible level or a state of functional disturbance that can be remedied by restored protein synthesis, is not known.

In our study MAP-2 immunostaining was not significantly diminished after severe lateral FP injury, except after secondary ICP increase, and then at the FP-TBI administration site. The affected area was so small (0.8 cm^2) in comparison with the remaining cortex that it did not influence the total MAP-2 cortical staining index. This result is in contrast to some findings in the literature, which show a substantial decrease of MAP-2 expression outside the FP-TBI administration site [33, 52]. The dramatic loss of MAP-2 reactivity in the normothermic animals with a secondary ICP increase is, however, in line with the literature. The diffuse reduction of MAP-2 immunoreactivity most likely reflects changes due to decreased cerebral blood flow and global ischemia. In the porcine model

used in this study, we suggest that decreased MAP-2 outside the FP-TBI administration site is a reliable early marker for diffuse brain oxygen deprivation [48].

The number of βAPP-immunopositive axons is slightly reduced after hypothermia

βAPP is a membrane-spanning glycoprotein of nerve cells. It is transported by fast axoplasmic transport [54] and accumulates following cytoskeletal disruption [55] due to inhibition of axoplasmic flow [56]. Intra-axonal accumulation of βAPP is a sensitive and early marker for diffuse axonal injury (DAI) [57]. DAI is an important consequence of TBI, and its extent is in most cases correlated with the severity of trauma and the development of coma [58, 59, 60, 61]. Axonal damage is not necessarily a primary traumatic event [56]. When DAI appears after a certain time interval, it is considered to reflect a progressive change after primary traumatic events. Indeed, axonal damage after lateral FP injury has been described as a progressive alteration over a 2-week period [62]. Our data on axonal swelling and axonal bulbs in traumatized normothermic pigs are in line with the literature. We also found a considerable number of βAPP-immunolabeled axons 24 h after TBI in pigs without a secondary ICP increase. The higher βAPP scores in the diencephalon in pigs with secondary ICP increase are not surprising and correlate with secondary brain insults. To date only one study has analyzed the effects of hypothermia on axonal injury after TBI [22]. This showed a significant reduction in βAPP-detected damaged axonal density in hypothermic rats. Hypothermia was performed either before or after injury, which might be one possible cause for brain protection in their study. In contrast, we observed only slight differences in βAPP accumulation under normothermia and hypothermia conditions, although traumatized hypothermic juvenile pigs lacked βAPP immunoreaction in the brain stem, which was demonstrable under normothermia. In addition, all traumatized animals showed axonal injury, demonstrating that axonal damage is a reliable event in our TBI model.

Hypothermia reduces TUNEL positivity at the site of traumatization

Although the TUNEL method was used mainly to assess apoptotic cells, labeling of necrotic cells could not be excluded. On the contrary, DNA fragmentation due to necrosis was in many cases more likely than apoptotic cell death. According to Rink et al. [63], cells with homogeneous dark nuclei are considered to be necrotic, while those with nuclear condensation and fragmentation are apoptotic. Therefore, the general term 'TUNEL positivity' has been used.

The TUNEL experiments yielded high scores in normothermic animals with a secondary ICP increase. It is important to note that the time period of 24 h between TBI and killing of the animals may not be long enough for the induction of significant apoptosis. Conti et al. [64] found apoptosis in adult rat brain 24 h after lateral FP injury only in the injured cortex, whereas 48 h or even weeks were needed for it to occur in other brain regions, such as hippocampus and thalamus. However, a study by Xu et al. [24] on cold-induced brain injury in rats demonstrated occurrence of apoptotic neuronal cell death already at 12 h with a peak at 24 h in the cortex and at 48 h in the white matter and hippocampus. Thus, apoptosis in brain injury is influenced by various factors including the experimental setting. Moreover, the mechanism of delayed cell death after brain injury remains to be determined. Clark et al. [65] investigated expression of the apoptosis-suppressor gene *bcl-2*, and Colicos and Dash [66] the role of apoptosis in spatial memory deficits. Alteration in the expression of immediate early genes and glutamate might trigger a rise in the intracellular free Ca^{2+} concentration by activating NMDA receptors and voltage-dependent Ca^{2+} channels. Hypothermia is able to reduce apoptosis via Ca^{2+}-mediated endonuclease activity, resulting in DNA fragmentation [67]. In a study of cold-induced brain damage [24], hypothermia for 12 h seemed to be more effective than hypothermia for 3 h, and hypothermia reduced apoptosis and essentially eliminated detectable DNA labeling not only at 24 and 48 h after injury but 1, 3 and 6 months later, arguing against the hypothesis of a simple delay of cerebral damage under hypothermia [68]. In our study, TUNEL-positive scores at the FP-TBI administration site were lowered after hypothermic treatment, indicating a protective effect.

In conclusion, severe FP-TBI combined with temporary blood loss consistently produced traumatic axonal injury with focal brain damage. Mild hypothermia was able to prevent a secondary increase in ICP and its sequelae of diffuse hypoxic-ischemic brain injury. However, mild hypothermia did not offer significant protection against traumatic axonal injury.

Acknowledgements The authors wish to thank Mrs. Renate Klupsch for her excellent technical work, Dr. H. Hoyer (Jena) for expert advice in medical statistics, and Dr. A. M. Carter (Odense, Denmark) for his collegial review of the manuscript. The study was supported by BMBF 01ZZ9602.

References

1. Gennarelli TA, Thibault LE, Adams JH, Graham DI, Thompson CJ, Marcincin RP (1982) Diffuse axonal injury and traumatic coma in the primate. Ann Neurol 12: 564–574
2. Adams JH, Doyle D, Ford I, Gennarelli TA, Graham DI, McLellan DR (1989) Diffuse axonal injury in head injury: definition, diagnosis and grading. Histopathology 15: 49–59
3. McIntosh TK, Vink R, Noble L, Yamakami I, Fernyak S, Soares H, Faden AL (1989) Traumatic brain injury in the rat: characterization of a lateral fluid-percussion model. Neuroscience 28: 233–244
4. Wladis A, Hjelmqvist H, Brismar B, Kjellstrom BT (1998) Acute metabolic and endocrine effects of induced hypothermia in hemorrhagic shock: an experimental study in the pig. J Trauma 45: 527–533

5. Dixon CE, Lyeth BG, Povlishock JT, Findling RL, Hamm RJ, Marmarou A, Young HF, Hayes RL (1987) A fluid percussion model of experimental brain injury in the rat. J Neurosurg 67: 110–119
6. Hayes RL, Stalhammar D, Povlishock JT, Allen AM, Galinat BJ, Becker DP, Stonnington HH (1987) A new model of concussive brain injury in the cat produced by extradural fluid volume loading. II. Physiological and neuropathological observations. Brain Inj 1: 93–112
7. Lindgren S, Rinder L (1969) Production and distribution of intracranial and intraspinal pressure changes at sudden extradural fluid volume input in rabbits. Acta Physiol Scand 76: 340–351
8. Yamakami I, McIntosh TK (1991) Alterations in regional cerebral blood flow following brain injury in the rat. J Cereb Blood Flow Metab 11: 655–660
9. Cortez SC, McIntosh TK, Noble LJ (1989) Experimental fluid percussion brain injury: vascular disruption and neuronal and glial alterations. Brain Res 482: 271–282
10. Soares HD, Thomas M, Cloherty K, McIntosh TK (1992) Development of prolonged focal cerebral edema and regional cation changes following experimental brain injury in the rat. J Neurochem 58: 1845–1852
11. Hovda DA, Becker DP, Katayama Y (1992) Secondary injury and acidosis. J Neurotrauma 9 [Suppl 1]: S47–60
12. Bernard S (1996) Induced hypothermia in intensive care medicine. Anaesth Intensive Care 24: 382–388
13. Marion DW, Penrod LE, Kelsey SF, Obrist WD, Kochanek PM, Palmer AM, Wisniewski SR (1997) Treatment of traumatic brain injury with moderate hypothermia. N Engl J Med 336: 540–546
14. Shiozaki T, Sugimoto H, Taneda M, Oda J, Tanaka H, Hiraide A, Shimazu T (1998) Selection of severely head injured patients for mild hypothermia therapy. J Neurosurg 89: 206–211
15. Metz C, Holzschuh M, Bein T, Woertgen C, Frey A, Frey I, Taeger K, Brawanski A (1996) Moderate hypothermia in patients with severe head injury: cerebral and extracerebral effects. J Neurosurg 85: 533–541
16. Illievich UM, Zornow MH, Choi KT, Scheller MS, Strnat MA (1994) Effects of hypothermic metabolic suppression on hippocampal glutamate concentrations after transient global cerebral ischemia. Anesth Analg 78: 905–911
17. Suehiro E, Fujisawa H, Ito H, Ishikawa T, Maekawa T (1999) Brain temperature modifies glutamate neurotoxicity in vivo. J Neurotrauma 16: 285–297
18. Bramlett HM, Dietrich WD, Green EJ, Busto R (1997) Chronic histopathological consequences of fluid-percussion brain injury in rats: effects of post-traumatic hypothermia. Acta Neuropathol 93: 190–199
19. Clifton GL, Jiang JY, Lyeth BG, Jenkins LW, Hamm RJ, Hayes RL (1991) Marked protection by moderate hypothermia after experimental traumatic brain injury. J Cereb Blood Flow Metab 11: 114–121
20. Clifton GL (1995) Systemic hypothermia in treatment of severe brain injury: a review and update. J Neurotrauma 12: 923–927
21. Dietrich WD, Alonso O, Busto R, Globus MY, Ginsberg MD (1994) Post-traumatic brain hypothermia reduces histopathological damage following concussive brain injury in the rat. Acta Neuropathol 87: 250–258
22. Koizumi H, Povlishock JT (1998) Posttraumatic hypothermia in the treatment of axonal damage in an animal model of traumatic axonal injury. J Neurosurg 89: 303–309
23. Laptook AR, Corbett RJ, Sterett R, Burns DK, Garcia D, Tollefsbol G (1997) Modest hypothermia provides partial neuroprotection when used for immediate resuscitation after brain ischemia. Pediatr Res 42: 17–23
24. Xu RX, Nakamura T, Nagao S, Miyamoto O, Jin L, Toyoshima T, Itano T (1998) Specific inhibition of apoptosis after cold-induced brain injury by moderate postinjury hypothermia. Neurosurgery 43: 107–114
25. Yu WR, Westergren H, Farooque M, Holtz A, Olsson Y (1999) Systemic hypothermia following compression injury of rat spinal cord: reduction of plasma protein extravasation demonstrated by immunohistochemistry. Acta Neuropathol 98: 15–21
26. Mansfield RT, Schiding JK, Hamilton RL, Kochanek PM (1996) Effects of hypothermia on traumatic brain injury in immature rats. J Cereb Blood Flow Metab 16: 244–252
27. Sullivan HG, Martinez J, Becker DP, Miller JD, Griffith R, Wist AO (1976) Fluid-percussion model of mechanical brain injury in the cat. J Neurosurg 45: 521–534
28. Armstead WM, Kurth CD (1994) Different cerebral hemodynamic responses following fluid percussion brain injury in the newborn and juvenile pig. J Neurotrauma 11: 487–497
29. DeWitt DS, Jenkins LW, Wei EP, Lutz H, Becker DP, Kontos HA (1986) Effects of fluid-percussion brain injury on regional cerebral blood flow and pial arteriolar diameter. J Neurosurg 64: 787–794
30. McIntosh TK, Faden AI, Bendall MR, Vink R (1987) Traumatic brain injury in the rat: alterations in brain lactate and pH as characterized by ^{1}H and ^{31}P nuclear magnetic resonance. J Neurochem 49: 1530–1540
31. Prins ML, Lee SM, Cheng CL, Becker DP, Hovda DA (1996) Fluid percussion brain injury in the developing and adult rat: a comparative study of mortality, morphology, intracranial pressure and mean arterial blood pressure. Dev Brain Res 95: 272–282
32. Shima K, Marmarou A (1991) Evaluation of brain-stem dysfunction following severe fluid-percussion head injury to the cat. J Neurosurg 74: 270–277
33. Hicks RR, Smith DH, McIntosh TK (1995) Temporal response and effects of excitatory amino acid antagonism on microtubule-associated protein 2 immunoreactivity following experimental brain injury in rats. Brain Res 678: 151–160
34. Maxwell WL, Povlishock JT, Graham DL (1997) A mechanistic analysis of nondisruptive axonal injury: a review. J Neurotrauma 14: 419–440
35. Yoshikawa T (1968) Atlas of the brains of domestic animals. University of Tokyo Press, Tokyo
36. McKenzie KJ, McLellan DR, Gentleman SM, Maxwell WL, Gennarelli TA, Graham DI (1996) Is beta-APP a marker of axonal damage in short-surviving head injury? Acta Neuropathol 92: 608–613
37. Gentleman SM, McKenzie JE, Royston MC, McIntosh TK, Graham DI (1999) A comparison of manual and semi-automated methods in the assessment of axonal injury. Neuropathol Appl Neurobiol 25: 41–47
38. Aickin M, Gensler H (1996) Adjusting for multiple testing when reporting research results: the Bonferroni vs Holm methods. Am J Public Health 86: 726–728
39. Arani RB, Chen JJ (1998) A power study of a sequential method of p-value adjustment for correlated continuous endpoints. J Biopharm Stat 8: 585–598
40. Walter B, Bauer R, Fritz H, Jochum T, Wunder L, Zwiener U, Reinhart K (1997) Biomechanical characteristics of lateral fluid percussion and pathomorphological findings after severe traumatic brain injury in juvenile pigs. Pflügers Arch 433 [Suppl]: R 63
41. Signorini DF, Andrews PJ, Jones PA, Wardlaw JM, Miller JD (1999) Adding insult to injury: the prognostic value of early secondary insults for survival after traumatic brain injury. J Neurol Neurosurg Psychiatry 66: 26–31
42. Sundbarg G, Nordstrom CH, Messeter K, Soderstrom S (1987) A comparison of intraparenchymatous and intraventricular pressure recording in clinical practice. J Neurosurg 67: 841–845
43. Crutchfield JS, Narayan RK, Robertson CS, Michael LH (1990) Evaluation of a fiberoptic intracranial pressure monitor. J Neurosurg 72: 482–487
44. De Camilli P, Miller PE, Navone F, Theurkauf WE, Vallee RB (1984) Distribution of microtubule-associated protein 2 in the nervous system of the rat studied by immunofluorescence. Neuroscience 11: 817–846
45. Dawson DA, Hallenbeck JM (1996) Acute focal ischemia-induced alterations in MAP2 immunostaining: description of temporal changes and utilization as a marker for volumetric assessment of acute brain injury. J Cereb Blood Flow Metab 16: 170–174

46. Kitagawa K, Matsumoto M, Niinobe M, et al (1989) Microtubule-associated protein 2 as a sensitive marker for cerebral ischemic damage – immunohistochemical investigation of dendritic damage. Neuroscience 31: 401–411
47. Miyazawa T, Bonnekoh P, Hossmann KA (1993) Temperature effect on immunostaining of microtubule-associated protein 2 and synaptophysin after 30 minutes of forebrain ischemia in rat. Acta Neuropathol 85: 526–532
48. Schwab M, Antonow Schlorke I, Zwiener U, Bauer R (1998) Brain-derived peptides reduce the size of cerebral infarction and loss of MAP2 immunoreactivity after focal ischemia in rats. J Neural Transm Suppl 53: 299–311
49. Yanagihara T, Brengman JM, Mushynski WE (1990) Differential vulnerability of microtubule components in cerebral ischemia. Acta Neuropathol 80: 499–505
50. Saatman KE, Graham DI, McIntosh TK (1998) The neuronal cytoskeleton is at risk after mild and moderate brain injury. J Neurotrauma 15: 1047–1058
51. Posmantur RM, Kampfl A, Taft WC, Bhattacharjee M, Dixon CE, Bao J, Hayes RL (1996) Diminished microtubule-associated protein 2 (MAP2) immunoreactivity following cortical impact brain injury. J Neurotrauma 13: 125–137
52. Folkerts MM, Berman RF, Muizelaar JP, Rafols JA (1998) Disruption of MAP-2 immunostaining in rat hippocampus after traumatic brain injury. J Neurotrauma 15: 349–363
53. Taft WC, Yang K, Dixon CE, Hayes RL (1992) Microtubule-associated protein 2 levels decrease in hippocampus following traumatic brain injury. J Neurotrauma 9: 281–290
54. Koo EH, Sisodia SS, Archer DR, Martin LJ, Weidemann A, Beyreuther K, Fischer P, Masters CL, Price DL (1990) Precursor of amyloid protein in Alzheimer disease undergoes fast anterograde axonal transport. Proc Natl Acad Sci USA 87: 1561–1565
55. Otsuka N, Tomonaga M, Ikeda K (1991) Rapid appearance of beta-amyloid precursor protein immunoreactivity in damaged axons and reactive glial cells in rat brain following needle stab injury. Brain Res 568: 335–338
56. Povlishock JT, Jenkins LW (1995) Are the pathobiological changes evoked by traumatic brain injury immediate and irreversible? Brain Pathol 5: 415–426
57. Gentleman SM, Nash MJ, Sweeting CJ, Graham DI, Roberts GW (1993) Beta-amyloid precursor protein (beta APP) as a marker for axonal injury after head injury. Neurosci Lett 160: 139–144
58. Graham DI, Gennarelli TA (1997) Trauma. In: Graham DI, Lantos PL (eds): Greenfield's neuropathology, 6th edn. Arnold, London, pp 198–262
59. Patt S, Brodhun M (1999) Neuropathological sequelae of traumatic injury in the brain. An overview. Exp Toxicol Pathol 51: 119–123
60. Pilz P (1983) Axonal injury in head injury. Acta Neurochir Suppl Wien 32: 119–123
61. Povlishock JT (1992) Traumatically induced axonal injury: pathogenesis and pathobiological implications. Brain Pathol 2: 1–12
62. Pierce JE, Trojanowski JQ, Graham DI, Smith DH, McIntosh TK (1996) Immunohistochemical characterization of alterations in the distribution of amyloid precursor proteins and beta-amyloid peptide after experimental brain injury in the rat. J Neurosci 16: 1083–1090
63. Rink A, Fung KM, Trojanowski JQ, Lee VM, Neugebauer E, McIntosh TK (1995) Evidence of apoptotic cell death after experimental traumatic brain injury in the rat. Am J Pathol 147: 1575–1583
64. Conti AC, Raghupathi R, Trojanowski JQ, McIntosh TK (1998) Experimental brain injury induces regionally distinct apoptosis during the acute and delayed post-traumatic period. J Neurosci 18: 5663–5672
65. Clark RS, Chen J, Watkins SC, Kochanek PM, Chen M, Stetler RA, Loeffert JE, Graham SH (1997) Apoptosis-suppressor gene bcl-2 expression after traumatic brain injury in rats. J Neurosci 17: 9172–9182
66. Colicos MA, Dash PK (1996) Apoptotic morphology of dentate gyrus granule cells following experimental cortical impact injury in rats: possible role in spatial memory deficits. Brain Res 739: 120–131
67. Tominaga T, Kure S, Narisawa K, Yoshimoto T (1993) Endonuclease activation following focal ischemic injury in the rat brain. Brain Res 608: 21–26
68. Edwards AD, Yue X, Squier MV, Thoresen M, Cady EB, Penrice J, Cooper CE, Wyatt JS, Reynolds EO, Mehmet H (1995) Specific inhibition of apoptosis after cerebral hypoxia-ischaemia by moderate post-insult hypothermia. Biochem Biophys Res Commun 217: 1193–1199

The Effect of Mild Hypothermia on Plasma Fentanyl Concentration and Biotransformation in Juvenile Pigs

Harald G. Fritz, MD*, Martin Holzmayr†, Bernd Walter, MD†‡, Klaus-Uwe Moeritz, PhD‖, Amelie Lupp, MD§, and Reinhard Bauer, MD, PhD†

Departments of *Anesthesiology and Intensive Care Medicine and †Pathobiochemistry, Institute for Pathophysiology and Pathobiochemistry, ‡Department of Neurosurgery and §Institute for Pharmacology and Toxicology, Friedrich-Schiller-University, Jena; and ‖Institute of Pharmacology, Ernst Moritz Arndt University, Greifswald, Germany

Therapeutic hypothermia may alter the required dosage of analgesics and sedatives, but no data are available on the effects of mild hypothermia on plasma fentanyl concentration during continuous, long-term administration. We therefore assessed in a porcine model the effect of prolonged hypothermia on plasma fentanyl concentration during 33 h of continuous fentanyl administration. Seven female piglets (weight: 11.8 ± 1.1 kg) were anesthetized by IV fentanyl (15 $\mu g \cdot kg^{-1} \cdot h^{-1}$) and midazolam (1.0 $mg \cdot kg^{-1} \cdot h^{-1}$). After preparation and stabilization (12 h), the animals were cooled to a core temperature of 31.6° ± 0.2°C for 6 h and were then rewarmed and kept normothermic at 37.7° ± 0.3°C for 6 more hours. Plasma fentanyl concentrations were measured by radioimmunoassay, cardiac index by thermodilution, and blood flows of the kidney, spleen, pancreas, stomach, gut, and hepatic artery by a colored microspheres technique. Furthermore, in an additional 4 pigs, temperature dependency of hepatic microsomal cytochrome P450 3A4 (CYP3A4) was determined *in vitro* by ethylmorphine *N*-demethylation. Plasma fentanyl concentration increased by 25% ± 11% ($P < 0.05$) during hypothermia and remained increased for at least 6 h after rewarming. Hypothermia reduced the cardiac index (41% ± 15%, $P < 0.05$), as well as all organ blood flows except the hepatic artery. A strong temperature dependency of CYP3A4 was found ($P < 0.01$). Mild hypothermia induced a distribution and/or elimination-dependent increase in plasma fentanyl concentration which remained increased for several hours after rewarming. Consequently, a prolonged increase of the plasma fentanyl concentration should be anticipated for appropriate control of the analgesia/sedatives during and early after therapeutic hypothermia.

(Anesth Analg 2005;100:996–1002)

Mild hypothermia has been effective after cardiac arrest, ischemic and traumatic brain injury (TBI), neonatal asphyxia, and neurosurgical procedures (1–3). However, there is controversy on the effects of hypothermia on patient outcome in these applications, especially after TBI (2). The results may be influenced by the complex effects of hypothermia, the modalities of hypothermia application, and side effects of hypothermia.

Background anesthesia seems to be an independent factor that may influence both the putative protective and detrimental effects of hypothermia. Indeed, hypothermia itself may alter the pharmacokinetics of anesthetics. The plasma concentration of propofol increases about 28% during mild hypothermia in humans (4). During reduced core temperature, a doubling of vecuronium-induced neuromuscular block duration has been demonstrated in humans (5). Additionally, the anesthetic/analgesic regimen after TBI may dramatically influence the response to hypothermia (6).

The synthetic opioid fentanyl, when administered IV, is cleared predominantly by hepatic biotransformation (7). Fentanyl is metabolized by the microsomal cytochrome P450 3A4 (CYP3A4) isoform in humans (8), which is also present in the pig liver with similar activity (9). However, the effects of mild hypothermia on the action of continuously administered opioids for long-term analgesia and sedation (e.g., fentanyl) are not well understood.

We therefore examined, in a porcine model, the effect of mild hypothermia (32°C) on the plasma concentration of fentanyl during continuous long-term

This study was supported by Grant 01ZZ9602 from the Bundesministerium für Bildung und Forschung, Germany, and Janssen-Cilag G.m.b.H. Neuss, Germany.

Accepted for publication September 8, 2004.

Address correspondence and reprint requests to Harald G. Fritz, MD, Department of Anesthesiology and Intensive Care Medicine, Martha-Maria Hospital Halle D*lau gGmbH, Roentgenstr. 1, D-06120 Halle/S., Germany. Address e-mail to harald_fritz_2000@yahoo.de.

DOI: 10.1213/01.ANE.0000146517.17910.54

©2005 by the International Anesthesia Research Society
0003-2999/05

administration (33 h). We also investigated the effect of hypothermia on perfusion of organs that are involved in fentanyl metabolism and excretion, using color-labeled microspheres (CMS) (10). Furthermore, we determined temperature dependency of porcine hepatic microsomal CYP3A4 activity *in vitro* by ethylmorphine *N*-demethylation. We studied whether a temporarily decreased and subsequently reestablished body temperature, by altering the enzyme activity responsible for hepatic biotransformation, would influence the plasma concentration of fentanyl during continuous infusion.

Methods

The study protocol was approved by the committee of the Thuringian State Government for animal research. The animals were managed in accordance with the guidelines of the American Physiological Society.

In Vivo *Study*

Seven female juvenile pigs of mixed German domestic breed (6-wk-old, weight: 11.8 ± 1.1 kg) were initially sedated with ketamine hydrochloride (20 mg/kg) and midazolam (1 mg/kg), and anesthesia was maintained during surgery by 70% nitrous oxide in 30% oxygen and 2% isoflurane. After tracheotomy (tube size: 5.5-mm inner diameter) and insertion of a central venous catheter into the left external jugular vein for drug administration and fluid therapy (lactated Ringer's solution: 4 $mL \cdot kg^{-1} \cdot h^{-1}$), muscular relaxation was achieved with IV pancuronium bromide (0.4 $mg \cdot kg^{-1} \cdot h^{-1}$). The lungs of the pigs were mechanically ventilated using pressure-controlled ventilation (Servo Ventilator 900C; Siemens-Elema, Solna, Sweden) with an oxygen/air mixture (FIO_2 0.35). Ventilation was controlled by continuous end-expiratory CO_2 monitoring and arterial blood gas check with α-stat regime hourly.

The left brachial artery was cannulated for continuous monitoring of mean arterial blood pressure (MABP). A thermodilution catheter for cardiac index (CI) measurement was inserted into the abdominal aorta 2 cm below the diaphragm via the femoral artery. A left atrium catheter (inner diameter 1.0 mm) was placed via a left thoracotomy for CMS injection. In addition, a catheter (inner diameter 0.5 mm) was inserted into a branch of the pulmonary artery for mixed venous blood sampling. Another catheter (inner diameter 1.4 mm) was advanced from the left femoral artery into the abdominal aorta in order to withdrawal reference samples during regional blood flow measurement (see below).

An electrocardiogram was recorded from standard limb leads using stainless steel needle electrodes. Body temperature was controlled by a rectal thermoprobe, maintained throughout instrumentation at 37.5° ± 0.5°C using a water-filled pad connected to a heating-cooling thermostat and a feedback-controlled heating lamp. Physiological variables were recorded on a multichannel polygraph (MT95K2; Astro-Med).

Experimental Protocol and Management of Hypothermia. After instrumentation, anesthesia was maintained throughout the experiment with a continuous infusion of fentanyl (15 $\mu g \cdot kg^{-1} \cdot h^{-1}$) and midazolam (1.0 $mg \cdot kg^{-1} \cdot h^{-1}$). During the baseline stabilization period of 12 h, values were recorded at 6 h (measuring point one, MP1) and 12 h (MP2). Systemic hypothermia was started 1 h after MP2 by means of a cooling blanket and forced air cooling. Hypothermia was guided by a rectal thermocouple probe. The animals were surface cooled within 217 ± 101 min to a core temperature of 31.6° ± 0.2°C for 6 h (MP3). Afterward, animals were rewarmed (MP4) within 258 ± 55 min and kept normothermic at 37.7° ± 0.3°C for a further 6 h (MP5) (Fig. 1).

Measurements. Blood samples for analysis of plasma fentanyl concentrations were injected into glass tubes. The plasma was separated in a refrigerated centrifuge (4°C) and placed in polypropylene tubes. Plasma fentanyl concentrations were measured by radioimmunoassay (Fa. Janssen Biotech, Olen, Belgium) at the five time points (MP1–5) (11). The assay sensitivity was 0.05 ng/mL, with intra- and intercoefficients of variation 6.0% and 6.9%, respectively. The assay was specific for fentanyl and did not include the metabolites.

Organ blood flows were measured using the reference sample CMS technique (10). Briefly, a known amount (approximately 3×10^6 per injection) of polystyrene CMS (diameter: 15.5 ± 0.33 μm) in 0.01% Tween 80, surface coated with 1 of 5 dyes (blue, yellow, white, red, violet) (Dye-Trak; Triton Technology, San Diego, CA) were thoroughly vortexed and sonicated and immediately injected within 20 s into the left atrium. CMS injected had a different color for each measuring point (MP1–5). A blood sample was withdrawn from the descending aorta as the reference sample, beginning 15 s before the CMS injection and continuing for 2 min at a rate of 3 mL/min (syringe pump SP210iw; World Precision Instruments, Inc., Sarasota, FL). The CMS injection did not alter MABP. At the end of each experiment, the pigs were killed with potassium chloride and the organ tissue samples from pancreas, spleen, liver, kidney, stomach (cardia, fundus, and pylorus, 4–6 g each), and gut (duodenum, jejunum, and ileum, 4–6 g each) were removed for processing. Blood and tissue samples were digested and the dye content of the contained CMS was estimated by photometric absorption with a diode-array ultraviolet/visible spectrophotometer (model 7500, wave length range 300–800 nm with a 2-nm

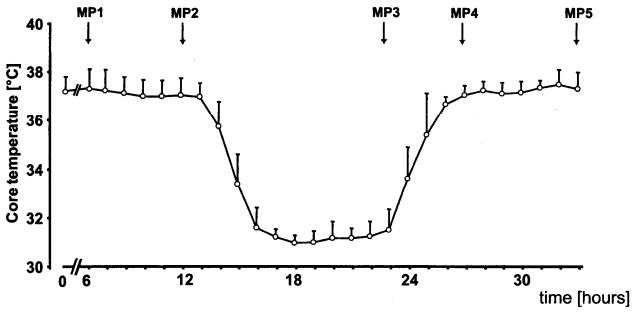

Figure 1. Temperature pattern during the 33-h experiment. MP = measurement points for organ blood flow and plasma fentanyl concentration. Values are presented as means + SD.

optical band width; Beckman Instruments, Fullerton, CA). Calculations were performed using the MISS software (Triton Technology). The number of CMS was calculated using the specific absorbency value of the different dyes (provided by the manufacturer). Absolute tissue blood flows measured by CMS were calculated by the formula: $flow_{tissue}$ = number of $microspheres_{tissue} \cdot (flow_{reference}/number\ of\ microspheres_{reference})$. Flows are expressed in mL/min per 100 g of tissue.

Assuming the oxygen capacity of hemoglobin to be 1.39 mL O_2/g hemoglobin in pigs, blood O_2 content was calculated as equal to grams of hemoglobin/mL · 1.39 mL O_2/g hemoglobin · O_2 saturation and expressed in mL/100 mL. Dissolved oxygen was added by calculation, using the measured Po_2 and the temperature-corrected solubility coefficient for oxygen. The systemic oxygen consumption ($\dot{V}o_2$) was calculated by multiplying CI by the difference in arteriovenous O_2 content. Systemic oxygen extraction rate was calculated by arteriovenous O_2 content divided by arterial oxygen content.

In Vitro *Study*

Biological Material. To determine temperature dependency of CYP3A4 activity, 9000*g* supernatants from pig liver specimens were used. Four juvenile pigs of mixed German domestic breed (age: 6 wk, weight: 12.7 ± 1.5 kg) were initially sedated with ketamine hydrochloride (20 mg/kg) and midazolam (1 mg/kg) and afterward killed for organ removal by IV injection of 10 mL of saturated magnesium chloride. Subsequently, the liver specimens (approximately 1 g each) were quickly removed and shock-frozen in liquid nitrogen and kept therein until processing. For preparation of the 9000*g* supernatants, the specimens were homogenized in ice-cold 0.1 M sodium phosphate buffer pH 7.4 (1:3 w/v) and centrifuged at 9000*g* for 20 min at 4°C. The protein content of the supernatants was determined by modified Biuret method.

Cytochrome P450-Dependent Monooxygenase Model Reactions. Ethylmorphine *N*-demethylation activity was assessed in the supernatants by photometrical determination of the reaction product formaldehyde (12). For this reaction, the supernatants were diluted 1:4 with 0.1 M sodium phosphate buffer pH 7.4. Reactions were performed in a shaking water bath for 10 min at the temperatures indicated (26°, 32°, 38°, 44°C). Before starting the reaction with the substrate ethylmorphine, samples were allowed to equilibrate to the temperature for 5 min. The activities of the model reactions were referenced to the protein content of the supernatants.

Values were presented as means ± SD. One-way analysis of variance with repeated measures was performed within the group. *Post hoc* comparisons were done using paired Student's *t*-test with Bonferroni correction for multiple comparisons. Differences were considered significant at $P < 0.05$. All statistical tests were done using the statistical package SPSS for Windows release 10.0 (SPSS Inc., Chicago, IL).

Results

Blood gases, arterial glucose and lactate contents, as well as systemic hemodynamics are presented in Table 1. Hypothermia resulted in a decrease in CI of 41% ± 15% and heart rate of 21% ± 4% ($P < 0.05$), whereas arterial glucose and lactate concentrations were slightly increased ($P < 0.05$). After rewarming, both CI and heart rate returned to baseline levels. MABP decreased 22% ± 8% ($P < 0.05$) during hypothermia, but remained slightly reduced after rewarming. Furthermore, during hypothermia, the systemic $\dot{V}o_2$ was reduced by 44% ± 11% ($P < 0.05$) and returned to prehypothermic values after rewarming.

The baseline plasma fentanyl concentration did not change during the prehypothermic period (MP1, MP2) (Fig. 2). At the end of the cooling period, the plasma fentanyl concentration increased by 25% ± 11% (MP3, $P < 0.001$). After rewarming (MP4) and 6 h of normothermia (MP5), plasma fentanyl concentration remained increased ($P < 0.05$).

As shown in Figure 3, hypothermia was associated with markedly reduced blood flows ($P < 0.05$) to the kidney (38% ± 32%), spleen (45% ± 33%), stomach (53% ± 31%), and gut (49% ± 26%). Pancreatic blood flow was also reduced during hypothermia (49% ± 46%), and remained so even after rewarming ($P < 0.05$). In contrast, hepatic artery blood flow remained unchanged throughout the experiment.

Hypothermia induced a strong temperature-dependent reduction in hepatic CYP3A4 activity (at 26°C: 48% ± 2%, at 32°C: 69% ± 1%, compared with values obtained at 38°C) ($P < 0.001$). Temperature increase was associated with a mildly reduced CYP3A4 activity (at 44°C: 94% ± 3%) ($P < 0.01$) (Fig. 4).

Table 1. Hemodynamic and Blood Variables

	MP1	MP2	MP3	MP4	MP5
pH	7.49 ± 0.04	7.49 ± 0.03	7.41 ± 0.07*	7.51 ± 0.03	7.51 ± 0.07
Pao_2 (mm Hg)	146 ± 18	152 ± 10	183 ± 17*	157 ± 6*	144 ± 13
$Paco_2$ (mm Hg)	40 ± 4	39 ± 3	43 ± 3*	38 ± 4	38 ± 3
Arterial glucose (mmoL/L)	6.4 ± 1.2	6.5 ± 1.0	9.9 ± 3.1*	8.4 ± 3.6*	6.3 ± 1.0
Arterial lactate (mmoL/L)	1.4 ± 0.6	1.5 ± 0.5	2.6 ± 1.4*	1.4 ± 0.5	1.2 ± 0.3
HR (bpm)	206 ± 11	200 ± 20	163 ± 9*	192 ± 22	197 ± 23
MABP (mm Hg)	119 ± 15	118 ± 15	93 ± 9*	104 ± 10	96 ± 17*
CI ($mL \cdot min^{-1} \cdot kg^{-1}$)	199 ± 34	195 ± 26	118 ± 30*	193 ± 46	198 ± 40
O_2ER (%)	44 ± 8	43 ± 9	43 ± 5	51 ± 9	49 ± 6
$\dot{V}o_2$ ($mL \cdot min^{-1} \cdot kg^{-1}$)	5.4 ± 9.0	5.6 ± 1.6	3.0 ± 6.0*	5.1 ± 9.1	4.9 ± 6.4

Values are presented as means ± SD.
MP1 = baseline, MP2 = control of baseline, MP3 = after 6 h of hypothermia at 32°C, MP4 = return of normothermia; MP5 = end of the experiment; MP = measuring point; Pao_2 = arterial oxygen partial pressure; $Paco_2$ = arterial carbon dioxide partial pressure; HR = heart rate; MABP = mean arterial blood pressure; CI = cardiac index; O_2ER = systemic oxygen extraction rate; $\dot{V}o_2$ = systemic oxygen consumption.
* $P < 0.05$ versus baseline (MP1).

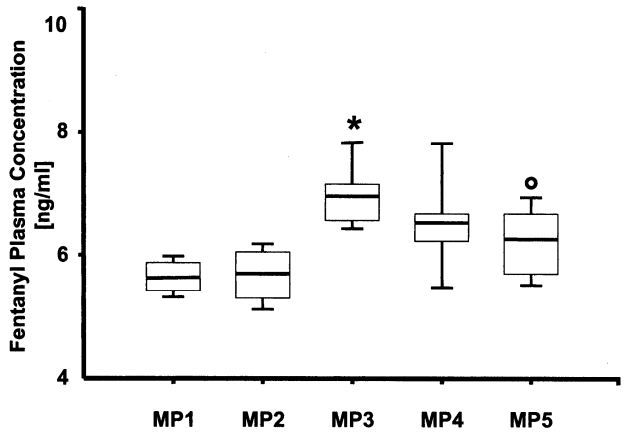

Figure 2. The baseline plasma fentanyl concentration did not change during the first 12 h (MP1, MP2) before cooling (MP = measurement points for organ blood flow and plasma fentanyl concentration). At the end of the cooling period (MP3), the plasma fentanyl concentration increased significantly to 7.0 ± 0.6 ng/mL. After rewarming (MP4) and a further 6 h at normothermia (MP5), the plasma fentanyl concentration decreased significantly to 6.3 ± 0.6 ng/mL ($P < 0.05$) compared with MP3, but remained increased compared with baseline (MP1, MP2). Horizontal lines in the boxes represent median, the boxes represent the interquartile ranges (25th and 75th percentiles); error bars represent 10th and 90th percentiles,*$P < 0.001$, °$P < 0.05$, MP versus control.

Discussion

The present study demonstrates an increase of approximately 25% in the plasma concentration of fentanyl, when infused at a constant rate during a 6-hour period of hypothermia at approximately 32°C. This observation is consistent with other reports describing the effect of hypothermia on the pharmacokinetics of other drugs with a high hepatic extraction ratio such as propofol (4), propanolol (13), and fentanyl (14) and also those having a low hepatic extraction ratio, such as phenytoin (15) or metabolized by nonspecific esterases like remifentanil (16). However, these studies differed with regard to drug administration, observation time, and level of hypothermia. Although continuous fentanyl infusion over a prolonged period is a common approach for analgesia and sedation in intensive care medicine, there are few data on plasma fentanyl concentrations during hypothermia.

We chose a porcine model because of the similarities between swine and humans in the basic cardiovascular variables, including CI and $\dot{V}o_2$, as well as regional distribution of blood flows (17). Furthermore, there is a remarkable similarity in biotransformation pathways, because the activity of the most important CYP isoform in humans, CYP3A4, also responsible for hepatic fentanyl metabolism, is present in pigs with comparable levels and activities (9).

Under normal conditions, fentanyl is cleared predominantly by hepatic biotransformation (7), and the metabolism is extensive and rapid under physiological conditions. Furthermore, fentanyl is preferentially oxidized to norfentanyl by hepatic microsomal cytochrome P450 3A isoform (8) and excreted renally. Other pathways such as intestinal metabolism seem less likely with parenteral administration (18).

There are several processes that may be responsible for an increase in plasma fentanyl concentration during hypothermia. The pharmacokinetics of fentanyl, a drug with a large distribution volume and a high hepatic extraction ratio, could be altered. After a bolus injection, distribution volume and total body clearance were markedly reduced during hypothermia (14). A reduced total body clearance can be a result of reduced hepatic biotransformation and/or slower distribution caused by reduced cardiac output and organ perfusion rate estimated in this study. Simulation studies have demonstrated that the amount of reduced perfusion reported in this study can be responsible for increased blood fentanyl concentration (19).

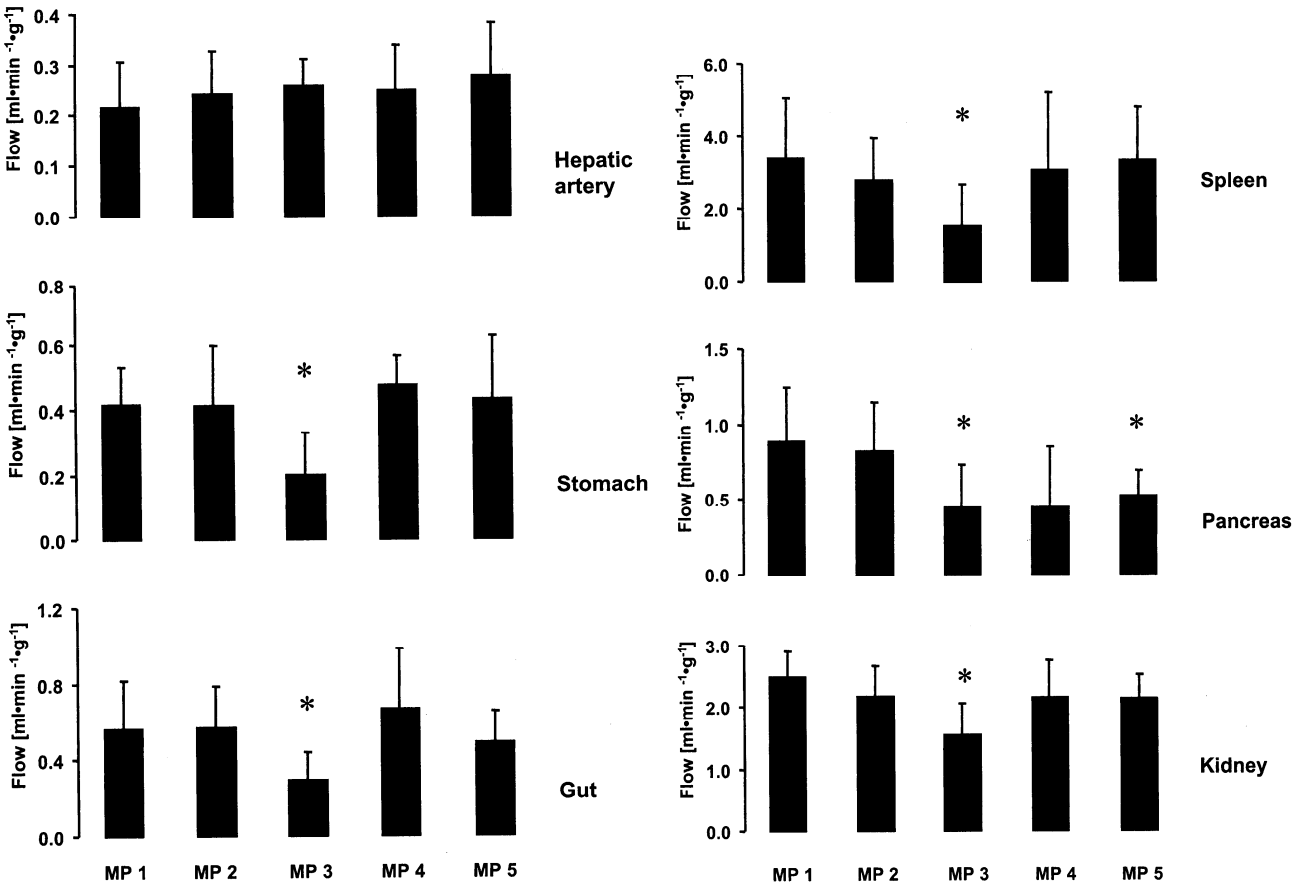

Figure 3. Organ blood flow during the prehypothermic period (MP1, MP2), after 6 h of hypothermia at 31.6° ± 0.2°C (MP3), after rewarming to normothermia (MP4), and at the end of the experiment at 6 h after rewarming (MP5). MP = measurement points for organ blood flow and plasma fentanyl concentration. Values are presented as means + SD, *$P < 0.05$ MP versus control.

However, the experimental design does not allow discrimination between alterations in distribution and elimination influences.

With regard to hypothermia-dependent alterations of fentanyl elimination, several aspects have to be considered. We have shown that hepatic CYP3A4 activity in juvenile pigs is strongly temperature dependent. At 32°C, the conversion rate was reduced by about one-third. Therefore, a relevant component of the reduction in total body clearance seems to be a reduced hepatic biotransformation of fentanyl. Furthermore, total hepatic blood flow is assumed to be reduced, despite the surprising finding that only arterial hepatic influx remained unaltered during mild hypothermia. Under normal conditions, arterial hepatic blood flow represents no more than one-fifth of total hepatic blood flow in the juvenile pig (20). The other influx arrives via the portal vein. Indeed, there is no doubt that portal blood flow was markedly reduced during hypothermia, because all perfusion rates of splanchnic organs drained by the portal vein were reduced. Because fentanyl has a high liver extraction ratio, hepatic elimination of fentanyl is expected to be more sensitive to blood flow alterations than to enzymatic activity (21). We suggest that both mechanisms, i.e., reduced total liver blood flow and reduced hepatic CYP3A4 activity, are involved in the reduced hepatic elimination, which may in turn be responsible for the increased efficient levels of fentanyl during hypothermia.

Hemodynamic data support our opinion that hypothermia-dependent alteration of fentanyl turnover is not primarily caused by compromised hepatic energy metabolism. The expected effects of mild hypothermia on systemic hemodynamics and oxygen uptake were similar to that reported earlier with a comparable anesthetic/analgesic regimen (22). Our data demonstrate a marked decrease in CI (CI decreased by an average 41%), and concomitant decrease in whole body O_2 uptake which suggests an appropriate decreasing of metabolic demand. This assumption is supported by an unaltered arteriovenous oxygen

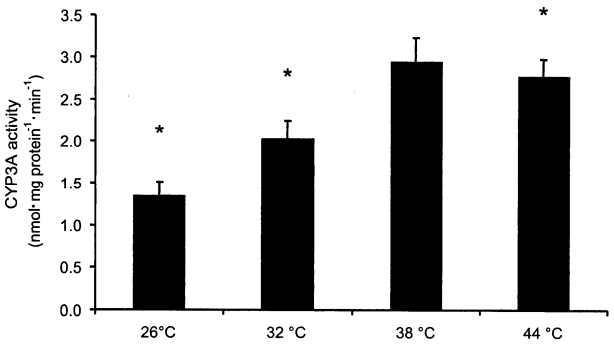

Figure 4. Temperature-dependency of pig hepatic microsomal cytochrome P450 3A4 (CYP3A) activity *in vitro* by ethylmorphine *N*-demethylation. MP = measurement points for organ blood flow and plasma fentanyl concentration. Values are presented as means + SD, *$P < 0.05$ versus 38°C).

extraction rate during and after mild hypothermia (Table 1). Furthermore, during hypothermia, similar reductions in blood flow have been shown for the splanchnic organs studied, suggesting portal blood flow to the liver appropriate to a reduced oxidative metabolism. The maintained hepatic artery influx tends to exclude hepatic hypoperfusion and restricted hepatic O_2 availability for the reduced fentanyl metabolism.

Thus, a risk for increased blood concentrations during long-term administration of fentanyl depends mainly on portal blood flow, which is proportional to cardiac output. Hence, maintenance of cardiac output to normal values may suggest that fentanyl concentration is likely stable whereas a decrease in cardiac output should suggest decreasing fentanyl doses.

The reason for a delayed normalization of plasma fentanyl level after rewarming remains unclear. A prolonged inhibition of hepatic CYP3A4 activity seems rather implausible, because after long-term deep hypothermic liver preservation, hepatic drug extraction was reestablished within 30 min of rewarming (23). An augmented tissue accumulation of fentanyl during the hypothermic period of reduced clearance, and subsequent rebound of plasma levels after rewarming increases tissue blood flow, may be involved.

Additionally, it should be noted that hepatic CYP3A4 is also responsible for midazolam biotransformation, hence this drug could also accumulate during mild hypothermia. In this study, however, we did not estimate plasma midazolam levels. There is no information about the effects of hypothermia on midazolam pharmacology. Nevertheless, it is quite possible that a decreased midazolam metabolism during hypothermia might have resulted in increased midazolam concentration with a possible competition on fentanyl metabolism. Provided that a similar response occurs as with fentanyl, a prolonged accumulation of two drugs could overcome the transforming capacity of CYP3A4 for xenobiotics, resulting in a delayed normalization of the respected plasma levels. Furthermore, midazolam could presumably enhance the hemodynamic effect of hypothermia on regional blood flow and fentanyl transport to the liver. A biphasic response of portal blood flow to bolus administration of midazolam has been reported with an early increase and a following decrease. This is probably related to redistribution of blood within the splanchnic system (blood mobilization from spleen and intestine), whereas hepatic arterial flow decreased immediately after administration (24).

Although the underlying mechanisms of the persistent increase of plasma fentanyl concentration remain speculative, the description of the phenomenon may be of clinical relevance with respect to the recovery from sedation of intensive care unit (ICU) patients after therapeutic hypothermia. However, the range of concentrations usually required in ICU can be smaller than in anesthesia. Therefore, the consequences of hypothermia-related fentanyl accumulation *per se* seem less relevant. However, hypothermia can aggravate a fentanyl overdosage during continuous long-term administration and can result in negative side effects such as decreased intestinal motility, hypotension, reduced tissue extraction capabilities, prolonged ICU stay, increased costs, and acute withdrawal syndrome (25). Consequently, an optimal analgesic/sedative regimen during the application of hypothermia should be carefully chosen.

Nevertheless, we can conclude that hypothermia of 32°C induces a reduction of CI, hypoperfusion in several organs, and an increase in plasma fentanyl concentrations. With rewarming, there is a prolonged recovery phase which may include increased side effects and prolonged recovery from analgesia/sedation.

The authors acknowledge the advice of U. Jaeger, I. Witte, and L. Wunder and their skillful technical assistance (Institute for Pathophysiology and Pathobiochemistry, University Jena, Germany), and Don Bredle, PhD (Department of Kinesiology, University of Wisconsin, Eau Claire, WI), for advice in preparing the manuscript.

References

1. Battin MR, Penrice J, Gunn TR, Gunn AJ. Treatment of term infants with head cooling and mild systemic hypothermia (35.0 degrees C and 34.5 degrees C) after perinatal asphyxia. Pediatrics 2003;111:244–51.
2. Fritz HG, Bauer R. Secondary injuries in brain trauma: effects of hypothermia. J Neurosurg Anesthesiol 2004;16:43–52.
3. Hindman BJ, Todd MM, Gelb AW, et al. Mild hypothermia as a protective therapy during intracranial aneurysm surgery: a randomized prospective pilot trial. Neurosurgery 1999;44:23–32.
4. Leslie K, Sessler DI, Bjorksten AR, Moayeri A. Mild hypothermia alters propofol pharmacokinetics and increases the duration of action of atracurium. Anesth Analg 1995;80:1007–14.

5. Caldwell JE, Heier T, Wright PM, et al. Temperature-dependent pharmacokinetics and pharmacodynamics of vecuronium. Anesthesiology 2000;92:84–93.
6. Statler KD, Alexander HL, Vagni VA, et al. Moderate hypothermia may be detrimental after traumatic brain injury in fentanyl-anesthetized rats. Crit Care Med 2003;31:1134–9.
7. McClain DA, Hug CC Jr. Intravenous fentanyl kinetics. Clin Pharmacol Ther 1980;28:106–14.
8. Tateishi T, Krivoruk Y, Ueng YF, et al. Identification of human liver cytochrome P-450 3A4 as the enzyme responsible for fentanyl and sufentanil N-dealkylation. Anesth Analg 1996;82: 167–72.
9. Anzenbacher P, Soucek P, Anzenbacherova E, et al. Presence and activity of cytochrome P450 isoforms in minipig liver microsomes: comparison with human liver samples. Drug Metab Dispos 1998;26:56–9.
10. Walter B, Bauer R, Gaser E, Zwiener U. Validation of the multiple colored microsphere technique for regional blood flow measurements in newborn piglets. Basic Res Cardiol 1997;92: 191–200.
11. Michiels M, Hendriks R, Heykants J. A sensitive radioimmunoassay for fentanyl: plasma level in dogs and man. Eur J Clin Pharmacol 1977;12:153–8.
12. Klinger W, Muller D. Ethylmorphine-N-demethylation by liver homogenate of newborn and adult rats; enzyme kinetics and age course of Vmax and Km1. Acta Biol Med Ger 1977;36: 1149–59.
13. McAllister RG Jr, Tan TG. Effect of hypothermia on drug metabolism: *in vitro* studies with propranolol and verapamil. Pharmacology 1980;20:95–100.
14. Koren G, Barker C, Goresky G, et al. The influence of hypothermia on the disposition of fentanyl: human and animal studies. Eur J Clin Pharmacol 1987;32:373–6.
15. Iida Y, Nishi S, Asada A. Effect of mild therapeutic hypothermia on phenytoin pharmacokinetics. Ther Drug Monit 2001;23: 192–7.
16. Russell D, Royston D, Rees PH, et al. Effect of temperature and cardiopulmonary bypass on the pharmacokinetics of remifentanil. Br J Anaesth 1997;79:456–9.
17. McKirnan MD, White FC, Guth BD, Bloor CM. Exercise and hemodynamic studies in swine. In: Stanton HC, Mersmann HJ, eds. Swine in cardiovascular research. Boca Raton, FL: CRC Press, 1986:105–20.
18. Labroo RB, Paine MF, Thummel KE, Kharasch ED. Fentanyl metabolism by human hepatic and intestinal cytochrome P450 3A4: implications for interindividual variability in disposition, efficacy, and drug interactions. Drug Metab Dispos 1997;25: 1072–80.
19. Bjorkman S, Wada DR, Stanski DR. Application of physiologic models to predict the influence of changes in body composition and blood flows on the pharmacokinetics of fentanyl and alfentanil in patients. Anesthesiology 1998;88:657–67.
20. Tranquilli WJ, Parks CM, Thurmon JC, et al. Organ blood flow and distribution of cardiac output in nonanesthetized swine. Am J Vet Res 1982;43:895–7.
21. Scholz J, Steinfath M, Schulz M. Clinical pharmacokinetics of alfentanil, fentanyl, and sufentanil: an update. Clin Pharmacokinet 1996;31:275–92.
22. Perez-de-Sa V, Roscher R, Cunha-Goncalves D, et al. Mild hypothermia has minimal effects on the tolerance to severe progressive normovolemic anemia in swine. Anesthesiology 2002; 97:1189–97.
23. Kelley SD, Cauldwell CB, Fisher DM, et al. Recovery of hepatic drug extraction after hypothermic preservation. Anesthesiology 1995;82:251–8.
24. Gelman S, Reves JG, Harris D. Circulatory responses to midazolam anesthesia: emphasis on canine splanchnic circulation. Anesth Analg 1983;62:135–9.
25. Soliman HM, Melot C, Vincent JL. Sedative and analgesic practice in the intensive care unit: the results of a European survey. Br J Anaesth 2001;87:186–92.

JOURNAL OF NEUROTRAUMA
Volume 22, Number 7, 2005
© Mary Ann Liebert, Inc.
Pp. 807–821

A Pig Model with Secondary Increase of Intracranial Pressure after Severe Traumatic Brain Injury and Temporary Blood Loss

HARALD G. FRITZ,[1] BERND WALTER,[2] MARTIN HOLZMAYR,[3] MICHAEL BRODHUN,[4] STEPHAN PATT,[4] and REINHARD BAUER[3]

ABSTRACT

There is a lack of animal models of traumatic brain injury (TBI) that adequately simulate the long-term changes in intracranial pressure (ICP) increase following clinical TBI. We therefore reproduced the clinical scenario in an animal model of TBI and studied long-term postinjury changes in ICP and indices of brain injury. After induction of anesthesia, juvenile piglets were randomly traumatized using fluid-percussion injury (FPI) to induce either moderate (mTBI = 6 pigs: 3.2 ± 0.6 atm) or severe (sTBI = 7 pigs: 4.1 ± 1.0 atm) TBI. Injury was followed by a 30% withdrawal of blood volume. ICP and systemic hemodynamic were monitored continuously. Repeated measurements of global cerebral blood flow (CBF) and cerebral metabolic rate of oxygen ($CMRO_2$) were performed at baseline, at the end of blood withdrawal, after volume replacement, and at 8 and 24 h postinjury. Histological and immunocytochemical studies have also performed. ICP peaked immediately following FPI (mTBI: 33 ± 16 mm Hg; sTBI: 47 ± 14 mm Hg, $p < 0.05$) in both groups. In the sTBI group, we noted a second peak at 5 ± 1.5 h postinjury. This second ICP peak was accompanied by a 50% reduction in CBF (44 ± 31 mL · min · 100 g^{-1}) and $CMRO_2$ (2.5 ± 2.0 mL · min · 100 g^{-1}). Moderate TBI typically resulted in focal pathological change whereas sTBI caused more diffuse change, particularly in terms of the ensuing axonal damage. We thus describe an animal model of severe TBI with a reproducible secondary ICP increase accompanied by patterns of diffuse brain damage. This model may be helpful in the study of pathogenetic relevance of concomitant affections and verify new therapeutic approaches in severe TBI.

Key words: fluid-percussion injury; hemorrhagic hypotension; intracranial pressure; piglets; secondary injury

INTRODUCTION

Severe traumatic brain injury (TBI) is often associated with elevation of intracranial pressure (ICP). According to one estimate (Ward, 1994), approximately 60% of severely head-injured patients develop increased ICP. Intracranial hypertension following TBI is of considerable prognostic value (Ciricillo et al., 1992; Juul et al., 2000) and correlates with adverse outcome (Miller et al., 1981; Signorini et al., 1999).

[1]Department for Anesthesiology and Intensive Care Medicine and Matha-Maria Hospital, Halle, Germany, [2]Department of Neurosurgery, [3]Institute for Pathophysiology and Pathobiochemistry, [4]Institute of Pathology, Universitätsklinikum Jena, Friedrich Schiller University, Jena, Germany.

Although several groups of investigators have developed animal models of TBI in an attempt to reproduce diverse aspects of pathophysiological responses, long-term ICP changes have been assessed in only a limited number of studies (Shibata et al., 1993). One reason for this might be that the majority of investigations used rodents (Statler et al., 2001). The lisencephalic nature of the rodent cortex appears less susceptible to simulating intracranial changes leading to secondary ICP increase, as frequently observed in humans after severe TBI. The marked structural difference in the human brain morphology with its appearance of complex gyri and sulci may be involved in the different response of ICP to TBI (Povlishock et al., 1994). In contrast, animals showing similarities to human brain morphology (i.e., cat, dog, sheep, pig) have been successfully used as models for TBI with ICP alterations (Lindgren and Rinder, 1969; Millen et al., 1985; Pfenninger et al., 1989; Sullivan et al., 1976). One major difficulty in these animal models of TBI was that the reported ICP increases varied. Some reported no ICP change (Lewelt et al., 1982). Others reported moderate (Engelborghs et al., 1998), or only short-lived ICP elevations (Sullivan et al., 1976). Alternatively, some reported pronounced ICP elevations (Pfenninger et al., 1989). The reasons for "inconsistencies" in ICP response include differences in the injury methods used, observational durations, and/or species-specific characteristics.

Given that none of the known experimental TBI approaches are able to simulate the complex pathophysiology and the large variety of events occurring during clinical TBI, a main disadvantage of the study of the pathological ICP alterations as a main consequence of secondary brain injury, was their lack of reproducibility. Because of these limitations, other experimental models such as epidural balloon inflation (Bauer et al., 1999; Nilsson et al., 1995), intracranial fluid infusion (Leffler et al., 1989), or cryogenic lesion (Kroppenstedt et al., 1999) were used to investigate the compromising effects of increasing ICP or CPP reduction on brain metabolism and cerebral circulation.

However, these approaches simplified the complex interactions of secondary brain injury responsible for the secondary ICP increase after severe TBI. Therefore, we sought to simulate a scenario of two sequential insults known to be frequent at the scene and relevant for the subsequent consequences: a TBI of different intensity followed by temporary blood loss. We used the fluid percussion (FP) injury, which is known to induce TBI with different extents of brain damage, dependent on the intensity of impact administered (McIntosh et al., 1989; Prins and Hovda, 2003; Sullivan et al., 1976), leading to focal or diffuse brain injury. Subsequently, a temporary blood loss was used to induce short-lived hypotension. The aim of this study was to describe a model providing a consistent response of secondary ICP elevation with subsequent neuropathological consequences.

MATERIALS AND METHODS

Experiments were carried out according to the guidelines for animal care and use. Laboratory animal protocols were approved by the Animal Research Committee of the Thuringian State government.

General Instrumentation

Nineteen female juvenile pigs of mixed German domestic breed (6 weeks old, weighing 11.1–13.9 kg) were sedated with ketamine hydrochloride (20 mg/kg b.w.) and midazolam (1 mg/kg b.w.), and were anesthetized with 70% nitrous oxide in 30% oxygen and 2 Vol-% isoflurane (Vapour 19.3, Draegerwerk AG, Lübeck, Germany). Tracheotomy (tube size: 5.5 mm I.D.) was performed, and a central venous catheter was inserted in the left external jugular vein for drug administration and fluid therapy (lactated Ringer's solution: 4 mL//kg b.w./h). Anesthesia was then maintained throughout the experiment with continuous infusion of fentanyl (0.015 mg/kg b.w. /h) and midazolam (1.1 mg/kg b.w./h). Therefore, nitrous oxide and isoflurane were exchanged by air. An inspired fraction of oxygen of about 0.35 was used. Muscle relaxation was achieved with pancuronium bromide (0.4 mg/kg b.w./h, i.v.). All animals were ventilated in a pressure-controlled mode (Servo Ventilator 900C, Siemens-Elema, Sweden). Ventilation was controlled by continuous endexpiratory CO_2 monitoring and hourly arterial blood gas samples. The ventilator was set with a positive inspiratory pressure of 15–20 mbar and a positive end-expiratory pressure of 2–4 mbar. Respiratory rate and inspired oxygen fraction were titrated to maintain a $Paco_2$ of 35 to 40 mm Hg and Pao_2 of 100–130 mm Hg.

Body temperature was controlled by a rectal thermoprobe, maintained throughout instrumentation at 37.5 $\pm$ 0.5°C using a water-filled pad connected to a heating-cooling thermostat and a feedback-controlled heating lamp. The urinary bladder was punctured and permanently drained (Cystofix, Braun Melsungen AG, Germany).

The left brachial artery was catheterized for continuous arterial blood pressure (ABP) monitoring, and a further catheter (inner diameter 1.4 mm) was advanced from the left femoral artery into the abdominal aorta and positioned 1 cm above the aortic bifurcation in order to withdraw reference samples for the colored microsphere measurements. A thermodilution catheter for cardiac in-

dex (CI) measurement was placed into the abdominal aorta 2 cm below the diaphragm through the saphenous artery. After left-sided thoracotomy between the second and third rib, a polyurethane catheter (inner diameter 1.0 mm) was introduced into the left atrium for colored microsphere injection. A further catheter (inner diameter 0.8 mm) was inserted in a pulmonary lobe artery of the left lower lung lobe for withdrawal of mixed venous blood samples. Correct positions of the catheter tips were checked by continuous pressure trace recordings and by autopsy at the end of the experiment.

Arterial and central venous catheters were connected with pressure transducers (P23Db, Statham Instruments, Puerto Rico). An electrocardiogram was recorded from standard limb leads using stainless steel needle electrodes. All animals underwent craniotomy, centered between lambda and bregma over the right parietal cortex in order to fix the fluid percussion adapter (with an 11-mm-bore tube). The dura mater remained intact. A burr hole was drilled into the left frontal bone. A fiberoptic catheter for ICP measurements (Camino Laboratories, San Diego, CA) and a thermocouple serving as a temperature probe (LICOX, GMS, Kiel, Germany) were implanted into the left frontal subcortical white matter. A further burr hole was drilled midline between bregma and lambda suture. A polyurethane catheter (inner diameter 0.5 mm) was inserted into the superior sagittal sinus and advanced to the confluence of the sinuses for withdrawal of venous blood samples from the forebrain. Another burr hole was drilled over the left frontal cortex, and a laser Doppler flow probe was placed on the intact dura mater for continuous cortical blood flow recording (Laser Blood Flow Monitor MBF 3D, Moore Instruments, Axminster, England). Burr holes were sealed with bone wax and covered with dental acrylic resin in order to fix the probes and the fluid percussion adapter in place throughout the experiment.

Physiological parameters were recorded on a multichannel polygraph (MT95K2, Astro-Med, West Warwick, RI). In addition, data were recorded using a 16-channel A/D board (sample rate 128 Hz, Data Translation, DT2821F, Marlboro, MA) and stored on the hard disk of a personal computer for off-line data analysis.

Experimental Protocol

When surgical preparation was completed, the cerebral and cardiovascular monitoring was started and continued throughout the experiment. The animals were allowed to rest for 60 min. After baseline physiological values, including data of CBF and brain oxidative metabolism had been obtained, randomly chosen pigs were subjected to lateral fluid percussion injury (FP-TBI). A self-made device designed according to Sullivan et al. (1976) was used. Briefly, the fluid percussion adapter was connected to a transduced housing, and this in turn was connected to the fluid percussion device. The device itself consisted of a Plexiglas cylindrical reservoir 25 cm long and 50 mm in diameter. One end of the device was connected to the transducer housing, and the other end had a metal piston mounted on O-rings. The exposed end of the piston was covered with a rubber pad. The entire system was filled (air bubble-free) with physiologic solution. FP-TBI was produced by allowing a 6.2-kg pendulum to strike the Plexiglas cork and generate a hydraulic pressure transient traveling through the device and impacting upon the dura overlying the brain (the surface area amounted to 63.6 mm^2). The severity of the injury was randomly varied by modification of pendulum angle of deflection (moderate TBI [mTBI, $n = 6$]: 21.2 $\pm$ 1.2°; severe TBI [sTBI, $n = 7$]: 26.0 $\pm$ 3.6°). The resulting pressure pulse was recorded on a high time resolution transducer (Type 5011, Kistler, Germany) and saved on an oscilloscope (54600B Oscilloscope, Hewlett Packard, Colorado Springs, CO). Accordingly, the pressure pulse differed between mTBI (3.2 $\pm$ 0.6 atm) and sTBI (4.1 $\pm$ 1.0 atm), estimated as the mean pressure pulse amplitude between 2^{nd} and 5^{th} msec after FP onset. Immediately after TBI administration, a three-way stopcock mounted on the Plexiglas cylindrical reservoir of the TBI device was opened to allow decompression. Starting 3 min after traumatic injury, 30% of the calculated blood volume (BV, was assumed to be 8% of body weight [Pownall and Dalton, 1973]) was withdrawn continuously within 18 min. After a delay of 14 min, the withdrawn BV was replaced by a gelatin-based plasma expander (Gelafusal; Serum-Werk Bernburg, Germany) within 10 min.

Repeated measurements of blood gases, electrolytes, glucose, lactate, CI, and CBF (colored microspheres) were performed at baseline at the end of blood withdrawal (TBI and BW), immediately after volume replacement (1 h after TBI/VR), as well as 8 and 24 h after FPI. Another six animals received all experimental procedures except FP-TBI administration, blood withdrawal, and volume replacement, and served as control animals.

Immediately after the last measurement, animals were prepared for perfusion fixation of the brain. For this purpose, the chest was opened by a midline sternotomy. The ascending aorta was carefully prepared, and a lax double suture was placed. A stiff secured cannula (inner diameter 2.2 mm) was prepared and flushed with warmed saline. Then 30% potassium chloride solution was injected intracardially, so that the heart beat stopped immediately, followed by a fast insertion of the prepared perfusion cannula, which was tightly locked into the ascending aorta. Descending aorta, both subclavian arter-

ies, and the lower caval vein were clamped by forceps. Right cardiac atrium was opened widely, and subsequently about 500 mL of warmed heparinized physiological saline was infused to flush the perfused vessels from blood. When the returned solution was clear, the brain and adjacent tissues were perfused with 1500 mL of neutrally buffered 4% formalin solution. Afterwards, brain was fixed in situ by immersion in 4% formalin for 48 h at 4°C, then removed from the skull and processed for macro- and microscopical evaluation.

Analytical procedures and calculations

The regional CBF was measured by means of the reference sample color-labeled microsphere (Dye-Trak®, Triton Technology, San Diego, CA) technique, which represents a valid alternative to the radioactively labeled microsphere method for organ blood flow measurement in newborn piglets and avoids all disadvantages arising from radioactive labeling with long-lived isotopes (Walter et al., 1997). Application in piglets and methodical considerations have been presented and discussed in detail elsewhere (Bauer et al., 1996; Walter et al., 1997). Briefly, in random sequence, about 3 million colored polystyrene microspheres were injected into the left atrium. The injection line was then flushed with 2 mL of saline. A blood sample was withdrawn from the thoracic aorta as the reference sample, beginning 15 sec before the microsphere injection and continuing for 2 min at a rate of 3.53 mL/min (syringe pump SP210iw, World Precision Instruments Inc., Sarasota, FL). At the end of each experiment, the brains were removed and sectioned in the desired brain regions. For digestion, reference blood samples and tissue samples between 0.5 and 2.5 g were covered with an appropriate volume (approximately 3 mL/g) of digestive solution (4 N KOH with 4% Tween 80 in deionized water). All tissue and blood samples were digested for a minimum of 4 h at 60°C. In order to isolate the microspheres, each digested tissue sample was then filtered under vacuum suction through an 8-μm-pore polyester-membrane filter. Colored microspheres were quantified by their dye content. The dye was recovered from the microspheres by adding dimethylformamide. The photometric absorption of each dye solution was measured by a diode-array UV/visible spectrophotometer (model 7500, Beckman Instruments, Fullerton, CA). Calculations were performed using the MISS® software (Triton Technology, San Diego, CA). The number of microspheres was calculated using the specific absorbance value of the different dyes. All reference and tissue samples contained >400 microspheres.

Heart rate, ABP, arterial and brain venous pH, P_{CO_2}, and P_{O_2}, oxygen saturation, glucose, lactate, and hemoglobin values were measured immediately before the microsphere injection, respectively. Blood pH, P_{CO_2}, and P_{O_2} were measured with a blood gas analyzer (model ABL50, Radiometer, Copenhagen, Denmark), blood hemoglobin and oxygen saturation were measured using a hemoximeter (model OSM2, Radiometer, Copenhagen, Denmark), and blood glucose and lactate contents were measured with an electrolyte, metabolite laboratory EML105® (Radiometer, Copenhagen, Denmark) and corrected to the body temperature of the animal at the time of sampling.

Assuming the oxygen capacity of hemoglobin to be 1.39 mL/O_2/g hemoglobin in pigs (Bauer et al., 2001), blood O_2-content was calculated as equal to g hemoglobin/mL · 1.39 mL O_2/g hemoglobin · O_2-saturation and expressed in mL/100 mL blood. Dissolved oxygen was added by calculation, using the measured pO_2 and the temperature-corrected solubility coefficient for oxygen.

The absolute flows to the tissues measured by the colored microspheres were calculated by the formula: $\text{flow}_{\text{tissue}} = \text{number of microspheres}_{\text{tissue}} \cdot (\text{flow}_{\text{reference}}/\text{number of microspheres}_{\text{reference}})$. Flows are expressed in milliliters per min per 100 g tissue by normalizing for tissue weight. The $CMRO_2$ was obtained by multiplying the blood flow to the forebrain by the cerebral arteriovenous O_2 content difference, where the blood flow to the forebrain includes all regions drained by the sagittal sinus (cerebral cortex, cerebral white matter, some deep gray structures: basal ganglia, thalamus, and hippocampus) (Coyle et al., 1993). Cerebral perfusion pressure (CPP) was calculated continuously as the difference between ABP and ICP. Brain cortical blood flow was normalized by estimation of a mean value of arbitrary units during baseline (3-min period) and expressed as percentage of baseline. Furthermore, ICP amplitude was continuously estimated off-line using data acquisition and analysis software package "Watisa 1.1" (GJB Datentechnik Bolten & Jannek GbR, Ilmenau, Germany). Spectral analysis of ICP (sample rate 50 Hz) was performed for time intervals of 900 sec using the software package "MathLab®" Version 7.0.1 (The MathWorks GmbH, Aachen, Germany) and expressed as spectral power density.

Macropathologic Evaluation

Macroscopic inspection after skull removal confirmed an intact dura mater below the fluid percussion adapter in all animals with TBI. To assess subarachnoid bleeding, dura mater was carefully removed from the fixed brains. A 10-point scale of a brain-bleeding–surface index (BBSI) was used to score bleeding extent. Total volume of intracerebral bleeding could not

be quantified exactly, because of anatomically and dissection considerations. Bleeding scores were estimated independently by two investigators blinded to study groups.

Histology

The 7-mm-thick coronal slices of the frontal, temporoparietal brain, and brainstem were embedded in paraffin and cut into 7-μm-thick sections, which were stained with hematoxylin and eosin (H&E) for routine morphology or prepared for immunhistochemistry. For immunohistochemical analysis, tissue sections were permeabilized in 0.1% Triton X-100/PBS (3× for 5 min), followed by incubation in blocking buffer containing goat serum. The primary monoclonal antibody mouse anti-beta amyloid precursor protein (βAPP, MAb 22C11; Boehringer Mannheim, Indianapolis, IN; 1:200) was applied overnight at 4°C in TBS, 0.1% Triton X-100 and 5% goat serum. Cy3 or Cy2-linked goat anti-mouse secondary antibodies (1:200 for 2 h at 4°C, Jackson Immuno Research Laboratories, Inc., USA) were used to recognize the primary antibodies. Fluorescent signals were imaged by confocal laser scanning microscopy (Zeiss LSM 510) using standard filters. For negative controls, sections were incubated with normal goat serum in the absence of primary antibody and showed no immunostaining.

The total number of damaged βAPP-positive axons and axonal bulbs were estimated in the subcortical temporoparietal white matter and thalamus of both ipsi- and contralateral hemispheres as well as in the brainstem (counts/0.5 mm^2, 20× objective, extrapolated for the whole βAPP-positive area). In addition, a semiquantitative rating score was used to evaluate the extent of traumatic induced axonal injury for βAPP immunostaining (McKenzie et al., 1996). This score allows a differentiation between mild, moderate, and severe axonal damage. For morphological orientation, an atlas of the pig brain was used (Felix et al., 1999).

Statistical Analysis

Comparisons between groups were made with one-way ANOVA. One-way ANOVA with repeated measures was performed within each group. Post hoc comparisons were performed with Student's *t*-tests. Differences in frequencies of macro- and microscopical characteristics as well as patterns of ICP behavior were compared by the Fisher exact tests; immunomorphological data were compared by the Mann-Whitney U-test. The alpha-adjustment procedure of Bonferroni and Holm was performed to evaluate significant differences. Differences were considered significant when p was <0.05.

RESULTS

Functional Effects

Physiological data are shown in Table 1. Arterial blood gases and rectal temperature were within physiological ranges and not significantly altered from baseline in any group during the whole experiment. Baseline data of systemic and cerebral hemodynamics (Table 1) as well as of the cerebral oxygen metabolism were similar between all groups studied (Fig. 2). Furthermore, in the control group, physiological data remained similar throughout the experiment.

While the systemic hemodynamic response (ABP, HR, CI) did not differ between the two trauma groups, the higher intensity of FPI in the sTBI animals produced a biphasic ICP increase (Fig. 1). The first ICP peak of sTBI animals occurred 90 sec after the impact and was 1.5-fold greater than the corresponding peak in mTBI group ($p < 0.05$). The ICP increase in sTBI animals persisted until the blood withdrawal was started, whereas in the mTBI animals the ICP decreased immediately after reaching the peak ($p < 0.05$). A secondary ICP increase in sTBI animals occurred at 5 ± 1.5 h postinjury and persisted up to the end of the experiment (Table 1, $p < 0.05$). Reduction of cerebral perfusion pressure (CPP) was more pronounced after severe TBI and blood withdrawal ($p < 0.05$) and temporarily reestablished after volume replacement. A further progressive decrease occurred in sTBI animals ($p < 0.05$), whereas CPP remained sustained in mTBI animals. Brain temperature was slightly reduced in sTBI animals ($p < 0.05$).

Spontaneously occurring ICP patterns of compromised intracranial compliance appeared more frequently in the sTBI group (Fig. 3, Table 2, $p < 0.05$), whereas provoked ICP alterations due to tracheal aspiration occurred also regularly after moderate TBI and occasionally in untreated animals.

Under baseline conditions, juvenile piglets represent a CBF of 48 ± 11 mL · min · 100 g^{-1} and $CMRO_2$ of 3.2 ± 1.0 mL · min · 100 g^{-1}. Compared to baseline, CBF increased following volume replacement and remained elevated up to the end of the experiment in mTBI animals (Fig. 2, $p < 0.05$). In sTBI animals, however, global CBF decreased after the end of blood withdrawal and recovered insufficiently after volume substitution, compared to baseline. At the end of the experiment, CBF of sTBI animals was reduced to nearly half of the mTBI CBF values (44 ± 31 mL · min · 100 g^{-1} vs. 91 ± 18 mL · min · 100 g^{-1}, $p < 0.05$).

$CMRO_2$ of mTBI animals increased after blood loss to 120 ± 15% of baseline levels ($p < 0.05$), returned to baseline levels after volume replacement and remained unaltered throughout the recovery period. In contrast,

Table 1. Physiological Parameters during Baseline Conditions, after FP-TBI and 30% Blood Volume Withdrawal (TBI & BW), after Volume Replacement about 1 h after TBI (1 h after TBI/VR) as Well as 8 and 24 h after FP-TBI

Animal groups	*Control group (n = 6)*	*mTBI group (n = 6)*	*sTBI group (n = 7)*
Arterial pO_2 (mm Hg)			
Baseline	146.3 ± 5.1	139.3 ± 25.6	144.4 ± 20.6
TBI & BW	148.4 ± 22.3	138.9 ± 25.9	146.4 ± 12.4*
1 h after TBI/VR	154.2 ± 14.2	145.5 ± 28.6	150.1 ± 10.5
8 h after TBI	136.7 ± 34.1	139.2 ± 26.5	145.8 ± 11.8
24 h after TBI	149.0 ± 14.9	146.0 ± 22.0	144.6 ± 12.1
Arterial pCO_2 (mm Hg)			
Baseline	39.0 ± 4.4	42.4 ± 2.3	40.0 ± 4.0
TBI & BW	41.2 ± 1.5	41.9 ± 2.4	37.6 ± 4.3*
1 h after TBI/VR	40.3 ± 1.0	41.5 ± 1.7	37.5 ± 41.1*
8 h after TBI	42.8 ± 3.5	40.5 ± 3.1	36.6 ± 3.8*,†
24 h after TBI	39.8 ± 6.3	40.8 ± 1.4	36.7 ± 3.2*,†
Arterial pH			
Baseline	7.49 ± 0.03	7.45 ± 0.01	7.49 ± 0.05
TBI & BW	7.49 ± 0.02	7.44 ± 0.04	7.45 ± 0.07
1 h after TBI/VR	7.49 ± 0.02	7.45 ± 0.05	7.47 ± 0.07
8 h after TBI	7.48 ± 0.01	7.46 ± 0.05	7.54 ± 0.03†
24 h after TBI	7.52 ± 0.06	7.51 ± 0.04†	7.53 ± 0.06†
Arterial hemoglobin ($mmoL \cdot L^{-1}$)			
Baseline	6.4 ± 0.6	5.9 ± 0.5	5.9 ± 0.5
TBI & BW	6.1 ± 0.5	5.4 ± 0.6	5.4 ± 0.3†
1 h after TBI/VR	5.8 ± 0.4	3.2 ± 1.2†	3.2 ± 0.7†
8 h after TBI	5.4 ± 0.5†	4.0 ± 0.9†	4.0 ± 0.7†
24 h after TBI	4.9 ± 0.8	3.8 ± 1.1†	3.9 ± 0.6†
Blood glucose ($mmoL \cdot L^{-1}$)			
Baseline	6.3 ± 0.5	6.7 ± 1.1	6.2 ± 0.9†
TBI & BW	6.5 ± 0.5	10.7 ± 3.3†	11.0 ± 4.7†
1 h after TBI/VR	6.3 ± 0.3	7.0 ± 1.3	9.9 ± 4.3*,†
8 h after TBI	6.1 ± 0.3	7.4 ± 1.9	7.8 ± 2.3
24 h after TBI	6.1 ± 0.5	6.5 ± 1.0	6.8 ± 1.4
Arterial blood pressure (mm Hg)			
Baseline	104 ± 12	103 ± 17	102 ± 12
TBI & BW	107 ± 11	69 ± 23†	65 ± 24†
1 h after TBI/VR	110 ± 12	92 ± 17	99 ± 15
8 h after TBI	94 ± 11	75 ± 15	78 ± 18
24 h after TBI	108 ± 20	81 ± 11	72 ± 21†
Heart rate (min^{-1})			
Baseline	176 ± 32	177 ± 9	166 ± 15
TBI & BW	170 ± 23	208 ± 32	218 ± 38†
1 h after TBI/VR	163 ± 21	178 ± 15	170 ± 14
8 h after TBI	154 ± 22	173 ± 24	179 ± 32
24 h after TBI	161 ± 24	170 ± 13	171 ± 15

Table 1. Physiological Parameters during Baseline Conditions, after FP-TBI and 30% Blood Volume Withdrawal (TBI & BW), after Volume Replacement about 1 h after TBI (1 h after TBI/VR) as Well as 8 and 24 h after FP-TBI (*Continued*)

Animal groups	*Control group* (n = 6)	*mTBI group* (n = 6)	*sTBI group* (n = 7)
Cardiac index ($mL \cdot kg^{-1} \cdot min^{-1}$)			
Baseline	248 ± 15	256 ± 33	260 ± 59
TBI & BW	248 ± 27	137 ± 61†	128 ± 40†
1 h after TBI/VR	248 ± 23	267 ± 40	295 ± 49
8 h after TBI	267 ± 56	249 ± 60	256 ± 39
24 h after TBI	258 ± 45	289 ± 49	265 ± 74
Whole body O_2 uptake ($mL \cdot kg^{-1} \cdot min^{-1}$)			
Baseline	5.6 ± 0.9	6.4 ± 1.1	6.4 ± 2.1
TBI & BW	6.3 ± 1.6	5.4 ± 1.6	5.1 ± 1.4
1 h after TBI/VR	6.1 ± 1.7	5.5 ± 1.0	5.9 ± 1.9
8 h after TBI	7.1 ± 1.8	6.3 ± 1.3	5.8 ± 1.0
24 h after TBI	6.0 ± 1.2	5.9 ± 1.9	5.2 ± 1.8
Rectal temperature (°C)			
Baseline	38.9 ± 0.4	38.8 ± 0.7	38.7 ± 0.6
TBI & BW	38.3 ± 0.4	38.9 ± 0.9	38.5 ± 0.7
1 h after TBI/VR	38.3 ± 0.6	83.4 ± 0.7	37.8 ± 0.6†
8 h after TBI	38.1 ± 0.3	38.5 ± 0.8	38.1 ± 0.4
24 h after TBI	38.0 ± 0.6	38.6 ± 0.7	38.1 ± 0.9
Intracranial pressure (mm Hg)			
Baseline	8 ± 2	9 ± 3	8 ± 2
TBI & BW	8 ± 2	4 ± 7	16 ± 12
1 h after TBI/VR	8 ± 2	9 ± 8	18 ± 8
8 h after TBI	6 ± 3	7 ± 2	26 ± 21
24 h after TBI	4 ± 4	7 ± 3	48 ± 24*,†
Cerebral perfusion pressure (mm Hg)			
Baseline	97 ± 13	94 ± 19	93 ± 12
TBI & BW	99 ± 12	65 ± 26	50 ± 24†
1 h after TBI/VR	102 ± 12	83 ± 25	82 ± 14
8 h after TBI	88 ± 13	68 ± 17	52 ± 29†
24 h after TBI	104 ± 22	75 ± 13	31 ± 29*†
Brain temperature (°C)			
Baseline	38.3 ± 0.8	38.8 ± 1.0	38.5 ± 0.7
TBI & BW	38.0 ± 1.1	38.6 ± 0.9	37.4 ± 1.2*,†
1 h after TBI/VR	38.3 ± 1.2	38.3 ± 0.6†	37.7 ± 0.7*,†
8 h after TBI	37.9 ± 0.3†	38.9 ± 1.0	37.5 ± 2.3*
24 h after TBI	38.6 ± 0.9	38.8 ± 0.8	37.1 ± 2.7*,†

*$p < 0.05$ mTBI versus sTBI.

†$p < 0.05$ value versus baseline.

Data expressed as mean ± SD.

FP, fluid percussion; TBI, traumatic brain injury; BW, blood withdrawal; VR, volume replacement; mTBI, moderate traumatic brain injury; sTBI, severe traumatic brain injury.

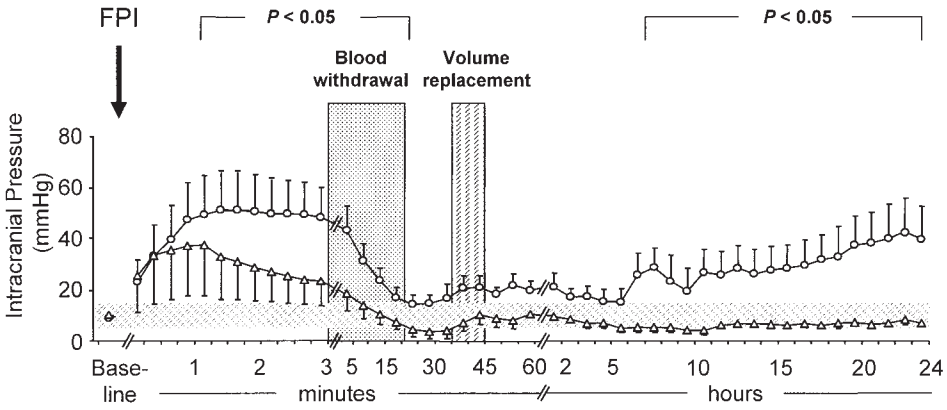

FIG. 1. Recordings of intracranial pressure before and after moderate (mTBI, triangles) and severe (sTBI, circles) fluid-percussion injury (FPI) subsequently followed by withdrawal of 30% of the calculated blood volume (Blood withdrawal) and replacement by a gelatin-based plasma expander (Volume replacement). Recordings are from the first 3 min (value sampling: every 15 sec), from the first hours (value sampling: every 5 min), and to 24 h (value sampling hourly). Data are presented as mean ± SD. The gray hatched area represents ±2 SD from control group.

sTBI animals represented a triphasic behavior in $CMRO_2$ with a marked decrease immediately after TBI application and blood withdrawal (70 ± 6% of baseline levels) and a distinct increase of cerebral O_2 uptake after volume replacement (130 ± 12% of baseline), followed by a re-decline at 24 h postinjury (75 ± 24% of baseline; Fig. 2, $p < 0.05$).

Morphological Effects

In the control animals small amounts of bleeding and tissue distortions were observed around the FP-adapter. In all traumatized animals subarachnoid hemorrhage was seen on the ipsilateral hemisphere. In both traumatized groups small amounts of subarachnoid hemorrhage were noted over the brainstem. Small amounts of supratentorial intraparenchymal bleeding (mainly in subcortical white matter) was seen in all sTBI animals but only in one of six mTBI animals. Subarachnoid hemorrhage over the contralateral hemisphere and the cerebellum were seen in all sTBI animals. Consequently, the semi quantitative evaluation of the extent of bleeding showed a significantly higher score in the sTBI compared to the mTBI group (Table 3, $p < 0.05$). Four sTBI animals showed severe and the other three sTBI animals showed moderate features of raised intracranial pressure (narrowing of sulci and flattening of gyri, reduction in size of ventricles, tentorial and tonsillar hernia). In addition, one animal showed brainstem infarction.

Histological examination showed in all traumatized animals, slight subarachnoid hemorrhage near the craniotomy for FP-adapter, and small intraparenchymal bleeding in the temporoparietal subcortical white matter around gliding contusions. In animals of the sTBI group, subarachnoid hemorrhage was also observed at the contralateral right hemisphere as described already. In all traumatized animals, foci of triangular hemorrhagic necroses were found accompanied by an almost complete loss of nerve cells in the center of the injury. In the adjacent areas, shrunken neurons with eosinophilic homogenization of the cytoplasm and triangular dark nuclei were abundant. The next zone was characterized by shrunken neurons without cell homogenization. Adjacent to this region (approximately 1.5 cm from the center of trauma), morphologically intact neurons were observed in mTBI, whereas shrunken neurons with triangular cell bodies and nuclei, eosinophilic cytoplasm, and perineuronal edema could be found scattered throughout the whole ipsi- and contralateral temporoparietal cortex of sTBI animals (Table 4, $p < 0.05$). In the sTBI group, neuronal injury in the hippocampus was observed in all subfields of both hemispheres, whereas in the mTBI group, necrotic neurons were observed in only two cases and were restricted to the CA2 subfield of the ipsilateral hippocampus (Table 4, $p < 0.05$). Additional neuronal damage in the brainstem could be observed in three animals of the sTBI group, whereas no damage was detected in the brains of mTBI group. Taken together, mTBI animals showed mainly focal brain damage, whereas sTBI animals showed signs of both focal and diffuse damage.

Using βAPP staining, no axonal damage was found in the control animals. In animals of mTBI, moderate axonal damage was observed in the subcortical temporoparietal white matter near the contusion but not in the subcortical white matter of the contralateral hemisphere. Axonal damage was moderate in the ipsilateral

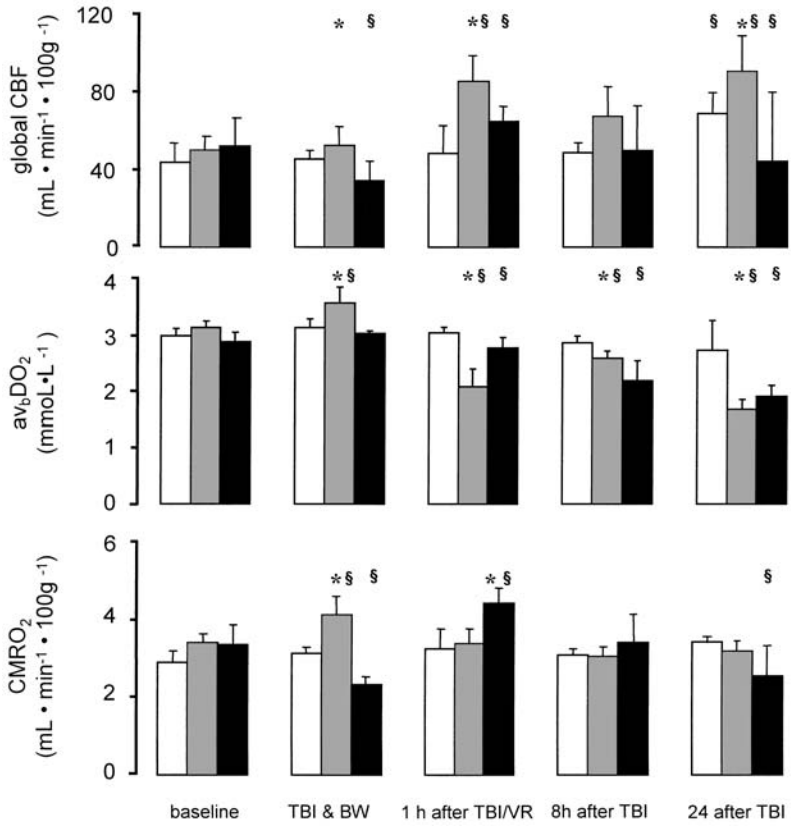

FIG. 2. Effect of gradual fluid-percussion induced TBI (mTBI, moderate traumatic brain injury, shaded columns; sTBI, severe traumatic brain injury, black columns) and temporary blood withdrawal (~30% blood volume [TBI & BW]) with subsequent volume replacement with plasma expander about 1 h after TBI (1 h after TBI/VR) as well as 8 h and 24 h after FP-TBI on global cerebral blood flow (CBF), cerebral arteriovenous O_2 content difference (av_bDO_2), and cerebral metabolic rate of oxygen ($CMRO_2$). Open columns represent data from control group. Values are presented as means ± SD. §Significant differences to baseline (comparisons within each group), $p < 0.05$. *Significant differences between mTBI and sTBI animals (comparisons between treated groups at different experimental stages), $p < 0.05$.

thalamus and sparse in the contralateral thalamus. Only one animal showed additional axonal damage in the left and right superior cerebellar peduncle and in the medial longitudinal bundle of the brainstem.

In brains of sTBI animals, moderate to severe axonal damage was detected scattered in the subcortical temporoparietal white matter, in the corpus callosum, and in the thalamus of the ipsilateral hemisphere. Moderate axonal damage was found in the temporoparietal subcortical white matter and in the thalamus of the contralateral hemisphere. Nearly all animals showed moderate to severe axonal damage in the left and right superior cerebellar peduncle as well as in the medial longitudinal bundle of the brainstem. In comparison to mTBI and control, sTBI showed significant pronounced axonal damage in the ipsi- and contralateral hemisphere as well as in the brainstem (Fig. 4, $p < 0.05$). Taken together, mTBI animals represented focal axonal damage, whereas in sTBI animals signs of diffuse axonal damage (DAI) were found frequently.

DISCUSSION

We described a large animal model of TBI that closely simulates frequently observed courses of events after TBI in humans. Here we were able to show that a high-intensity FP-TBI together with a temporary induced marked blood loss provoked consistently a secondary ICP increase combined with disturbances of brain function and signs of diffuse brain damage. In contrast to previous studies (Dixon et al., 1987), which reported early ICP elevation immediately following trauma, corresponding to the time course of the primary ICP peak in this study, a secondary ICP elevation occurred gradually after a free interval of several hours. This was reproducible after high

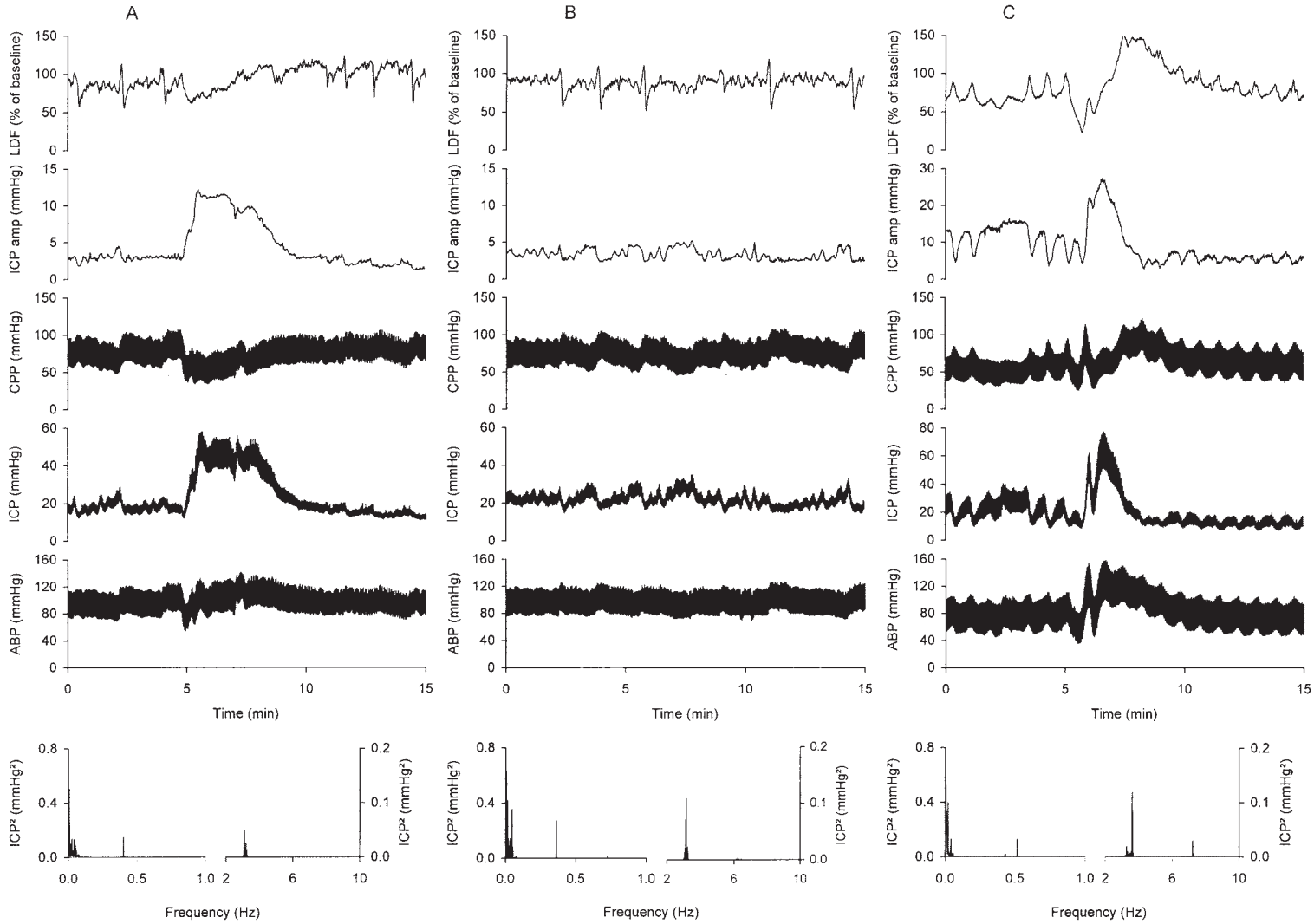

FIG. 3. Representative recordings of arterial blood pressure (ABP), intracranial pressure (ICP), cerebral perfusion pressure (CPP), ICP amplitude (ICP amp), and brain cortical blood flow (LDF), derived from two different animals of sTBI group with typical patterns of transient ICP elevation. (**A**) Plateau wave of ICP, which usually occurs when cerebrospinal compensatory reserve is low. At the height of the wave, CPP and brain cortical blood flow are distinctly reduced despite maintained ABP. After the plateau wave, ICP falls below baseline level and cerebrospinal compensatory reserve appears to be improved. (**B**) "B" waves of ICP were shown in almost all animals suffering sTBI. They are suggested to indicate decreased intracranial compliance and enhanced risk of intracranial hypertension. (**C**) High, spiky wave of ICP caused by sudden increase in ABP. The initial period is associated with marked brain cortical blood flow reduction, whereas an outlasting cortical hyperemia appeared after ICP lowering induced by sustained CPP elevation. Frequency components of ICP recordings were resolved and separately presented by frequency analysis (lowest panel) and represent main components of ICP fluctuations, for example, showing pulse wave and harmonics (frequency range, 2–10 Hz), respiratory wave and the first harmonic (small frequency band at ~0.4 and ~0.8 Hz owing to artificial ventilation) and "slow waves" (frequency range, 0.05–0.0055 Hz, which represents 20-sec to 3-min period).

Table 2. Appearance of Specific ICP Patterns Throughout the Observational Period

Patterns of ICP behavior	*Control*	*mTBI*	*sTBI*
Low stable ICP	6/6[a]	6/6[b]	0/7
Stable and elevated ICP	0/6	0/6	7/7[a,b]
"B" waves of ICP	0/6	0/6	6/7[a,b]
Plateau waves of ICP	0/6	0/6	4/7
High, spiky waves of ICP during sudden increases in ABP	0/6	0/6	3/7
Spiky waves of ICP caused by sucking out the trachea	2/6	4/6	7/7[a]

[a]Differences in frequencies in the appearance of specific patterns of ICP behavior between control group and sTBI group, at $p < 0.05$.

[b]Differences in frequencies in the appearance of specific patterns of ICP behavior between mTBI group and sTBI group, at $p < 0.05$.

Data pairs represent number of animals with specific ICP patterns per total number of experimental animals of each group.

ICP, intracranial pressure; mTBI, moderate traumatic brain injury; sTBI, severe traumatic brain injury; ABP, arterial blood pressure.

intensity FP-TBI, subsequent blood withdrawal and volume replacement. In contrast, a reduced intensity of FP-TBI was accompanied by a short-lasting ICP increase early after TBI induction. Subsequently, mild functional alterations of the brain were observed together with rather focal brain damage.

We used transient hemorrhagic hypotension as a complicating pathophysiological factor, followed by a substitution of colloids 35 minutes following injury. This scenario is comparable to the primary resuscitation management of severely head injured patients. Data from the Traumatic Coma Data Bank have been shown that early hypotension occurs in about 35% of the patients and is associated with a doubling of mortality (Chesnut et al., 1993). Secondary insults after experimental TBI have been shown to aggravate cerebral hypoperfusion and lead to energy failure and cerebral edema development. It has further been shown that animals subjected to a secondary hypoxemic insult after TBI have worse motor and histological outcomes than those subjected to TBI alone (Bramlett et al., 1999; Clark et al., 1997; Ishige et al., 1988; Nawashiro et al., 1995).

Furthermore, this experimental approach offers improved possibilities to investigate resuscitation procedures on outcome after TBI and early hypotension. Despite clinical importance, there is still controversy about treatment standards because comprehensive prospective studies are missing.

Recently it has been shown that early aggressive resuscitation to re-establish preinjury arterial blood pressure after combined fluid-percussion injury and uncontrolled hemorrhage resulted in increased hemorrhage and failure to optimize cerebrovascular function. In contrast, a period of moderate hypotension was well tolerated and did not compromise cerebrovascular hemodynamics, as evidenced by physiological parameters that remained within the limits of cerebral autoregulation. In addition, a tendency of improved short-term survival was reported (Stern et al., 2000). In a similar pig model of severe FP-TBI and controlled hemorrhagic hypotension, it was shown that CPP directed therapy improved brain oxygenation and maintained the cerebrovascular CO_2 reactivity within the first 5 h post-TBI. Brain edema was lower, but lung edema was greater, suggesting a higher propensity for pulmonary complications (Mattioli et al., 2003).

Indeed, respiratory disturbance represents a frequently occurring complication owing to severe TBI and hemorrhagic hypotension, which may cause hypoxic hypoxia and hypercapnia. We did not focus on this issue in this study. However, it represents a main area of clinical relevance, especially after resuscitation and should be considered in future to mimic more closely human severe brain injury. Indeed, the endangering consequences of respiratory disturbances are not only characterized by systemic O_2 deficit and disturbed acid-base balance but also by specific effects on intracranial volume regulation early after brain trauma. Given, that under those circumstances intracranial compliance is rather compromised, any additional volume increase can be responsible for critical ICP elevation with concomitant CPP reduction. It is well-known that the components of respiratory insufficiency, that is, hypoxemia, hypercapnia, and acidosis, induce cerebral hyperemia, mainly in the cerebrovascular bed outside the traumatically injured brain tissue in order to maintain adequate O_2 availability. However, the underlying vasodilation of resistance brain ves-

Table 3. Brain-Bleeding–Surface Index (BBSI) from Animals Suffering from Moderate (mTBI) and High Intensity FP-TBI (sTBI) Evaluated by Two Blinded Investigators

	Control (n = 6)	*mTBI* (n = 6)	*sTBI* (n = 7)
Investigator 1	1.4 ± 0.5	4.4 ± 1.5	6.6 ± 2.7
Investigator 2	1.8 ± 0.6	2.8 ± 0.8	6.4 ± 2.5
Mean	1.6 ± 0.6	3.6 ± 1.1[†]	6.5 ± 2.6[*,†]

[*]$p < 0.05$ mTBI versus sTBI.

[†]$p < 0.05$ value versus control group.

Data expressed as mean ± SD.

Table 4. Appearance and Distribution of Hypoxic-Ischemic Cells in Ipsi- and Contralateral Hemispheres Using H & E Histology

	Gray matter		*Thalamus*		*Hippocampus*		*Pons*	
Group	*Ipsilateral*	*Contralateral*	*Ipsilateral*	*Contralateral*	*Ipsilateral*	*Contralateral*	*Ipsilateral*	*Contralateral*
Control	0/6	0/6	0/6	0/6	0/6	0/6	0/6	0/6
mTBI	6/6	0/6	1/6	0/6	2/6	0/6	0/6	0/6
sTBI	7/7*	7/7*,†	7/7*,†	5/7*,†	7/7*,†	6/7*,†	5/7*,†	5/7*,†

*Differences in frequencies in the appearance of hypoxic-ischemic cells between control group and sTBI group, at $p < 0.05$.
†Differences in frequencies in the appearance of hypoxic-ischemic cells between mTBI group and sTBI group, at $p < 0.05$.
Data pairs represent number of animals with morphologic changes per total number of experimental animals of each group.

sels represent a distinct enlargement of intracranial blood volume, and hence an additional intracranial volume increase. Because traumatic brain injury induces disturbance of cerebrovascular autoregulation within the affected brain tissue with shift of the lower limit of the autoregulatory threshold to higher pressure values (Chan et al., 1992), even a limited CPP reduction can be responsible for CBF restriction with secondary regional ischemia.

The experimental approach, used in this study, did not clarify the underlying mechanisms responsible for secondary ICP increase. Nevertheless, sophisticated elaboration of the continuously monitored cardiovascular, ventilatory and neurological parameters allows us to exclude relevant alterations in ventilatory gas exchange or systemic hemodynamics in animals after mTBI and sTBI. However, a critical compromise in CPP was always induced by a pathologically increased ICP. Therefore, we suggest that intracranial processes are predominantly responsible for secondary ICP elevation. This assumption is supported by regularly occurring patterns of ICP increase in animals after sTBI suggesting a compromised intracranial compliance and increased risk to induce subsequently states of stable and elevated ICP (Fig. 3, Table 2, $p < 0.05$). Traumatic brain swelling appears to be the main cause for mass expansion and subsequent ICP increase. It has been reported that early after FP-TBI a transient ICP occurred regularly (Dixon et al., 1987). We suggest that the ICP increase immediately after FP administration is caused by the amount of the rapidly injected fluid volumes into the cranial cavity, which is trapped extradurally. In all cases of FP-TBI administration a dural integrity has been confirmed by inspection immediately after impact and at autopsy. The maintenance of early ICP increase may be caused by vascular swelling (Marmarou and Shima, 1990). A further component of space occupation occurring early after FP-TBI is that of intracranial bleeding. The semi quantitative evaluation of the extent of bleeding showed a significantly higher score after high intensity FP-TBI compared to moderate intensity FP-TBI ($p < 0.05$). We suggest that the FP impact induced predominantly bleeding by cerebral and cerebellar vein disruption. However, because the ICP exhibited normalization with failed progression during blood withdrawal and several hours after volume replacement, we assume that intracranial bleedings stopped spontaneously. Nevertheless, enhanced masses of clotting blood may compromise intracranial compliance with increased risk of secondary ICP elevation after high intensity FP-TBI.

Furthermore, high intensity FP-TBI was associated with a more pronounced reduction of CPP at the end of

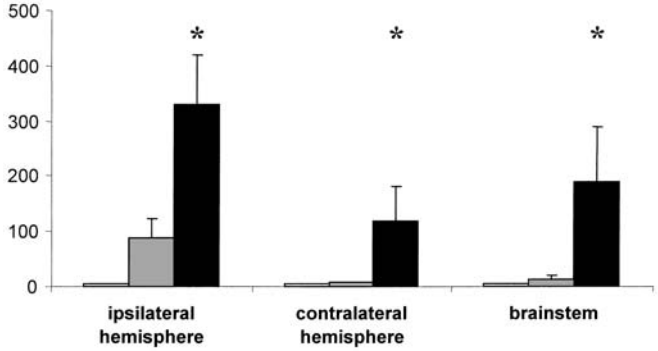

FIG. 4. Total number of damaged β-APP positive axons and axonal bulbs in the ipsi- and contralateral hemisphere. Values are presented as means ± SE. Control group, open columns; moderate traumatic brain injury group (mTBI), shaded columns; severe traumatic brain injury group (sTBI), black columns. *Significant differences between mTBI and sTBI group, $p < 0.05$.

blood withdrawal leading to a temporary compromise of CBF and brain oxygen uptake. We have observed in the sTBI group after withdrawal of 30% of estimated blood volume a CPP reduction of 47 ± 23% with concomitant decline in CBF and $CMRO_2$ whereas in the mTBI group a CPP reduction of 31 ± 22% occurred with unaltered CBF and increased $CMRO_2$. However, gradual ABP reduction was similar after both moderate and high intensity FP-TBI. In addition, whole body O_2 uptake appears unaltered after TBI and blood withdrawal. Hence, systemic cardiovascular regulation was apparently intact and the gradual undershoot of the lower autoregulatory threshold was mainly induced by sustained ICP elevation. Consequently, TBI intensity used in this application did not alter the ability of short-time cardiovascular centralization owing to pronounced blood loss early after mechanical brain injury.

Previous studies using porcine TBI models have also addressed the effects of fluid replacement (Schmoker et al., 1992; Shackford, 1997) or early resuscitation after posttraumatic hypotension (Malhotra et al., 2003; Stern et al., 2000). Similar to our investigation, they also found an ICP increase immediately after fluid resuscitation. Contrary our findings, they failed to show a substantial secondary ICP increase. This difference may result from the use of less severe brain injury (Glass et al., 1999) and cryogenic lesion (Schmoker et al., 1992; Shackford, 1997), which may reflect a rather focal TBI. Furthermore, in other studies the observation period may have been too short to acquire secondary changes with later onset (Malhotra et al., 2003; Stern et al., 2000).

Moreover, there is evidence that in this animal model of severe TBI and temporary blood loss transient increases in cerebral blood volume occurred in the majority of cases resulting in considerable sudden ICP elevation (Table 2, Fig. 3). We found signs in systemic and ICP behaviour typical of plateau waves or Lundberg "A-waves" (Lundberg, 1960). Here, a widely maintained cerebrovascular autoregulation can be suggested, despite critically compromised intracranial compliance (Rosner and Becker, 1984). A compromised autoregulatory response was also recorded characterized by synchronous elevation of ABP and ICP. We found such patterns occasionally early after TBI and registered it in two cases before plateau waves occurred. Therefore, we assume that in this model the consequences of combined brain injury are able to induce a temporary disturbance of cerebral autoregulation, which is followed by a re-established cerebrovascular autoregulation. However, a subsequently developing stable ICP elevation occurred despite the passing normalization in cerebrovascular regulation. We suggest that the above mentioned processes of edema formation are presumably responsible for the renewed deterioration.

Intraparenchymatous or intracerebral hemorrhages frequently accompany and aggravate diffuse traumatic brain injury. Such bleeding patterns have also been reported in adults and children after severe traumatic brain injury and have been associated with worse outcome (Graham et al., 1989; Mattioli et al., 2003). Previous experimental studies have also shown evidence of significant diffuse bleeding in various TBI models (Adelson et al., 2001). The FPI model, although frequently used to study focal pathological or physiological responses (Armstead, 2002; Armstead and Kurth, 1994; Prins and Hovda, 2003), has frequently shown pathological evidence of diffuse brain injury (Dixon et al., 1987). Interestingly, patterns of diffuse brain injury were observed more frequently when TBI was accompanied by hemorrhagic hypotension and hypoxemia (Ito et al., 1996). In the present study, we also found an increase in incidence and quantity of intracerebral bleeding in the severe brain injury group.

Neuropathological consequences were associated with the TBI intensity. We observed a considerable number of βAPP-immunolabeled axons in the ipsi- and contralateral temporoparietal subcortical white matter, thalamus and brainstem in the sTBI animals. The intra-axonal accumulation of βAPP serve as a sensitive and early marker for the diffuse traumatic axonal injury (Buki et al., 2000; Maxwell et al., 1997) and underlines in addition to the histological findings diffuse brain damage in the sTBI group.

However, altogether we have to realize that despite the efforts towards standardization of experimental approaches to induce severe TBI a considerable heterogeneity in brain reactivity has been found. Time course of ICP alteration and related effects on CBF and brain oxidative metabolism as well as morphopathological consequences showed distinct quantitative differences despite maintained systemic conditions. Therefore, the need for further clarification of key pathogenetic mechanisms in the development of secondary brain injury due to TBI and related complications, like hemorrhagic hypotension or respiratory disturbances are necessary. The current animal model appears to be an experimental tool to provide useful findings.

In conclusion, we present a model of traumatic brain injury which closely simulates the clinical scenario. We have reproduced the secondary ICP increase after severe brain injury and described the complex hemodynamic, metabolic, functional, and histopathologic changes during the first 24 h. Beside the induction of secondary ICP increase this model is suitable to induce experimental focal or diffuse neuronal damage and traumatic axonal damage depending on the trauma intensity. This experimental model appears to be helpful in the study of new therapeutic approaches. Furthermore, it enables in-depth

studies such as resuscitation thresholds, effects of hypovolema, hypoxemia, hypercarbia, hyperthermia, and their influence on neuropathology to be studied.

ACKNOWLEDGMENTS

We acknowledge the advice of U. Jaeger, I. Witte, and L. Wunder for their skillful technical assistance and of Wahedullah Karzai, M.D. (Dept. of Anesthesiology and Intensive Care Medicine, Zentralklinikum Bad Berka, Germany) on the preparation of the manuscript. This study was supported by grant by BMBF/IZKF 01ZZ9602 (Federal Republic of Germany).

REFERENCES

ADELSON, P.D., JENKINS, L.W., HAMILTON, R.L., et al. (2001). Histopathologic response of the immature rat to diffuse traumatic brain injury. J. Neurotrauma **18,** 967–976.

ARMSTEAD, W.M. (2002). Age-dependent NMDA contribution to impaired hypotensive cerebral hemodynamics following brain injury. Brain Res. Dev. Brain Res. **139,** 19–28.

ARMSTEAD, W.M., and KURTH, C.D. (1994). Different cerebral hemodynamic responses following fluid percussion brain injury in the newborn and juvenile pig. J. Neurotrauma **11,** 487–497.

BAUER, R., WALTER, B., TOROSSIAN, A., et al. (1999). A piglet model for evaluation of cerebral blood flow and brain oxidative metabolism during gradual cerebral perfusion pressure decrease. Pediatr. Neurosurg. **30,** 62–69.

BAUER, R., WALTER, B., WURKER, E., et al. (1996). Colored microsphere technique as a new method for quantitative-multiple estimation of regional hepatic and portal blood flow. Exp. Toxicol. Pathol. **48,** 415–420.

BAUER, R., WALTER, B., VORWIEGER, G., et al. (2001). Intrauterine growth restriction induces up-regulation of cerebral aromatic amino acid decarboxylase activity in newborn piglets: [^{18}F]fluorodopa positron emission tomographis study. Pediatr. Res. **49,** 474–480.

BRAMLETT, H.M., DIETRICH, W.D., and GREEN, E.J. (1999). Secondary hypoxia following moderate fluid percussion brain injury in rats exacerbates sensorimotor and cognitive deficits. J. Neurotrauma **16,** 1035–1047.

BUKI, A., OKONKWO, D.O., WANG, K.K., et al. (2000). Cytochrome c release and caspase activation in traumatic axonal injury. J. Neurosci. **20,** 2825–2834.

CHAN, K.H., MILLER, J.D., DEARDEN, N.M., et al. (1992). The effect of changes in cerebral perfusion pressure upon middle cerebral artery blood flow velocity and jugular bulb venous oxygen saturation after severe brain injury. J. Neurosurg. **77,** 55–61.

CHESNUT, R.M., MARSHALL, S.B., PIEK, J., et al. (1993). Early and late systemic hypotension as a frequent and fundamental source of cerebral ischemia following severe brain injury in the Traumatic Coma Data Bank. Acta Neurochir. (Wien) Suppl. **59,** 121–125.

CIRICILLO, S.F., ANDREWS, B.T., DAMRON, S.L., et al. (1992). Severity and outcome of intracranial lesions in pedestrians injured by motor vehicles. J. Trauma **33,** 899–903.

CLARK, R.S., KOCHANEK, P.M., DIXON, C.E., et al. (1997). Early neuropathologic effects of mild or moderate hypoxemia after controlled cortical impact injury in rats. J. Neurotrauma **14,** 179–189.

COYLE, M.G., OH, W., and STONESTREET, B.S. (1993). Effects of indomethacin on brain blood flow and cerebral metabolism in hypoxic newborn piglets. Am. J. Physiol. **264,** H141–H149.

DIXON, C.E., LYETH, B.G., POVLISHOCK, J.T., et al. (1987). A fluid percussion model of experimental brain injury in the rat. J. Neurosurg. **67,** 110–119.

ENGELBORGHS, K., VERLOOY, J., VAN REEMPTS, J., et al. (1998). Temporal changes in intracranial pressure in a modified experimental model of closed head injury. J. Neurosurg. **89,** 796–806.

FELIX, B., LEGER, M.E., ALBE-FESSARD, D., et al. (1999). Stereotaxic atlas of the pig brain. Brain Res. Bull. **49,** 1–137.

GLASS, T.F., FABIAN, M.J., SCHWEITZER, J.B., et al. (1999). Secondary neurologic injury resulting from nonhypotensive hemorrhage combined with mild traumatic brain injury. J. Neurotrauma **16,** 771–782.

GRAHAM, D.I., FORD, I., ADAMS, J.H., et al. (1989). Fatal head injury in children. J. Clin. Pathol. **42,** 18–22.

ISHIGE, N., PITTS, L.H., BERRY, I., et al. (1988). The effects of hypovolemic hypotension on high-energy phosphate metabolism of traumatized brain in rats. J. Neurosurg. **68,** 129–136.

ITO, J., MARMAROU, A., BARZO, P., et al. (1996). Characterization of edema by diffusion-weighted imaging in experimental traumatic brain injury. J. Neurosurg. **84,** 97–103.

JUUL, N., MORRIS, G.F., MARSHALL, S.B., et al. (2000). Intracranial hypertension and cerebral perfusion pressure: influence on neurological deterioration and outcome in severe head injury. The Executive Committee of the International Selfotel Trial. J. Neurosurg. **92,** 1–6.

KROPPENSTEDT, S.N., KERN, M., THOMALE, U.W., et al. (1999). Effect of cerebral perfusion pressure on contusion volume following impact injury. J. Neurosurg. **90,** 520–526.

LEFFLER, C.W., BUSIJA, D.W., MIRRO, R., et al. (1989). Effects of ischemia on brain blood flow and oxygen consumption of newborn pigs. Am. J. Physiol. **257,** H1917–H1926.

LEWELT, W., JENKINS, L.W., and MILLER, J.D. (1982). Effects of experimental fluid-percussion injury of the brain on

cerebrovascular reactivity of hypoxia and to hypercapnia. J. Neurosurg. **56,** 332–338.

LINDGREN, S., and RINDER, L. (1969). Production and distribution of intracranial and intraspinal pressure changes at sudden extradural fluid volume input in rabbits. Acta Physiol. Scand. **76,** 340–351.

LUNDBERG, N. (1960). Continuous recording and control of ventricular fluid pressure in neurosurgical patients. Acta Psychiatr. Neurol. Scand. **149,** 158–167.

MALHOTRA, A.K., SCHWEITZER, J.B., FOX, J.L., et al. (2003). Cerebral perfusion pressure directed therapy following traumatic brain injury and hypotension in swine. J. Neurotrauma **20,** 827–839.

MARMAROU, A., and SHIMA, K. (1990). Comparative studies of edema produced by fluid percussion injury with lateral and central modes of injury in cats. Adv. Neurol. **52,** 233–236.

MATTIOLI, C., BERETTA, L., GEREVINI, S., et al. (2003). Traumatic subarachnoid hemorrhage on the computerized tomography scan obtained at admission: a multicenter assessment of the accuracy of diagnosis and the potential impact on patient outcome. J. Neurosurg. **98,** 37–42.

MAXWELL, W.L., POVLISHOCK, J.T., and GRAHAM, D.L. (1997). A mechanistic analysis of nondisruptive axonal injury: a review. J. Neurotrauma **14,** 419–440.

McINTOSH, T.K., VINK, R., NOBLE, L., et al. (1989). Traumatic brain injury in the rat: characterization of a lateral fluid-percussion model. Neuroscience **28,** 233–244.

McKENZIE, K.J., McLELLAN, D.R., GENTLEMAN, S.M., et al. (1996). Is beta-APP a marker of axonal damage in short-surviving head injury? Acta Neuropathol. (Berl.) **92,** 608–613.

MILLEN, J.E., GLAUSER, F.L., and FAIRMAN, R.P. (1985). A comparison of physiological responses to percussive brain trauma in dogs and sheep. J. Neurosurg. **62,** 587–591.

MILLER, J.D., BUTTERWORTH, J.F., GUDEMAN, S.K., et al. (1981). Further experience in the management of severe head injury. J. Neurosurg. **54,** 289–299.

NAWASHIRO, H., SHIMA, K., and CHIGASAKI, H. (1995). Selective vulnerability of hippocampal CA3 neurons to hypoxia after mild concussion in the rat. Neurol. Res. **17,** 455–460.

NILSSON, F., AKESON, J., MESSETER, K., et al. (1995). A porcine model for evaluation of cerebral haemodynamics and metabolism during increased intracranial pressure. Acta Anaesthesiol. Scand. **39,** 827–834.

PFENNINGER, E.G., REITH, A., BREITIG, D., et al. (1989). Early changes of intracranial pressure, perfusion pressure, and blood flow after acute head injury. Part 1: An experimental study of the underlying pathophysiology. J. Neurosurg. **70,** 774–779.

POVLISHOCK, J.T., HAYES, R.L., MICHEL, M.E., et al. (1994). Workshop on animal models of traumatic brain injury. J. Neurotrauma **11,** 723–732.

POWNALL, R., and DALTON, R.G. (1973). Blood and plasma volumes of neonatal pigs expressed relative to bodyweight and total body water. Br. Vet. J. **129,** 583–588.

PRINS, M.L., and HOVDA, D.A. (2003). Developing experimental models to address traumatic brain injury in children. J. Neurotrauma **20,** 123–137.

ROSNER, M.J., and BECKER, D.P. (1984). Origin and evolution of plateau waves. Experimental observations and a theoretical model. J. Neurosurg. **60,** 312–324.

SCHMOKER, J.D., ZHUANG, J., and SHACKFORD, S.R. (1992). Hemorrhagic hypotension after brain injury causes an early and sustained reduction in cerebral oxygen delivery despite normalization of systemic oxygen delivery. J. Trauma **32,** 714–722.

SHACKFORD, S.R. (1997). Effect of small-volume resuscitation on intracranial pressure and related cerebral variables. J. Trauma **42,** S48–S53.

SHIBATA, M., EINHAUS, S., SCHWEITZER, J.B., et al. (1993). Cerebral blood flow decreased by adrenergic stimulation of cerebral vessels in anesthetized newborn pigs with traumatic brain injury. J. Neurosurg. **79,** 696–704.

SIGNORINI, D.F., ANDREWS, P.J., JONES, P.A., et al. (1999). Adding insult to injury: the prognostic value of early secondary insults for survival after traumatic brain injury. J. Neurol. Neurosurg. Psychiatry **66,** 26–31.

STATLER, K.D., JENKINS, L.W., DIXON, C.E., et al. (2001). The simple model versus the super model: translating experimental traumatic brain injury research to the bedside. J. Neurotrauma **18,** 1195–1206.

STERN, S.A., ZINK, B.J., MERTZ, M., et al. (2000). Effect of initially limited resuscitation in a combined model of fluid-percussion brain injury and severe uncontrolled hemorrhagic shock. J. Neurosurg. **93,** 305–314.

SULLIVAN, H.G., MARTINEZ, J., BECKER, D.P., et al. (1976). Fluid-percussion model of mechanical brain injury in the cat. J. Neurosurg. **45,** 521–534.

WALTER, B., BAUER, R., GASER, E., et al. (1997). Validation of the multiple colored microsphere technique for regional blood flow measurements in newborn piglets. Basic Res. Cardiol. **92,** 191–200.

WARD, J.D. (1994). Pediatric head injury: a further experience. Pediatr. Neurosurg. **20,** 183–185.

Address reprint requests to:
Reinhard Bauer, M.D., Ph.D.
Institute for Pathophysiology and Pathobiochemistry
Friedrich Schiller University
D-07740 Jena, Germany

E-mail: Reinhard.Bauer@mti.uni-jena.de

10. Weitere, im Zusammenhang mit der Thematik stehende Publikationen

1. Fritz H, Schwarzkopf K, Hoff H, Kurzweg V, Hartmann M, Klein U: Urapidil zur Therapie von postanästhetischem Shivering nach Allgemeinanästhesie. Anaesthesist 50 (2001) 406-410

2. Fritz HG, Hoff H, Hartmann M, Karzai W, Schwarzkopf KR: The effects of urapidil on thermoregulatory thresholds in volunteers. Anesth Analg 94 (2002) 626-630

3. Fritz H, Bauer R: Präklinische Versorgung des schweren kindlichen Schädel-Hirn-Traumas. Notfall & Rettungsmedizin 5 (2002) 335-340

4. Fritz HG, Bauer R: Traumatic injury in the developing brain--effects of hypothermia. Exp Toxicol Pathol 56 (2004) 91-102

5. Fritz HG, Bauer R: Secondary injuries in brain trauma: effects of hypothermia. J Neurosurg Anesthesiol 16 (2004) 43-52

6. Walter B, Bauer R, Fritz H, Jochum T, Wunder L, Zwiener U: Evaluation of micro tip pressure transducers for the measurement of intracerebral pressure transients induced by fluid percussion. Exp Toxicol Pathol 51 (1999) 124-129

7. Bauer R, Walter B, Fritz H, Zwiener U: Ontogenetic aspects of traumatic brain edema--facts and suggestions. Exp Toxicol Pathol 51 (1999) 143-150

8. Walter B, Bauer R, Kuhnen G, Fritz H, Zwiener U: Coupling of cerebral blood flow and oxygen metabolism in infant pigs during selective brain hypothermia. J Cereb Blood Flow Metab 20 (2000) 1215-1224

9. Schwarzkopf KR, Hoff H, Hartmann M, Fritz HG: A comparison between meperidine, clonidine and urapidil in the treatment of postanesthetic shivering. Anesth Analg 92 (2001) 257-260

10. Walter B, Brust P, Fuchtner F, Muller M, Hinz R, Kuwabara H, Fritz H et al.: Age-dependent effects of severe traumatic brain injury on cerebral dopaminergic activity in newborn and juvenile pigs. J Neurotrauma 21 (2004) 1076-1089

11. Bauer R, Fritz H: Pathophysiology of traumatic injury in the developing brain: an introduction and short update. Exp Toxicol Pathol 56 (2004) 65-73

Aus der Universitätsklinik für Anästhesiologie und operative Intensivmedizin
an der Martin-Luther-Universität Halle-Wittenberg,
(Direktor: Prof. Dr. med. J. Radke)
dem Institut für Pathophysiologie des Bereiches Medizin
an der Friedrich-Schiller-Universität Jena
(komm. Direktor: PD Dr. med. R. Bauer)
und der Klinik für Anästhesiologie und Intensivmedizin
am Krankenhaus Martha-Maria Halle-Dölau gGmbH,
Akademisches Lehrkrankenhaus der Martin-Luther-Universität Halle-Wittenberg
(Chefarzt: Dr. med. Harald Fritz)

Thesen zur Habilitationsschrift

Effekte der milden Hypothermie auf das traumatisierte Gehirn und extrazerebrale Organe des juvenilen Schweines

zur Erlangung des akademischen Grades

Dr. med. habil

vorgelegt

der Medizinischen Fakultät

der Martin-Luther-Universität Halle-Wittenberg

von Dr. med. Harald Georg Fritz

geboren am 09. September 1958 in Erfurt

1. Die komplexe Dynamik der Pathogenese des kindlichen Schädel-Hirn-Traumas weist eine Reihe von Aspekten auf, die grundsätzlich vom Schädel-Hirn-Trauma des Erwachsenen differieren.

2. Das kindliche Schädel-Hirn-Trauma benötigt adaptierte experimentelle Modelle, um seine spezifischen pathophysiologischen Aspekte zu untersuchen.

3. Eine Vielzahl von experimentellen Untersuchungen erfolgt bis heute am lisencephalen Gehirn, weshalb die Ergebnisse dieser Untersuchungen nur sehr begrenzt auf das menschliche Gehirn übertragbar sind.

4. Untersuchungen am gyrierten Gehirn des Schweines sind auf Grund der Vergleichbarkeit zum menschlichen Gehirn bezüglich Anatomie und physiologischer Reaktion besser geeignet, in kliniknahen Modellen die Frühphase nach einem Schädel-Hirn-Trauma zu modellieren.

5. Das epidurale Ballonmodell ist geeignet, Veränderungen der zerebralen Hämodynamik während stufenweiser Steigerung des intrakraniellen Druckes beim juvenilen Schwein zu modellieren.

6. Die stufenweise Steigerung des intrakraniellen Druckes auf 25, 35 und 45 mmHg reduziert den zerebralen Perfusionsdruck reproduzierbar auf 70, 50 und 30% des Ausgangsniveaus. Voraussetzung hierfür ist die Regulation des mittleren arteriellen Blutdruckes über eine closed-loop-Schleife mit Blutentzug oder Bluttransfusion zur Konstanz des arteriellen Blutdruckes.

7. Mit der stufenweisen Reduktion des zerebralen Perfusionsdruckes assoziiert ist eine Verminderung des globalen zerebralen Blutflusses. Die milde Reduktion des CPP auf 70% (ICP=25 mmHg) verursacht zunächst eine Steigerung der regionalen Durchblutung in der Medulla oblongata. Ein überproportionaler Abfall der kortikalen Durchblutung ist bei weiterer CPP-Reduktion zu beobachten.

8. Die elektrische kortikale Funktion ist schon bei milder Reduktion der zerebralen Perfusion auf 70 % (ICP = 25 mmHg) des Ausgangswertes erheblich beeinträchtigt. Sie ist bei weiterer Reduktion des CPP durch Amplituden - und Frequenzverlangsamung gekennzeichnet und resultiert bei CPP-Reduktion auf 35 % in einem Null-Linien-ECoG bzw. in Burst-Suppression-Mustern.

9. Die milde Hypothermie reduziert den zerebralen Sauerstoffmetabolismus stärker als den zerebralen Blutfluss beim juvenilen Schwein.

10. Während stufenweiser CPP-Reduktion reduziert die milde Hypothermie das Ausmaß der perfusionsabhängigen Beeinträchtigung von Hirndurchblutung und Sauerstoffmetabolismus. Die kortikale Funktion bleibt länger erhalten.

11. Das schwere flüssigkeitsvermittelte Perkussionstrauma mit nachfolgendem Blutentzug erlaubt die Modellierung der schweren traumatischen Hirnschädigung beim juvenilen Gehirn.

12. Innerhalb der ersten 24 Stunden nach schwerem flüssigkeitsvermittelten Perkussionstrauma treten ca. 5 Stunden posttraumatisch beginnend, reproduzierbare Hirndruckanstiege auf.

13. Die milde Hypothermie reduziert den histopathologischen Schaden nach schwerem flüssigkeitsvermittelten Perkussionstrauma nach 24 Stunden. Es ist jedoch möglich, dass die Beeinflussung des intrakraniellen Druckes durch die Hypothermie die wesentliche Komponente für die Reduktion des histopathologischen Schadens darstellt.

14. Die Pharmakokinetik von Fentanyl wird beim juvenilen Schwein durch die Hypothermie wesentlich verändert. So steigen die Fentanyl-Plasmaspiegel während 6-stündiger Hypothermie um 25 % an und normalisieren sich nach Wiedererwärmung nur langsam.

15. Die Aktivität der hepatischen CYP3A4-Cytochrom P 450-Untereinheit ist temperaturabhängig. Sie ist während milder Hypothermie (32°C) um 30%

reduziert, während moderater Hypothermie (26°C) um 52%. Der arterielle hepatische Blutfluss wird dagegen durch die Hypothermie nur unwesentlich beeinflusst. Es ist deshalb anzunehmen, dass die Erhöhung der Fentanyl-Plasmaspiegel wesentlich durch die reduzierte Aktivität CYP3A4 verursacht wird.

16. Die Hypothermie vermag sowohl indirekt über eine reduzierte Organperfusion als auch direkt durch Verminderung von Enzymaktivitäten die Pharmakokinetik von Analgetika zu beeinflussen.

Lebenslauf

Personalien:

Name	Harald Georg Fritz
Geburtsdatum	09.09.1958
Geburtsort	Erfurt
Staatsangehörigkeit	Deutsch
Konfession	evang.-luth.
Familienstand	verheiratet, 4 Kinder

Schulbildung:

1965 – 1973	24. Polytechnische Oberschule „Friedrich Schiller“ Erfurt
1973 – 1977	Erweiterte Oberschule Heinrich-Mann Erfurt
1975	Abschlusszeugnis 10.Klasse
1977	Abitur

Ausbildung/Studium:

09/1977 – 10/1977	Medizinische Akademie Erfurt , Hilfspfleger
10/1977 – 10/1980	Militärdienst: Eilenburg, Potsdam Wildpark-West, Sanitätsdienst Unteroffizier,
1980 – 1982	Humanmedizin, Vorklinik, Karl-Marx-Universität, Leipzig,
1982	Physikum
1982 – 1986	Klinische Ausbildung, Medizinische Akademie Erfurt
31.08.1985	Staatsexamen
1985 – 1986	Pflichtassistenz an der Zentralklinik f. Herz- und Lungenkrankheiten Bad Berka und den Kliniken und Polikliniken der Stadt Weimar

Qualifikationen:

14.12.1985	Diplom: " Ergebnisse einer alternierenden Polychemotherapie bei 30 Patienten mit Hodentumoren"
01.09.1986	Approbation als Arzt
07.11.1990	Facharztanerkennung „Anästhesiologie und Intensivtherapie“
06.08.1991	Fachkunde: Rettungsdienst
17.02. 1993	Promotion: „Klinische Wertigkeit der Schallspektrographie mechanischer Herzklappenprothesen"
11. –15.04.2000	Kurs zum Erwerb der Fachkunde „Leitender Notarzt“
20.02.2002	Fakultative Weiterbildung: „Spezielle Anästhesiologische Intensivmedizin“

Beruflicher Werdegang:

09/1986 – 12/1989	Assistenzarzt, Abt. f. Anästhesie und Intensivtherapie Zentralklinik für Herz- und Lungenkrankheiten, Bad Berka
01/1990 – 06/1992	Assistenzarzt/Facharzt, Klinik f. Anästhesiologie und Intensivtherapie, Medizinische Akademie, Erfurt
07/1992 – 08/1993	Facharzt, Abt. f. Anästhesiologie und Intensivmedizin, Ev. Stift St. Martin, Koblenz
09/1993 – 05/1994	Facharzt, Klinik f. Anästhesiologie und Intensivtherapie, Friedrich-Schiller-Universität, Jena
06/1994 – 09/2004	Oberarzt in der Neuroanästhesie, der Anästhesiologischen Intensivtherapiestation und der Kardioanästhesie, Klinik f. Anästhesiologie und Intensivtherapie Friedrich-Schiller-Universität, Jena
Seit 10/2004	Chefarzt, Klinik f. Anästhesiologie und Intensivmedizin, Krankenhaus Martha-Maria gGmbH, Halle-Dölau

Danksagung

An dieser Stelle möchte ich mich bei allen bedanken, die mich auf dem langen Weg der Fertigstellung der Arbeit begleitet und unterstützt haben.
Mein ganz besonderer Dank gilt Herrn Priv.-Doz. Dr. med. Reinhard Bauer für die Überlassung des Themas, das Vertrauen für die unbegrenzte Nutzung der umfangreichen Laboreinrichtungen und für seine Unterstützung bei Präsentationen und Veröffentlichungen der Ergebnisse. Ihm verdanke ich zahlreiche konstruktive Diskussionen, die mir stets Anregung zur inhaltlichen und methodischen Auseinandersetzung mit den zu bearbeitenden Fragestellungen waren. Er hat mich an das experimentelle Arbeiten herangeführt.
Des Weiteren möchte ich mich bei Herrn Dr. med. Bernd Walter bedanken, der zu den vielen Experimenten durch sein außerordentliches Engagement und überdurchschnittlichen Fleiß sowie Sorgfalt und Fachkenntnis einen unschätzbaren Beitrag geleistet hat.
Ein weiterer Dank gilt Herrn Prof. Dr. med. Stephan Patt und Herrn Dr. med. Michael Brodhun für die sehr sorgfältige und umfangreiche Aufarbeitung des histologischen Untersuchungsmaterials.
Mein Dank gilt auch den Mitarbeitern des Labors, den medizinisch technischen Assistentinnen Frau Ute Jäger und Frau Ilona Witte für die vielen zusätzlichen Arbeitsstunden, ohne die das Gelingen der Experimente in Frage gestellt gewesen wäre, sowie Herrn Dipl. Ing. Lothar Wunder, der für die Lösung vieler kniffliger technischer Probleme unentbehrlich war.
Ein besonderer Dank gilt meinem langjährigen Lehrer und Kliniksdirektor Herrn Prof. Dr. med. Konrad Reinhart, der mir die zeitlichen Freiräume für die Durchführung der Experimente schuf und durch sein hartnäckiges Intervenieren die Fertigstellung der dieser Arbeit zugrunde liegenden Publikationen katalysierte.
Nicht zuletzt gilt mein Dank auch Herrn Prof. Dr. med. Joachim Radke, der mich ermutigte, nach dem Wechsel von Jena nach Halle, die Arbeit auch als „Externer“ zu vollenden. Von ihm erhielt ich die notwendige universitäre Unterstützung.

Eidesstattliche Erklärung

Hiermit versichere ich an Eides statt, dass ich die vorliegende Habilitationsleistung selbständig verfasst und keine anderen als die angegebenen Quellen und Hilfsmittel verwendet habe.

Zugleich erkläre ich, dass an keiner anderen Fakultät oder Universität ein Habilitationsverfahren derzeit anhängig ist bzw. jemals anhängig war.

Halle, den 29.05.2007 Dr. med. Harald Fritz